Advances in the Theory of Fixed-time Stability with Applications in Constrained Control and Optimization

by

Kunal Garg

A dissertation submitted in partial fulfillment
of the requirements for the degree of
Doctor of Philosophy
(Aerospace Engineering)
in the University of Michigan
2021

Doctoral Committee:

Associate Professor Dimitra Panagou, Chair
Professor Dennis S. Bernstein
Professor Ilya V. Kolmanovsky
Associate Professor Necmiye Ozay

Kunal Garg

kgarg@umich.edu

ORCID iD: 0000-0002-1895-4991

To my parents.

Acknowledgments

It would be unfair to this dissertation if I started by thanking anyone but my advisor, Prof. Dimitra Panagou. She believed in me, allowed me to pursue my passion, gave me all the freedom in the world to let me explore all the different directions, and at the same time, kept me on track and focused. She has been really patient with me, particularly in the process of writing technical papers. I would imagine anyone else would have given up on me, given the number of rejections I received for my papers, but Prof. Panagou did not. She even encouraged me after each of those rejections, taking the fault on herself and motivating me to keep working on the stuff I was passionate about. She always had a plan for me, a very important aspect for someone like me who is highly susceptible to lose focus. I could not have asked for a better Ph.D. advisor, and I can only say that she is the Ph.D. advisor that I needed, not the one I probably deserved.

I wish to acknowledge my collaborators and colleagues. Thank you, Dr. Dongkun Han, who introduced me to the art of writing technical papers in the very first year of my Ph.D., a skill that would go a long way. Dr. Rohit Gupta and Dr. Mayank Baranwal introduced me to the new avenues of research in continuous-time optimization which contributed to a great portion of this dissertation. They not only introduced me to a ton of useful mathematical results, but they also helped me understand some of the very complex ideas and results. I would like to thank both of them for their friendship, and all their support in the last 3 years. I would like to thank James Usevitch, the kindest and the most encouraging person I have ever met, for all his support throughout my Ph.D. Apart from all the long technical discussions I was fortunate enough to have with him, I am also going to miss his jolly personality and the liveliness that he would bring into anything. I am grateful to him and all the other DASC Lab members for reviewing all my papers and giving me valuable feedback on my research. Special thanks to Dr. Parag Bobade and Dr. Ehsan Arabi for introducing me to new research avenues, and to Dr. Lars Lindemann for clarifying some of the very crucial technical concepts to me.

I would like to thank all of my friends here in Michigan and back in India. Thank you, Larry and Lucy Champoux, for the numerous dinner parties, the free furniture, the drives

to and from the airport (and the Niagara Falls trip!), and for making my life as an international student much better. I do not even know how to express my gratitude towards my friend, my brother, Vikalp Aggarwal. If it were not for the trips to NYC to meet him, I do not know how I would have coped with all the stress of Ph.D. life. Another person who made the Ph.D. life so easy for me, especially in the time of the pandemic, is my roommate and my dear friend, Aaditya Lakshmanan. Thanks for your invaluable help, both personal and academic. I am also grateful to have met Aditya Sundar, Vishnu Chipade, Harsh Agrawal, Gurmeet Singh, Vishwas Goel, Dr. Siddartha Srivastava, and Akshay Sarin who made my Ph.D. life easier in one way or the other. I would like to give a very special thank you to all the members of the "Juwaris" group, Dr. Kumar Aanjaneya, Poorwa Shekhar (extra special thank you for all the BWWs nights!), Saurabh Mahajan, Harshad Dharmatti, Dr. Shriya Sethuraman, Dr. Vaibhav Gogte, Dr. Ripudaman Singh, Dr. Niket Prakash, Dr. Keval Ramani, Sneha Joshi, and most of all, Aditi Kulkarni for not only introducing me to this group but also for being the nicest person I have ever met and for being an inspiring cook and sharing all those amazing recipes with me. I am thankful to Ashu Bapna and Akanksha Jethani for instilling confidence in me and keeping me motivated. Thank you all for the virtual game nights and for keeping the human touch in the trying times of the pandemic that saved me from going paranoid. Finally, I would like to offer a special thank you to Shalini Yadav for always being there for me.

I am thankful to the staff members of the Department of Aerospace Engineering, especially Denise Phelps for being *the* point-of-contact for anything even remotely related to graduate studies. I would like to acknowledge Thomas Griffin and David McLean for all their logistic and technical help, and especially for allowing me to take the necessary equipment from the department to my apartment in the time of the pandemic, without which surviving the last and the most crucial year of my Ph.D. would have been a nightmare.

I thank my little brother, Nitin Garg, for being there with our parents when I could not be. I would always be grateful to have a sister like you, Ankita Goyal, who has been and would forever remain my go-to person for any personal advice. My first Europe trip would always be memorable, thanks to you. Last but not least, I thank my parents, Sunil Garg and Anju Garg, for all their love and caring. I dedicate this dissertation to my parents for all the sacrifices they have made for me. Without their love and support, I would not be whatever I am today.

Finally, I would like to thank NASA Grant NNX16AH81A and Air Force Office of Scientific Research (AFOSR) award number FA9550-17-1-0284 whose support made my research possible.

Table of Contents

List of Figures

Figure

List of Appendices

Appendix

List of Abbreviations

w.r.t. with respect to

AS asymptotic stability

ES exponential stability

LS Lyapunov stable

FTS finite-time stability

FxT fixed-time

FxT-CLF fixed-time CLF

FxTS fixed-time stability

CLF control Lyapunov function

CBF control barrier function

ZCBF zeroing control barrier function

QP quadratic program

STL signal temporal logic

KKT Karush-Kuhn-Tucker

UAV unmanned aerial vehicle

RRT rapidly-exploring random tree

GF gradient flow

PL Polyak-Łojasiewicz

MPC model predictive control

SP saddle-point

Abstract

Driving the state of dynamical systems to a desired point or set is a problem of crucial practical importance. Various constraints are present in real-world applications due to structural and operational requirements. Spatial constraints, i.e., constraints requiring the system trajectories to evolve in some *safe* set, while visiting some goal set(s), are typical in safety-critical applications. Furthermore, temporal constraints, i.e., constraints pertaining to the time of convergence, appear in time-critical applications, for instance, when a task must complete within a fixed time due to an internal or an external deadline. Moreover, imperfect knowledge of the operational environment and/or system dynamics, and the presence of external disturbances render offline control policies impractical and make it essential to develop methods for online control synthesis. Thus, from the implementation point-of-view, it is desired to design fast optimization algorithms so that an optimal control input, e.g., min-norm control input, can be computed online. As compared to exponential stability, the notion of fixed-time stability is stronger, with the time of convergence being finite and is bounded for all initial conditions. This dissertation studies the theory of fixed-time stability with applications in multi-agent control design under spatiotemporal and input constraints, and in the field of continuous-time optimization.

First, multi-agent control design problems under spatiotemporal constraints are studied. A vector-field-based controller is presented for distributed control of multi-agent systems for a class of agents modeled under double-integrator dynamics. A finite-time controller that utilizes the state estimates obtained from a finite-time state observer is designed to guarantee that each agent reaches its goal location within a finite time while maintaining safety with respect to other agents as well as dynamic obstacles.

Next, new conditions for fixed-time stability are developed to use fixed-time stability along with input constraints. It is shown that these new conditions capture the relationship between the time of convergence, the domain of attraction, and the input constraints for fixed-time stability. Additionally, the new conditions establish the robustness of fixed-time stable systems with respect to a class of vanishing and non-vanishing additive disturbances. Utilizing these new fixed-time stability results, a control design method using convex opti-

mization is presented for a general class of systems having nonlinear, control-affine dynamics. Control barrier and control Lyapunov function conditions are used as linear constraints in the optimization problem for set-invariance and goal-reachability requirements. Various practical issues, such as input constraints, additive disturbance, and state-estimation error, are considered.

Next, new results on finite-time stability for a class of hybrid and switched systems are proposed using a multiple-Lyapunov-functions framework. The presented framework allows the system to have unstable modes. Finally, novel continuous-time optimization methods are studied with guarantees for fixed-time convergence to an optimal point. Fixed-time stable gradient flows are developed for unconstrained convex optimization problems under conditions such as strict convexity and gradient dominance of the objective function, which is a relaxation of strong convexity. Furthermore, min-max problems are considered and modifications of saddle-point dynamics are proposed with fixed-time stability guarantees under various conditions on the objective function.

CHAPTER 1

Introduction

This dissertation studies finite- and fixed-time stability of dynamical systems with applications in multi-agent control synthesis and convex optimization problems. This chapter provides the motivation for this research and a brief literature review for each of the topics studied in the dissertation, the contributions of the dissertation, the relevant publications that provide the base for it, and its outline.

1.1 Motivation

The stability of the equilibrium points or sets of dynamical systems is an essential property since they typically are designed to capture desired specifications and performance requirements of the system response. The traditional notions of stability for dynamical systems with Lipschitz or locally Lipschitz dynamics have been studied extensively in the literature. In contrast to asymptotic stability (AS) or exponential stability (ES), which pertains to the convergence of system trajectories as time tends to infinity, finite-time stability (FTS) [1] is a concept that guarantees convergence in a finite time. A stronger notion, termed as fixed-time stability (FxTS), requires that this finite time of convergence is uniformly bounded for all initial conditions, thus requiring the system trajectories to reach an equilibrium point or set within a *fixed* time independent of the initial conditions. Hence, for specifications involving temporal constraints and time-critical systems, the theory of finite- and fixed-time stability can be leveraged in the control design to guarantee that such specifications are met. It has been shown that a faster rate of convergence generally implies that the closed-loop system has better disturbance rejection properties; in particular, under the effect of added vanishing disturbance, finite-time convergence is preserved and under the effect of non-vanishing, bounded disturbance, the ultimate bound on the state-error is of

[1] With a slight abuse of notation, the acronyms FTS (similarly, FxTS) is used to denote both finite-time *stability* and finite-time *stable*, depending on the context.

a lower magnitude (see e.g., [1, 2]). This further motivates the study of finite- and fixed-time stability in this dissertation for time-critical motion planning problems as well as for gradient flows to solve convex optimization problems. However, achieving fixed-time stability under input constraints is a challenging problem since in this case it is not possible to guarantee convergence within a fixed time for arbitrary initial conditions. There is no prior work on incorporating input constraints while characterizing a domain of attraction from which fixed-time convergence can be guaranteed. This motivates the study of new fixed-time stability conditions that incorporate input constraints and characterize a domain of attraction of fixed-time stability.

With the advent of fast computational tools, online control synthesis through solving an optimization problem has attracted much attention, particularly in the fields of robot motion planning and safety- and time-critical control. In particular, computation of minimum norm control input via a quadratic program (QP), satisfying certain conditions on forward invariance of a safe set and convergence to a required goal set, has become very popular since QPs, being convex optimization problem, can be solved very efficiently. Here, safety and convergence requirements can be formulated as linear inequalities using the notion of control barrier function (CBF) and control Lyapunov function (CLF), respectively. CBF is used to ensure that system trajectories do not leave a zero sub-level set of a barrier function, rendering this set forward invariant. Furthermore, input constraints, that are inevitable in real-world problems, can be incorporated in a QP formulation via linear inequalities, leading to realizable control synthesis. The notion of CLF requires the system trajectories to reach a zero sub-level set of a Lyapunov function asymptotically, thus, naturally motivating the concept of fixed-time CLF (FxT-CLF), requiring that the same is achieved within a fixed amount of time. Combining FxT-CLF and CBF in a QP results in an effective control synthesis technique guaranteeing both safety and fixed-time convergence under input constraints. This, along with the fact that QPs can be solved very efficiently for real-time implementation, motivates the study of QP based control synthesis techniques in this dissertation.

There is a variety of practical examples where certain stability properties cannot be achieved using a continuous feedback controller; for instance, the authors in [3] make their case for the well-studied pendulum on a cart problem. Many control-theoretic examples have been proposed where switched controller systems can provide stability and performance guarantees; see e.g. [4–6]. Thus, the design and analysis of *hybrid* controllers, leading to hybrid closed-loop dynamics, become essential. In addition, hybrid systems are capable of modeling a large class of complex dynamical systems, e.g. walking bipedal robots [7, 8] and gear-shift in automated vehicles [9]. Leveraging a *common* Lyapunov

function, restrictive conditions for FTS have been studied in past, requiring, in part, that each of the subsystems of the hybrid system is FTS in itself. A *multiple* Lyapunov functions based approach lifts this restriction and allows the system to have unstable subsystems, and thus, such an approach is very important from a practical point of view, where unstable subsystems arising from various reasons, e.g. presence of an unobservable or an uncontrollable subsystem, are inevitable. Motivated from this, this dissertation studies the notion of FTS in the context of hybrid and switched dynamical systems.

Finally, exploring connections and applications of the theory of FTS and FxTS to other domains can give new insights on just how useful these stability notions are from a practical point of view. Continuous-time optimization is currently an active field of research in optimization theory; prior work in this area has yielded useful insights and elegant methods for proving stability and convergence properties of the optimization algorithms. Development of FxTS schemes for convex optimization problems can lead to the fast computation of the optimal solutions, advancing the field of optimization-based control synthesis one step further in the direction of real-time implementability. This motivates the study of FxTS gradient flows in this dissertation to solve a class of convex optimization problems.

Though the theory presented in this dissertation treats continuous-time dynamics, the discrete-time implementation manifests the applicability of the proposed methods in practice. The study of discretization methods that preserve the finite- and fixed-time convergence behavior of the continuous-time dynamical systems upon discretization is an active field of research. In particular, whether there exists a discretization scheme for FTS and FxTS dynamical systems such that the resulting discrete dynamical system has a finite and fixed number of steps convergence, respectively, thus *preserving* the convergence rate, is an open problem. Recent work on rate-preserving schemes [10, 11] and *consistent-discretization* schemes [12, 13] for finite or fixed-time stable dynamical systems motivates the future work of studying discretization schemes for the proposed methods, which would guarantee convergence of the solutions in a finite or fixed number of steps for all initial conditions (see also, discussion in Sections 4.5 and 6.4).

1.2 Literature review

1.2.1 Robust multi-agent control design with finite-time stability

In recent years, the usability of unmanned aerial vehicles (UAVs) has increased due to availability and technology maturity; examples of applications include package transportation [14] and distributed sensing [15]. Large-scale problems make centralized algorithms

intractable with the number of agents, motivating the research in the field of distributed coordination and control. The problem of decentralized multi-agent motion planning, which mainly focuses on generating collision-free trajectories for multiple agents (e.g., UAVs) so that they reach preassigned goal locations under limited sensing, communication, and interaction capabilities has been studied by many researchers [16–18].

Numerous methodologies on distributed motion planning of multi-agent systems have appeared in recent years, with the most popular being (i) optimization-based techniques [19–21]; (ii) Lyapunov-based methods [22, 23]; (iii) Voronoi-based methods [24, 25]; (iv) graph search methods, e.g., A^* planning [26], and sampling-based methods (e.g., rapidly-exploring random tree (RRT)) [27,28]. The main issue with sampling-based or graph-based methods is scalability with the number of agents. The scalability issues can be circumvented by using Lyapunov-based methods, such as navigation fields or vector fields.

From a practical and robustness point of view, sensing uncertainties along with the case when only partial state measurements are available should be considered. In particular, while the state vector of a 6 degree-of-freedom UAV or an underwater vehicle consists of the pose (position and orientation) and the velocity vector, certain common localization sensors, e.g. GPS, Sonar, LiDAR, only measure a few of the states of the vehicle. Furthermore, these sensors are noisy, something that needs to be taken into account during the control design, and thus, the problem of designing an observer-based controller for robust full-state feedback arises. Another important aspect in multi-agent control design is the limited capabilities of the considered vehicles, in terms of limited sensing and communication radii. From the safety perspective, the agents must be able to avoid collisions with each other and with obstacles under these limitations. In [29], the authors consider a limited sensing radius for a pair of nonholonomic vehicles for cooperative and non-cooperative collision avoidance. In [30], the authors used potential functions for formation control and obstacle avoidance under limited sensing. In [31] (see also [32]), the authors design a centralized *supervisor* for collision avoidance in the presence of disturbances and uncontrolled vehicles. However, the work in [29–32] assumes complete knowledge of the states of the agents and no sensing uncertainties.

Ensuring certain levels of robustness against modeling uncertainties and external disturbances is of primary concern for real-world applications. Much work is done in the case of matched disturbances, i.e. when the control input and the disturbance enter the plant via the same channel. In [33], a stable uncertainty is assumed to be bounded in $\mathcal{H}_\infty$-norm by a *prior* given desired tolerance, and an observer-based controller is designed by using the algebraic Riccati equation. Related work considering bounded deterministic disturbances can be found in the design of finite-time consensus algorithms with matched

disturbances [34–36], mismatched disturbances [37], and the rotating consensus control with mixed model uncertainties and external disturbances [38].

Wind, modeled as a state disturbance, affects the position dynamics of the aerial vehicles. For most of the practical systems, such as fixed-wing (or rotary-wing) aircraft, the control inputs are the deflection of control surfaces and thrust (or the rotor speed), which take effect in the velocity dynamics of the vehicle. Hence, the study of systems with unmatched disturbance becomes significantly important. Nevertheless, there is only a little work in this field for the case of multi-agent systems: in [39], the authors assumed that the dynamics of the unmatched disturbance are known, and leverage this knowledge to design a disturbance observer. In [40], the authors show input-to-state stability via full-state feedback for the cases when 1) the disturbance is matched and is uniformly bounded, and 2) the disturbance is unmatched, is uniformly bounded as well as *integral-bounded*. In [41] and [42], the authors assumed that the disturbance is at least twice continuously differentiable for a second-order system and that all the derivatives of the disturbance are bounded with known bounds. While under these *strong* assumptions, the aforementioned work showed that the effect of the disturbance can be nullified, it is worth noting that one cannot always assume such smoothness or vanishing properties for wind disturbances. In this dissertation, a distributed robust observer-based controller is developed that addresses most of these drawbacks by considering a limited and erroneous sensing model, partial erroneous state measurements, wind disturbances, and dynamical obstacles.

It is generally desired that the agents achieve their tasks of reaching given locations in a finite time. For example, a UAV tasked with a package delivery must reach its destination within the desired time. In contrast to AS, which pertains to convergence as time goes to infinity, FTS is a concept that requires the convergence of solutions in finite time. In the seminal work [2], the authors introduce necessary and sufficient conditions in terms of a Lyapunov function for the equilibrium of a continuous-time, autonomous system to exhibit FTS. Finite-time controllers have been used for applications such as consensus or formation control in [43–45], but without consideration of safety or collision avoidance. There is a large body of literature on collision avoidance schemes along with finite-time convergence, e.g. [46–50]. The work in [46–48] considers finite-time consensus with inter-agent collision avoidance, whereas [49] incorporates collision avoidance in finite-time flocking of *Cucker-Smale* agents. [50] considers the problem of parallel formation (or, velocity alignment) in a finite time in a stationary-obstacle environment. Although the aforementioned work considers inter-agent collision avoidance or obstacle avoidance, none of them considers external disturbances or uncertainties in the state measurements. [51] considers bounded, matched disturbance, and presents a method of achieving robust finite-

time consensus for multi-agent systems. The work in [35, 36] consider bounded, matched disturbances, whereas [52] considers unknown nonlinearities in the dynamics, and design protocols to achieve consensus in a *fixed time*. However, [35, 36, 51, 52] do not consider collision avoidance. The work in this dissertation addresses the problem of finite-time convergence in distributed multi-agent control while guaranteeing inter-agent safety as well as collision avoidance with dynamic obstacles under the presence of state disturbances and measurement uncertainties.

1.2.2 Control synthesis via quadratic programming

Forward invariance of a safe set in addition to convergence to a desired set (or point) can be achieved via a combination of CLF and CBF [53–55]. In recent years, online optimization, particularly, QP based approaches have gained popularity for control synthesis since the convergence requirements encoded via CLFs and safety requirements via CBFs can be incorporated together in a QP formulation; see [53, 56–58]. Other notions such as exponential CBFs (see [59, 60] and zeroing control barrier function (ZCBF)s (see [53, 54]) can also be used in a QP formulation for forward invariance. These methods are suitable for real-time implementation as QPs can be solved efficiently [23, 57, 61].

Input constraints, such as actuator saturation, are inevitable in practice. Since a limited control input can affect the region of convergence, addressing spatiotemporal and input constraints simultaneously is a challenging control problem. Most of the aforementioned contributions address control design that achieves convergence to the desired goal set (or point), but without explicitly considering control input constraints. Such constraints are considered in [53], where performance and safety objectives are represented using CLFs and CBFs, respectively, along with control input constraints in a QP. More recently, the authors in [57] address the issue of sampling effects and additive bounded disturbances in guaranteeing safety using robust control barrier functions; more specifically, they formulate a QP to design a zero-order hold control input for a mechanical system in the presence of component-wise input constraints.

Most of the aforementioned work imposes asymptotic or exponential convergence requirements through a CLF. The authors of [62] formulate a QP for finite-time convergence to the desired set, yet without considering input constraints. This limitation is removed in [63], where the authors consider a QP formulation incorporating input constraints as well, in addition to the safety and convergence constraints. The authors in [64] use CBFs to encode signal-temporal logic (STL) based specifications, involving reaching a goal set within a finite time, and formulate a QP to compute the control input. While FTS leads

to convergence within a finite time, this time of convergence can grow unbounded as the initial conditions go farther away from the equilibrium point. In order to meet temporal requirements, it is required that convergence is achieved within a user-defined time. A stronger notion termed as FxTS, introduced in [65] where the time of convergence does not depend upon the initial conditions, can be used to address such temporal constraints. The concept of FxTS has been studied widely in the past decade; the authors in [66, 67] discuss necessary and sufficient conditions for FxTS; [68, 69] present FxTS results from a sliding-mode perspective (see also [70–72] for certain examples of applications of FxTS theory in control and estimation problems). The work in this dissertation combines the notion of CLF and FxTS to introduce a class of functions termed as FxT-CLF, thus guaranteeing convergence within a fixed time.

Encoding safety in the presence of disturbances can be done using robust CBFs [57, 58, 73]. While the work in [57, 58, 73] considers bounded additive disturbance in the system dynamics, it is generally assumed that the system states are available without errors. In their majority, earlier work in the literature on multi-agent collision avoidance using CBFs [21, 23, 29, 30] assumes perfect knowledge of the states of the agents and no sensing uncertainties. The work in this dissertation uses a combination of robust CBFs and robust FxT-CLFs in a QP to compute a controller that guarantees robust safety and fixed-time convergence in the presence of additive disturbance, state-estimation error, and input constraints.

1.2.3 Finite-time stabilization of hybrid systems

The stability of the equilibrium point or equilibrium set of hybrid systems has been studied extensively in the literature; for an overview of the theory of hybrid systems, i.e., on solution concepts and the notion of stability, the interested readers are referred to [74, 75]. Switched systems are a special class of hybrid systems, where only the system dynamics are allowed to switch without discrete jumps in the system states. Stability of switched systems is typically studied using either a *common* Lyapunov function, or *multiple* Lyapunov functions. In [76], the author introduces the concept of multiple Lyapunov functions to analyze the stability of switched systems; since then, a lot of work has been done on the stability of switched systems using multiple Lyapunov functions, see e.g., [77, 78]. In [77], the authors relax the non-increasing condition on the Lyapunov functions used in [76], by introducing the notion of generalized Lyapunov functions. They present necessary and sufficient conditions for Lyapunov and AS of switched systems under arbitrary switching.

Inspired by the results in [76, 77], this dissertation studies conditions for FTS of a class

of hybrid systems, using multiple generalized Lyapunov functions. FTS of switched and hybrid systems have gained popularity in the last few years. The authors in [79] consider the problem of designing a controller for a linear switched system under delay and external disturbance with finite-time convergence. In [80], the authors design a hybrid observer and show finite-time convergence in the presence of unknown, constant bias. In [81], the authors study FTS of nonlinear impulsive dynamical systems, and present sufficient conditions to guarantee FTS. The work in [80, 81] considers discrete jumps in the states of a continuous dynamical system, i.e., in a system one model for the continuous dynamics, and one model for the discrete dynamics. The authors in [82] present conditions in terms of a common Lyapunov function for FTS of hybrid systems. They require the value of the Lyapunov function to be decreasing during the continuous flow and non-increasing at the discrete jumps. The authors in [83] design an FTS state-observer for switched systems via a sliding-mode technique under the assumption that each subsystem is observable on a domain. More recently, the authors in [84] study FTS of homogeneous switched systems by introducing the concept of hybrid homogeneous degree and relating negative homogeneity with FTS. They consider switched systems with an assumption that each subsystem possesses a homogeneous Lyapunov function, and that the switching-intervals are constant. In [85], the authors consider systems in the strict-feedback form with positive powers and design a controller as well as a switching law so that the closed-loop system is FTS. In [86], the authors design an FTS observer for switched systems with unknown inputs. They assume that each linear subsystem is *strongly* observable and that the first switching occurs after an *a priori* known time. In contrast, the work in this dissertation does not assume that the subsystems are homogeneous or in the strict feedback form, and studies conditions in terms of multiple Lyapunov functions for FTS of the origin for a general class of hybrid and switched systems.

1.2.4 Continuous-time optimization

The study of continuous-time optimization methods has been a very important part of the optimization theory from very early days [87]. Research in this area continues to this day intending to develop and study differential equations that model the commonly used discrete-time optimization algorithms [10, 88]. Establishing connections between ordinary differential equations (ODEs) and optimization has been an active topic of interest, see [88–90] and the references therein. The theory of ODEs offers useful insights into optimization theory and the corresponding techniques [88]. As noted by the authors in [91], the continuous-time perspective of optimization problems provides simple and elegant proofs

for the convergence of solutions to the equilibrium points using Lyapunov stability theory.

It is well known that the strict minima of a locally convex function $f : \mathbb{R}^n \to \mathbb{R}$ are stable equilibria of the gradient flow (GF) dynamics $\dot{x} = -\nabla f(x)$, and that, if the sub-level sets of f are compact, then the trajectories converge asymptotically to the set of critical points of f. In recent years, GFs have been employed in a wide range of applications, including image processing [92] and motion planning [93]. There is a plethora of work on asymptotic convergence analysis of GF, for an overview, see [10]. Recent work, for example, [88], has focused on exponential stability of the GF based methods. The *strong* or *strict convexity* of the objective function is a standard assumption for exponential stability. As shown in [94], the condition can be relaxed by assuming that the objective function satisfies the Polyak-Łojasiewicz (PL) inequality, i.e., the objective function is *gradient dominated*. In [95], the authors develop cubic regularization of Newton's method with super-linear convergence rate. Another set of problems where GF is used is the *saddle-point dynamics* for *min-max problems*, where a multivariate function needs to be minimized over one set of variables and maximized over another set of variables. Saddle-point dynamics and its variations have been used extensively in the design and analysis of distributed feedback controllers [96] and optimization algorithms in several domains, including active power loss minimization [97], network optimization [98], and zero-sum games [99] (see [100] for a detailed presentation on various applications where saddle-point dynamics naturally arise).

It is worth noticing that while there is a lot of work on continuous-time optimization, most of it addresses asymptotic or exponential convergence of the solutions to the optimal point, i.e., convergence as time tends to infinity. In [93], the authors introduce normalized gradient flows to show finite-time convergence of the solutions to the optimal point. The authors in [101] consider convex optimization problems with equality constraints under strong convexity of the objective function and design discontinuous dynamics that converge to the optimal solution in finite time. Finite-time distributed optimization is studied in [102, 103], where the authors assume very specific initial conditions, such that the sum of the gradient of the objective functions is zero. In [68], the authors design a sliding-mode-based technique for distributed optimization with fixed-time convergence guarantees assuming that the objective functions are strongly convex. In [104], a method of finding the optimal solution of a linear program in a fixed time is proposed. In [105] and [106], the authors design finite-time converging schemes for distributed optimization where the objective function is a sum of quadratic functions and strictly convex functions, respectively.

In this dissertation, modified GF schemes are designed for unconstrained and constrained convex optimization problems, as well as for min-max problems, with fixed-time

convergence guarantees. In [102, 103], the authors assume that the Hessian of the objective function is Lipschitz continuous. This assumption as well as the strong-convexity assumption in [68, 101] are relaxed in this work, and it is shown that fixed-time convergence can be guaranteed for a larger class of problems where the objective function satisfies the PL inequality. In contrast to [93, 104], the work in this dissertation studies convex optimization problems with linear equality constraints and proposes a novel method to obtain the optimal point in fixed time under certain conditions on the smoothness and convexity of the objective function.

1.3 Contributions and outline

This dissertation advances the theoretical results in the field of finite- and fixed-time stability with applications in provably safe control synthesis for multi-task problems under input constraints and convex optimization problems. The following is a summary of the contributions of this research:

- Chapter 2 presents a framework for multi-agent motion planning with finite-time stability guarantees under additive disturbances and partial state information. In this chapter, agents modeled via double-integrators are considered and a finite-time observer-based robust controller is designed with provable safety with respect to other agents and dynamic obstacles. It is also shown that under the effect of the carefully designed vector field, there is no deadlock. The results in this chapter are based on the work in [107].

- Under the notion of FTS as studied in Chapter 2, the time of convergence can grow unbounded. For the satisfaction of temporal constraints, the notion of FxTS can be used in control synthesis. However, it is not possible to guarantee FxTS in the presence of input constraints. Chapter 3 presents two new results on FxTS of dynamical systems relaxing the prior conditions so that the modified conditions can be used to guarantee FxTS for control systems with input constraints. The relationship between the time of convergence, the domain of attraction, and the input bounds are established. The proposed results also establish the robustness of FxTS dynamical systems with respect to a class of additive disturbances. The results in this chapter are partly based on the work in [108, 109].

- In contrast to Chapter 2 where systems modeled under double-integrator dynamics are studied, Chapter 4 studies the problem of control synthesis for a general class of

nonlinear control affine systems and presents a general control synthesis framework for safety-critical systems. Leveraging the new FxTS conditions from Chapter 3, a QP is proposed with guaranteed feasibility such that the control input defined as a solution of the QP solves a multi-task problem involving safety and fixed-time convergence under input constraints. A framework for handling a class of additive disturbances and measurement errors is proposed using the notion of robust CLFs and robust CBFs. The results in this chapter are partly based on the work in [110–112].

- Chapter 5 presents novel multiple-Lyapunov function based FTS conditions for a class of hybrid and switched systems. Utilizing the proposed conditions, an FTS switching law design procedure is proposed and an FTS observer-based controller is designed for a class of switched linear systems with only one controllable and observable mode. The results in this chapter are based on the work in [113, 114].

- Chapter 6 presents novel FxTS gradient flows for a class of convex optimization problems including constrained and unconstrained optimization problems as well as min-max problems. Assumptions on strong convexity are relaxed and novel FxTS gradient flows are proposed such that the resulting system trajectories reach the optimal point of the underlying optimization problem within a fixed amount of time. The results in this chapter are partly based on the work in [115].

Finally, Chapter 7 presents the conclusions of the dissertation and directions for future research, and lists of the other related work by the author which are not discussed in detail in the dissertation.

CHAPTER 2

Finite-time Multi-Agent Control Design

In this chapter, the problem of safe trajectory generation for multi-rotor type UAVs is considered. Specifically, the considered problem seeks to generate safe trajectories from all initial conditions to a goal location for double integrator vehicles with limited, erroneous sensing capabilities, in the presence of unknown wind disturbance and moving obstacles.

First, a full-state feedback controller using attractive and repulsive vector fields is designed in Section 2.1. The agents are modeled using double integrator dynamics for 2-D (or planar) motion of multi-rotor aircraft. This is motivated by the problem of safe trajectory generation of multi-rotor aircraft flying in a low-altitude urban airfield with restrictions on the airspace available for such operations, particularly in terms of altitude restrictions. With the anticipated increase in the number of vehicles in the airspace, it might be desired to have altitude bands designated to different classes of UAVs depending upon their capabilities. Thus, it is of interest to design safe trajectories of aircraft with fixed altitude constraints. The problem of avoiding a form of deadlocks is also addressed by properly defining the direction of motion for the agents when the vector field vanishes so that *global* convergence is guaranteed. Furthermore, the theory of FTS is utilized so that the agents accomplish the assigned tasks of reaching their respective goal locations in a finite time.

Then, a general class of unmatched state disturbances is considered in the agents' dynamics to account for wind disturbances in Section 2.2. It is also assumed that only position measurements are available. An FTS state-feedback control law is designed that uses state estimates derived from an FTS state-estimator. A limited sensing model is assumed that is erroneous, i.e., the agents can sense the position and the velocity of their neighboring agents within a bounded error.

Finally, Section 2.3 studies the motion of *class-A* or controlled agents is considered in a dynamic obstacle environment induced by *class-B* or uncontrolled agents (or simply, dynamic obstacles), as defined in [116]. The dynamic obstacles do not cooperate to

avoid collisions. A robust controller is designed that guarantees inter-agent safety and convergence of each agent to their respective goal locations within a finite time even in the presence of dynamic obstacles. Two simulation case studies are presented in Section 2.4, demonstrating the efficacy of the proposed method. The results in this chapter are based on [107].

The following notation is frequently used in this chapter:

$\boldsymbol{r}_i$	Position of the agent i
$\boldsymbol{u}_i$	Velocity of agent i
$\boldsymbol{a}_i$	Acceleration of agent i
$\boldsymbol{r}_{gi}$	Desired goal location of agent i
$\boldsymbol{w}$	Wind disturbance
$\boldsymbol{w}_{av}$	Mean value of the wind disturbance
δ_{av}	Variation of the wind disturbance from the mean value
d_{ij}	Distance between agent i and j
d_m	Minimum safety distance
R_c	Sensing radius of each agent
δ_e	Estimation error
$\boldsymbol{r}_{js}^i$	Position of the agent j as sensed by agent i
$\boldsymbol{u}_{js}^i$	Velocity of agent j as sensed by agent i
ϵ_s	Sensing error
$\mathbf{F}_i$	Nominal vector field for agent i
γ_i	Desired direction of motion for agent i
u_{id}	Desired speed for agent i
$\hat{\boldsymbol{r}}_i$	Estimated position of the agent i
$\hat{\boldsymbol{u}}_i$	Estimated velocity of agent i
$\hat{\boldsymbol{u}}_{id}$	Desired estimated velocity for the estimated agent i
$\hat{d}_{ij}$	Distance between agent i and j as estimated by agent i
$\mathbb{R}$	Set of reals
$\mathbb{R}_+$	Set of non-negative reals
$\|\cdot\|$	Euclidean norm (2-norm) of $(\cdot)$
$\angle(\boldsymbol{x})$	Orientation of the vector $\boldsymbol{x}$
$\mathbf{0}$	Zero vector
$\emptyset$	Empty set

2.1 Modeling and problem statement

Consider N identical agents $i \in \{1, \ldots, N\}$, that are assigned to move to goal locations of position coordinates $\boldsymbol{r}_{gi} = \begin{bmatrix} x_{gi} & y_{gi} \end{bmatrix}^T$ while avoiding collisions, i.e., for all agents $i \neq j$, $\|\boldsymbol{r}_i(t) - \boldsymbol{r}_j(t)\| \geq d_m$ for all $t \geq 0$, where d_m is a user-defined safety distance. Each agent i is assumed to be a multi-rotor aircraft whose equations of motion for 2-D planar motion are approximated via double integrator dynamics. The following dynamics model the motion of the agents:

$$\dot{\boldsymbol{r}}_i(t) = \boldsymbol{u}_i(t) + \boldsymbol{w}(\boldsymbol{r}_i(t), t), \tag{2.1a}$$

$$\dot{\boldsymbol{u}}_i(t) = \boldsymbol{a}_i(t), \tag{2.1b}$$

$$\boldsymbol{y}_i(t) = \boldsymbol{r}_i(t), \tag{2.1c}$$

where $\boldsymbol{r}_i(t) = \begin{bmatrix} x_i(t) & y_i(t) \end{bmatrix}^T$ is the position vector of agent i, $\boldsymbol{y}_i(t)$ is the output map of the system consisting of the position of agent i, $\boldsymbol{u}_i(t) = \begin{bmatrix} u_{ix}(t) & u_{iy}(t) \end{bmatrix}^T$ is the velocity vector comprising the linear velocities of the agent i and $\boldsymbol{a}_i(t) = \begin{bmatrix} a_{ix}(t) & a_{iy}(t) \end{bmatrix}^T$ is the acceleration input to agent i. The position r_i, the velocity u_i and the acceleration u_i, all are measured with respect to (w.r.t.) a global reference frame. The term $\boldsymbol{w}(\boldsymbol{r}_i, t) : \mathbb{R}^2 \times \mathbb{R}_+ \to \mathbb{R}^2$ is the unknown wind disturbance, which can vary in space and time. As can be seen from (2.1), the disturbance $\boldsymbol{w}(\boldsymbol{r}_i, t)$ is unmatched. The arguments $t, \boldsymbol{r}$ are dropped whenever clear from the context. The following assumption is made about the disturbance $\boldsymbol{w}$.

Assumption 2.1 (Boundedness of wind disturbance). *The norm of the wind disturbance is bounded as*

$$\|\boldsymbol{w}(\boldsymbol{r}, t) - \boldsymbol{w}_{av}\| \leq \delta_w \quad \forall (\boldsymbol{r}, t) \in \mathcal{D} \subseteq \mathbb{R}^2 \times \mathbb{R}_+ \tag{2.2}$$

where $\boldsymbol{w}_{av}$ is the average or mean value of the disturbance over the domain $\mathcal{D}$, with $\|\boldsymbol{w}_{av}\| < \infty$ and $\delta_w < \infty$ is the maximum deviation of the disturbance from the mean value. Furthermore, the parameters $\boldsymbol{w}_{av}$ and δ_w are known.

Remark 2.1. *It is assumed that the disturbance is bounded with a known bound and known mean value. This assumption on unmatched disturbance $\boldsymbol{w}(\boldsymbol{r}, t)$ is much less restrictive as compared to the following literature: (i) in [39], the authors assume that the dynamics of the disturbance are known; (ii) in [40], the authors assume that the disturbance is an*

element of $\mathcal{L}_\infty$; (iii) in [41], the authors assumed that the disturbance satisfies a stronger regularity assumption, i.e., it should be at least twice differentiable for double-integrator systems.

The main problem statement considered in this chapter is given as follows:

Problem 2.1. *For each agent $i \in \{1, 2, \ldots, N\}$, design an output feedback $\boldsymbol{u}_i = \boldsymbol{u}_i(\boldsymbol{y}_i)$ such that the closed-loop trajectories of (2.1) satisfy $\|\boldsymbol{r}_i(t) - \boldsymbol{r}_j(t)\| \geq d_m$ for all $t \geq 0$ and $\lim_{t \to T_i} \boldsymbol{r}_i(t) = \boldsymbol{r}_{gi}$ where $T_i < \infty$.*

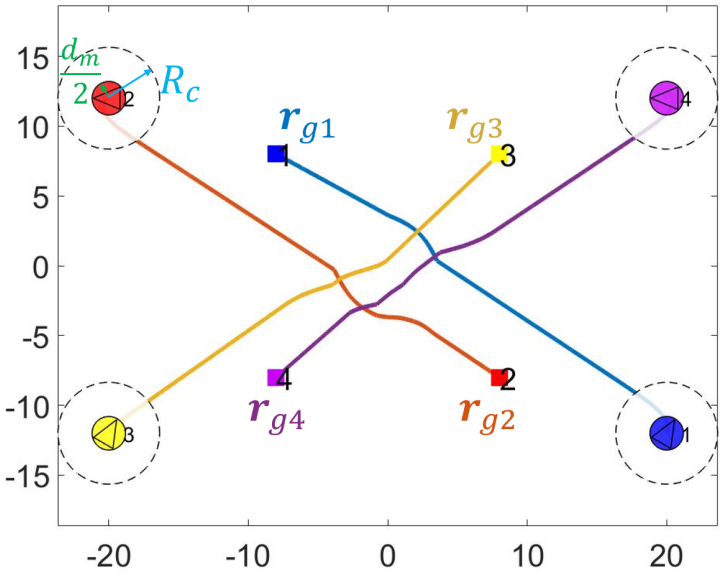

Figure 2.1: An example scenario consisting of 4 agents.

Each agent i is assumed to be a circular disk of radius $\frac{d_m}{2}$ centered at $\boldsymbol{r}_i = \begin{bmatrix} x_i & y_i \end{bmatrix}^T$ (so that the inter-agent safety is ensured when $\|\boldsymbol{r}_i - \boldsymbol{r}_j\| \geq d_m$), and has a circular sensing region $\mathcal{C}_i$ of radius R_c, denoted as $\mathcal{C}_i := \{\boldsymbol{r} \in \mathbb{R}^2 \mid \|\boldsymbol{r}_i - \boldsymbol{r}\| \leq R_c\}$ (see Figure 2.1). Denote by $\mathcal{N}_i := \{j \mid \boldsymbol{r}_j \in \mathcal{C}_i\}$ the set of agents that are in the sensing region of agent i, and call them neighbors of agent i. Agent i can sense the position and velocity of a neighbor $j \in \mathcal{N}_i$. To this end, the following assumption is made on the sensing error for each agent i.

Assumption 2.2 (Sensing model). *Agent i can sense the position (denoted as $\boldsymbol{r}_{js}^i$) and velocity (denoted as $\boldsymbol{u}_{js}^i$) of an agent $j \in \mathcal{N}_i$ within a bounded error ϵ_s, i.e., $\|\boldsymbol{r}_j(t) - \boldsymbol{r}_{js}^i(t)\| \leq \epsilon_s$ and $\|\boldsymbol{u}_j(t) - \boldsymbol{u}_{js}^i(t)\| \leq \epsilon_s$.*

The following assumption is made on the initial and goal location of the agents, and the sensing radius, R_c to ensure safety and convergence.

Assumption 2.3 (Initial and goal locations). *For each pair (i, j) such that $i \neq j$, $\|\boldsymbol{r}_i(0) - \boldsymbol{r}_j(0)\| > d_s$ and $\|\boldsymbol{r}_{gi} - \boldsymbol{r}_{gj}\| \geq 3R_c$, where d_s is the modified safety distance as defined in Theorem 2.5. Furthermore, the sensing radius satisfies $R_c > 2d_s$.*

2.1.1 Overview of finite-time stability

First, the required definitions and results on the notion of FTS are reviewed. Consider the system:

$$\dot{x}(t) = f(x(t)), \tag{2.3}$$

where $x \in \mathbb{R}^n$, $f : \mathcal{D} \to \mathbb{R}^n$ is continuous on an open neighborhood $\mathcal{D} \subseteq \mathbb{R}^n$ of the origin and $f(0) = 0$. Assume that the solution of (2.3) exists and is unique for all initial conditions $x(0) \in \mathbb{R}^n$. The following definition is adapted from [2].

Definition 2.1 (FTS). *The origin is an FTS equilibrium of (2.3) if it is Lyapunov stable and there exists a neighborhood $\mathcal{N}$ of the origin such that for all $x(0) \in \mathcal{N} \setminus \{0\}$, $\lim_{t \to T} x(t) = 0$, where $T = T(x(0)) < \infty$. The origin is a globally FTS equilibrium if $\mathcal{N} = \mathbb{R}^n$.*

Here, T is termed as the *settling-time* function. The authors also presented Lyapunov conditions for FTS. The following result is adapted from [2]:

Theorem 2.1 (Lyapunov conditions for FTS). *Suppose there exist a continuously differentiable, positive definite function $V : \mathcal{D} \to \mathbb{R}$ for (2.3), real numbers $\alpha > 0$ and $\gamma \in (0, 1)$, and an open neighborhood $\mathcal{V} \subseteq \mathcal{D} \subset \mathbb{R}^n$ of the origin such that its time derivative $\dot{V}(x)$ satisfies*

$$\dot{V}(x) \leq -\alpha\, V(x)^{\gamma},\ \forall x \in \mathcal{V} \setminus \{0\}. \tag{2.4}$$

Then the origin is an FTS equilibrium. Furthermore, the settling-time function T satisfies

$$T(x(0)) \leq \frac{V(x(0))^{1-\gamma}}{\alpha(1-\gamma)}, \forall x(0) \in \mathbb{R}^n. \tag{2.5}$$

Next the notion of homogeneity and its relation to FTS is reviewed from [117].

Definition 2.2 (Homogeneity). *A function $\boldsymbol{f} : \mathbb{R}^n \to \mathbb{R}^n$ is called a homogeneous function with degree d w.r.t. a dilation function $\Delta_\epsilon(\boldsymbol{x}) \coloneqq (\epsilon^{r_1} x_1, \epsilon^{r_2} x_2, \ldots, \epsilon^{r_n} x_n)$ where $r_i > 0$ and*

$\boldsymbol{x} = \begin{bmatrix} x_1 & x_2 & \dots & x_n \end{bmatrix}^T$, *if it holds that*

$$f_i(\epsilon^{r_1} x_1, \epsilon^{r_2} x_2, \dots, \epsilon^{r_n} x_n) = \epsilon^{d+r_i} f_i(x_1, x_2, \dots, x_n)$$

for each $i = \{1, 2, \dots, n\}$ *and for all* $\epsilon > 0$.

Theorem 2.2 (Homogeneity and FTS). *Suppose the vector field* $\boldsymbol{f}$ *is homogeneous with degree* d*. Then, the origin of the system* (2.3) *is FTS if and only if it is asymptotically stable and* $d < 0$.

Theorem 2.3 ([118])**.** *The origin of the system* $\dot{\boldsymbol{x}}(t) = -k\boldsymbol{x}\|\boldsymbol{x}\|^{\alpha-1}$ *is globally FTS for all* $k > 0$ *and* $0 < \alpha < 1$.

2.1.2 Vector field design

For each agent i, a vector-field-based feedback controller is designed. First, a vector field is defined that can steer the agents towards their goal locations while maintaining safe inter-agent distances. Then, a feedback law to follow this vector field is designed. Two categories of vector fields are sought to achieve the objectives of safety and convergence.

Attractive vector field: A radially attractive vector field that navigates agent i towards its goal location $\boldsymbol{r}_{gi}$ is defined as:

$$\mathbf{F}_{gi} := \begin{cases} -\frac{(\boldsymbol{r}_i - \boldsymbol{r}_{gi})}{\|\boldsymbol{r}_i - \boldsymbol{r}_{gi}\|}; & \boldsymbol{r}_i \neq \boldsymbol{r}_{gi}, \\ \mathbf{0}; & \boldsymbol{r}_i = \boldsymbol{r}_{gi}. \end{cases} \tag{2.6}$$

Vector field (2.6) is globally attractive towards $\boldsymbol{r}_{gi}$, which ensures that whenever agent i is conflict-free, i.e., $\mathcal{N}_i = \emptyset$, it moves towards its goal location. Note that at $\boldsymbol{r}_i = \boldsymbol{r}_{gi}$, the vector field $\mathbf{F}_{gi}$ is defined to be $\mathbf{0}$, so that it is defined everywhere on $\mathbb{R}^2$.

Repulsive vector field: In order to maintain a safe distance from agent $j \in \mathcal{N}_i$, agent i operates under a radially-repulsive field $\mathbf{F}_{ij}$ given by:

$$\mathbf{F}_{ij} := \begin{cases} \frac{\boldsymbol{r}_i - \boldsymbol{r}_j}{\|\boldsymbol{r}_i - \boldsymbol{r}_j\|}; & \boldsymbol{r}_i \neq \boldsymbol{r}_j, \\ \mathbf{0}; & \boldsymbol{r}_i = \boldsymbol{r}_j. \end{cases} \tag{2.7}$$

This is a radially repulsive field from the point $\boldsymbol{r}_j$, which makes agent i move away from all agents $j \in \mathcal{N}_i$.

2.1.3 Blending attractive and repulsive vector fields

Let $d_{ij} = \|\boldsymbol{r}_i - \boldsymbol{r}_j\|$ be the inter-agent distance between agent i and j. Since limited sensing radius R_c is assumed for agent i and it is required for the agent i to maintain a minimum separation d_m from all the other agents, the following *bump-function* $\sigma_{ij}(\cdot) : \mathbb{R}_+ \to [0, 1]$ is defined to blend the attractive and repulsive fields [116]:

$$\sigma_{ij}(d_{ij}) \coloneqq \begin{cases} 1, & d_m \leq d_{ij} < d_r; \\ a\ {d_{ij}}^3 + b\ {d_{ij}}^2 + c\ d_{ij} + d, & d_r \leq d_{ij} \leq R_c; \\ 0, & d_{ij} > R_c; \end{cases} \tag{2.8}$$

where d_r is a positive constant that satisfies $d_m < d_r < R_c$. The coefficients a, b, c, d have been computed as:

$$a = -\frac{2}{(d_r - R_c)^3}, b = \frac{3(d_r + R_c)}{(d_r - R_c)^3}, c = -\frac{6\ d_r R_c}{(d_r - R_c)^3}, d = \frac{{R_c}^2(3d_r - R_c)}{(d_r - R_c)^3},$$

so that the bump function σ_{ij} given as per (2.8) is a $\mathcal{C}^1$ function. One may now define the vector field for each agent i as:

$$\mathbf{F}_i \coloneqq \sum_{j \in \mathcal{N}_i} \sigma_{ij} \mathbf{F}_{ij} + \prod_j (1 - \sigma_{ij}) \mathbf{F}_{gi}. \tag{2.9}$$

The blending of the vector fields according to (2.9) means that whenever agent i is far away from all the other agents, i.e., $d_{ij} > R_c$ for all j, then only the globally attractive vector field is active, whereas if there are other agents in its vicinity, the net vector field is a weighted average of the attractive field $\mathbf{F}_{gi}$ and the repulsive field $\mathbf{F}_{ij}$, and, in the case when there is an agent j very close to the agent i, i.e., $d_{ij} < d_r$, then only the repulsive vector field $\mathbf{F}_{ij}$ is active.

The controller objective is to design the control inputs $\boldsymbol{a}_i$ for each agent i, so that the motion of each agent i is along the vector field $\mathbf{F}_i$. To this end, a backstepping approach is used where first, a desired velocity $\boldsymbol{u}_{id}$ to be tracked is designed, and then, the controller $\boldsymbol{a}_i$ is designed so that the desired velocity can be tracked. The direction $\angle \boldsymbol{u}_{id}$ along (2.9) and magnitude $\|\boldsymbol{u}_{id}\|$ of the desired velocity $\boldsymbol{u}_{id}$ are designed separately. The desired direction of motion of agent i is set to be:

$$\gamma_i \coloneqq \begin{cases} \tan^{-1}\left(\frac{\mathbf{F}_{iy}}{\mathbf{F}_{ix}}\right), & \|\mathbf{F}_i\| > 0; \\ \gamma_i^0, & \|\mathbf{F}_i\| = 0, \end{cases} \tag{2.10}$$

where $\gamma_i^0 = \tan^{-1}\left(\frac{x_i - x_{gi}}{-(y_i - y_{gi})}\right)$. Note that $\tan^{-1}\left(\frac{x_i - x_{gi}}{-(y_i - y_{gi})}\right)$ is the orientation of the vector perpendicular to the vector $\boldsymbol{r}_i - \boldsymbol{r}_{gi}$ pointing to the direction at an angle of $-\frac{pi}{2}$ from the vector $\boldsymbol{r}_i - \boldsymbol{r}_{gi}$. This desired direction for the case when $\|\mathbf{F}_i\| = 0$ is defined in such a manner so that there is no deadlock, as showed in the following lemma.

Lemma 2.1 (Deadlock resolution). *If the direction of the motion of each agent i is along γ_i given by (2.10), then the agents resolve their deadlocks, i.e., the agents do not stay indefinitely at a location other than their goal location $\boldsymbol{r}_{gi}$ for all times.*

The proof is provided in Appendix A.1. Thus, it is shown that the agents do not converge in a deadlock while moving along their respective vector fields. Next, a desired velocity command with magnitude u_{id} and direction $\boldsymbol{u}_{idn} = \begin{bmatrix}\cos\gamma_i & \sin\gamma_i\end{bmatrix}^T$ is designed for each agent i, which tracks the vector field (2.9), so that the trajectories of the agent i are collision-free and reach the goal location $\boldsymbol{r}_{gi}$. Then, the error between the actual velocity $\boldsymbol{u}_i$ and the desired linear velocity $\boldsymbol{u}_{id}$ of agent i is considered in designing an acceleration controller $\boldsymbol{a}_i$ that drives this error to zero in finite-time. It is ensured that the safety is maintained by enlarging the safety distance d_m by the maximum transient error induced by the velocity error $\boldsymbol{u}_i - \boldsymbol{u}_{id}$.

2.1.4 State feedback design

In order to design the desired velocity command $\boldsymbol{u}_{id}$ that generates collision-free position trajectories for the kinematic subsystem (2.1a) of each agent i, the control design in [22] is used. In [119], the desired velocity vector is defined as $\boldsymbol{u}_{id} = u_{id}\boldsymbol{u}_{idn}$ where $\boldsymbol{u}_{idn} = \begin{bmatrix}\cos\gamma_i & \sin\gamma_i\end{bmatrix}^T$ and u_{id} of agent i is defined as:

$$u_{id} := \begin{cases} \frac{1}{\mu}\log\left(\left(\sum_{j\in\mathcal{N}_i|J_i<0} e^{-\mu\, u_{i|j}}\right)^{-1} + 1\right), & d_m \le d_{ij} \le R_c; \\ u_{ic}, & d_{ij} > R_c; \end{cases} \tag{2.11}$$

where $u_{i|j}$ denotes the velocity adjustment mechanism of agent i w.r.t. agent j, defined as:

$$u_{i|j} := u_{ic}\frac{d_{ij} - d_m}{R_c - d_m} + \varepsilon_i u_{is|j}\frac{R_c - d_{ij}}{R_c - d_m}, \tag{2.12}$$

with the terms in (2.12) defined as:

$$u_{ic}(\boldsymbol{r}_i) \coloneqq \begin{cases} k_{i1} \tanh\left(\|\boldsymbol{r}_i - \boldsymbol{r}_{gi}\|\right), & \|\boldsymbol{r}_i - \boldsymbol{r}_{gi}\| > R_1; \\ k_{i2}\|\boldsymbol{r}_i - \boldsymbol{r}_{gi}\|^{\alpha_r}, & \|\boldsymbol{r}_i - \boldsymbol{r}_{gi}\| \leq R_1; \end{cases}, \tag{2.13a}$$

$$u_{is|j} \coloneqq u_{jd} \frac{\boldsymbol{r}_{ji}{}^T \boldsymbol{u}_{jdn}}{\boldsymbol{r}_{ji}{}^T \boldsymbol{u}_{idn}}, \quad J_i \coloneqq \boldsymbol{r}_{ji}{}^T \boldsymbol{u}_{idn}, \quad \boldsymbol{r}_{ji} \coloneqq \boldsymbol{r}_i - \boldsymbol{r}_j, \tag{2.13b}$$

where $0 < \alpha_r, \varepsilon_i < 1$ and $\mu \gg 1$ is a large positive number. Note that the term u_{ic} given in (2.13a) is defined differently from [116, 119], so that finite-time convergence can be guaranteed unlike the prior work where asymptotic convergence is guaranteed. Gains k_{i1}, k_{i2} and parameter R_1 are chosen such that u_{ic} is continuously differentiable for all $\boldsymbol{r}_i$. Hence, enforcing continuity of u_{ic} and its derivative when $\|\boldsymbol{r}_i - \boldsymbol{r}_{gi}\| = R_1$, it holds that:

$$k_{i1} \tanh R_1 = k_{i2} R_1^{\alpha_r} \quad \text{and} \quad k_{i1}(1 - \tanh^2 R_1) = \alpha_r k_{i2} R_1^{\alpha_r - 1}. \tag{2.14}$$

From the above equations, R_1 can be obtained as the solution of

$$(1 - \tanh^2 R_1) = \alpha_r \frac{\tanh(R_1)}{R_1}. \tag{2.15}$$

The above expression has a unique positive solution R_1 for all $0 < \alpha_r < 1$. For a given positive gain $k_{i1} > 0$, k_{i2} is given as $k_{i2} = k_{i1} \frac{\tanh R_1}{R_1^{\alpha_r}}$. The term $\|\boldsymbol{r}_i - \boldsymbol{r}_{gi}\|^{\alpha_r}$ ensures finite-time convergence (Theorem 2.6). The definition of u_{ic} is (2.13a) ensures that the magnitude of the desired speed u_{ic} is bounded for all $\boldsymbol{r}_i$.

Remark 2.2. *The expression given in* (2.11) *is a smooth approximation of the following function*

$$\max\left\{0, \min_{k \in \mathcal{N}_i | J_k < 0} u_{i|k}\right\}.$$

The min *function is approximated by*

$$g(a) \coloneqq -\frac{1}{\mu} \log(\sum_i e^{-\mu a_i}),$$

with $\mu \gg 1$ *where* $a = \begin{bmatrix} a_1 & a_2 & \cdots a_l \end{bmatrix}$. *Using the smooth approximation for* max *function*

$$h(b) \coloneqq \frac{1}{\mu} \log(\sum_i e^{\mu b_i}),$$

for $b = \begin{bmatrix} g(a) & 0 \end{bmatrix}$, *it follows that* $h(b) = \frac{1}{\mu} \log(e^{\mu g(a)} + 1)$. *Using the fact that* $e^{\mu g(a)} =$

$e^{-\log(\sum_i e^{-\mu a_i})} = (\sum_i e^{-\mu a_i})^{-1}$, *the expression as* (2.11) *can be obtained.*

Remark 2.3. *Note that the desired velocity in* (2.11) *assumes that agent* i *has perfect knowledge of its neighbor* j*'s position and velocity. This assumption is relaxed in the robust control design in Section 2.2. Also, the protocol defined in* (2.11) *is not used directly but is used as a base to design for the robust controller design. The equation* (2.11) *is included here, taken directly from [116], for the sake of completeness.*

With this desired velocity in hand, the acceleration command is chosen to be

$$\boldsymbol{a}_i \coloneqq \dot{\boldsymbol{u}}_{id} - \lambda_i(\boldsymbol{u}_i - \boldsymbol{u}_{id})\|\boldsymbol{u}_i - \boldsymbol{u}_{id}\|^{\alpha-1}, \tag{2.16}$$

where $\lambda_i > 0$, $0 < \alpha < 1$ so that the velocity error $\boldsymbol{u}_i - \boldsymbol{u}_{id}$ converges to $\mathbf{0}$ in finite time [1]. Since in this work, it is assumed that only the position of agent i is measured, first, a state-estimator is designed in order to implement a full-state feedback. Then, the desired velocity command (denoted as $\hat{\boldsymbol{u}}_{id}$) is redesigned for the estimator dynamics so that it is robust w.r.t. the state-disturbance $\boldsymbol{w}(\boldsymbol{r}, t)$ and sensing uncertainties.

2.2 Robust Control Design

2.2.1 Finite-time stable state-estimator

The feedback control law (2.16) requires full-state information. Since only partial state is available via the system output, an FTS state-estimator inspired from [120] is used, given by:

$$\dot{\hat{\boldsymbol{r}}}_i = \hat{\boldsymbol{u}}_i + k_{i3}(\boldsymbol{y}_i - \hat{\boldsymbol{y}}_i)\|\boldsymbol{y}_i - \hat{\boldsymbol{y}}_i\|^{\alpha_1-1} + \boldsymbol{w}_{av} \tag{2.17a}$$

$$\dot{\hat{\boldsymbol{u}}}_i = \boldsymbol{a}_i + k_{i4}(\boldsymbol{y}_i - \hat{\boldsymbol{y}}_i)\|\boldsymbol{y}_i - \hat{\boldsymbol{y}}_i\|^{\alpha_2-1}, \tag{2.17b}$$

where $\hat{\boldsymbol{y}}_i = \hat{\boldsymbol{r}}_i$ is the estimated output, $0 < \alpha_1, \alpha_2 < 1$, and $k_{i3}, k_{i4} > 0$. Define the error terms $\boldsymbol{r}_{ie} \coloneqq \boldsymbol{r}_i - \hat{\boldsymbol{r}}_i = \boldsymbol{y}_i - \hat{\boldsymbol{y}}_i$ and $\boldsymbol{u}_{ie} \coloneqq \boldsymbol{u}_i - \hat{\boldsymbol{u}}_i$, so that from (2.1) and (2.17), it follows that:

$$\dot{\boldsymbol{r}}_{ie} = \boldsymbol{u}_{ie} - k_{i3}\boldsymbol{r}_{ie}\|\boldsymbol{r}_{ie}\|^{\alpha_1-1} + \boldsymbol{w}(\boldsymbol{r}_i, t) - \boldsymbol{w}_{av} \tag{2.18a}$$

$$\dot{\boldsymbol{u}}_{ie} = -k_{i4}\boldsymbol{r}_{ie}\|\boldsymbol{r}_{ie}\|^{\alpha_2-1}. \tag{2.18b}$$

[1] This can be verified using $\boldsymbol{x} = \boldsymbol{u}_i - \boldsymbol{u}_{id}$ in Theorem 2.3.

In order to show the finite-time convergence of the estimation error, the following results are needed:

Lemma 2.2 (AS of error dynamics). *If $\boldsymbol{w}(\boldsymbol{r}_i, t) \equiv \mathbf{0}$, the origin is an asymptotically stable equilibrium of the system* (2.18).

Proof. Note that $\boldsymbol{w}(\boldsymbol{r}_i, t) \equiv \mathbf{0}$ implies that there is no external disturbance and the system (2.18) is autonomous. Choose the candidate Lyapunov function

$$V(\boldsymbol{r}_{ie}, \boldsymbol{u}_{ie}) \coloneqq \frac{k_{i4}}{1+\alpha_2}\|\boldsymbol{r}_{ie}\|^{1+\alpha_2} + \frac{1}{2}\|\boldsymbol{u}_{ie}\|^2,$$

which is a positive definite function. Taking its time derivative along the trajectories of (2.18), it follows that:

$$\begin{aligned}\dot{V}(\boldsymbol{r}_{ie}, \boldsymbol{u}_{ie}) &= k_{i4}\|\boldsymbol{r}_{ie}\|^{\alpha_2-1}\boldsymbol{r}_{ie}^T(\boldsymbol{u}_{ie} - k_{i3}\boldsymbol{r}_{ie}\|\boldsymbol{r}_{ie}\|^{\alpha_1-1}) + \boldsymbol{u}_{ie}^T(-k_{i4}\boldsymbol{r}_{ie}\|\boldsymbol{r}_{ie}\|^{\alpha_2-1}) \\ &= -k_{i3}k_{i4}\|\boldsymbol{r}_{ie}\|^{\alpha_1+\alpha_2} \leq 0.\end{aligned}$$

Now, since $\alpha_1 + \alpha_2 > 0$, $\dot{V}(\boldsymbol{r}_{ie}, \boldsymbol{u}_{ie}) = 0$ at $\boldsymbol{r}_{ie} \equiv \mathbf{0}$ for all $\boldsymbol{u}_{ie} \in \mathbb{R}^2$. Using LaSalle's invariance principle, it holds that the origin is the only point where the trajectories of the system (2.18) can identically stay. Hence, the origin is an asymptotically stable equilibrium of the system (2.18) when $\boldsymbol{w}(\boldsymbol{r}_i, t) = \mathbf{0}$. □

Lemma 2.3 (Homogeneity of error dynamics). *For $\boldsymbol{w}(\boldsymbol{r}_i, t) \equiv \mathbf{0}$ and $\alpha_1 = \alpha$, $\alpha_2 = 2\alpha - 1$, where $\frac{1}{2} < \alpha < 1$, the error dynamics* (2.18) *is homogeneous with degree of homogeneity $d = \alpha - 1 < 0$.*

Proof. Let $r_1 = 1$ and $r_2 = \alpha$, with $\frac{1}{2} < \alpha < 1$. With these parameters, define the dilation function $\Delta_\epsilon(\boldsymbol{r}, \boldsymbol{u}) = (\epsilon\boldsymbol{r}, \epsilon^\alpha\boldsymbol{u})$. Define the right hand side of (2.18) as $\boldsymbol{f}^{err}(\boldsymbol{r}_{ie}, \boldsymbol{u}_{ie}) = \begin{bmatrix} f_1^{err}(\boldsymbol{r}_{ie}, \boldsymbol{u}_{ie}) & f_2^{err}(\boldsymbol{r}_{ie}, \boldsymbol{u}_{ie}) \end{bmatrix}^T$. Now, for $\boldsymbol{w}(\boldsymbol{r}_i, t) = \mathbf{0}$, define $d \coloneqq \alpha - 1$ so that for all $\epsilon > 0$ it follows that:

$$\begin{aligned}f_1^{err}(\epsilon^{r_1}\boldsymbol{r}_{ie}, \epsilon^{r_2}\boldsymbol{u}_{ie}) &= \epsilon^{r_2}\boldsymbol{u}_e - k_{i3}\epsilon^{r_1\alpha_1}\boldsymbol{r}_{ie}\|\boldsymbol{r}_{ie}\|^{\alpha_1-1} = \epsilon^{d+r_1}f_1^{err}(\epsilon^{r_1}\boldsymbol{r}_{ie}, \epsilon^{r_2}\boldsymbol{u}_{ie}), \\ f_2^{err}(\epsilon^{r_1}\boldsymbol{r}_{ie}, \epsilon^{r_2}\boldsymbol{u}_{ie}) &= -k_{i4}\epsilon^{r_1\alpha_2}r_e\|\boldsymbol{r}_{ie}\|^{\alpha_2-1} = \epsilon^{d+r_2}f_2^{err}(\epsilon^{r_1}\boldsymbol{r}_{ie}, \epsilon^{r_2}\boldsymbol{u}_{ie}).\end{aligned}$$

Thus, from Definition 2.2, the error dynamics is homogeneous with degree $d = \alpha - 1 < 0$. □

From [117, Theorem 7.1], it holds that the origin is a finite-time stable equilibrium for (2.18) if $\boldsymbol{w}(\boldsymbol{r}_i, t) = \mathbf{0}$, i.e. in the absence of the disturbance. Now, it is shown that in the presence of the disturbance $\boldsymbol{w}(\boldsymbol{r}_i, t)$, the estimation error remains bounded:

Theorem 2.4 (**Estimation error bound**). *With α_1, α_2 as per Lemma 2.3, the norm of the state estimation error is bounded as*

$$\left\| \begin{bmatrix} \boldsymbol{r}_{ie}(t)^T & \boldsymbol{u}_{ie}(t)^T \end{bmatrix}^T \right\| \leq \delta_{ie}(t)$$

for all $t \geq 0$, where $\delta_{ie}(t)$ is defined as

$$\delta_{ie}(t) := \begin{cases} \|\boldsymbol{u}_{ie}(0)\|, & 0 \leq t \leq T_i^{est}; \\ l_i \delta_w^{c_i}, & t > T_i^{est}; \end{cases} \tag{2.19}$$

where $l_i = (2(1-\beta))^{\frac{1-\beta}{\beta}} \|\boldsymbol{u}_{ie}(0)\| > 0$, $c_i = \frac{1-\beta}{\beta} > 1, 0 < \beta < \frac{1}{2}$, and $0 \leq T_i^{est} < \infty$ is a finite constant.

Proof. Define $\boldsymbol{z}(t) := \begin{bmatrix} \boldsymbol{r}_{ie}(t)^T & \boldsymbol{u}_{ie}(t)^T \end{bmatrix}^T$. First, note that the *nominal* error dynamics, i.e. when the disturbance $\boldsymbol{w}(\boldsymbol{r}_i, t) = 0$, the origin is finite-time stable for the system (2.18). Using [117, Theorems 4.1, 6.2], it holds that there exists a function $T(\boldsymbol{r}_{ie}, \boldsymbol{u}_{ie})$ that is continuous at origin. Now, using this function as the settling time, from [2, Theorem 4.3], it holds that there exists a continuous Lyapunov function $V(\boldsymbol{r}_{ie}, \boldsymbol{u}_{ie})$ satisfying the condition $\dot{V}(\boldsymbol{r}_{ie}, \boldsymbol{u}_{ie}) + c(V(\boldsymbol{r}_{ie}, \boldsymbol{u}_{ie}))^{\beta} \leq 0$, where $c > 0$ and $0 < \beta < 1$ (namely, $V(\boldsymbol{r}_{ie}, \boldsymbol{u}_{ie}) = (T(\boldsymbol{r}_{ie}, \boldsymbol{u}_{ie}))^{\frac{1}{1-\beta}}$). Let β satisfy $\beta \in (0, \frac{1}{2})$. Since $\|\boldsymbol{w}(\boldsymbol{r}_i, t) - \boldsymbol{w}_{av}\| \leq \delta_w$, using [2, Theorem 5.2], it follows that with $\boldsymbol{z}(0) \in \mathcal{U}$, where $\mathcal{U}$ is an open neighborhood of origin, $\boldsymbol{z}(t) \in \mathcal{U}$ for all time $t \geq 0$. Define $\mathcal{U} := \{\boldsymbol{z} \mid \|\boldsymbol{z}\| \leq \|\boldsymbol{z}(0)\|\}$ so that $\boldsymbol{z}(0) \in \mathcal{U}$. Since one can choose $\hat{\boldsymbol{r}}_i(0) = \boldsymbol{r}_i(0)$, it holds that $\|\boldsymbol{z}(t)\| \leq \|\boldsymbol{z}(0)\| = \|\boldsymbol{u}_{ie}(0)\|$. From this, it holds that $\|\boldsymbol{z}(t)\| \leq \|\boldsymbol{u}_{ie}(0)\|$ for all time $t \geq 0$. Furthermore, again as per [2, Theorem 5.2], there exists a finite time T_i^{est} such that for all $t \geq T_i^{est}$

$$\|\boldsymbol{z}(t)\| \leq l_i \delta_w^{c_i}, \tag{2.20}$$

where $l_i = ((2(1-\beta))^{\frac{1-\beta}{\beta}} \|\boldsymbol{u}_{ie}(0)\| > 0$, $c_i = \frac{1-\beta}{\beta} > 1$. Hence, with choice of $\delta_{ie}(t)$ as per (2.19), it follows that $\|\boldsymbol{z}(t)\| \leq \delta_{ie}(t)$ for all $t \geq 0$. □

Remark 2.4. *The reason for using a finite-time state-estimator instead of a Luenberger observer is that, as shown in [2], the bound on the state (in this case, state-estimation*

error) δ_{ie} in Theorem 2.4 is of a higher order than the bound on the disturbance δ_w ($c_i > 1$), leading to improved rejection of low-level persistent disturbances.

Next, a robust controller using the estimated states $\hat{\boldsymbol{r}}_i, \hat{\boldsymbol{u}}_i$ is designed.

2.2.2 Observer-based robust controller

First, the desired velocity is redesigned using the estimated states as follows:

$$\hat{\boldsymbol{u}}_{id} \coloneqq \hat{u}_{id}\hat{\boldsymbol{u}}_{idn} - k_{i3}\boldsymbol{r}_{ie}\|\boldsymbol{r}_{ie}\|^{\alpha_1 - 1} - \boldsymbol{w}_{av}, \tag{2.21a}$$

$$\hat{\boldsymbol{u}}_{idn} \coloneqq \begin{bmatrix}\cos\hat{\gamma}_i & \sin\hat{\gamma}_i\end{bmatrix}^T, \tag{2.21b}$$

where $\hat{\gamma}_i \coloneqq \gamma_i(\hat{\boldsymbol{r}}_i)$. Note that in the absence of actual state measurements, the vector field $\mathbf{F}_i, \hat{\gamma}_i$ and the bump function $\sigma = \sigma(\hat{d}_{ij})$, where $\hat{d}_{ij}$ is given by (2.25), are functions of the estimated/sensed positions. Define the set I_i as

$$I_i \coloneqq \{j \in \mathcal{N}_i | \hat{J}_i < 0, d_s \leq \hat{d}_{ij} \leq R_c\}, \tag{2.22}$$

as the set of agents who are in the sensing range of agent i such that the agent i is moving towards them, i.e., $\hat{J}_i \coloneqq \hat{\boldsymbol{r}}_{ji}^T\hat{\boldsymbol{u}}_{idn} < 0$. The new desired speed $\hat{u}_{id}$ for agent i is set as:

$$\hat{u}_{id} \coloneqq \begin{cases} \frac{1}{\mu}\log\left(\left(\sum\limits_{j\in\mathcal{N}_i|\hat{d}_{ij}\leq d_s} e^{-\mu\,\hat{u}_{is|j}}\right)^{-1} + 1\right), & I_i = \emptyset \;\&\; \hat{d}_{ij} \leq d_s; \\ u_{ic}, & I_i = \emptyset \;\&\; \hat{d}_{ij} > d_s; \\ \frac{1}{\mu}\log\left(\left(\sum\limits_{j\in I_i} e^{-\mu\,\hat{u}_{i|j}}\right)^{-1} + 1\right), & I_i \neq \emptyset; \end{cases} \tag{2.23}$$

where $\hat{u}_{i|j}$ is defined as:

$$\hat{u}_{i|j} \coloneqq u_{ic}\frac{\hat{d}_{ij} - d_s}{R_c - d_s} + \hat{u}_{is|j}\frac{R_c - \hat{d}_{ij}}{R_c - d_s}, \tag{2.24}$$

where d_s is defined as per Theorem 2.5, $u_{ic} = u_{ic}(\hat{\boldsymbol{r}}_i)$ is as per (2.13a) and rest of the terms in (2.24) are given as:

$$\hat{u}_{is|j} \coloneqq \varepsilon_i\frac{\hat{\boldsymbol{r}}_{ji}^T\boldsymbol{u}_{js}^i}{\hat{\boldsymbol{r}}_{ji}^T\hat{\boldsymbol{u}}_{idn}} + (1-\varepsilon_i)\frac{u_e d_s}{\hat{\boldsymbol{r}}_{ji}^T\hat{\boldsymbol{u}}_{idn}}, \quad 0 < \varepsilon_i < 1, \tag{2.25}$$

$$\hat{J}_j \coloneqq \hat{\boldsymbol{r}}_{ji}^T\hat{\boldsymbol{u}}_{idn}, \quad \hat{\boldsymbol{r}}_{ji} \coloneqq \hat{\boldsymbol{r}}_i - \boldsymbol{r}_{js}^i, \quad \hat{d}_{ij} \coloneqq \|\hat{\boldsymbol{r}}_{ji}\|, \tag{2.26}$$

where $\boldsymbol{u}_{js}^i$ and $\boldsymbol{r}_{js}^i$ are the position and velocity of agent $j \in \mathcal{N}_i$ as *sensed* by agent i and u_e is defined later as per (A.8). Consider the dynamics (2.17) with an objective of tracking the velocity command $\hat{\boldsymbol{u}}_{id}$ given as per (2.21). The acceleration controller is designed as follows:

$$\boldsymbol{a}_i = \dot{\hat{\boldsymbol{u}}}_{id} - \lambda_i \boldsymbol{u}_{ide} \|\boldsymbol{u}_{ide}\|^{\beta_2 - 1} - k_{i4} \boldsymbol{r}_{ie} \|\boldsymbol{r}_{ie}\|^{\alpha_2 - 1}, \tag{2.27a}$$

$$\boldsymbol{u}_{ide} = \hat{\boldsymbol{u}}_i - \hat{\boldsymbol{u}}_{id}, \tag{2.27b}$$

where $\lambda_i > 0$, $0 < \beta_2 < 1$ and $\boldsymbol{u}_{ide}$ is the velocity error between the desired velocity $\hat{\boldsymbol{u}}_{id}$ and the velocity of the observer $\hat{\boldsymbol{u}}_i$. In the next sections, it is shown that the system (2.1) converges to a small neighborhood of the desired goal location $\boldsymbol{r}_{gi}$, while maintaining safety.

2.2.3 Safety analysis

First, define the estimation error parameter δ_e as

$$\delta_e := \max_{i,t} \delta_{ie}(t) = \max_i \{\boldsymbol{u}_{ie}(0), l_i \delta_w^{c_i}\}, \tag{2.28}$$

so that $\|\boldsymbol{r}_i(t) - \hat{\boldsymbol{r}}_i(t)\| \leq \delta_e$ and $\|\boldsymbol{u}_i(t) - \hat{\boldsymbol{u}}_i(t)\| \leq \delta_e$ for all agents i and for all time $t \geq 0$.

Theorem 2.5 (Safety w.r.t. other agents). *Assume N agents $i \in \{1, 2, \ldots, N\}$ are moving under the effect of acceleration controller (2.27). If the safe separation of each agent i is taken as $d_s = d_m + r_e + \delta_e + \epsilon_s$, with r_e being the maximum overshoot of the position error in the transient period of the closed-loop system (2.17) given as $r_e := \max_i \|\boldsymbol{r}_{ieMax}\|$ where $\boldsymbol{r}_{ieMax} = \frac{\boldsymbol{u}_{ide}(0)\|\boldsymbol{u}_{ide}(0)\|^{1-\beta_2}}{\lambda_i(2-\beta_2)}$ with $\boldsymbol{u}_{ide}(0) = \hat{\boldsymbol{u}}_i(0) - \hat{\boldsymbol{u}}_{id}(0)$, and δ_e is defined as in (2.28), then the motion of all agents is collision free, i.e. $\|\boldsymbol{r}_i(t) - \boldsymbol{r}_j(t)\| \geq d_m$ for all $i \neq j$ and for all $t \geq 0$.*

The proof is provided in Appendix A.2.

2.2.4 Convergence analysis

Now it is shown that under the effect of the designed control law (2.27), the closed-loop trajectories of agent i reach the $\delta_{ie}-$neighborhood around the goal location $\boldsymbol{r}_{gi}$ in a finite time. The following intermediate result is presented before proceeding with the main result.

Lemma 2.4. *Consider the system* $\dot{\boldsymbol{x}}(t) = -k\boldsymbol{x}(t)\frac{\tanh(\|\boldsymbol{x}(t)\|)}{\|\boldsymbol{x}(t)\|}$ *where* $k > 0$. *Assume that* $\boldsymbol{x}(0) \neq \mathbf{0}$. *Then, for all* $\epsilon > 0$, *there exists a time* $T_\epsilon < \infty$ *such that* $\|\boldsymbol{x}(t)\| \leq \epsilon$ *for all* $t \geq T_\epsilon$.

Proof. Let $V(\boldsymbol{x}) \coloneqq \frac{1}{2}\|\boldsymbol{x}(t)\|^2$ be the candidate Lyapunov function. Taking the time derivative of $V(\boldsymbol{x})$ along the system trajectories, it follows that

$$\dot{V}(\boldsymbol{x}) = \boldsymbol{x}(t)^T(-k\boldsymbol{x}(t)\frac{\tanh\|\boldsymbol{x}(t)\|}{\|\boldsymbol{x}(t)\|}) = -k\|\boldsymbol{x}(t)\|\tanh(\|\boldsymbol{x}(t)\|).$$

This shows that $\dot{V}(\boldsymbol{x}(t)) < 0$ for all $\boldsymbol{x}(t) \neq \mathbf{0}$. Hence, it holds that $V(\boldsymbol{x}(t)) \leq V(\boldsymbol{x}(0))$ or $\|\boldsymbol{x}(t)\| \leq \|\boldsymbol{x}(0)\|$ for all $t \geq 0$. Define $x_0 \coloneqq \|\boldsymbol{x}(0)\|$ so that it holds that $\|\boldsymbol{x}(t)\| \leq x_0$ and since $\boldsymbol{x}(0) \neq \mathbf{0}$, $x_0 > 0$. It is easy to check that the system trajectories satisfy $\tanh(\|\boldsymbol{x}(t)\|) \geq \frac{\tanh(x_0)}{x_0}\|\boldsymbol{x}(t)\|$ for all $t \geq 0$, i.e., the graph of $\tanh(\|\boldsymbol{x}(t)\|)$ lies above the straight line $y = c\|\boldsymbol{x}(t)\|$ with slope $c = \frac{\tanh(x_0)}{x_0}$ for all $\|\boldsymbol{x}(t)\| \leq x_0$. Hence, it holds that $\dot{V}(\boldsymbol{x}) = -k\|\boldsymbol{x}(t)\|\tanh(\|\boldsymbol{x}(t)\|) \leq -\frac{k\tanh(x_0)}{x_0}\|\boldsymbol{x}(t)\|^2 = -cV(\boldsymbol{x})$ where $c = \frac{2k\tanh(x_0)}{x_0}$. From the Comparison Lemma [121, Section 5.2], it follows that $V(\boldsymbol{x}(t)) \leq e^{-ct}V(\boldsymbol{x}(0))$.

For a given $\epsilon > 0$, define $T_\epsilon = -\frac{1}{c}\log(\frac{\epsilon^2}{2V(\boldsymbol{x}(0))})$, so that it holds that $V(\boldsymbol{x}(T_\epsilon)) \leq e^{-cT_\epsilon}V(\boldsymbol{x}(0)) = \frac{1}{2}\epsilon^2$. Now, since $V(\boldsymbol{x}(t)) \leq V(\boldsymbol{x}(T_\epsilon))$ for all $t \geq T_\epsilon$, it follows that $V(\boldsymbol{x}(t)) \leq \frac{1}{2}\epsilon^2$ or $\|\boldsymbol{x}(t)\| \leq \epsilon$ for all $t \geq T_\epsilon$. Also, since $\|\boldsymbol{x}_0\| \neq 0$, it holds that $T_\epsilon < \infty$. □

Now the main result for finite-time convergence can be stated.

Theorem 2.6 (Convergence). *Under the effect of control law (2.27), the closed-loop trajectories of (2.1) for each agent* i *reach a* δ_{ie}*-neighborhood around the goal location* $\boldsymbol{r}_{gi}$ *in finite time, i.e.,* $\exists\, T_i < \infty$, *such that* $\|\boldsymbol{r}_i(t) - \boldsymbol{r}_{gi}\| \leq l_i\delta_w^{c_i}$ *for all time* $t \geq T_i$.

Proof. The agents follow the vector field (2.9) under the desired direction of motion given by (2.10), which takes each agent i away from the other agents and towards its goal location, i.e., each class-A agent resolves the conflict with all other agents. From Lemma 2.1, there is no deadlock so that the agents are always attracted to their desired goal locations. Thus, there exists a finite time $T_i^{cr} \geq 0$ in which, the agent i resolves all the conflicts and starts moving towards its goal location. Also, from Assumption 2.3, once all agents reach their respective goal locations, they are out of each others' sensing region. Hence, once all the agents reached their respective goal locations, they stay there.

Now, it can be shown that once agent i resolves all its conflicts with the other agents, it would reach its goal location in finite time. Consider the error dynamics for $\hat{\boldsymbol{u}}_{ide}$ which,

as per (A.10), reads $\dot{\hat{\boldsymbol{u}}}_{ide} = -\lambda_i(\boldsymbol{u}_{ide})\|\boldsymbol{u}_{ide}\|^{\beta_2-1}$. From Theorem 2.3, it holds that the origin of the system (A.10) is FTS, which implies that there exists a time t_i such that for all $t \geq t_i$, $\hat{\boldsymbol{u}}_i(t) = \boldsymbol{u}_{id}(t)$. Note that from (2.21) and (2.17), it follows that $\dot{\hat{\boldsymbol{r}}}_i(t) = \hat{u}_{id}\hat{\boldsymbol{u}}_{idn}$ for all $t \geq t_i$. Now, in the absence of neighbors, from (2.21), it holds that $\hat{u}_{id} = \hat{u}_{ic}$ and the direction of vector field $\hat{\boldsymbol{u}}_{idn}$ is along $\mathbf{F}_i(\hat{\boldsymbol{r}}_i) = \mathbf{F}_{gi}(\hat{\boldsymbol{r}}_i)$, i.e., along $-(\hat{\boldsymbol{r}}_i - \boldsymbol{r}_{gi})$. Hence, the dynamics of the desired trajectory $\hat{\boldsymbol{r}}_{id}$ reads

$$\dot{\hat{\boldsymbol{r}}}_i = -\hat{u}_{ic}\frac{(\hat{\boldsymbol{r}}_i - \boldsymbol{r}_{gi})}{\|\hat{\boldsymbol{r}}_i - \boldsymbol{r}_{gi}\|}. \tag{2.29}$$

Now, if at the instant when the error $\hat{\boldsymbol{u}}_{ide}(t)$ becomes $\mathbf{0}$, the value of the norm $\|\hat{\boldsymbol{r}}_i - \boldsymbol{r}_{gi}\| \leq R_1$, then $\hat{u}_{ic}$ in (2.29) directly takes the form $\hat{u}_{ic} = k_{i2}\|\hat{\boldsymbol{r}}_i - \boldsymbol{r}_{gi}\|^{\alpha_r}$. If this is not the case, then by Lemma 2.4, there exits a finite time $\tilde{t}_i$, after which $\|\hat{\boldsymbol{r}}_i - \boldsymbol{r}_{gi}\|$ is less than R_1. Now, after this point, the value $\hat{u}_{ic}$ as per (2.13a) reads $\hat{u}_{ic} = k_{i2}\|\hat{\boldsymbol{r}}_i - \boldsymbol{r}_{gi}\|^{\alpha_r}$. Hence, it follows that

$$\dot{\hat{\boldsymbol{r}}}_i = -k_{i2}\|\hat{\boldsymbol{r}}_i - \boldsymbol{r}_{gi}\|^{\alpha_r}\frac{(\hat{\boldsymbol{r}}_i - \boldsymbol{r}_{gi})}{\|\hat{\boldsymbol{r}}_i - \boldsymbol{r}_{gi}\|} = -k_{i2}(\hat{\boldsymbol{r}}_i - \boldsymbol{r}_{gi})\|\hat{\boldsymbol{r}}_i - \boldsymbol{r}_{gi}\|^{\alpha_r-1}. \tag{2.30}$$

From Theorem 2.3, $\boldsymbol{r}_{gi}$ is a finite-time stable equilibrium for (2.30). Hence, there exists a finite-time T_i^* such that, for all $t \geq T_i^*$, it holds that $\hat{\boldsymbol{r}}_i(t) = \boldsymbol{r}_{gi}$. Now, from Theorem 2.4, $\|\boldsymbol{r}_i(t) - \hat{\boldsymbol{r}}_i(t)\| \leq l_i\delta_w^{c_i}$ for all $t \geq T_i^{est}$. Define $T_i := T_i^{est} + T_i^* + T_i^{cr} < \infty$, so that for all $t \geq T_i$, $\|\boldsymbol{r}_i(t) - \hat{\boldsymbol{r}}_i(t)\| = \|\boldsymbol{r}_i(t) - \boldsymbol{r}_{gi}\| \leq l_i\delta_w^{c_i}$, which completes the proof. □

Theorem 2.6, in light of Theorem 2.5, guarantees that within a finite time, all the agents reach a small neighborhood of their respective goal locations, which depends upon δ_w, while maintaining inter-agent safety at all times. This also implies that in the absence of the wind disturbance, or the case when $\boldsymbol{w} \equiv \boldsymbol{w}_{av}$, the agents reach exactly their respective goal locations. Note that the time T_i^{cr} required by each agent i to resolve all the conflicts, though finite, depends on the number, the initial and the goal locations of all the agents, and cannot be estimated beforehand without further assumptions on these parameters.

2.3 Dynamic obstacle environment

Let us now consider the case when the agents, termed as class-A agents subsequently, have to navigate in an obstacle environment. Consider M dynamic obstacles $o \in \mathcal{N}_B = \{N+1, \ldots, N+M\}$ that are moving with upper-bounded linear velocity $\|\boldsymbol{u}_o\| \geq 0$. These can model agents of higher priority, adversarial agents that are non-cooperative to the motion of the class-A agents, or failed class-A agents whose motion is uncontrollable.

In what follows, this class of dynamic obstacles is referred to as class-B agents [116]. The following assumptions are made in order to guarantee the safety of the system in the presence of dynamic obstacles.

Assumption 2.4 (Class-B agents). *The class-B agents are assumed to have a circular shape of the same size. The velocity of the class-B agents are bounded as* $\|\boldsymbol{u}_o\| \leq u_o$ *with* $0 \leq u_o < \infty$.

Assumption 2.5 (Inter-agent distance). *For two class-B agents* o_1, o_2*, the inter-agent distance is* $\|\boldsymbol{r}_{o_1}(t) - \boldsymbol{r}_{o_2}(t)\| > 2d_s$ *for almost all* $t \geq 0$*. Furthermore, for all class-B agents* o *and for all* $i \in \{1, \cdots, N\}$*,* $\|\boldsymbol{r}_o(t) - \boldsymbol{r}_{gi}\| \geq R_c + \delta_e$ *for almost all* $t \geq 0$.

Remark 2.5. *Assumption 2.5 is needed to guarantee that no class-A agent can become permanently occluded by a group of class-B agents and that they are not in conflict with class-B agents at their goal locations. Note that this is a sufficient condition to eliminate this situation. It might happen that even if the class-B agents are very close to each other, the class-A agents can skip through and reach their goal location*

Note that unlike [116], an *active* communication between agents is not considered in this work. The class-A agents do not even need to know whether their neighboring agents are class-A or class-B. The coordination protocol for the multi-agent system in the presence of dynamic obstacles can now be presented.

2.3.1 Safe velocity design

The desired linear velocity $\hat{\boldsymbol{u}}_{id}$ of each agent i is defined as per (2.21) where the modified $\hat{u}_{id}$ is

$$\hat{u}_{id} \coloneqq \begin{cases} -\frac{1}{\mu}\log\left(\sum\limits_{j\in\mathcal{N}_i|\hat{d}_{ij}\leq d_s} e^{-\mu\,\hat{u}^1_{is|j}}\right) & \hat{d}_{ij} \leq d_s, \\ -\frac{1}{\mu}\log\left(\sum\limits_{j\in\mathcal{N}_i} e^{-\mu\,\hat{u}^1_{i|j}}\right), & d_s \leq \hat{d}_{ij} \leq R_c, \\ u_{ic}, & \hat{d}_{ij} > R_c; \end{cases}, \tag{2.31}$$

where

$$\hat{u}^1_{i|j} \coloneqq \hat{u}_{ic}\frac{\hat{d}_{ij}-d_s}{R_c-d_s}+\hat{u}^1_{is|j}\frac{R_c-\hat{d}_{ij}}{R_c-d_s}, \tag{2.32}$$

$$\hat{u}^1_{is|j} \coloneqq \begin{cases} (1+\varepsilon_i)\frac{\hat{\boldsymbol{r}}^T_{ji}\boldsymbol{u}^i_{js}}{\hat{\boldsymbol{r}}^T_{ji}\hat{\boldsymbol{u}}_{idn}}, & \hat{J}_j > 0, \\ \varepsilon_i\frac{\hat{\boldsymbol{r}}^T_{ji}\boldsymbol{u}^i_{js}}{\hat{\boldsymbol{r}}^T_{ji}\hat{\boldsymbol{u}}_{idn}}, & \hat{J}_j \leq 0; \end{cases}, \tag{2.33}$$

with $\hat{J}_j \coloneqq \hat{\boldsymbol{r}}^T_{ji}\hat{\boldsymbol{u}}^i_{js}$, and rest of the terms such as $\varepsilon_i, \hat{d}_{ij}$ are given as in (2.25).

Remark 2.6. *Note that the expression in* (2.31) *is different from* (2.23) *since, in the latter case, the desired $\hat{u}_{id}$ is restricted to be always positive. In* (2.31)*, the $(+1)$ term is removed in the argument of the logarithm, allowing $\hat{u}_{id}$ to take negative values as well.*

2.3.2 Safety analysis

With this definition of the desired velocity $\hat{\boldsymbol{u}}_{id}$ with $\hat{u}_{id}$ given by (2.31), the following result can be stated:

Theorem 2.7 (Safety w.r.t. class-B agents). *Consider N class-A agents $i \in \{1,\dots,N\}$ assigned to move to goal locations $\boldsymbol{r}_{gi}$, and M class-B agents $o \in \{N+1,\dots,N+M\}$ serving as dynamic obstacles satisfying Assumption 2.4-2.5. Then, with d_s given as per Theorem 2.5, under the coordination protocol* (2.27) *with desired velocity defined as in* (2.21) *and $\hat{u}_{id}$ given as per* (2.31)*, each class-A agent maintains safe distance d_m with other agents.*

Proof. As per the analysis in the proof of Theorem 2.5, it follows that for all $j \in \mathcal{N}_i$, $\hat{d}_{ij} = \|\hat{\boldsymbol{r}}_i - \hat{\boldsymbol{r}}_j\| \geq d_s \implies \|\boldsymbol{r}_i - \boldsymbol{r}_j\| \geq d_m$. So, it is sufficient to prove that $\hat{d}_{ij} \geq d_s$ for all time t and for all $i \neq j$, i in class A, or equivalently, to prove that at $\hat{d}_{ij} = d_s$, the time derivative $\dot{\hat{d}}_{ij} \geq 0$. According to the control law (2.31), the agent i adjusts its linear velocity u_i so that it avoids colliding with the neighbor $j \in \mathcal{N}_i$ whose motion maximizes the rate of change of relative distance d_{ij}. Consider that $\hat{J}_j = \hat{\boldsymbol{r}}^T_{ji}\hat{\boldsymbol{u}}^i_{js} > 0$, i.e., the class-B agent o is moving towards the agent i. The time derivative of the inter-agent distance, evaluated at $\hat{d}_{ij} = d_s$, given by (A.6) under the closed-loop protocol (2.31) reads

$$\dot{\hat{d}}_{ij} = \frac{\hat{u}_{id}\,\hat{\boldsymbol{r}}^T_{ji}\hat{\boldsymbol{u}}_{idn} - \hat{\boldsymbol{r}}^T_{ji}\hat{\boldsymbol{u}}^i_{js}}{\hat{d}_{ij}} = \frac{(1+\varepsilon_i)\hat{\boldsymbol{r}}^T_{ji}\boldsymbol{u}^i_{js} - \hat{\boldsymbol{r}}^T_{ji}\hat{\boldsymbol{u}}^i_{js}}{\hat{d}_{ij}} = \frac{\varepsilon_i\hat{\boldsymbol{r}}^T_{ji}\boldsymbol{u}^i_{os}}{\hat{d}_{ij}} \geq 0.$$

Similarly, when $\hat{J}_j = \hat{\boldsymbol{r}}_{ji}^T \hat{\boldsymbol{u}}_{js}^i \leq 0$, i.e. the agent j is moving away from the agent i, the time derivative of the inter-agent distance at $\hat{d}_{ij} = d_s$ reads

$$\dot{\hat{d}}_{ij} = \frac{\hat{u}_{id}\, \hat{\boldsymbol{r}}_{ji}^T \hat{\boldsymbol{u}}_{idn} - \hat{\boldsymbol{r}}_{ji}^T \hat{\boldsymbol{u}}_{js}^i}{\hat{d}_{ij}} = \frac{\varepsilon_i \hat{\boldsymbol{r}}_{ji}^T \boldsymbol{u}_{js} - \hat{\boldsymbol{r}}_{ji}^T \hat{\boldsymbol{u}}_{js}^i}{\hat{d}_{ij}} = \frac{(\varepsilon_i - 1)\hat{\boldsymbol{r}}_{ji}^T \boldsymbol{u}_{js}^i}{\hat{d}_{ij}} \geq 0.$$

Note that the last inequality is true since $0 < \varepsilon_i < 1$. Hence, every agent i maintains a safe distance from its class-B neighbors. This shows that in all possible scenarios, each class-A agent maintains a safe distance from all the other agents. □

2.3.3 Convergence analysis

Theorem 2.8 (Convergence). *Under the effect of coordination protocol (2.27) with desired velocity $\hat{\boldsymbol{u}}_{id}$ defined as in (2.21) and $\hat{u}_{id}$ given as per (2.31), the closed-loop trajectories (2.1) of each class-A agent i reach a δ_{ie}-neighborhood around the goal location $\boldsymbol{r}_{gi}$ in finite time, i.e., $\exists\, T_i < \infty$, such that $\|\boldsymbol{r}_i(t) - \boldsymbol{r}_{gi}\| \leq \delta_{ie}(t)$ for all time $t \geq T_i$.*

Proof. According to the Assumption 2.5, there are no two class-B agents whose distance is less than $2d_s$ for all times, which implies that there will always be space between the two obstacles from where the class-A agent can pass through. The rest of the proof directly follows from Theorem 2.6. Also, since the class-B agents are not always near the goal locations $\boldsymbol{r}_{gi}$ (Assumption 2.5), once the class-A agent i reaches its goal location, it can stay there. □

Remark 2.7. *While as per Lemma 1, there would be no deadlocks in the motion of the agents, it is still possible that there are livelocks. Livelock occurs when periodic motions are executed by the agents, which may be induced by a periodic motion of class-B agents or under certain control gains, the direction of the wind, and the set of initial and goal locations for the class-A agents. Although in the presence of external disturbances that vary both in space and time, it is difficult for the class-B agents to plan their motion in order to induce a livelock for the class-A agents, it is still possible. Excluding the livelocks is a rather difficult problem, is out of the scope of the current work, and is left as a problem for future investigation.*

Hence, it is shown that in the presence of moving obstacles, or class-B agents, the class-A agents would be able to reach very close to the desired goal location while maintaining safety. Next, a few simulation results showing the efficacy of the proposed control design are presented.

2.4 Simulations

Two scenarios involve $N = 46$ agents out of which 20 are class-B agents and 26 are class-A agents are presented (interested reader is referred to [107] for more simulation case studies[2]). In Figure 2.3, class-A agents are colored blue and the class-B agents are colored red. The goal locations are selected sufficiently far apart so that the agents' sensing regions do not overlap when agents lie on their goal locations (i.e., $\|\boldsymbol{r}_{gi} - \boldsymbol{r}_{gj}\| > R_c$ for $i \neq j$). The simulation parameters are listed below:

- $d_m = 4m$, $\epsilon_s = 5$, $\delta_e = 15$, $d_s = 29\ m$ and $R_c = 3.5d_s$. Define $\Delta_e = \max_i\{l_i\delta_w^{c_i}\}$, so that from Theorem 2.8, we have $\|\boldsymbol{r}_{ie}\| \leq \Delta_e$ for all times $t \geq \max_i T_i$. In this case, $\Delta_e = 0.8824\ m$.
- $\boldsymbol{w}_{av} = [5.86, 2.96]^T\ m/sec$ and $\delta_w = 1.92\ m/sec$
- $\varepsilon_i = 0.01$, $k_{i1} = 5$, $k_{i3} = 0.8538$, $k_{i4} = 0.3149$, $\alpha_r = 0.9, R_1 = 0.4017m, \alpha_1 = 0.9$ and $\alpha_2 = 0.8$.

Figure 2.2 shows the spatial variation of the wind speed used as the external disturbance in the simulations. The the wind speed at each $x - y$ location is plotted. The figure shows the variation of the wind speed in the $x - y$ plane in the domain $[-100, 100] \times [-100, 100]$. The following formulation is used to scale up the domain of the disturbance:

$$\boldsymbol{w}(x \pm 200, y \pm 200, t) = \boldsymbol{w}(x, y, t) \tag{2.34}$$

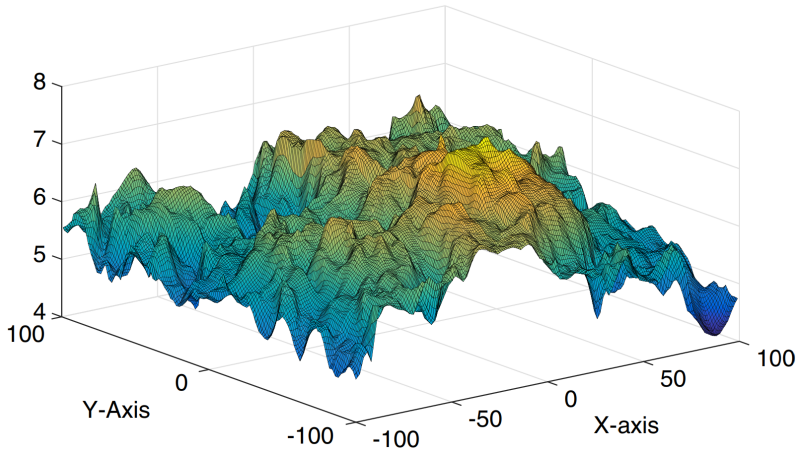

Figure 2.2: The wind profile used as external disturbance.

[2]Simulation videos are available online at https://tinyurl.com/y7syd8la

The goal locations are chosen such that they form the characters UM for the aesthetic appeal of the simulations. In Figure 2.3, the initial positions of the agents are marked by diamonds: blue diamonds are the initial positions of class-A agents and red diamonds are those of class-B agents. In the first scenario, class-B agents are moving outwards and class-A agents are moving inwards. The black ellipse is used to denote the agents that are moving in the same direction with arrows representing their direction of motion. In Scenario 2, the class-B agents (red-diamonds) start in V-formation as represented by the black-lines.

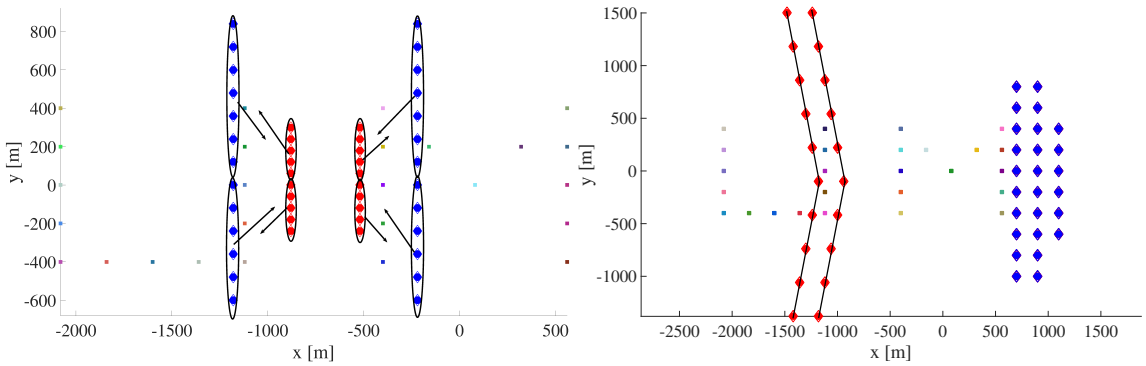

Figure 2.3: Initial configuration of Scenario 1 and 2.

The motion of the class-B agents is such that the Assumption 2.5 is satisfied while in scenario 3, the motion of class-B agents is chosen such that Assumption 2.5 is not satisfied. In brief:

- In the first scenario, the class-B agents start in-between the class-A agents and move outwards, while class-A agents move inwards. The set of initial locations, target locations, and initial directions of movement is given in Figure 2.3. This scenario shows how effectively class-A agents can avoid collisions with class-B agents. Furthermore, we assume that the wind disturbance in this case varies only with $\boldsymbol{r}$ and is constant in t, i.e. $\boldsymbol{w} = \boldsymbol{w}(\boldsymbol{r})$.

- In the second scenario, the class-B agents come as a swarm in the V-formation towards the class-A agents. This scenario shows how class-A agents can avoid collisions with other class-A agents as well as class-B agents. In this case, we allow the wind disturbance to vary both in space and time, i.e. $\boldsymbol{w} = \boldsymbol{w}(\boldsymbol{r}, t)$. We discuss the difference in the results in the first two scenarios arising because of the difference in assumptions on the wind disturbance.

Figures 2.4 and 2.6 show the performance of the presented protocol both in terms of safety and convergence. In all the figures, it can be seen that class-A agents are able to

maintain the safe distance, d_m with all the other agents (both class-A and class-B agents). Also, it can be seen that the class-A agents reach a much smaller neighborhood of their desired goal locations (i.e. their final distance from their goal location $\|\boldsymbol{r}_i - \boldsymbol{r}_{gi}\|$) than the theoretical (conservative) bound given as per Theorem 2.8.

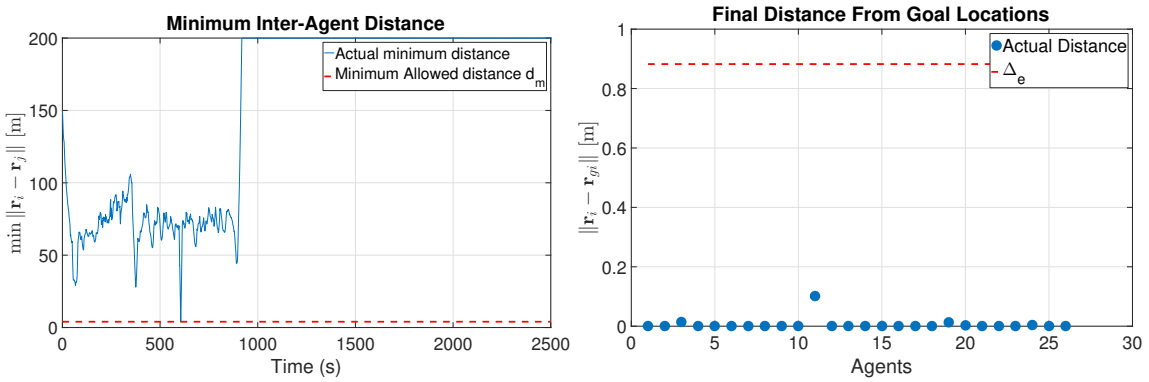

Figure 2.4: Scenario 1: minimum inter-agent distance and final distance from the goal.

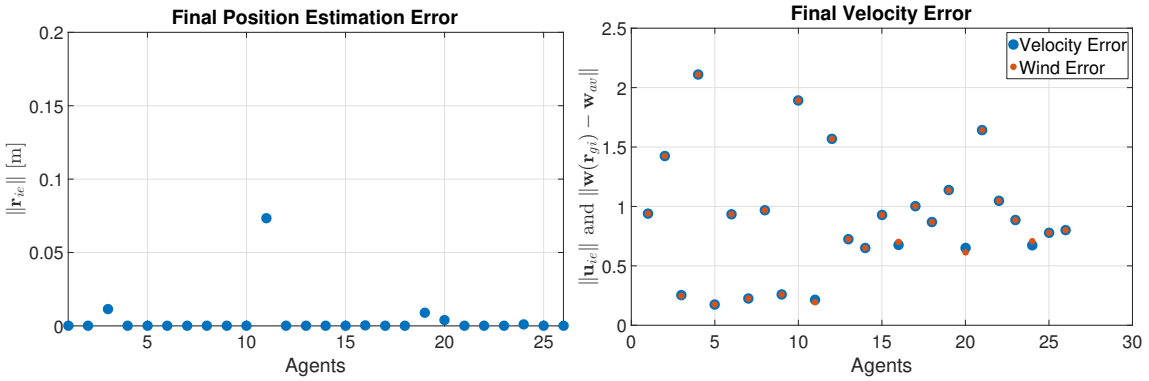

Figure 2.5: Scenario 1: Final position error $\|\boldsymbol{r}_{ie}\|$, velocity estimation error $\|\boldsymbol{u}_{ie}\|$ and $\|\boldsymbol{w}(\boldsymbol{r}_{gi}, t) - \boldsymbol{w}_{av}\|$

Note that for the observer dynamics (2.18), the equilibrium point is $\boldsymbol{r}^*_{ie}(t) = 0$ and $\boldsymbol{u}^*_{ie}(t) = -(\boldsymbol{w}(\boldsymbol{r}_i, t) - \boldsymbol{w}_{av})$. Since this equilibrium point varies both in space and time and the time derivative of the disturbance $\boldsymbol{w}(\boldsymbol{r}_i, t)$ is assumed to be unknown, one cannot prove that the system (2.18) would actually stay at this time varying equilibrium. As can be seen in the Figures 2.5, the error $\|\boldsymbol{r}_{ie}\|$ is close to 0 while $\|\boldsymbol{u}_{ie}(t)\|$ is close to $\|\boldsymbol{w}(\boldsymbol{r}_{gi}, t) - \boldsymbol{w}_{av}\|$ under the assumption that $\boldsymbol{w}(\boldsymbol{r}_i, t)$ does not vary with time. In the case when the wind is indeed a function of time, it can be seen from Figure 2.7 that while the final estimation error is still very small, the velocity error does not converge to the actual wind error.

Figure 2.8 shows the norm of the accelerations and the velocities of one of the class-A agents. Once the class-A agent reaches its goal location, its velocity becomes constant,

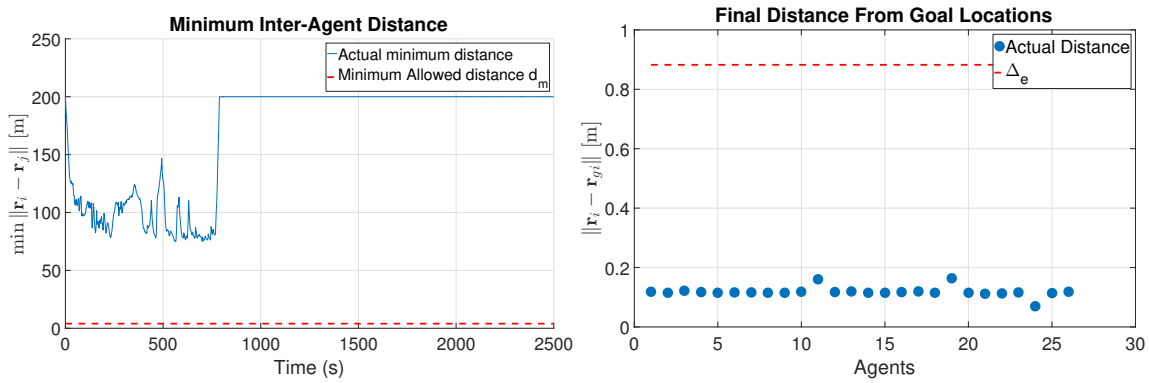

Figure 2.6: Scenario 2: minimum inter-agent distance and final distance from the goal.

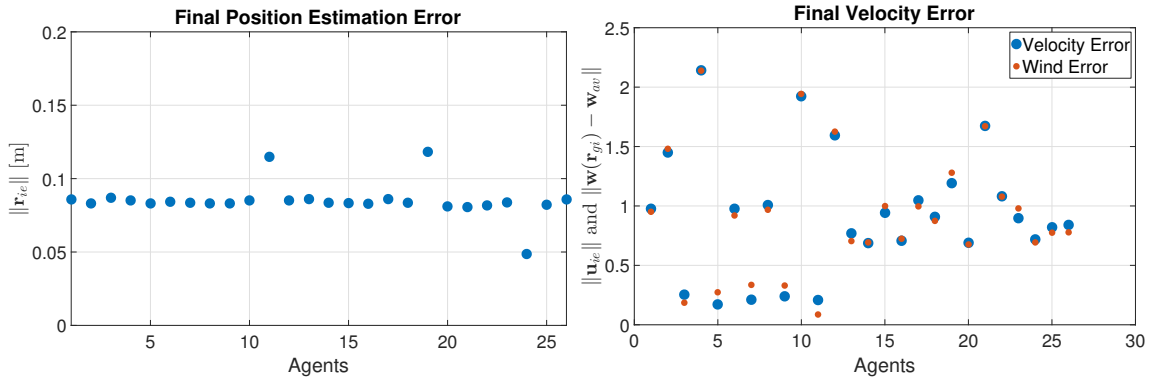

Figure 2.7: Scenario 2: Final position error $\|\boldsymbol{r}_{ie}\|$, velocity estimation error $\|\boldsymbol{u}_{ie}\|$ and the error term $\|\boldsymbol{w}(\boldsymbol{r}_{gi}, t) - \boldsymbol{w}_{av}\|$

equal and the opposite of the wind disturbance at the location and the acceleration becomes zero. The commanded acceleration and the velocity are noisy because of the disturbance $\boldsymbol{w}$ and the sensing uncertainties.

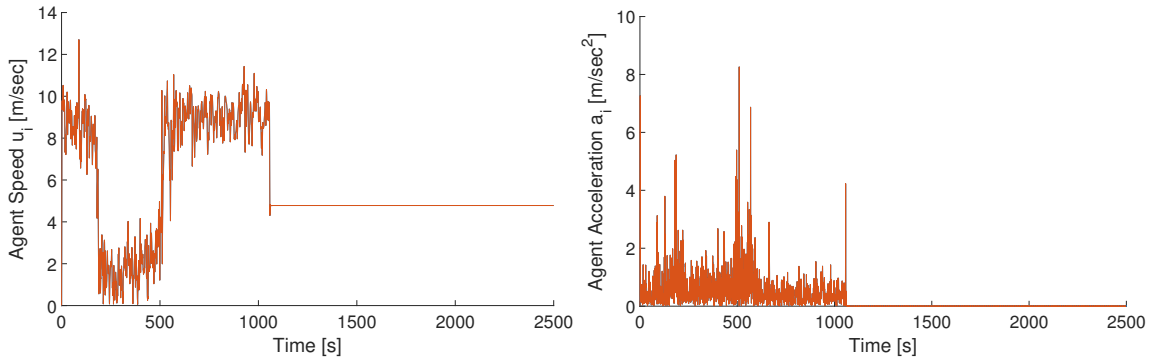

Figure 2.8: Scenario 2: magnitude of velocity and acceleration of a class-A agent.

2.5 Discussion

As demonstrated via various simulation scenarios, the proposed protocol can de-conflict a large number of agents while maintaining safety and guaranteed convergence to the neighborhood of the desired goal location in the presence of unknown state-disturbances. The main strength of the proposed approach is the scalability with the number of agents and the ability to counteract a class of state-disturbance and sensing uncertainties. One of the main drawbacks of the presented work is the assumption on the motion of the dynamic obstacles. It is important to note that Assumption 2.5 is a sufficient condition to avoid the herding of the class-A agents by a formation of class-B agents. Furthermore, it is required that the class-B agents do not hover around the goal location of the class-A agents so that there is no conflict once the class-A agents reach their respective goal locations. As demonstrated in Scenario 3, even if this condition fails to hold, the class-A agents can still reach their goal locations. This outcome is because the external disturbance $\boldsymbol{w}$ and the sensing uncertainty in the positions of the neighboring agents can result in a vector field taking the class-A agents through the narrow gap between the class-B agents while maintaining safety.

One of the directions for future work is the identification of the non-cooperative neighbors. Once a class-A agent identifies a dynamic obstacle, it can use the knowledge of the upper bound on the velocity of the obstacle to avoid herding.

2.6 Conclusion

A robust distributed estimation and control scheme is presented to generate collision-free trajectories for multiple agents in the presence of dynamic obstacles, and unmatched state disturbances standing for wind effects. It is shown that under the adopted disturbance (dynamic obstacle and wind) modeling and assumptions, the safety and convergence of the system can be guaranteed. A finite-time observer and a finite-time feedback controller are designed and it is shown that the closed-trajectories of each agent converge to a δ-neighborhood of their respective goal locations in a finite time, where δ depends upon the external disturbances acting on the system. The proposed method, being completely distributed with analytical expressions for the observer and control laws, is scalable with the number of agents.

CHAPTER 3

New Results on Fixed-time Stability

In contrast to FTS studied in Chapter 2, the notion of FxTS requires that the time of convergence is uniformly bounded for all initial conditions. This stronger notion can be used in time-critical problems where a system objective is required to be completed within a user-defined time, irrespective of the system's initial conditions. However, faster convergence also requires higher control input requirements. For a real-world control system, FxTS from arbitrary initial conditions presumes unbounded control authority. To address the problem of FxTS in the presence of input constraints, new Lyapunov conditions for FxTS are presented in this chapter.

First new Lyapunov conditions on FxTS are presented in Section 3.2 by introducing a (possibly positive) a linear term in the upper bound of the derivative of the Lyapunov function in addition to the two negative terms introduced in [65]. It is shown that FxTS is guaranteed from a domain of attraction that depends upon the ratio of the coefficients of the (possibly positive) new and the older, negative, terms in the bound of the time derivative of the Lyapunov function. An upper-bound on the time of convergence to the equilibrium is computed, which is also a function of this ratio. The new Lyapunov conditions, when used in a QP, introduce a slack term, resulting in feasibility guarantees even with input constraints. The relation between the domain of attraction for fixed-time stability, the input bounds, and the time of convergence is established for a 1-D control affine system. Finally, it is shown that the proposed results on FxTS also characterizes the robustness of FxTS systems under additive vanishing disturbances. The results in this section are partly based on [108].

Second new Lyapunov conditions with a (possibly positive) constant term in the time derivative of the Lyapunov function is studied in Section 3.3 to model bounded, non-vanishing disturbances in the system dynamics. In the presence of non-vanishing disturbances, typically only boundedness of the trajectories in a neighborhood of the equilibrium point (or set) can be guaranteed (see, e.g., [122, Section 9.2]). The neighborhood to which

the system trajectories converge, as well the time of convergence to this neighborhood, are characterized in terms of the positive and negative terms that appear in the time derivative of the Lyapunov function. The results in this section are partly based on [109]. The author wishes to acknowledge his co-author Mitchell Black for contributions in the development of some of the results presented in this section.

The following notation is frequently used in this chapter:

$\mathbb{R}$	the set of real numbers
$\mathbb{R}_+$	Set of non-negative reals
$\|\cdot\|$	Euclidean norm (2-norm) of $(\cdot)$
$\mathcal{C}^k$	$k-$times continuously differentiable functions
$L_f V(x)$	Lie derivative of $V \in \mathcal{C}^1$ along f defined as $\frac{\partial V}{\partial x} f(x)$
$x^\star$	Optimal value of the variable x
∂S	Boundary of a closed set S

3.1 Preliminaries

In this section, the notion of FTS and FxTS and the related prior results are reviewed. Consider the autonomous dynamical system:

$$\dot{x}(t) = f(x(t)), \tag{3.1}$$

where $x \in \mathbb{R}^n$, $f : \mathcal{D} \to \mathbb{R}^n$ is continuous on an open neighborhood $\mathcal{D} \subseteq \mathbb{R}^n$ of the origin and $f(0) = 0$. The arguments t, x are dropped whenever clear from the context. In this work, the results are presented under the assumption that the solution of (3.1) exists and is unique for all $x(0) \in \mathbb{R}^n$. For results on FTS and FxTS for systems with non-unique solutions, the interested reader is referred to [82, 123–126]. First, various notions of stability for autonomous systems are reviewed.

Definition 3.1 (Stability). *The origin of* (3.1) *is said to be:*

(i) Lyapunov stable (LS) or simply, stable, if for every $\epsilon > 0$, there exists $\delta(\epsilon) > 0$ such that if $\|x(0)\| < \delta$, then $\|x(t)\| < \epsilon$ for all $t \geq 0$.

(ii) Asymptotic stable (AS) (respectively, globally AS), if it is stable, and there exists $c > 0$ such that for all $\|x(0)\| < c$ (respectively, for all $x(0) \in \mathbb{R}^n$), the solution of (3.1) *satisfies $\lim_{t\to\infty} x(t) = 0$.*

(iii) Exponentially stable (ES) (respectively, globally ES), if there exist $c, a, \gamma > 0$ *such that*

$$\|x(t)\| \leq ae^{-\gamma\, t}\|x(0)\|,$$

for all $\|x(0)\| < c$ *(respectively, for all* $x(0) \in \mathbb{R}^n$*), and* $t \geq 0$*.*

(iv) Finite-time stable (FTS), if it is stable and there exists an open neighborhood $\mathcal{N}$ *of the origin such that for all* $x(0) \in \mathcal{N} \setminus \{0\}$, $\lim_{t\to T} x(t) = 0$*, where* $T = T(x(0)) < \infty$*. The origin is a globally FTS equilibrium if* $\mathcal{N} = \mathbb{R}^n$*.*

For the sake of completeness, the Lyapunov conditions for FTS, adapted from [2], are repeated here:

Theorem 3.1 (Lyapunov conditions for FTS). *Suppose there exist a continuously differentiable, positive definite function* $V : \mathcal{D} \to \mathbb{R}$ *for* (3.1)*, real numbers* $\alpha > 0$ *and* $\gamma \in (0, 1)$*, and an open neighborhood* $\mathcal{V} \subseteq \mathcal{D} \subset \mathbb{R}^n$ *of the origin such that the time derivative* $\dot{V}(x)$ *satisfies*

$$\dot{V}(x) \leq -\alpha\, V(x)^{\gamma},\ \forall x \in \mathcal{V} \setminus \{0\}. \tag{3.2}$$

Then the origin is an FTS equilibrium. Furthermore, the settling-time function T *satisfies*

$$T(x(0)) \leq \frac{V(x(0))^{1-\gamma}}{\alpha(1-\gamma)}. \tag{3.3}$$

Note that under the notion of FTS, the upper-bound on the settling-time function T as given in Theorem 3.1, though *finite*, depends upon the initial condition $x(0)$ and grows unbounded as $\|x(0)\|$ increases. The notion of FxTS, as defined below, allows the settling time to remain uniformly bounded for all initial conditions. The following definition of FxTS and the corresponding Lyapunov conditions are adapted from [65].

Definition 3.2 (FxTS). *The origin is said to be an FxTS equilibrium of* (3.1) *if it is globally FTS and the settling time function is uniformly bounded for all* $x(0) \in \mathbb{R}^n$*, i.e.,* $\sup_{x(0)\in\mathbb{R}^n} T(x(0)) < \infty$.

Theorem 3.2 (Old Lyapunov conditions for FxTS). *Suppose there exists a continuously differentiable, positive definite, radially unbounded function* $V : \mathbb{R}^n \to \mathbb{R}$ *such that*

$$\dot{V}(x) \leq -\alpha_1 V(x)^{\gamma_1} - \alpha_2 V(x)^{\gamma_2}, \tag{3.4}$$

holds for all $x \in \mathbb{R}^n \setminus \{0\}$*, with* $\alpha_1, \alpha_2 > 0$*,* $\gamma_1 > 1$ *and* $0 < \gamma_2 < 1$*. Then, the origin of* (3.1) *is FxTS with continuous settling-time function* T *that satisfies:*

$$T \leq \frac{1}{\alpha_1(\gamma_1 - 1)} + \frac{1}{\alpha_2(1 - \gamma_2)}. \tag{3.5}$$

Note that the upper-bound on the time of convergence in the case of FxTS is *fixed*, i.e., independent of the initial conditions. In the case when $\gamma_1 = 1 + \frac{1}{\mu}, \gamma_2 = 1 - \frac{1}{\mu}$ with $\mu > 1$, the authors in [127, Lemma 2] proposed a tighter upper-bound on the time of convergence given as

$$T \leq \frac{\mu\pi}{2\sqrt{\alpha_1\alpha_2}}. \tag{3.6}$$

Remark 3.1. *Intuitively, for* $V(x) > 1$*, it holds that* $V(x)^{\gamma_1} > V(x)$ *and so, the first term in* (3.4) *leads to convergence of the system trajectories to the set* $\{x \mid V(x) \leq 1\}$ *within a fixed amount of time given by the first term in* (3.5)*. For* $V(x) \leq 1$*, it holds that* $V(x)^{\gamma_2} > V(x)$ *and so, the second term in* (3.4) *leads to convergence of the system trajectories from the set* $\{x \mid V(x) \leq 1\}$ *to the origin within a fixed amount of time given by the second term in* (3.5)*. Since the FTS condition in* (2.4) *contains only the second term, which dominates when* V *is small, the time of convergence, though finite, grows as the initial distance from the equilibrium point increases.*

3.2 New Lyapunov conditions for fixed-time stability: first result

3.2.1 Motivating example

The inspiration for the new FxTS result comes from the problem of control synthesis for fixed-time convergence under input constraints. Consider a 1-dimensional control affine system

$$\dot{x} = f(x) + g(x)u, \tag{3.7}$$

where $f, g : \mathbb{R} \to \mathbb{R}$ are continuous functions. Suppose that the control objective is to drive the closed-loop trajectories of (3.7) to a set $S_G := \{x \mid V(x) \leq 0\}$ within a user-defined

time $T_{ud} > 0$ where $V : \mathbb{R} \to \mathbb{R}$ is a continuously differentiable function. Additionally, consider the input constraints $u_m \leq u \leq u_M$ where $u_m < u_M$.

As pointed out in [63], QPs can be solved very efficiently and can be used for real-time implementation. To this end, following the work in [53, 59] and using the FxTS conditions from Theorem 3.2, a QP can be formulated as follows :

$$\min_{u} \quad \frac{1}{2}u^2 \tag{3.8a}$$

$$\text{s.t.} \quad \begin{bmatrix} 1 \\ -1 \end{bmatrix} u \leq \begin{bmatrix} u_M \\ -u_m \end{bmatrix}, \tag{3.8b}$$

$$L_f V(x) + L_g V(x) u \leq -\alpha_1 V(x)^{\gamma_1} - \alpha_2 V(x)^{\gamma_2}, \tag{3.8c}$$

for $x \notin S_G$, where $c > 0$, and $\alpha_1, \alpha_2, \gamma_1, \gamma_2$ are chosen as $\alpha_1 = \alpha_2 = \frac{\mu\pi}{2T_{ud}}$, $\gamma_1 = 1 + \frac{1}{\mu}$ and $\gamma_2 = 1 - \frac{1}{\mu}$ with $\mu > 1$. Existence of the solution of (3.8) implies existence of a control input under the effect of which, the closed-loop trajectories of (3.7) reach the set S_G within a fixed time T, which, per (3.6), satisfies $T \leq \frac{\mu\pi}{2\sqrt{\alpha_1\alpha_2}}$, and with the choice of $\alpha_1 = \alpha_2 = \frac{\mu\pi}{2T_{ud}}$, further satisfies $T \leq T_{ud}$. The issue with the QP in (3.8) is that it might not be feasible for all initial conditions due to the presence of input constraints. The authors in [53] introduce a slack variable in the CLF constraint in order to guarantee feasibility of the QP when additional constraints are present. Inspired from that, a slack term in the constraint (3.8c) can be introduced. In order to guarantee FxTS in the presence of such a slack term, a new FxTS result is presented next.

3.2.2 Lyapunov conditions

Previously, conditions of the form (3.4) are considered by various authors, where the time derivative of the Lyapunov candidate is upper bounded by two negative terms. The result in this section relaxes these conditions by allowing a linear term to appear in the upper bound of the time derivative. In particular, the following Lyapunov condition is considered for a positive definite, continuously differentiable $V : \mathbb{R}^n \to \mathbb{R}$:

$$\dot{V}(x) \leq -\alpha_1 V(x)^{\gamma_1} - \alpha_2 V(x)^{\gamma_2} + \delta_1 V(x), \tag{3.9}$$

with $\alpha_1, \alpha_2 > 0$, $\delta_1 \in \mathbb{R}$, $\gamma_1 = 1 + \frac{1}{\mu}$, $\gamma_2 = 1 - \frac{1}{\mu}$ where $\mu > 1$, which introduces $\delta_1 V(x)$ as the additional *linear* term in the time derivative of $V(x)$ as compared to (3.4). Before presenting the main result, the following lemma is needed, which gives the expressions for the upper-bounds on time when (3.9) is integrated, for various relative values of δ_1 and

$2\sqrt{\alpha_1\alpha_2}$.

Lemma 3.1 (Bounds on convergence time). *Let $V_0, \tilde{V}, \alpha_1, \alpha_2 > 0$, $\delta_1 \in \mathbb{R}$, $\gamma_1 = 1 + \frac{1}{\mu}$ and $\gamma_2 = 1 - \frac{1}{\mu}$, where $\mu > 1$. Define*

$$I_1 \coloneqq \int_{V_0}^{0} \frac{dV}{-\alpha_1 V^{\gamma_1} - \alpha_2 V^{\gamma_2} + \delta_1 V}, \tag{3.10}$$

$$I_2 \coloneqq \int_{V_0}^{\tilde{V}} \frac{dV}{-\alpha_1 V^{\gamma_1} - \alpha_2 V^{\gamma_2} + \delta_1 V}. \tag{3.11}$$

Then, the following holds:

(i) If $0 \leq \frac{\delta_1}{2\sqrt{\alpha_1\alpha_2}} < 1$, it holds that for all $V_0 \geq 0$

$$I_1 \leq \frac{\mu}{\alpha_1 k_1}\left(\frac{\pi}{2} - \tan^{-1} k_2\right), \tag{3.12}$$

where $k_1 = \sqrt{\frac{4\alpha_1\alpha_2 - \delta_1^2}{4\alpha_1^2}}$ and $k_2 = -\frac{\delta_1}{\sqrt{4\alpha_1\alpha_2 - \delta_1^2}}$;

(ii) If $\frac{\delta_1}{2\sqrt{\alpha_1\alpha_2}} \geq 1$ and $0 \leq V_0 \leq k^\mu \left(\frac{\delta_1 - \sqrt{\delta_1^2 - 4\alpha_1\alpha_2}}{2\alpha_1}\right)^\mu$ with $0 < k < 1$, it holds that

$$I_1 \leq \frac{\mu}{\alpha_1(b-a)}\left(\log\left(\frac{b - ka}{a(1-k)}\right) - \log\left(\frac{b}{a}\right)\right), \tag{3.13}$$

where $a \leq b$ are the roots of $\gamma(z) \coloneqq \alpha_1 z^2 - \delta_1 z + \alpha_2 = 0$;

(iii) If $\frac{\delta_1}{2\sqrt{\alpha_1\alpha_2}} \geq 1$ and $V_0 \geq \tilde{V} \coloneqq \tilde{k}^\mu \left(\frac{\delta_1 + \sqrt{\delta_1^2 - 4\alpha_1\alpha_2}}{2\alpha_1}\right)^\mu$ with $\tilde{k} > 1$, it holds that

$$I_2 \leq \frac{\mu}{\alpha_1(b-a)} \log\left(\frac{\tilde{k}b - a}{\tilde{k}b - b}\right). \tag{3.14}$$

The proof is provided in Appendix B.1. The first new FxTS condition can now be stated.

Theorem 3.3 (New Lyapunov conditions for FxTS). *Let $V : \mathbb{R}^n \to \mathbb{R}$ be a continuously differentiable, positive definite, radially unbounded function, satisfying*

$$\dot{V}(x) \leq -\alpha_1 V(x)^{\gamma_1} - \alpha_2 V(x)^{\gamma_2} + \delta_1 V(x), \tag{3.15}$$

for all $x \in \mathbb{R}^n \setminus \{0\}$ along the trajectories of (3.1) with $\alpha_1, \alpha_2 > 0$, $\delta_1 \in \mathbb{R}$, $\gamma_1 = 1 + \frac{1}{\mu}$, $\gamma_2 = 1 - \frac{1}{\mu}$ and $\mu > 1$. Then, there exists a neighborhood $D \subseteq \mathbb{R}^n$ of the origin such that

for all $x(0) \in D$, the closed-trajectories of (3.1) reach the origin within a fixed time T, where

$$D = \begin{cases} \mathbb{R}^n; & \frac{\delta_1}{2\sqrt{\alpha_1\alpha_2}} < 1, \\ \left\{ x \mid V(x) \leq k^\mu \left(\frac{\delta_1 - \sqrt{\delta_1^2 - 4\alpha_1\alpha_2}}{2\alpha_1} \right)^\mu \right\}; & \frac{\delta_1}{2\sqrt{\alpha_1\alpha_2}} \geq 1, \end{cases}, \tag{3.16}$$

$$T \leq \begin{cases} \frac{\mu\pi}{2\sqrt{\alpha_1\alpha_2}}; & \frac{\delta_1}{2\sqrt{\alpha_1\alpha_2}} \leq 0, \\ \frac{\mu}{\alpha_1 k_1}\left(\frac{\pi}{2} - \tan^{-1} k_2\right); & 0 \leq \frac{\delta_1}{2\sqrt{\alpha_1\alpha_2}} < 1, , \\ \frac{\mu}{\alpha_1(b-a)}\left(\log\left(\frac{b-ka}{a(1-k)}\right) - \log\left(\frac{b}{a}\right)\right); & \frac{\delta_1}{2\sqrt{\alpha_1\alpha_2}} \geq 1, \end{cases} \tag{3.17}$$

where $0 < k < 1$, $a < b$ are the solutions of $\gamma(z) := \alpha_1 z^2 - \delta_1 z + \alpha_2 = 0$, $k_1 = \sqrt{\frac{4\alpha_1\alpha_2 - \delta_1^2}{4\alpha_1^2}}$ and $k_2 = -\frac{\delta_1}{\sqrt{4\alpha_1\alpha_2 - \delta_1^2}}$.

Proof. Note that the domain of attraction D and the time of convergence T are functions of the ratio $r := \frac{\delta_1}{2\sqrt{\alpha_1\alpha_2}}$. The three cases, namely, $r \leq 0$, $0 \geq r < 1$ and $r \geq 1$ are studied separately.

For $r \leq 0$, one can recover the right-hand side of (3.4) from (3.15), and it follows from Theorem 3.2 that $D = \mathbb{R}^n$, and from part (3.6), it follows that $T \leq \frac{\mu\pi}{2\sqrt{\alpha_1\alpha_2}}$.

Next, consider the case when $0 \leq r < 1$. First it is shown that there exists $D \subseteq \mathbb{R}^n$ containing the origin such that $\dot{V}(x) < 0$ for all $x \in D \setminus \{0\}$, so that all sub-level sets of the function V contained in D are forward invariant. The right-hand side of (3.15) can be re-arranged so that (3.15) reads

$$\dot{V}(x) \leq V(x)\left(-\alpha_1 V(x)^{\gamma_1 - 1} - \alpha_2 V(x)^{\gamma_2 - 1} + \delta_1\right).$$

Note that $V(x) > 0$ for all $x \neq 0$. Thus, for $\dot{V}(x)$ to take negative values for all $x \neq 0$, it is needed that

$$\begin{aligned} \min_{x \neq 0}\left(-\alpha_1 V(x)^{\gamma_1 - 1} - \alpha_2 V(x)^{\gamma_2 - 1} + \delta_1\right) < 0 &\iff \delta_1 < \min_{x \neq 0}\left(\alpha_1 V(x)^{\gamma_1 - 1} + \alpha_2 V(x)^{\gamma_2 - 1}\right) \\ &\iff \delta_1 < \min_{x \neq 0}\left(\alpha_1 V(x)^{\frac{1}{\mu}} + \alpha_2 V(x)^{-\frac{1}{\mu}}\right). \end{aligned}$$

Substitute $s = V(x)^{\frac{1}{\mu}}$ to denote $\alpha_1 V(x)^{\frac{1}{\mu}} + \alpha_2 V(x)^{-\frac{1}{\mu}}$ as $\alpha_1 s + \frac{\alpha_2}{s}$. Then, the function $p : \mathbb{R}_+ \to \mathbb{R}$ defined as

$$p(s) := \alpha_1 s + \frac{\alpha_2}{s}$$

is a strictly convex function since $\frac{d^2p}{ds^2} = \frac{2\alpha_2}{s^3} > 0$ for all $k > 0$ and therefore, p has a

unique minimizer in $\mathbb{R}_+$ (see Figure 3.1). The derivative of p reads $\frac{dp}{ds} = \alpha_1 - \frac{\alpha_2}{s^2}$, which has a unique root in $\mathbb{R}_+$ at $s = \sqrt{\frac{\alpha_2}{\alpha_1}}$.[1] Thus the function p attains its minimum value at $s = \left(\frac{\alpha_2}{\alpha_1}\right)^{\frac{1}{2}}$, or equivalently, $\alpha_1 V(x)^{\frac{1}{\mu}} + \alpha_2 V(x)^{-\frac{1}{\mu}}$ attains its minimum value when $V(x) = \left(\frac{\alpha_2}{\alpha_1}\right)^{\frac{\mu}{2}}$. Define

$$V^\star := \left(\frac{\alpha_2}{\alpha_1}\right)^{\frac{\mu}{2}}, \quad \delta^\star := \alpha_1 (V^\star)^{\frac{1}{\mu}} + \alpha_2 (V^\star)^{-\frac{1}{\mu}} = 2\sqrt{\alpha_1 \alpha_2},$$

so that $\alpha_1 V(x)^{\frac{1}{\mu}} + \alpha_2 V(x)^{-\frac{1}{\mu}} \geq \delta^\star$ for all $x \in \mathbb{R}^n$. Thus, for $r < 1$, it holds that $\delta_1 < \delta^\star \leq \alpha_1 V(x)^{\frac{1}{\mu}} + \alpha_2 V(x)^{-\frac{1}{\mu}}$ for all x, and so, $\dot{V}(x) < 0$ for all $x \in \mathbb{R}^n \setminus \{0\}$. Thus, it holds that $D = \mathbb{R}^n$ in the case when $0 \leq r < 1$.

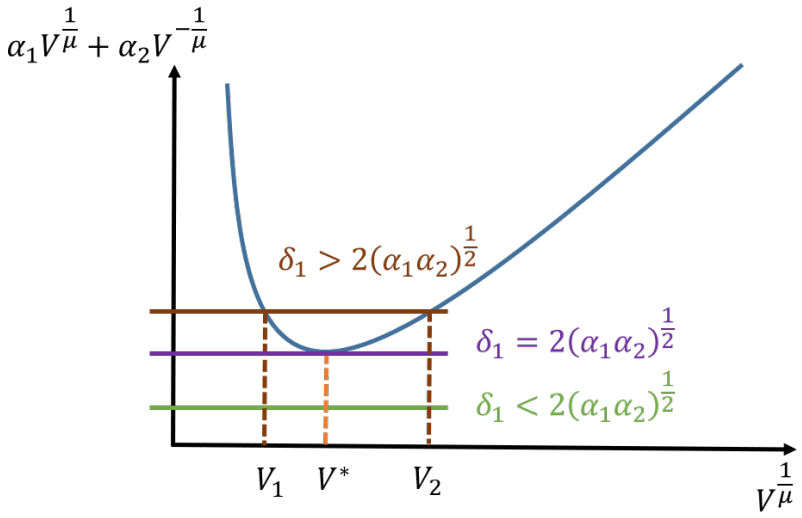

Figure 3.1: Qualitative variation of $h(V) = \alpha_1 V^{\frac{1}{\mu}} + \alpha_2 V^{-\frac{1}{\mu}}$ with V, for $\mu > 1$.

Now, for the case when $r \geq 1$, it holds that $\delta_1 = \alpha_1 V(x)^{\frac{1}{\mu}} + \alpha_2 V(x)^{-\frac{1}{\mu}}$ for all x such that $V(x)^{\frac{1}{\mu}} = V_1$ or $V(x)^{\frac{1}{\mu}} = V_2$, where V_1 and V_2 are given as

$$V_1 := \frac{\delta_1 - \sqrt{\delta_1^2 - 4\alpha_1\alpha_2}}{2\alpha_1}, \quad V_2 := \frac{\delta_1 + \sqrt{\delta_1^2 - 4\alpha_1\alpha_2}}{2\alpha_1},$$

(see Figure 3.1). It can be easily verified that if $r \geq 1$, then for all x such that $V_1 \leq V(x)^{\frac{1}{\mu}} \leq V_2$, the expression $-\alpha_1 V(x)^{\gamma_1} - \alpha_2 V(x)^{\gamma_2} + \delta_1 V(x)$ evaluates to a non-negative value. Also, for all x such that $V(x)^{\frac{1}{\mu}} < V_1$, it holds that $\delta_1 V(x) < \alpha_1 V(x)^{\gamma_1} + \alpha_2 V(x)^{\gamma_2}$.

[1] Only the non-negative root is of interest, since $s = V(x)^{\frac{1}{\mu}} \geq 0$.

Thus, $\dot{V}(x) < 0$ for all $x \in D \setminus \{0\}$ where

$$D = \{x \mid V(x) \leq (kV_1)^\mu\} = \left\{ x \mid V(x) \leq k^\mu \left(\frac{\delta_1 - \sqrt{\delta_1^2 - 4\alpha_1\alpha_2}}{2\alpha_1} \right)^\mu \right\},$$

for all $0 < k < 1$.

So far, the domain of attraction D is computed such that starting from $x(0) \in D$, the system trajectories reach the origin since $\dot{V}(x) < 0$ for all $x \in D \setminus \{0\}$. Next, it is shown that in all the aforementioned cases, the system trajectories reach the origin within a fixed time for all $x(0) \in D$.

Let $x(0) \in D$, so that $\dot{V}(x(t)) \leq 0$ for all $t \geq 0$ per the analysis above. In what follows, the argument $x(t)$ might be omitted for the function V for the sake of brevity. From (3.15), it follows that

$$\begin{aligned}
&\frac{1}{-\alpha_1 V^{\gamma_1} - \alpha_2 V^{\gamma_2} + \delta_1 V} \frac{dV}{dt} \geq 1, \\
\implies &\int_0^T \frac{1}{-\alpha_1 V^{\gamma_1} - \alpha_2 V^{\gamma_2} + \delta_1 V} \frac{dV}{dt} dt = \int_0^T dt, \\
\implies &\int_{V(x(0))}^{V(x(T))} \frac{dV}{-\alpha_1 V^{\gamma_1} - \alpha_2 V^{\gamma_2} + \delta_1 V} \geq \int_0^T dt \\
\implies &\int_{V_0}^{0} \frac{dV}{-\alpha_1 V^{\gamma_1} - \alpha_2 V^{\gamma_2} + \delta_1 V} \geq T,
\end{aligned}$$

where $V_0 = V(x(0))$ and T is the time instant when the trajectories reach the origin, and thus, $V(x(T)) = 0$. The left-hand side of last inequality above is defined as I_1 in Lemma 3.1, and thus, it holds that $T \leq I_1$. The cases when $0 \leq r < 1$ and $r \geq 1$ are considered separately.

First, let $0 \leq r < 1$. Using part (i) in Lemma 3.1, it holds that

$$T \leq I_1 \overset{(3.12)}{\leq} \frac{\mu}{\alpha_1 k_1} \left(\frac{\pi}{2} - \tan^{-1} k_2 \right), \tag{3.18}$$

where $k_1 = \sqrt{\frac{4\alpha_1\alpha_2 - \delta_1^2}{4\alpha_1^2}}$ and $k_2 = -\frac{\sqrt{\delta_1}}{\sqrt{4\alpha_1\alpha_2 - \delta_1^2}}$. Hence, if $\delta_1 < 2\sqrt{\alpha_1\alpha_2}$, it holds that $\dot{V}(x(t)) < 0$ for all $t \geq 0$ and $V(x(t)) = 0$ for all $t \geq T$, for all $x(0) \in \mathbb{R}^n \setminus \{0\}$, where $T \leq \frac{\mu}{\alpha_1 k_1} \left(\frac{\pi}{2} - \tan^{-1} k_2 \right)$. Since V is radially unbounded, the origin is globally FxTS.

Now, for $r \geq 1$, using part (ii) in Lemma 3.1, it holds that

$$T \leq I_1 \overset{(3.13)}{\leq} \frac{\mu}{\alpha_1 (b-a)} \left(\log \left(\frac{b - ka}{a(1-k)} \right) - \log \left(\frac{b}{a} \right) \right), \tag{3.19}$$

where a, b are the roots of $\gamma(z) := \alpha_1 z^2 - \delta_1 z + \alpha_2 = 0$. The bounds on T in (3.18) and (3.19) are independent of the initial condition $x(0)$. Thus, for all $x(0) \in D \setminus \{0\}$, the origin is FxTS. □

A couple of remarks are given on the above result.

Remark 3.2. *Theorem 3.3 implies that satisfaction of (3.15) guarantees FxTS of the origin within a fixed time T for a domain of attraction D. Here the domain of attraction D in (3.16) and the time of convergence T in (3.17) are functions of the ratio $\frac{\delta_1}{2\sqrt{\alpha_1\alpha_2}}$. In particular, if $\frac{\delta_1}{2\sqrt{\alpha_1\alpha_2}} < 1$, then per (3.16), the domain of attraction is the entire $\mathbb{R}^n$, and for a given α_1, α_2, as δ_1 increases, the domain of attraction becomes smaller.*

Remark 3.3. *For the case when $\frac{\delta_1}{2\sqrt{\alpha_1\alpha_2}} > 1$, it holds that $\dot{V}(x) \leq 0$ for all x such that $V(x)^{\frac{1}{\mu}} = V_1$, and therefore, it might not be possible for the system trajectories to reach the origin starting from $x(0)$ such that $V(x(0))^{\frac{1}{\mu}} = V_1$. Thus, the domain D in (3.16) for the case when $\frac{\delta_1}{2\sqrt{\alpha_1\alpha_2}} \geq 1$ is defined using the parameter k in such a manner that it excludes the boundary $\{x \mid V(x)^{\frac{1}{\mu}} = V_1\}$ for all $0 < k < 1$. Note that while $\lim_{k\to 1} D = \{x \mid V(x)^{\frac{1}{\mu}} \leq V_1\}$, it also holds that $\lim_{k\to 1} \bar{T} = \infty$ where $\bar{T}$ is the upper-bound on T in (3.17), verifying that it might not be possible for the system trajectories to reach the origin starting from this boundary.*

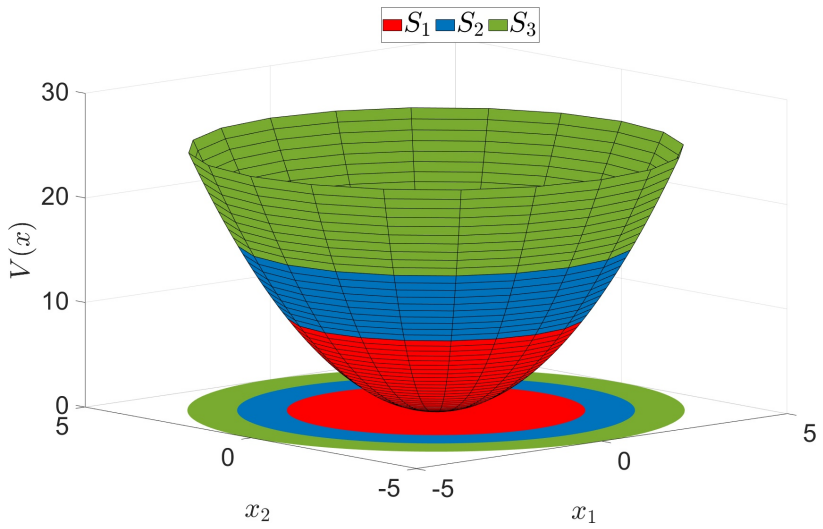

Figure 3.2: Illustration of domains S_1, S_2 and S_3 for the case when $\frac{\delta_1}{2\sqrt{\alpha_1\alpha_2}} > 1$.

The reason that the domain of attraction $D \neq \mathbb{R}^n$ when $\frac{\delta_1}{2\sqrt{\alpha_1\alpha_2}} \geq 1$ is because in this case, there exists a domain where the upper-bound of the time derivative of $V(x)$ takes

positive values. For $\frac{\delta_1}{2\sqrt{\alpha_1\alpha_2}} \geq 1$, the state space gets divided into three disjoint domains, namely $S_1 := \{x \mid V(x)^{\frac{1}{\mu}} < V_1\}$, $S_2 := \{x \mid V_1 \leq V(x)^{\frac{1}{\mu}} \leq V_2\}$ and $S_3 := \{x \mid V(x)^{\frac{1}{\mu}} > V_2\}$ satisfying $S_1 \cup S_2 \cup S_3 = \mathbb{R}^n$ and $S_i \cap S_j = \emptyset$ for all $i \neq j \in \{1, 2, 3\}$, such that $\dot{V}(x) < 0$ for all $x \in S_1 \setminus \{0\}$ as well as for all $x \in S_3$, but $\dot{V}(x)$ might take positive values for $x \in S_2$ (see Figure 3.2). Since $\{0\} \in S_1$ and $S_1 \cap S_3 = \emptyset$, it is not possible for the system trajectories to reach the origin when $x(0) \in S_3$. However, since $\dot{V}(x) < 0$ for all $x \in S_3$ and $S_1 \cup S_2 \subset \mathbb{R}^n \setminus S_3$, it follows that starting from $x(0) \in S_3$, the system trajectories reach an open neighborhood of the set $S_1 \cup S_2$ within a fixed time, as shown below.

Theorem 3.4. *Let $V : \mathbb{R}^n \to \mathbb{R}$ satisfies the assumptions of Theorem 3.3. If $\frac{\delta_1}{2\sqrt{\alpha_1\alpha_2}} > 1$, then the trajectories of (3.1) reach the set D_2 within a fixed time T_2 for all $x(0) \in \mathbb{R}^n \setminus D_2$, where*

$$D_2 = \left\{ x \mid V(x) \leq \tilde{k}^\mu \left(\frac{\delta_1 + \sqrt{\delta_1^2 - 4\alpha_1\alpha_2}}{2\alpha_1} \right)^\mu \right\}, \tag{3.20}$$

$$T_2 \leq \frac{\mu}{\alpha_1(b-a)} \log \left(\frac{\tilde{k}b - a}{\tilde{k}b - b} \right), \tag{3.21}$$

with $\tilde{k} > 1$.

Proof. If $\frac{\delta_1}{2\sqrt{\alpha_1\alpha_2}} \geq 1$, it holds that for all x such that $V(x) > V_2 = \tilde{V}$, the right-hand side of (3.15) is negative (see Figure 3.1). Thus, from part (iii) in Lemma 3.1 that the for all $V_0 \geq \tilde{V}$, the time T_2 required to reach the level set $\{V(x) \leq \tilde{k}^\mu \tilde{V}^\mu\}$ from all $x(0)$ satisfies $T_2 \leq I_2 \leq \frac{\mu}{\alpha_1(b-a)} \log \left(\frac{\tilde{k}b-a}{\tilde{k}b-b} \right)$. Thus, the system trajectories starting outside the set $D_2 = \{x \mid V(x) \leq \tilde{k}^\mu \tilde{V}^\mu\}$ with $\tilde{k} > 1$ reach the set D_2 within a fixed time T_2 where where

$$T_2 \leq \int_{V_0}^{\tilde{V}} \frac{dV}{-\alpha_1 V^{\gamma_1} - \alpha_2 V^{\gamma_2} + \delta_1 V},$$

with $\tilde{V} = k^\mu V_2^\mu$. From part (iii) in Lemma 3.1, it follows that $T_2 \leq I_2 \leq \frac{\mu}{\alpha_1(b-a)} \log \left(\frac{\tilde{k}b-a}{\tilde{k}b-b} \right)$. □

In conclusion, when $\frac{\delta_1}{2\sqrt{\alpha_1\alpha_2}} > 1$, there exits a neighborhood D of the origin, satisfying $D \subset S_1$, such that for all $x(0) \in D$, the system trajectories reach the origin within a fixed time, and there exists a neighborhood D_2 of the set $S_1 \cup S_2$, satisfying $\mathbb{R}^n \setminus D_2 \subset S_3$, such that for all $x(0) \in \mathbb{R}^n \setminus D_2$, the system trajectories reach the domain D_2 within a fixed time (see Figure 3.2 for the geometry of the sets S_1, S_2 and S_3).

3.2.3 Fixed-time stability under input constraints

To see how the condition (3.15) can be used to guarantee FxTS in the presence of control input constraints, consider the same example as in Section 3.2.1. Now, utilizing the new FxTS result from Theorem 3.3, a new QP can be formulated as follows:

$$\min_{u,\delta_1} \quad \frac{1}{2}u^2 + \frac{1}{2}\delta_1^2 + c\delta_1 \tag{3.22a}$$

$$\text{s.t.} \quad \begin{bmatrix} 1 \\ -1 \end{bmatrix} u \leq \begin{bmatrix} u_M \\ -u_m \end{bmatrix}, \tag{3.22b}$$

$$L_f V(x) + L_g V(x) u \leq \delta_1 V(x) - \alpha_1 V(x)^{\gamma_1} - \alpha_2 V(x)^{\gamma_2}, \tag{3.22c}$$

for $x \notin S_G$, where $c > 0$, and $\alpha_1, \alpha_2, \gamma_1, \gamma_2$ are chosen as $\alpha_1 = \alpha_2 = \frac{\mu\pi}{2T_{ud}}$, $\gamma_1 = 1 + \frac{1}{\mu}$ and $\gamma_2 = 1 - \frac{1}{\mu}$ with $\mu > 1$. It is desired that δ_1 takes negative values, since per (3.17), $\delta_1 \leq 0$ implies that the bound on time of convergence satisfies $T \leq \frac{\mu\pi}{2\sqrt{\alpha_1\alpha_2}}$, which in turn implies that $T \leq T_{ud}$, and so, convergence within the user-defined time T_{ud} can be achieved. Thus, the linear term $c\delta_1$ is introduced in the cost function with $c > 0$ in order to penalize non-positive values of δ_1. Here, the term $\delta_1 V(x)$ in (3.22c) can be thought of as a slack term, allowing for satisfaction of the constraint (3.22c) even in the presence of input constraints as shown below.

Lemma 3.2 (Feasibility of QP). *For each $x \notin S_G$, there exist $u(x) \in \mathbb{R}, \delta_1(x) \in \mathbb{R}$ satisfying (3.22b)-(3.22c), i.e., the QP (3.22) is feasible for all $x \notin S_G$.*

Proof. Choose $\bar{u}(x) \in [u_m, u_M]$ so that $\bar{u}(x)$ satisfies the input constraints. Since $x \notin S_G$, it holds that $V(x) > 0$ and so,

$$\bar{\delta}_1(x) := \frac{L_f V(x) + L_g V(x)\bar{u}(x) + \alpha_1 V(x)^{\gamma_1} + \alpha_2 V(x)^{\gamma_2}}{V(x)},$$

is well-defined for all $x \notin S_G$. Note that with $u = \bar{u}(x), \delta_1 = \bar{\delta}_1(x)$, (3.22c) is satisfied with equality. Thus, the pair $(\bar{u}(x), \bar{\delta}_1(x))$ satisfy (3.22b)-(3.22c) for all $x \notin S_G$, and thus, the QP (3.22) is feasible for all $x \notin S_G$. □

As mentioned above, the slack term δ_1 is used to guarantee feasibility of the underlying QP. Now, the relation of this slack term with domain of attraction, input constraints and time of convergence is explored. Let us hypothesize that the slack term corresponding to δ_1 in the QP (3.22) characterizes the trade-off between the domain of attraction and time of convergence for given control input bounds, and between the domain of attraction and the

input bounds for a given time of convergence. Intuitively, for given control input bounds, a larger value of T_{ud} (which results into smaller values of α_1, α_2), i.e., relaxation of time of convergence, should result in satisfaction of (3.22c) with smaller value of δ_1. Conversely, for a given T_{ud} (and thus, for a given pair α_1, α_2), a larger control authority should result into satisfaction of (3.22c) with smaller δ_1. In order to verify this intuition, one can compute the closed-form solution of (3.22) for the case when the control input constraint is active, and see how the parameters T_{ud}, u_m, u_M affect the optimal value of δ_1. To this end, consider the Lagrangian of the QP in (3.22):

$$\begin{aligned} L(u, \delta_1, \lambda_1, \lambda_2, \lambda_3) :=& \frac{1}{2}u^2 + \frac{1}{2}\delta_1^2 + c\delta_1 + \lambda_2(u - u_M) + \lambda_3(u_m - u) \\ &+ \lambda_1(L_f V(x) + L_g V(x)u - \delta_1 V(x) + \alpha_1 V(x)^{\gamma_1} + \alpha_2 V(x)^{\gamma_2}). \end{aligned} \tag{3.23}$$

Now, in order to see the effect of how input constraints affect δ_1, the case when the constraint $u = u_M$ is active is studied under the assumption that $u_M > 0$. Lemma 3.2 guarantees feasibility of the QP in (3.22) for all $x \notin S_G$. Thus, the Slater's condition holds and the Karush-Kuhn-Tucker (KKT) conditions are both necessary and sufficient for optimality (see e.g., [128, Chapter 5]). Using the KKT conditions, it follows that the optimal solution $(u^\star, \delta_1^\star, \lambda_1^\star, \lambda_2^\star, \lambda_3^\star)$ satisfies

$$\begin{aligned} &\delta_1^\star(x) = -c + \lambda_1^\star(x)V(x), \quad u^\star(x) = -\lambda_2^\star(x) + \lambda_3^\star(x) - \lambda_1^\star(x)L_g V(x), \\ &\lambda_1^\star(x) \geq 0, \quad \lambda_2^\star(x) \geq 0, \quad \lambda_3^\star(x) \geq 0, \end{aligned}$$

for all $x \notin S_G$. The following result establishes the optimal value of $\delta_1^\star$ for the case when the upper-bound input constraint is active.

Theorem 3.5 (Slack variable under control saturation). *Consider the QP (3.22) and let $a(x) := L_f V(x) + L_g V(x)u_M + cV + \alpha_1 V(x)^{\gamma_1} + \alpha_2 V(x)^{\gamma_2}$. Then, for $x \in S_M$ where*

$$S_M := \{x \mid a(x)L_g V(x) + u_M V(x)^2 < 0, a(x) > 0\},$$

the optimal value of u is given $u^\star(x) = u_M$ and that of δ_1 is given as

$$\delta_1^\star = \frac{L_f V(x) + L_g V(x)u_M}{V(x)} + \alpha_1 V(x)^{\gamma_1 - 1} + \alpha_2 V(x)^{\gamma_2 - 1}. \tag{3.24}$$

Proof. For $u^\star(x) = u_M$, it is required that $\lambda_2^\star(x) > 0$. Since $u^\star(x) = u_M$ and $u_m < u_M$, it follows that $u^\star(x) > u_m$ (i.e., the lower-bound constraint is inactive) and so $\lambda_3^\star(x) = 0$. It

follows that $\lambda_2^\star(x) = -u_M - \lambda_1^\star(x) L_g V(x)$. In the case when $u = u_M$, it is not possible that (3.22c) is inactive as it requires $\lambda_1^\star(x) = 0$, which implies that $\lambda_2^\star(x) = -u_M < 0$, which violates the optimality condition $\lambda_2^\star(x) \geq 0$. Thus, it is required that $\lambda_1^\star(x) > 0$, which in turn implies that the constraint (3.22c) is active and it follows that the optimal value of δ_1 is given as:

$$\begin{aligned}\delta_1^\star &= \frac{L_f V(x) + L_g V(x) u_M + \alpha_1 V(x)^{\gamma_1} + \alpha_2 V(x)^{\gamma_2}}{V(x)} \\ &= \frac{L_f V(x) + L_g V(x) u_M}{V(x)} + \alpha_1 V(x)^{\gamma_1 - 1} + \alpha_2 V(x)^{\gamma_2 - 1}.\end{aligned}$$

It follows that

$$\begin{aligned}\lambda_1^\star(x) &= \frac{L_f V(x) + L_g V(x) u_M + cV(x) + \alpha_1 V(x)^{\gamma_1} + \alpha_2 V(x)^{\gamma_2}}{V(x)^2} \\ \lambda_2^\star(x) &= -u_M - L_g V(x) \frac{L_f V(x) + L_g V(x) u_M + cV(x) + \alpha_1 V(x)^{\gamma_1} + \alpha_2 V(x)^{\gamma_2}}{V(x)^2}.\end{aligned}$$

Using the definition of function $a(x)$, it follows that

$$\lambda_1^\star(x) = \frac{a(x)}{V(x)^2}, \quad \lambda_2^\star(x) = -u_m - L_g V(x) \frac{a(x)}{V(x)^2}.$$

Now, for $x \in S_M$, it holds that $\lambda_1^\star(x) > 0$ and $\lambda_2^\star(x) > 0$ and thus, the optimal value of δ_1 is given by (3.24) and that of u as $u^\star = u_M$ holds when $x \in S_M$.[2] □

The expression for the optimal value of δ_1 in (3.24) is a function of T_{ud}, the required time of convergence and u_M, the upper-bound on the control input. Recall that the QP (3.22) is defined for $x \notin S_G$ and for $x \in S_M \setminus S_G$, $L_g V(x) < 0$ and $V(x) > 0$. Define $r^\star := \frac{\delta_1^\star}{2\sqrt{\alpha_1 \alpha_2}}$ so that

$$r^\star(x) = \left(\frac{L_f V(x) + L_g V(x) u_M}{V(x)} \right) \frac{T_{ud}}{\mu \pi} + \frac{1}{2} V(x)^{\gamma_1 - 1} + \frac{1}{2} V(x)^{\gamma_2 - 1}. \tag{3.25}$$

Since the region of interest is the one from where the closed-loop trajectories converge to the set S_G, consider (3.25) for the case when $x \in S := S_M \cap \{x \mid L_f V(x) + L_g V(x) u_M < 0\}$. For the restricted domain S, it is clear that $r^\star$ decreases as the control authority increases (i.e., as u_M increases), or the time of convergence requirement relaxes (i.e., as T_{ud} increases). The case when $u = u_m < 0$ can be dealt with using similar arguments.

[2] If the set $S_M = \emptyset$, it implies that there does not exist x such that $u^\star(x) = u_M$, or in other words, the control input never saturates with the upper bound.

Now, in the particular case when $\alpha_1 = \alpha_2$, let us examine how the domain of attraction D in (3.16) is affected by the ratio $r^\star$. Define $r_M = \sup_{x\in S} r^\star(x)$. For $r_M < 1$, it holds that $D = \mathbb{R}^n$, which is the largest possible domain of attraction. For $r_M \geq 1$, it holds that

$$\begin{aligned} D &= \left\{ x \mid V(x) \leq \inf_{z\in S} k^\mu \left(\frac{\delta_1^\star(z) - \sqrt{(\delta_1^\star(z))^2 - 4\alpha_1\alpha_2}}{2\alpha_1} \right)^\mu \right\} \\ &= \left\{ x \mid V(x) \leq \inf_{z\in S} k^\mu \left(r^\star(z) - \sqrt{(r^\star(z))^2 - 1} \right)^\mu \right\}. \end{aligned}$$

Let $D_r := \left\{ x \mid V(x) \leq k^\mu \left(r - \sqrt{r^2-1} \right)^\mu \right\}$ so that $D = D_r$ for all $r \geq 1$. It can be readily verified that $\left(r - \sqrt{r^2-1} \right)$ is a monotonically decreasing function for $r \geq 1$, i.e., $(r_1 - \sqrt{r_1^2-1}) < (r_2 - \sqrt{r_2^2-1})$ and thus, $D_{r_1} \subset D_{r_2}$ for $r_1 > r_2$. Thus, the set D_r shrinks as r increases and therefore, it holds that

$$D = \left\{ x \mid V(x) \leq k^\mu \left(r_M - \sqrt{r_M^2 - 1} \right)^\mu \right\}.$$

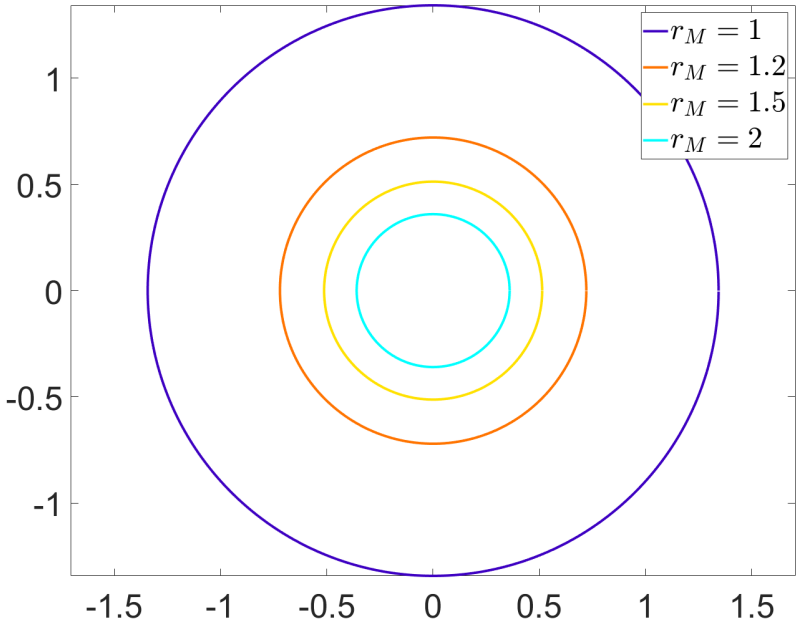

Figure 3.3: Domain of attraction D for $k = 0.95$ and $\mu = 2$.

Figure 3.3 plots the domain of attraction D for $V(x) = \frac{1}{2}\|x\|^2$. It can be seen that the domain D shrinks rapidly as r_M increases. So, it is desired that r_M takes smaller values for the domain of attraction D to be large. Using this and the discussion below (3.25), it can be concluded that for a given input bound, relaxing T_{ud} results in a larger domain of attraction

D, and conversely, for a given T_{ud}, increasing the input bounds results into a larger domain of attraction. Thus, the hypothesis that the parameter for fixed α_1, α_2, the parameter δ_1 characterizes the trade-off between the domain of attraction, time of convergence, and the input bounds is verified.

3.2.4 Robustness perspective

In comparison to Theorem 3.2, Theorem 3.3 allows a linear term $\delta_1 V$ in the upper bound of the time derivative of the Lyapunov function. This property can also capture robustness against a class of Lipschitz continuous, or vanishing, additive disturbance in the system dynamics, as shown in the following result.

Corollary 3.1 (Robustness w.r.t. vanishing disturbances). *Consider the* perturbed *dynamical system*

$$\dot{x} = f(x) + \psi(x), \tag{3.26}$$

where $f, \psi : \mathbb{R}^n \to \mathbb{R}^n$, $f(0) = 0$ *and there exists* $l_\psi > 0$ *such that for all* $x \in \mathbb{R}^n$, $\|\psi(x)\| \leq l_\psi \|x\|$. *Assume that the origin of the* nominal *system* $\dot{x} = f(x)$ *is fixed-time stable, and that there exists a Lyapunov function* V *satisfying conditions of Theorem 3.2 with* $\alpha_1, \alpha_2 > 0$, $\gamma_1 > 1$ *and* $0 < \gamma_2 < 1$. *Additionally, assume that there exist* $k, L > 0$ *such that* $V(x) \geq k\|x\|^2$ *and* $\left\|\frac{\partial V}{\partial x}\right\| \leq L\|x\|$ *for all* $x \in \mathbb{R}^n$. *Then, the origin of the perturbed system* (3.26) *is also FxTS.*

Proof. The time derivative of V along the system trajectories of (3.26) reads

$$\begin{aligned}\dot{V} = \frac{\partial V}{\partial x} f(x) + \frac{\partial V}{\partial x}\psi(x) &\leq -\alpha_1 V^{\gamma_1} - \alpha_2 V^{\gamma_2} + L l_\psi \|x\|^2 \\ &\leq -\alpha_1 V^{\gamma_1} - \alpha_2 V^{\gamma_2} + \frac{L l_\psi}{k} V.\end{aligned}$$

Hence, using Theorem 3.3, it holds that the origin of (3.26) is FxTS for all $x(0) \in D$, where D is a neighborhood of the origin. As per the conditions of Theorem 3.3, $D \subset \mathbb{R}^n$ or $D = \mathbb{R}^n$, depending upon the parameters $\alpha_1, \alpha_2, \gamma_1, \gamma_2, k, L$ and l_ψ. □

Thus, the new FxTS conditions in Theorem 3.3 can also be used to guarantee FxTS of the origin in the presence of a class of vanishing disturbances. In particular, Corollary 3.1 shows that FxTS is preserved under the effect of a class of additive, vanishing disturbances.

3.3 New Lyapunov conditions for fixed-time stability: second result

3.3.1 Lyapunov conditions

Inspired from results in the previous section, this section explores the possibility of introducing a constant term, as opposed to a linear term, in the upper-bound of the time derivative of the Lyapunov function. In particular, the following Lyapunov condition is considered for a positive definite, proper, continuously differentiable $V : \mathbb{R}^n \to \mathbb{R}$:

$$\dot{V}(x) \leq -\alpha_1 V(x)^{\gamma_1} - \alpha_2 V(x)^{\gamma_2} + \bar{\delta}_1, \tag{3.27}$$

with $\alpha_1, \alpha_2 > 0$, $\bar{\delta}_1 \in \mathbb{R}$, $\gamma_1 = 1 + \frac{1}{\mu}$, $\gamma_2 = 1 - \frac{1}{\mu}$ and $\mu > 1$, introducing $\bar{\delta}_1$ as the additional *constant* term in the time derivative of $V(x)$ as compared to (3.4). Before presenting the main result, the following lemma is needed, which gives the expressions for the integration of (3.27) for various relative values of $\bar{\delta}_1$ and $2\sqrt{\alpha_1\alpha_2}$. The following lemma is needed to prove the second main result of this chapter.

Lemma 3.3 (Bounds on convergence time). *Let $V_0, \alpha_1, \alpha_2 > 0$, $\gamma_1 = 1 + \frac{1}{\mu}$ and $\gamma_2 = 1 - \frac{1}{\mu}$, where $\mu > 1$. Define*

$$I := \int_{V_0}^{\bar{V}} \frac{dV}{-\alpha_1 V^{\gamma_1} - \alpha_2 V^{\gamma_2} + \bar{\delta}_1}. \tag{3.28}$$

Then, the following holds:

(i) If $0 \leq \bar{\delta}_1 < 2\sqrt{\alpha_1\alpha_2}$, it holds that for all $V_0 \geq \bar{V} = 1$

$$I \leq \frac{\mu}{\alpha_1 k_1}\left(\frac{\pi}{2} - \tan^{-1} k_2\right), \tag{3.29}$$

where $k_1 = \sqrt{\frac{4\alpha_1\alpha_2 - \bar{\delta}_1^2}{4\alpha_1^2}}$ and $k_2 = \frac{2\alpha_1 - \bar{\delta}_1}{\sqrt{4\alpha_1\alpha_2 - \bar{\delta}_1^2}}$;

(ii) If $\bar{\delta}_1 \geq 2\sqrt{\alpha_1\alpha_2}$ and $V_0 \geq \bar{V} = k^\mu\left(\frac{\bar{\delta}_1 + \sqrt{\bar{\delta}_1^2 - 4\alpha_1\alpha_2}}{2\alpha_1}\right)^\mu$ with $k > 1$, it holds that for all $V_0 \geq \bar{V}$

$$I \leq \frac{\mu}{\alpha_1(b-a)} \log\left(\frac{kb-a}{kb-b}\right),$$

where a, b are the roots of $\gamma(z) := \alpha_1 z^2 - \bar{\delta}_1 z + \alpha_2 = 0$;

The proof is provided in Appendix B.2. The second new result on FxTS can now be stated.

Theorem 3.6 (New Lyapunov conditions for FxTS). *Let $V : \mathbb{R}^n \to \mathbb{R}$ be a continuously differentiable, positive definite, radially unbounded function, satisfying*

$$\dot{V}(x) \leq -\alpha_1 V(x)^{\gamma_1} - \alpha_2 V(x)^{\gamma_2} + \bar{\delta}_1, \tag{3.30}$$

for all $x \in \mathbb{R}^n$ with $\alpha_1, \alpha_2 > 0$, $\bar{\delta}_1 \in \mathbb{R}$, $a_1 = 1 + \frac{1}{\mu}$, $a_2 = 1 - \frac{1}{\mu}$ and $\mu > 1$, along the trajectories of (3.1). Then, there exists a neighborhood $\bar{D}$ of the origin such that for all $x(0) \in \mathbb{R}^n \setminus \bar{D}$, the trajectories of (3.1) reach $\bar{D}$ in a fixed time $\bar{T}$, where

$$\bar{D} = \begin{cases} \{0\}, & \frac{\bar{\delta}_1}{2\sqrt{\alpha_1\alpha_2}} \leq 0, \\ \{x \mid V(x) \leq \frac{\bar{\delta}_1}{2\sqrt{\alpha_1\alpha_2}}\}, & 0 < \frac{\bar{\delta}_1}{2\sqrt{\alpha_1\alpha_2}} < 1, , \\ \{x \mid V(x) \leq k^{\mu}\left(\frac{\bar{\delta}_1 + \sqrt{\bar{\delta}_1^2 - 4\alpha_1\alpha_2}}{2\alpha_1}\right)^{\mu}\}; & \frac{\bar{\delta}_1}{2\sqrt{\alpha_1\alpha_2}} \geq 1, \end{cases} \tag{3.31}$$

$$\bar{T} \leq \begin{cases} \frac{\mu\pi}{2\sqrt{\alpha_1\alpha_2}}, & \frac{\bar{\delta}_1}{2\sqrt{\alpha_1\alpha_2}} \leq 0, \\ \frac{\mu}{\alpha_1 k_1}\left(\frac{\pi}{2} - \tan^{-1} k_2\right), & 0 < \frac{\bar{\delta}_1}{2\sqrt{\alpha_1\alpha_2}} < 1, , \\ \frac{\mu}{\alpha_1(b-a)} \log\left(\frac{kb-b}{kb-a}\right); & \frac{\bar{\delta}_1}{2\sqrt{\alpha_1\alpha_2}} \geq 1, \end{cases} \tag{3.32}$$

where $k > 1$, a, b are the solutions of $\gamma(z) = \alpha_1 z^2 - \delta_1 z + \alpha_2 = 0$, $k_1 = \sqrt{\frac{4\alpha_1\alpha_2 - \bar{\delta}_1^2}{4\alpha_1^2}}$, and $k_2 = -\frac{\bar{\delta}_1}{\sqrt{4\alpha_1\alpha_2 - \delta_1^2}}$.

Proof. Note that for $\bar{\delta}_1 \leq 0$, the inequality (3.4) can be obtained from (3.30), and so FxTS of the origin is guaranteed for all $x \in \mathbb{R}^n$, and thus, $\bar{D} = \{0\}$. Thus, the case when $\bar{\delta}_1 > 0$ is considered, for which sufficiently small values of $V(x)$ cause the right hand side of (3.30) to become positive. The proof follows from Lemma 3.3. Consider (3.30) and let $x(0)$ be such that $\bar{\delta}_1 < \alpha_1 V(x(0))^{\gamma_1} + \alpha_2 V(x(0))^{\gamma_2}$. Integrate $\dot{V}(x)$ to obtain:

$$\int_{V_0}^{V(x(T))} \frac{1}{-\alpha_1 V^{\gamma_1} - \alpha_2 V^{\gamma_2} + \bar{\delta}_1} dV \geq \int_0^T dt = T, \tag{3.33}$$

where $V_0 \coloneqq V(x(0))$ and T is the time when the system trajectories first reach the domain $\bar{D}$. It is easy to show that for each of the cases listed in the theorem statement, $\alpha_1 V(x)^{\gamma_1} + \alpha_2 V(x)^{\gamma_2} > \bar{\delta}_1$ for all $x \in \mathbb{R}^n \setminus \bar{D}$ and thus the right-hand side of (3.30) is negative for all $x \notin \bar{D}$ for the corresponding $\bar{D}$. Now, to show that the system trajectories converge to $\bar{D}$ within a fixed time, the upper bounds on $\bar{T}$ are computed.

For the case when $\bar{\delta}_1 < 2\sqrt{\alpha_1\alpha_2}$, part (i) in Lemma 3.3 provides an upper bound on the left-hand side of (3.33) for $x \notin \bar{D} = \{x \mid V(x) \leq \frac{\bar{\delta}_1}{2\sqrt{\alpha_1\alpha_2}}\}$. Similarly, for the case $\bar{\delta}_1 \geq 2\sqrt{\alpha_1\alpha_2}$, part (ii) of Lemma 3.3 provides upper bounds on the left-hand side of (3.33). Thus, the domains $\bar{D}$ and the bounds on convergence times $\bar{T}$ for the various cases can be obtained directly from Lemma 3.3. Since for all three cases, $\bar{T} < \infty$ and is independent of the initial conditions, it follows that the system trajectories reach the set $\bar{D}$ within a fixed time $\bar{T}$. □

Note the difference between the results in Theorem 3.3 and Theorem 3.6. The first part of Theorem 3.3 guarantees that there exists a domain D such that for all $x(0) \in D$, the system trajectories converge to the origin within a fixed time T, i.e., the trajectories starting in the domain D reach the origin within a fixed time. On the other hand, analogues to the second part in Theorem 3.3 with $\frac{\delta_1}{2\sqrt{\alpha_2\alpha_2}}$, Theorem 3.6 guarantees that there exists a domain $\bar{D}$ such that for all $x(0) \in \mathbb{R}^n \setminus \bar{D}$, the system trajectories converge to the set $\bar{D}$ within a fixed time $\bar{T}$, i.e., the trajectories starting outside the set $\bar{D}$ reach this set within a fixed time.

3.3.2 Relation to input constraints

Similar as in Section 3.2.3, in order to see how the condition (3.30) can be used to guarantee FxTS to a domain D in the presence of control input constraints, consider the system (3.7) with the objective of driving the closed-loop trajectories of (3.7) to the set $S_G = \{x \mid V(x) \leq 0\}$ where $V : \mathbb{R} \to \mathbb{R}$ is a continuously differentiable function with the input constraints $u_m \leq u \leq u_M$ where $u_m < u_M$. Consider the QP :

$$\min_{\bar{u},\bar{\delta}_1} \ \frac{1}{2}\bar{u}^2 + \frac{1}{2}\bar{\delta}_1^2 + c\bar{\delta}_1 \tag{3.34a}$$

$$\text{s.t.} \quad u_m \leq \bar{u}, \tag{3.34b}$$

$$\bar{u} \leq u_M, \tag{3.34c}$$

$$L_fV(x) + L_gV(x)\bar{u} \leq \bar{\delta}_1 - \alpha_1 V(x)^{\gamma_1} - \alpha_2 V(x)^{\gamma_2}, \tag{3.34d}$$

for $x \notin S_G$, where $c > 0$, and $\alpha_1, \alpha_2, \gamma_1, \gamma_2$ are chosen as $\alpha_1 = \alpha_2 = \frac{\mu\pi}{2T_{ud}}$, $\gamma_1 = 1 + \frac{1}{\mu}$ and $\gamma_2 = 1 - \frac{1}{\mu}$ with $\mu > 1$ for a user-defined time $T_{ud} > 0$.

Let us again hypothesize that the slack term corresponding to $\bar{\delta}_1$ in the QP (3.34) characterizes the trade-off between the domain of convergence and time of convergence for given control input bounds, and between the domain of convergence and the input bounds for a given time of convergence. Intuitively, for given control bounds, a larger value of T_{ud}

(which results into smaller values of α_1, α_2), i.e., relaxation of time of convergence, should result in satisfaction of (3.34d) with smaller value of $\bar{\delta}_1$. Conversely, for a given T_{ud} (and thus, for a given pair α_1, α_2), a larger control authority should result into satisfaction of (3.34d) with smaller $\bar{\delta}_1$. In order to verify this intuition, one can compute the closed-form solution of (3.34) for the case when the control input constraint is active, and see how the parameters T_{ud}, u_m, u_M affect the optimal value of $\bar{\delta}_1$. To this end, consider the Lagrangian of the QP in (3.34):

$$\begin{aligned}\bar{L}(\bar{u}, \bar{\delta}_1, \bar{\lambda}_1, \bar{\lambda}_2, \bar{\lambda}_3) :=& \frac{1}{2}u^2 + \frac{1}{2}\bar{\delta}_1^2 + c\bar{\delta}_1 + \bar{\lambda}_2(u - u_M) + \bar{\lambda}_3(u_m - u) \\ &+ \bar{\lambda}_1(L_f V(x) + L_g V(x)u - \bar{\delta}_1 + \alpha_1 V^{\gamma_1} + \alpha_2 V^{\gamma_2}).\end{aligned} \tag{3.35}$$

Now, in order to see the effect of how input constraints affect $\bar{\delta}_1$, assume that the constraint $u = u_M$ is active and that $u_M > 0$. Following the analysis in Section 3.2.3, it can be shown that the optimal value of the ratio $\bar{r} := \frac{\bar{\delta}_1}{2\sqrt{\alpha_1\alpha_2}}$ and u are given as:

$$\bar{r}^\star(x) = (L_f V(x) + L_g V(x) u_M)\frac{T_{ud}}{\mu\pi} + \frac{1}{2}V(x)^{\gamma_1} + \frac{1}{2}V(x)^{\gamma_2}, \tag{3.36}$$

$$\bar{u}^\star(x) = u_M, \tag{3.37}$$

for $x \in \bar{S}_M \setminus S_G$ where $\bar{S}_M := \{x \mid \bar{a}(x)L_g V(x) + u_M < 0, \bar{a}(x) > 0\}$ with $\bar{a}(x) := L_f V(x) + L_g V(x)u_M + c + \alpha_1 V(x)^{\gamma_1} + \alpha_2 V(x)^{\gamma_2}$. Since the region of interest is the one from where the closed-loop trajectories converge to the neighborhood $\bar{D}$ of the set S_G, consider (3.36) for the case when $x \in \bar{S} := \bar{S}_M \cap \{x \mid L_f V(x) + L_g V(x)u_M \leq 0\}$. For this restricted domain, it is clear that $\bar{r}^\star$ in (3.36) decreases as the control authority increases (i.e., as u_M increases), or the time of convergence requirement relaxes (i.e., as T_{ud} increases).

Again, in the particular case when $\alpha_1 = \alpha_2$, let us examine how the domain of convergence D in (3.31) is affected by the ratio $\bar{r}$. Unlike domain of attraction D in Section 3.2.3, it is desired that the domain of convergence $\bar{D}$ in this case is as small as possible, so that the closed-loop trajectories reach closer to the goal set. Define $\bar{r}_M = \sup_{x\in\bar{S}} \bar{r}^\star$ so that for $\bar{r}_M \leq 0$, it holds that $\bar{D} = \{x \mid V(x) \leq 0\} = S_G$, which is the smallest possible domain of convergence. For $0 < \bar{r}_M < 1$, it holds that $D = \{x \mid V(x) \leq r_M\}$. For $\bar{r}_M \geq 1$, it holds

that

$$\bar{D} = \left\{ x \mid V(x) \leq k^{\mu} \sup_{z \in \bar{S}} \left(\frac{\bar{\delta}_1^{\star}(z) + \sqrt{(\bar{\delta}_1(z)^{\star})^2 - 4\alpha_1\alpha_2}}{2\alpha_1} \right)^{\mu} \right\}$$
$$= \left\{ x \mid V(x) \leq \sup_{z \in \bar{S}} k^{\mu} \left(\bar{r}^{\star}(z) + \sqrt{(\bar{r}(z)^{\star})^2 - 1} \right)^{\mu} \right\}.$$

Let $\bar{D}_r := \left\{ x \mid V(x) \leq k^{\mu} \left(r + \sqrt{r^2 - 1} \right)^{\mu} \right\}$ so that $\bar{D} = \bar{D}_r$ for all $r \geq 1$. It can be readily verified that $\left(r + \sqrt{r^2 - 1} \right)$ is a monotonically increasing function for $r \geq 1$, i.e., $(r_1 + \sqrt{r_1^2 - 1}) > (r_2 + \sqrt{r_2^2 - 1})$ and thus, $\bar{D}_{r_2} \subset \bar{D}_{r_1}$ for $r_1 > r_2$. Thus, it holds that

$$\bar{D} = \left\{ x \mid V(x) \leq k^{\mu} \left(\bar{r}_M + \sqrt{\bar{r}_M^2 - 1} \right)^{\mu} \right\}.$$

It is desired that $\bar{r}_M$ takes smaller values for the domain of convergence $\bar{D}$ to be small. Using this and the discussion above, it can be concluded that for a given input bound, relaxing $\bar{T}_{ud}$ results into a smaller domain of convergence $\bar{D}$, and conversely, for a given $\bar{T}_{ud}$, increasing the input bounds results into a smaller domain of convergence. Thus, the hypothesis that the parameter for fixed α_1, α_2, the parameter $\bar{\delta}_1$ characterizes the trade-off between the domain of convergence, time of convergence, and the input bounds is verified.

3.3.3 Robustness perspective

Theorem 3.6 can be used to show the robustness of a FxTS origin against a class of non-vanishing, bounded, additive disturbance in the system dynamics, as shown next.

Corollary 3.2 (Robustness w.r.t. non-vanishing disturbances). *Consider the* perturbed *dynamical system*

$$\dot{x} = f(x) + \phi(x), \tag{3.38}$$

where $f, \psi : \mathbb{R}^n \to \mathbb{R}^n$, $f(0) = 0$ and there exists $l_\phi > 0$ and a neighborhood $D_\phi \subset \mathbb{R}^n$ of the origin such that $\|\phi(x)\| \leq l_\phi$ for all $x \in D_\phi$. Assume that the origin of the nominal *system $\dot{x} = f(x)$ is fixed-time stable, and that there exists a Lyapunov function V satisfying conditions of Theorem 3.2 where $\alpha_1, \alpha_2 > 0$, $\gamma_1 > 1$ and $0 < \gamma_2 < 1$. Additionally, assume that there exists $L > 0$ such that $\left\| \frac{\partial V}{\partial x}(x) \right\| \leq L$ for all $x \in D_\phi$. Then, there exists $\bar{D} \subset D_\phi$ such that for all $x(0) \in \mathbb{R}^n \setminus \bar{D}$, the trajectories of (3.38) reach the set $\bar{D}$ within a fixed time $\bar{T} < \infty$.*

Proof. The time derivative of $V(x)$ along the system trajectories of (3.38) reads

$$\begin{aligned}\dot{V}(x) = \frac{\partial V}{\partial x}(f(x)+\phi(x)) = \frac{\partial V}{\partial x}f(x) + \frac{\partial V}{\partial x}\phi(x) &\leq -\alpha_1 V^{\gamma_1} - \alpha_2 V^{\gamma_2} + \frac{\partial V}{\partial x}\phi(x) \\ &\leq -\alpha_1 V^{\gamma_1} - \alpha_2 V^{\gamma_2} + L l_\phi.\end{aligned}$$

Hence, using Theorem 3.6, it follows that there exists $\bar{D} \subset D_\phi$ such that all solutions starting outside $\bar{D}$ reach the set $\bar{D}$ in a fixed time $\bar{T}$, where the set $\bar{D}$ and the convergence time $\bar{T}$ are functions of $\alpha_1, \alpha_2, \gamma_1, \gamma_2, L$ and l_ϕ. □

Note that in the presence of non-vanishing disturbances, it is not possible to guarantee that the system trajectories converge to the equilibrium point. Instead, (3.31) characterizes an estimate, $\bar{D}$, of a neighborhood of the equilibrium to where system trajectories are guaranteed to converge within a fixed-time, $\bar{T}$, and (3.32) provides an upper bound independent of $x(0)$ on $\bar{T}$.

3.4 Simulations

In this section, one numerical case study is presented on an academic example to demonstrate the relationship between the input constraints, time of convergence and the slack variable δ. Consider the following system:

$$\begin{aligned}\dot{x}_1 &= x_2 + x_1(x_1^2 + x_2^2 - 1) + x_1 u, \\ \dot{x}_2 &= -x_1 + \zeta(x_2)(x_1^2 + x_2^2 - 1) + x_2 u,\end{aligned}$$

where $x = [x_1, x_2]^T \in \mathbb{R}^2$, $u \in \mathbb{R}$, $\zeta(z) = (0.8 + 0.2e^{-100|z|})\tanh(z)$ and $S_G = \{x \mid \|x\| \leq 1\}$. Note that in the absence of the control input, the trajectories diverge away from S_G, i.e., the set S_G is unstable for the open-loop system. Define $h_G(x) = \|x\|^2 - 1$ and let the control input bounds be of the form $\|u\| \leq u_{max}$, where $u_{max} > 0$. The initial conditions are chosen as $x(0) = [3.33, 1.33]^T$.

The simulations are performed with $\mu = 2$. First, the effect of the control input bound on the maximum value of δ_1 is studied by fixing $T_{ud} = 1$, and varying u_{max}. Figure 3.4 plots the maximum value of $\max_x \delta_1(x)$ for various values of $u_{max} \in [16\ ,\ 25]$.[3] It can be observed that δ_1 decreases as the control authority u_{max} of the system increases.

Figure 3.5 plots the control input $u(t)$ with time for various values of u_{max}. The value of u_{max} increases from 16 to 25 from blue to red. Note that the input saturates in the beginning

[3] Since the open-loop system is unstable, for given set of initial conditions, it is observed that the closed-loop trajectories diverge for $u_{max} \leq 16$.

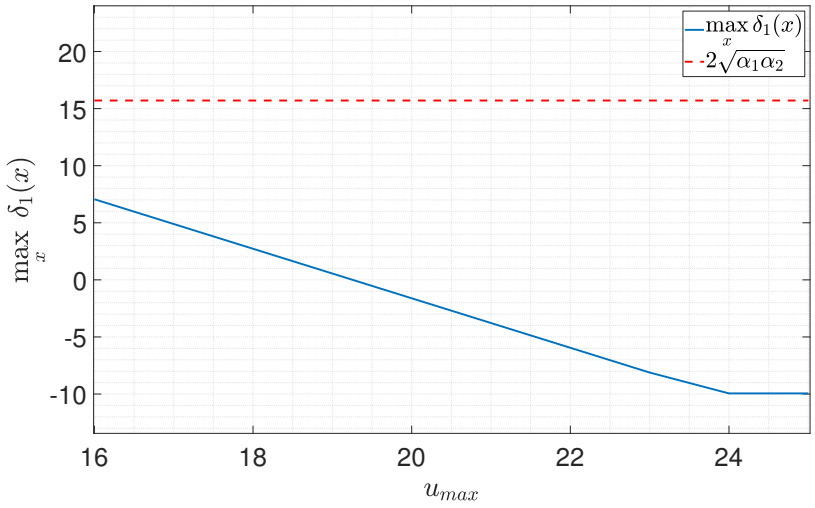

Figure 3.4: Variation of $\max \delta_1$ for various control input bounds u_{max}.

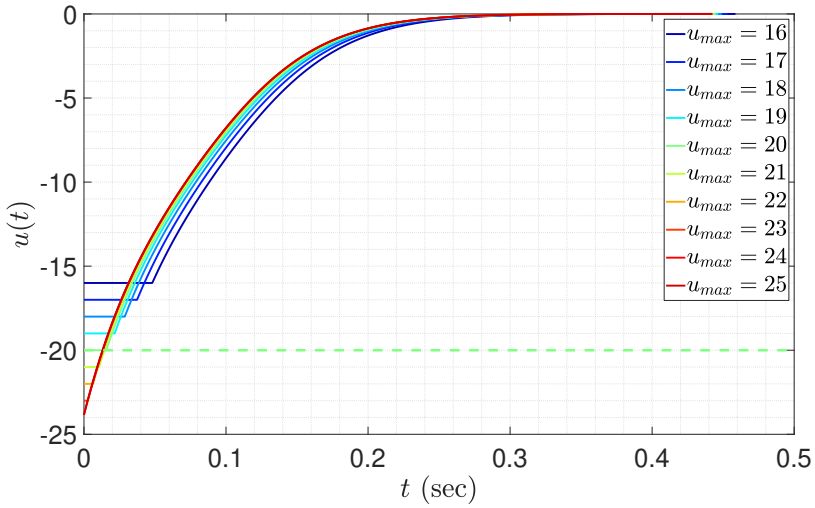

Figure 3.5: Control input $u(t)$ for various control input bounds u_{max}.

by u_{max} for $u_{max} \leq 24$ (the lower-bound input constraint is shown for the case when $u_{max} = 20$ with dashed line). It can be observed that in every case, the system trajectories do utilize the maximum available control authority at the beginning of the simulation, while the control input decreases to zero as the system trajectories approach the goal set.

Figure 3.6 plots the energy utilized by the system in terms of the integral $\int_0^T \|u(t)\|^2 dt$ for various values of u_{max}. The total energy decreases by about 8% as the maximum control authority increases from 16 to 25. This is also evident from Figure 3.7, which plots the different paths traced by the system from various values of u_{max}. It can be observed that as the control authority increases, the path length decreases, which results in a decrease in the utilized energy.

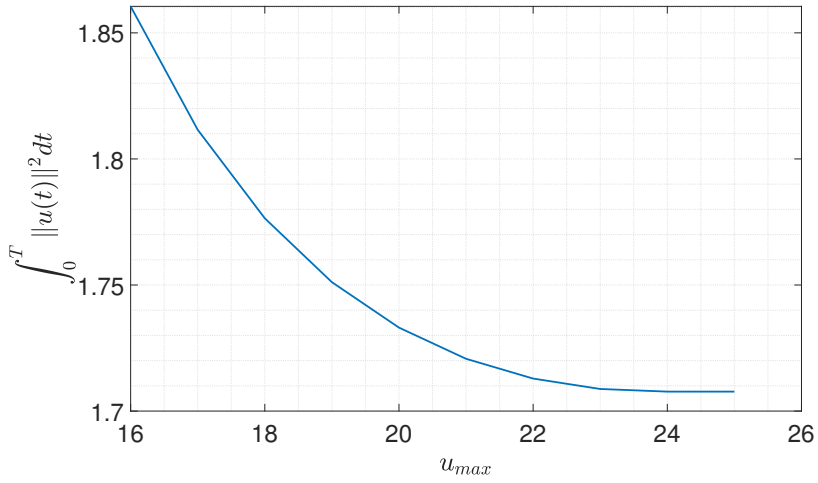

Figure 3.6: Energy $\int_0^T \|u(t)\|^2 dt$ for various control input bounds u_{max}.

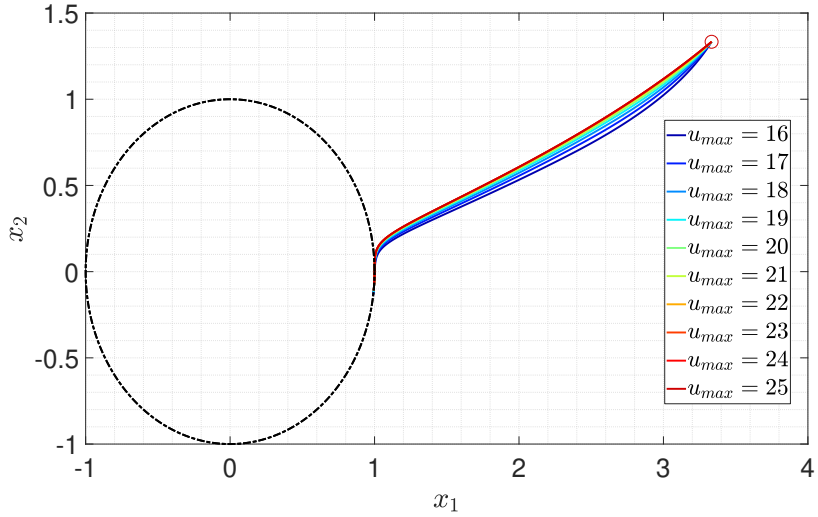

Figure 3.7: Closed-loop trajectories for various control input bounds u_{max}.

Next, control authority is kept fixed with $u_{max} = 16$ and the required time of convergence T is varied between 1 and 10. Figure 3.8 shows the variation of $\max_x \delta_1(x)$ as a function of the convergence time T. As T increases (or equivalently, α_1, α_2 decrease), the maximum value of $\delta_1(\cdot)$ decreases. This implies that for a larger time of convergence, there is a larger domain of attraction starting from which convergence can be achieved in the given time.

These (numerical) relations indicate that for a required domain of attraction D, one can choose the parameters u_{max} and T so that FxTS can be guaranteed for all initial conditions in D. Conversely, for a given input bound and required time of convergence, it is possible to find the largest domain of attraction by computing the maximum value of δ_1.

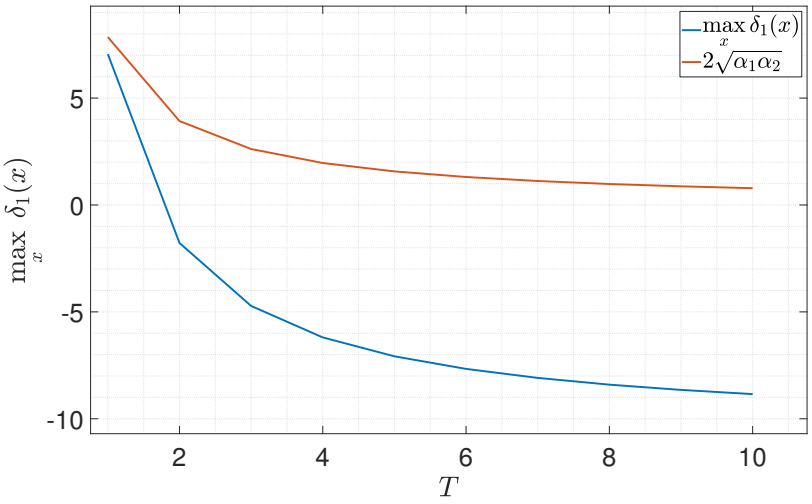

Figure 3.8: Variation of $\max \delta_1$ for various user-defined convergence time T.

3.5 Conclusions

In this chapter, two new results on FxTS are presented by allowing a possibly positive linear or constant term to appear in the time derivative of the Lyapunov function. In the first case, the domain of attraction, as well as the upper bound on the time of convergence for fixed-time stability, are characterized as functions of the coefficients of the positive and the negative terms in the upper bound of the time derivative of the Lyapunov function. The relationship between control authority, time of convergence, and the domain of attraction are discussed. In the second case, the estimate of the neighborhood of the equilibrium point, as well as the upper bound on the time of convergence to this neighborhood are characterized as functions of the ratio of the new constant and the coefficients of the negative terms in the upper bound of the time derivative of the Lyapunov function.

The proposed Lyapunov conditions can be used for control synthesis with FxTS guarantees. In the next chapter, problems involving both safety and convergence requirements are studied in the presence of input constraints, and a control synthesis framework based on quadratic programming is developed.

CHAPTER 4

Control Synthesis via Quadratic Programming

In this chapter, the problem of designing control inputs so that system trajectories remain in a safe set while converging to a goal set within a user-defined time is considered. Figure 4.1 shows a scenario of a motivating problem requiring a quadrotor to remain in a domain (acting as a safe set) that consists of the region bounded by the green boundary and excludes the regions marked in red. Furthermore, the blue regions denote the goal sets, which the quadrotor is required to visit in a given time sequence.

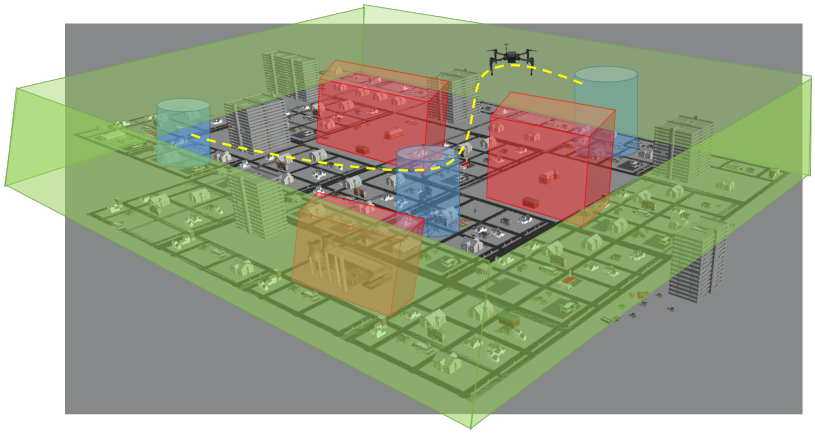

Figure 4.1: Motivating example scenario for a motion planning problem governed by spatiotemporal constraints.

In contrast to Chapter 2 where double-integrator systems are considered, this chapter studies the problem of control synthesis for systems modeled via a general class of nonlinear, control-affine dynamics. Furthermore, while the focus of Chapter 2 is on designing FTS controllers, in this chapter, the stronger notion of FxTS is considered to guarantee convergence within a user-defined time.

First, the nominal case without disturbances and with perfect state knowledge is considered in Section 4.2. Utilizing the new FxTS results from Chapter 3, this section studies a

QP-based formulation to compute the control input that renders a safe set forward invariant and drives the closed-loop trajectories to a goal set within a user-defined time. It is shown that the proposed QP is feasible, that the solution of the QP is a continuous function of the state variables, and the cases when the solution of the QP solves the considered problem of control design are discussed. The results in this section are based on [111]. The author wishes to acknowledge his co-author Dr. Ehsan Arabi for contributions in the development of some of the results presented in this section.

Then, the case with an additive disturbance in the system dynamics and imperfect state estimation is considered in Section 4.3. The notion of robust CBF is utilized to guarantee forward invariance of the safe set while incorporating both the disturbance in the system dynamics as well as the state estimation error. Besides, the novel concept of robust FxT-CLF is utilized to guarantee convergence to the goal set within the user-defined time. Finally, the robust FxT-CLF and the robust CBF conditions are utilized in a QP formulation, and it is shown that the proposed QP is feasible and that the control input defined as the solution of the QP solves the underlying constrained control design problem under certain assumptions. The results in this section are based on [112]. Two numerical case studies are presented in Section 4.4 corroborating the efficacy of the proposed method in control design for multi-task multi-agent problems.

The following notation is frequently used in this chapter:

$\mathbb{R}$	the set of real numbers
$\mathbb{R}_+$	Set of non-negative reals
$\|\cdot\|_p$	p-norm of $(\cdot)$
$\|\cdot\|$	Euclidean norm of $(\cdot)$
$\mathcal{C}^k$	k-times continuously differentiable functions
$L_f V(x)$	Lie derivative of $V \in \mathcal{C}^1$ along f defined as $\frac{\partial V}{\partial x} f(x)$
$\mathcal{U}$	Input-constraint set
S_S	Safe set
S_G	Goal set
T_{ud}	User-defined convergence time
∂S	Boundary of the closed set S
$\text{int}(S)$	Interior of the closed set S
$\|x\|_S$	Distance x from the set S defined as $\inf_{y \in S} \|x - y\|$
$x \leq y$	Element-wise inequalities $x_i \leq y_i, i = 1, 2, \ldots, n$
$\emptyset$	Empty set

4.1 Mathematical preliminaries

4.1.1 Problem formulation

Consider the control affine dynamical system:

$$\dot{x}(t) = f(x(t)) + g(x(t))u, \quad x(0) = x_0, \tag{4.1}$$

where $x \in \mathbb{R}^n$ is the state vector, $f : \mathbb{R}^n \to \mathbb{R}^n$ and $g : \mathbb{R}^n \to \mathbb{R}^{n\times m}$ are system vector fields, continuous in their arguments, and $u \in \mathbb{R}^m$ is the control input vector. In addition, define a safe set $S_S := \{x \mid h_S(x) \leq 0\}$, and consider a goal set to be reached in a user-defined time $T_{ud} > 0$ defined as $S_G := \{x \mid h_G(x) \leq 0\}$, where $h_S, h_G : \mathbb{R}^n \to \mathbb{R}$ are user-defined functions. The arguments t, x are dropped whenever clear from the context. A few special classes of functions are required in this chapter as defined below.

Definition 4.1. *A function $\alpha : \mathbb{R}_+ \to \mathbb{R}_+$ is called*

- ***Class-$\mathcal{K}$ function**: if it is continuous, increasing, i.e., for all $x > y \geq 0$, $\alpha(x) > \alpha(y)$ with $\alpha(0) = 0$;*
- ***Class-$\mathcal{K}_\infty$ function**: if it is a class-$\mathcal{K}$ function, and $\lim_{r\to\infty} \alpha(r) = \infty$;*

Definition 4.2. *(**Class-$\mathcal{KL}$ function**): A function $\kappa : \mathbb{R}_+ \times \mathbb{R}_+ \to \mathbb{R}_+$ is a class-$\mathcal{KL}$ function if*

1) for all $t \geq 0$, the map $\kappa(r, t)$ belongs to class-$\mathcal{K}$ and

2) for all $r \geq 0$, the map $\kappa(r, t)$ is decreasing in t with $\kappa(r, t) \to 0$ as $t \to \infty$.

The notion of positive-definiteness w.r.t. a set is defined below:

Definition 4.3 (Positive definite). *A function $V : \mathbb{R}^n \to \mathbb{R}$ is positive definite w.r.t. a compact set S if $V(x) = 0$ for all $x \in \partial S$ and $V(x) > 0$ for all $x \notin S$.*

Similarly, the notion of radial-unboundedness can be defined w.r.t. a compact set:

Definition 4.4 (Radially unbounded). *A function $V : \mathbb{R}^n \to \mathbb{R}$ is radially unbounded w.r.t. a compact set S if there exits $\alpha \in \mathcal{K}_\infty$ such that $V(x) \geq \alpha(|x|_S)$ for all $x \notin S$.*

Note that the traditional notions of positive definiteness and radial-unboundedness follows from the above definitions by setting $S = \{0\}$. The following standing assumption is made.

Assumption 4.1 (Safe and goal sets). *The functions $h_S(x), h_G(x) \in \mathcal{C}^1$, $S_G \bigcap S_S \neq \emptyset$, the set S_G is compact, and the sets S_S and S_G have non-empty interiors. Furthermore, the function h_G is radially unbounded w.r.t. S_G.*

4.1.2 Forward invariance

Since the system trajectories are required to stay in the set S_S at all times, the set S_S can be thought of as a safe set, or its complement set $\mathbb{R}^n \setminus S_S$, an unsafe set. Forward-invariance of a set is defined as:

Definition 4.5 (Forward invariance). *The set S is forward-invariant for the system (4.1) under the effect of a control input u if $x(0) \in S$ implies that $x(t) \in S$ for all $t \geq 0$.*

The following result, known as the Nagumo's theorem, is adapted from [129] for the forward-invariance of the set S_S for the control system (4.1):

Lemma 4.1 (Nagumo's theorem). *Let $u(x) \in \mathcal{U}$ be a continuous control input such that the resulting closed-loop trajectories of (4.1) are uniquely determined in the forward time. Then, the set S_S is forward invariant for the closed-loop system (4.1) if and only if the following holds:*

$$L_f h_S(x) + L_g h_S(x) u(x) \leq 0 \quad \forall x \in \partial S_S. \tag{4.2}$$

Thus, the following assumption is made to guarantee that the safe set S_S can be rendered forward invariant for (4.1).

Assumption 4.2 (Viability assumption). *For all $x \in \partial S_S$, there exists a control input $u \in \mathcal{U}$ such that the following condition holds:*

$$L_f h_S(x) + L_g h_S(x) u \leq 0. \tag{4.3}$$

Similar assumptions have been used in literature, either explicitly (see e.g. [55]) or implicitly (see e.g. [53]). A function that satisfies (4.3) is called a valid CBF by the authors in [64]. In this chapter, the conditions of ZCBF are used to ensure safety or forward invariance of the safe set S_S. The notion of ZCBF is defined by the authors in [53] as following.

Definition 4.6 (ZCBF). *For the dynamical system (4.1), a continuously differentiable function $B : \mathbb{R}^n \to \mathbb{R}$ is called a ZCBF for the set S_S if $B(x) < 0$ for $x \in \text{int}(S_S)$, $B(x) = 0$ for $x \in \partial S_S$, and there exists $\alpha \in \mathcal{K}$, such that*

$$\inf_{u \in \mathcal{U}} \{L_f B(x) + L_g B(x) u\} \leq \alpha(-B(x)), \quad \forall x \in S_S. \tag{4.4}$$

It is easy to see that if h_S is a ZCBF for (4.1), then it also satisfies (4.3). One special case of (4.4) is

$$\inf_{u \in \mathcal{U}} \{L_f B(x) + L_g B(x) u\} \leq -\delta B(x), \tag{4.5}$$

with $\delta \geq 0$, as discussed in [53, Remark 6]. In this work, the particular form of ZCBF condition in (4.5) is employed where δ is held as a free variable of optimization in a QP formulation. This condition helps guarantee the feasibility of the underlying QP while not jeopardizing forward invariance of the safe set.

Next, conditions for forward invariance of a time-varying set are reviewed. Define $S(t) = \{x \mid h(t,x) \leq 0\}$ where $h : \mathbb{R}_+ \times \mathbb{R}^n \to \mathbb{R}$ is continuously differentiable. The following assumption is made to guarantee that the safe set $S(t)$ can be rendered forward invariant for (4.1).

Assumption 4.3. *For all $x \in \partial S(t)$, $t \geq 0$, there exists a control input $u \in \mathcal{U}$ such that the following condition holds:*

$$L_f h(t, x(t)) + L_g h(t, x(t)) u + \frac{\partial h}{\partial t}(t, x(t)) \leq 0. \tag{4.6}$$

The following Lemma is also required to prove the main results later in the chapter.

Lemma 4.2 (Invariance of the interior). *Consider the following inequality*

$$L_f h(t, x(t)) + L_g h(t, x(t)) u + \frac{\partial h}{\partial t}(t, x(t)) \leq \alpha(-h(t, x(t))) \tag{4.7}$$

where α is a locally Lipschitz class-$\mathcal{K}$ function. Then, under the effect of a continuous control input $u \in \mathcal{U}$ satisfying (4.7) and for all initial conditions satisfying $h(0, x(0)) < 0$, it holds that the closed-loop trajectories satisfy $h(t, x(t)) < 0$ for all $0 \leq t \leq T$ where $T \in \mathbb{R}_+$, and $h(t, x(t)) \leq 0$ for all $t \geq 0$.

The proof can be completed using [122, Lemma 3.4] and [122, Lemma 4.4].

4.1.3 Fixed-time Convergence

First, the notion of CLF is reviewed. The following definition is adapted from [130].

Definition 4.7 (CLF-S). *: A continuously differentiable function $V : \mathbb{R}^n \to \mathbb{R}$ is called a CLF-S for (4.1), if it is positive definite and radially unbounded w.r.t. a compact set S and*

the following holds:

$$\inf_{u\in\mathcal{U}}\{L_fV(x)+L_gV(x)u\}<0,\quad \forall x\notin S. \tag{4.8}$$

Note that [130] defines CLF with $\mathcal{U}=\mathbb{R}^m$. Since this work deals with input constraints, the notion CLF is modified in Definition 4.7 so that it accounts for input constraints. Inspired from [66], a class of CLF, termed as FxT-CLF, is defined with a user-defined fixed-time convergence guarantees:

Definition 4.8 (FxT-CLF-S). *: A continuously differentiable function $V:\mathbb{R}^n\to\mathbb{R}$ is called FxT-CLF-S for (4.1) with parameters $\alpha_1,\alpha_2>0,\gamma_1>1,0<\gamma_2<1$, if it is positive definite and radially unbounded w.r.t. a compact set S and the following holds:*

$$\inf_{u\in\mathcal{U}}\{L_fV(x)+L_gV(x)u\}\leq-\alpha_1V(x)^{\gamma_1}-\alpha_2V(x)^{\gamma_2},\quad \forall x\notin S, \tag{4.9}$$

and the time of convergence T satisfies $T\leq T_{ud}$, where $T_{ud}>0$ is a user-defined fixed time.

Definition 4.8 defines the notion of FxT-CLF that guarantees convergence of the solutions to the set S within user-defined time T_{ud}. Note that the traditional notions of CLF [63] as defined in Definition 4.7 and exponential CLF [60] (defined with $\alpha_2=0$ and $\gamma_1=1$ in (4.9)) only guarantee asymptotic and exponential convergence, respectively.

Based on [66], the following sufficient conditions for existence of a control input u that renders the closed-loop trajectories reach the set goal S_G in the fixed time T_{ud} are presented in [110].

Theorem 4.1 (Convergence within T_{ud}). *If there exist constants $\alpha_1,\alpha_2>0$, $\gamma_1>1$ and $0<\gamma_2<1$, satisfying*

$$\frac{1}{\alpha_1(\gamma_1-1)}+\frac{1}{\alpha_2(1-\gamma_2)}\leq T_{ud}, \tag{4.10}$$

such that h_G is fixed-time (FxT) CLF-S_G with parameters $\alpha_1,\alpha_2,\gamma_1,\gamma_2$ for all $x\notin int(S_G)$, then there exists $u(t)\in\mathcal{U}$, such that the closed-loop trajectories of (4.1) reach the set S_G within fixed time T_{ud} for all initial conditions $x(0)\notin S_G$.

Another way to formulate the FxT-CLF-S_G condition is to require that

$$\inf_{u\in\mathcal{U}}\{L_fh_G(x)+L_gh_G(x)u\}\leq-\alpha_1\max\{0,h_G(x)\}^{\gamma_1}-\alpha_2\max\{0,h_G(x)\}^{\gamma_2}, \tag{4.11}$$

holds for all x. The condition (4.11) guarantees that the closed-loop trajectories reach the set S_G within fixed time T_{ud} and stay there for all future times, as shown below.

Corollary 4.1 (Forward invariance of goal set). *Assume that there exist $u \in \mathcal{U}$, and constants $\alpha_1, \alpha_2 > 0$, $\gamma_1 > 1$ and $0 < \gamma_2 < 1$ satisfying (4.10), such that the following holds:*

$$L_f h_G(x) + L_g h_G(x) u \leq -\alpha_1 \max\{0, h_G(x)\}^{\gamma_1} - \alpha_2 \max\{0, h_G(x)\}^{\gamma_2}, \tag{4.12}$$

for all $x \in \mathbb{R}^n$. Then, the closed-loop trajectories of (4.1) reach the set S_G within fixed time $T_{ud} < \infty$ for all initial conditions $x(0) \in \mathbb{R}^n$, and stay there for all future times.

Proof. For $x \notin S_G$, satisfaction of the inequality (4.12) implies that the function h_G is a FxT-CLF-S_G. Thus, using Theorem 4.1, it follows under the affect of a control input u that satisfies (4.12), the closed-loop trajectories of (4.1) reach the set S_G within a fixed time.

Once the closed-loop trajectories of (4.1) hit the boundary of the set S_G, it holds that $h_G(x) = 0$. From (4.12), it follows that $\dot{h}_G(x) \leq 0$ for all x such that $h_G(x) = 0$. Furthermore, compactness of the set S_G along with satisfaction of (4.12) for a continuous control input guarantees that the closed-loop solution of (4.1) exists and is uniquely determined for all $t \geq 0$ (see Theorem 4.3 for a detailed proof on existence and uniqueness). Thus, using Lemma 4.1, the set S_G is forward invariant under a continuous control input $u \in \mathcal{U}$ satisfying (4.12). □

4.2 Quadratic program formulation: nominal case

4.2.1 Problem setup

First, the main control synthesis problem studied in this section is discussed. The problem formulation is given as follows:

Problem 4.1. *Design a control input $u(t) \in \mathcal{U} := \{v \in \mathbb{R}^m \mid u_{min} \leq v \leq u_{max}\}$, so that the closed-loop trajectories $x(t)$ of (4.1) reach the set $S_G = \{x \mid h_G(x) \leq 0\}$ in a fixed time $T_{ud} > 0$ and satisfy $x(t) \in S_S = \{x \mid h_S(x) \leq 0\}$ for all $t \geq 0$ and $x_0 \in S_S$.*

Here, $u_{min} := \begin{bmatrix} u_{min_1} & \dots & u_{min_m} \end{bmatrix}^T$ and $u_{max} := \begin{bmatrix} u_{max_1} & \dots & u_{max_m} \end{bmatrix}^T$ where $u_{min_i} < u_{max_i}$ are the lower and upper bounds on the individual input u_i for $i = 1, 2, \dots, m$, respectively. Input constraints of this form are very commonly considered in the literature

[53, 57, 60]. This constraint set can be written in a compact form as $\mathcal{U} = \{v \mid A_u v \leq b_u\}$, where

$$A_u = \begin{bmatrix} \mathbf{I}_m \\ -\mathbf{I}_m \end{bmatrix}, \quad b_u = \begin{bmatrix} u_{max} \\ -u_{min} \end{bmatrix},$$

where $\mathbf{I}_m \in \mathbb{R}^{m \times m}$ is an identity matrix. Problem 4.1 can be readily translated into a temporal logic formula for the form of specifications that are encountered, for instance, in mission planning problems, The signal temporal logic (STL) specifications, given by formula ϕ include the following semantics:

1. $(x, t) \models \phi \iff h(x(t)) \leq 0$;
2. $(x, t) \models \neg\phi \iff h(x(t)) > 0$;
3. $(x, t) \models \phi_1 \wedge \phi_2 \iff (x, t) \models \phi_1 \wedge (x, t) \models \phi_2$;
4. $(x, t) \models G_{[a,b]}\phi \iff h(x(t)) \leq 0, \forall t \in [a, b]$;
5. $(x, t) \models F_{[a,b]}\phi \iff \exists t \in [a, b]$ such that $h(x(t)) \leq 0$,

where $\phi =$ true if $h(x) \leq 0$ and $\phi =$ false if $h(x) > 0$ (see [64] for more details). The temporal functions $G_{[a,b]}\phi$ and $F_{[a,b]}\phi$ stand for satisfaction of the formula ϕ *always* in the interval $[a, b]$, i.e., for all $t \in [a, b]$ and *eventually* in the interval $[a, b]$, i.e., for a $t \in [a, b]$, respectively. Problem 4.1 given in the form of spatiotemporal requirements can be written in the STL semantics as follows.

Problem 4.2. *Design control input $u \in \mathcal{U}$ so that the closed-loop trajectories satisfy*

$$(x, t) \models G_{[0,T]}\phi_S \wedge F_{[0,T]}\phi_G, \tag{4.13}$$

where ϕ_S (respectively, ϕ_G) = true if $h_S(x)$ (respectively, $h_G(x)) \leq 0$, and false otherwise.

Note that the requirements involving more complex STL formulae, for examples, requirements of the form

$$\begin{aligned}(x, 0) \models & G_{[t_0,t_N]}\phi_S \wedge G_{[t_0,t_1]}\phi_1 \wedge F_{[t_0,t_1]}\phi_1 \wedge G_{[t_1,t_2]}\phi_2 \\ & \wedge F_{[t_1,t_2]}\phi_2 \wedge \cdots \wedge G_{[t_{N-1},t_N]}\phi_{N-1} \wedge F_{[t_{N-1},t_N]}\phi_N,\end{aligned} \tag{4.14}$$

can also be considered in the proposed framework. Here $[t_0, t_1], [t_1, t_2], \ldots, [t_{N-1}, t_N]$ are intervals such that $t_{i+1} - t_i \geq T_{ud}$ where $0 < T_{ud} < \infty$, for all $0 \leq i \leq N - 1$, and ϕ_i is

true if $h_{G_i}(x) \leq 0$. The requirements (4.14) translate to the problem of designing control input u such that the closed-loop trajectories satisfy

$$x(t) \in S_S, \forall\, t \geq t_0, \tag{4.15a}$$

$$x(t) \in S_{G_i}, \forall\, t \in [t_{i-1}, t_i], \tag{4.15b}$$

where $S_{G_i} = \{x \mid h_{G_i}(x) \leq 0\}$, i.e., the closed-loop trajectories should stay in the set S at all times, and visit the sets S_{G_i} in the given time sequence, can also be considered in the proposed framework (Figure 4.2 illustrates the problem setting for one such scenario).

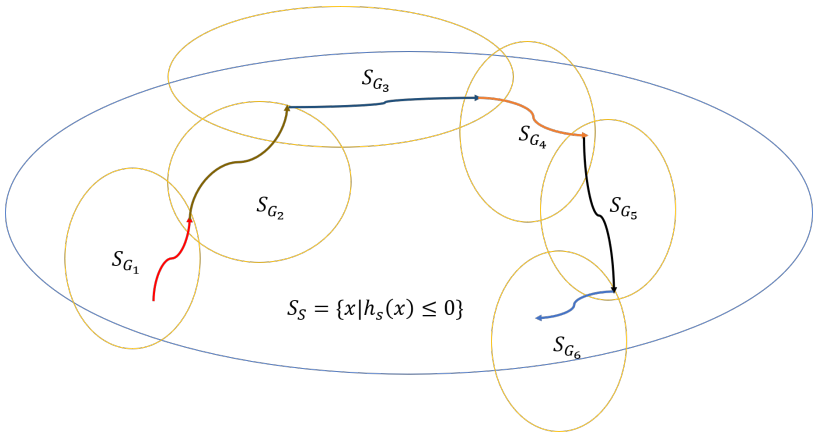

Figure 4.2: Illustration of a problem scenario with sequential tasks.

The requirements of the form (4.15) can be satisfied by solving Problem 4.1 sequentially with safe set defined as $\bar{S} = S_S \bigcap S_{G_i}$ and goal set as $\bar{S}_G = S_S \bigcap S_{G_{i+1}}$ for the time interval $[t_{i-1}, t_i]$ with $t_i - t_{i-1} \geq T_{ud} > 0$, and requiring the time of convergence to satisfy $T \leq T_{ud}$. It is needed that $S_{G_i} \bigcap S_{G_{i+1}} \neq \emptyset$ for the problem to be well-posed (Section 4.4 presents an instance of such an example of a two-robot motion planning case).

4.2.2 QP formulation

In this section, a QP is presented to address Problem 4.1 in the nominal case without disturbances and uncertainties. First, a QP is designed with guaranteed feasibility, then it is shown that the solution of the QP is a continuous function of x, and finally, the conditions under which the control input defined as the optimal solution of the proposed QP solves Problem 4.1 are discussed. In what follows, unless specified otherwise, all the results are presented under Assumptions 4.1-4.2. Define $z = \begin{bmatrix} v^T & \delta_1 & \delta_2 \end{bmatrix}^T \in \mathbb{R}^{m+2}$, and consider

the following QP:

$$\min_{v,\delta_1,\delta_2} \ \frac{1}{2} z^T H z + F^T z \tag{4.16a}$$

$$\text{s.t.} \quad A_u v \leq b_u, \tag{4.16b}$$

$$L_f h_G(x) + L_g h_G(x) v \leq \delta_1 h_G(x) - \alpha_1 \max\{0, h_G(x)\}^{\gamma_1} - \alpha_2 \max\{0, h_G(x)\}^{\gamma_2} \tag{4.16c}$$

$$L_f h_S(x) + L_g h_S(x) v \leq -\delta_2 h_S(x), \tag{4.16d}$$

where $H = \text{diag}\{w_{u_1}, \ldots, w_{u_m}, w_1, w_2\}$ is a diagonal matrix consisting of positive weights $w_{u_i}, w_i > 0$, $F = \begin{bmatrix} \mathbf{0}_m^T & q_1 & 0 \end{bmatrix}$ with $q_1 > 0$ and $\mathbf{0}_m \in \mathbb{R}^m$ a column vector consisting of zeros. The parameters $\alpha_1, \alpha_2, \gamma_1, \gamma_2$ are fixed, and are chosen as $\alpha_1 = \alpha_2 = \frac{\mu\pi}{2T_{ud}}$, $\gamma_1 = 1 + \frac{1}{\mu}$ and $\gamma_2 = 1 - \frac{1}{\mu}$ with $\mu > 1$. The choice of these parameters does not affect the feasibility of the QP, as discussed below. The linear term $F^T z = q_1 \delta_1$ in the objective function of (4.16) penalizes the positive values of δ_1 (see Theorem 4.4 for details on why δ_1 being non-positive could be useful). Constraint (4.16b) guarantees that the control input satisfies the control input constraints. Per Theorem 3.3, the constraint (4.16c) guarantees convergence and the constraint (4.16d) ensures safety.

The slack terms corresponding to δ_1, δ_2 allow the upper bounds of the time derivatives of $h_S(x)$ and $h_G(x)$, respectively, to have a positive term for x such that $h_S(x) < 0$ and $h_G(x) > 0$. This ensures the feasibility of the QP (4.16) for all x, as demonstrated below.

Lemma 4.3 (Feasibility of QP). *Under Assumptions 4.1-4.2, for each $x \in S_S \setminus S_G$, there exist $v(x) \in \mathbb{R}^m, \delta_1(x) \in \mathbb{R}, \delta_2(x) \in \mathbb{R}$ satisfying (4.16b)-(4.16d), i.e., the QP (4.16) is feasible for all $x \in S_S \setminus S_G$.*

Proof. Since $x \notin S_G$, it holds that $h_G(x) > 0$. Consider the following two cases separately: $h_S(x) = 0$ and $h_S(x) < 0$.

First, consider the case when $h_S(x) < 0$, i.e., $x \in \text{int}(S_S)$. Now, since $\mathcal{U}$ is non-empty, there exists $v = \bar{v}$ in $\mathcal{U}$ such that (4.16b) is satisfied. Choose $\bar{\delta}_2 := \frac{L_f h_S(x) + L_g h_S(x) \bar{v}}{-h_S(x)}$, so that (4.16d) is satisfied with equality. Also, for $x \in \text{int}(S_S) \setminus S_G$, it holds that $h_G(x) > 0$. Define $\bar{\delta}_1 := \frac{L_f h_G(x) + L_g h_G(x) \bar{v} + \alpha_1 h_G(x)^{\gamma_1} + \alpha_2 h_G(x)^{\gamma_2}}{h_G(x)}$, so that (4.16c) holds with equality. Thus, for the case when $h_S(x) < 0$, there exists $(\bar{v}, \bar{\delta}_1, \bar{\delta}_2)$ such that (4.16b)-(4.16d) holds.

Next, consider the case when $h_S(x) = 0$, i.e., $x \in \partial S_S$. Per Assumption 4.2, it holds that that there exists $v = \tilde{v} \in \mathcal{U}$ such that (4.16d) holds. Since $h_S(x) = 0$, all values of $\delta_2 \in \mathbb{R}$ are feasible, and hence, one can choose $\delta_2 = 0$. Hence, the choice of $(v, \delta_1, \delta_2) = (\tilde{v}, \bar{\delta}_1, 0)$ satisfies (4.16b)-(4.16d). Thus, the QP (4.16) is always feasible. □

Remark 4.1. *In comparison to [53], where conditions such as* $\frac{\partial h_S}{\partial x} \neq 0$ *or* $L_g h_S \neq 0$ *are imposed to guarantee feasibility of the QP, here, the slack terms corresponding to* δ_1, δ_2 *are used. Furthermore, in contrast to the prior work, where the feasibility is guaranteed only under the safety constraint* (4.16d) *and under a convergence constraint similar to* (4.16c)*, the presented formulation is guaranteed to have a feasible solution under the additional consideration of control input constraints* (4.16b)*. Furthermore, in contrast to the exponential convergence guarantees of the resulting closed-loop trajectories in [53], or, finite-time convergence guarantees without control input bounds in [62], the proposed formulation guarantees fixed-time convergence in the presence of control input constraints.*

4.2.3 Continuity of the solution of the QP

For guaranteeing forward invariance of the safe set S_S, Lemma 4.1 is utilized which requires the uniqueness of the system solutions. Traditionally, Lipschitz continuity of the right-hand side of (4.1) is utilized in order to guarantee existence and uniqueness of the solutions of (4.1), see e.g., [53, 58, 64]. When the right-hand side of (4.1) is only continuous, existence and uniqueness of the solutions can be established using the results in [131, Section 3.15-3.18] (see Theorem 4.3). Next, it is shown that the control input $u(x)$ as a solution of the QP (4.16) is continuous in its arguments. Define $A : \mathbb{R}^n \to \mathbb{R}^{(2m+2)\times(m+2)}$ and $b : \mathbb{R}^n \to \mathbb{R}^{(2m+2)}$ as

$$A(x) \coloneqq \begin{bmatrix} A_u & \mathbf{0}_{2m} & \mathbf{0}_{2m} \\ L_g h_G(x) & -h_G(x) & 0 \\ L_g h_S(x) & 0 & h_S(x) \end{bmatrix}$$

$$b(x) \coloneqq \begin{bmatrix} b_u \\ -L_f h_G(x) - \alpha_1 \max\{0, h_G(x)\}^{\gamma_1} - \alpha_2 \max\{0, h_G(x)\}^{\gamma_2} \\ -L_f h_S(x) \end{bmatrix}$$

where $\mathbf{0}_{2m} \in \mathbb{R}^{2m}$ is a column vector consisting of zeros. Also, define the functions $G_i(x, z) \coloneqq A_i(x)z - b_i(x)$ where $A_i \in \mathbb{R}^{1\times(m+2)}$ is the i-th row of the matrix A, and $b_i \in \mathbb{R}$ the i-th element of b, so that the constraints (4.16b)-(4.16d) can be written as $G_i(x, z) \leq 0$ for $i \in 1, 2, \ldots, 2m + 2$. Let $z^\star$ and $\lambda^\star \in \mathbb{R}_+^{2m+2}$ denote the optimal solution of (4.16), and the corresponding optimal Lagrange multiplier, respectively. The following assumption is made to prove the main results of this section.

Assumption 4.4 (Strict complementary slackness)**.** *The strict complementary slackness holds for* (4.16) *for all* $x \in \text{int}(S_S) \setminus S_G$*, i.e., for each* $i \in \{1, 2, \ldots, 2m + 2\}$*, it holds that*

either $\lambda_i^\star > 0$ *or* $G_i(x, z^\star) < 0$ *for all* $x \in \text{int}(S_S) \setminus S_G$.

Complimentary slackness, i.e., $\lambda_i^\star G_i(x, z^\star) = 0$, for all $i = 1, \ldots, 2m + 2$, is a both necessary and sufficient condition for optimality of the solution for QPs [128, Chapter 5]. Note that this condition permits existence of i such that both $\lambda_i^\star = 0$ and $G_i(x, z^\star) = 0$. *Strict* complimentary slackness rules out this possibility, and require that for each i, either $\lambda_i^\star$ or $G_i(x, z^\star)$ is non-zero.

Theorem 4.2 (Continuity of solution of QP)**.** *Under Assumptions 4.1 and 4.4, the solution* $z^* : \mathbb{R}^n \to \mathbb{R}^{m+2}$ *of* (4.16) *is continuous on* $\text{int}(S_S) \setminus S_G$.

Proof. The proof is based on [132, Theorem 2.1]. Denote by $I(x)$, the indices of rows of matrix $A(x)$ corresponding to the active constraints, i.e., $j \in I(x)$ implies $A_j(x)z^\star(x) = b_j(x)$, where $A_j \in \mathbb{R}^{1\times m+2}$ is the j-th row of the matrix A and $b_j \in \mathbb{R}$ the j-th element of b. Define matrix A_{ac} and b_{ac} by collecting $A_j(x)$, and of b_j, respectively, so that $A_{ac}(x)z^\star(x) = b_{ac}(x)$. Since at most one of the input constraints $u_i \le u_{M_i}$ or $u_{m_i} \le u_i$ can be active at a time, the matrix $A_{ac}(x)$ has k rows from $\begin{bmatrix} A_u & \mathbf{0}_{2m} & \mathbf{0}_{2m} \end{bmatrix}$, where $k \le m$, which are linearly independent. Furthermore, it has p rows from $\begin{bmatrix} L_g h_G & -h_G & 0 \\ L_g h_S & 0 & h_S \end{bmatrix}$, where $p \le 2$. Since $h_G, h_S \neq 0$ for $x \in \text{int}(S_S) \setminus S_G$, these $k + p$ rows are linearly independent. Thus, the matrix A_{ac} is full row-rank, i.e., the gradients of the active constraints $\{A_{ac_i}(x)\}$, where $A_{ac_i}(x)$ is the $i-$th row of matrix $A_{ac}(x)$, are linearly independent.

The second derivative $\nabla_{zz} L$ of the Lagrangian defined as

$$L(z, x, \lambda) \coloneqq \frac{1}{2} z^T H z + F^T z + \lambda^T (A(x)z - b(x)),$$

with respect to z is H, which is a positive definite matrix. Using this, and the fact that the QP (4.16) is feasible, it holds that the second-order sufficient conditions for optimality hold (see e.g. [132, Section 2.3]). Note that [132, Theorem 2.1] requires that the objective function and the functions $G_i(x, u)$ have the second derivatives jointly continuous in (x, u). Since the objective function $\frac{1}{2} z^T H z + F^T z$ is independent of x, and the constraint functions $G_i(x, u)$ are linear in u, the second derivative of these functions are independent of x, and thus, satisfy this condition trivially. Finally, the strict complementary slackness condition is satisfied per Assumption 4.4. Thus, all the conditions of [132, Theorem 2.1] are satisfied. Therefore, for every $x \in \text{int}(S_S) \setminus S_G$, there exists an open neighborhood $\mathcal{X} \subset \text{int}(S_S) \setminus S_G$ of x such that the solution $z^\star(x)$ is continuous for all $x \in \mathcal{X}$. Since this holds for all $x \in \text{int}(S_S) \setminus S_G$, it follows that the solution $z^\star(x)$ is continuous for all $x \in \text{int}(S_S) \setminus S_G$. □

Note that the above result guarantees that the control input defined as $u(x) = v^\star(x)$ is continuous on $\text{int}(S_S) \setminus S_G$. Under Assumption 4.4, the authors in [133] show that the solution is continuously differentiable if the objective function and the constraints functions are twice continuously differentiable. The authors in [53] assume that the functions f, g and the Lie derivatives $L_f h_S, L_f h_G, L_g h_S, L_g h_G$ are locally Lipschitz continuous to show Lipschitz continuity of the solution of QP in the absence of control input constraints. Under similar assumptions, the authors in [23] show that the solution of QP is guaranteed to be Lipschitz continuous (in the absence of input constraints) if the CBF constraints are inactive, i.e., the constraints are satisfied with strict inequality at the optimal solution $z^\star$, which is same as Assumption 4.4. The authors extend these results in [61] by utilizing the theory of non-smooth analysis, and strong forward invariance of sets even if the control input is not continuous. Under similar assumptions, the results in [134] utilize the concept of Clarke tangent cones to guarantee strong forward invariance when the control input is only Lebesgue measurable. Note that in the presented formulation, the only requirement is that the functions f, g are continuous, and h_S, h_G continuously differentiable in x, which is a relaxation of the prior assumptions.

Next, it is shown that closed-loop trajectories of (4.1) under $u = v^\star$ exist and are unique.

Theorem 4.3 (Uniqueness of closed-loop trajectory). *Let Assumptions 4.1-4.4 hold. If the solution of (4.16), given as $z^\star = [v^\star(\cdot)^T \ \delta_1^\star(\cdot) \ \delta_2^\star(\cdot)]^T$, satisfies $\mathfrak{d}_1 := \sup_{\text{int}(S_S)\setminus S_G} \delta_1^\star(x) < \infty$, then there exists a neighborhood D of the set $S_G \cap \text{int}(S_S)$ such that the closed-loop trajectory under $u(\cdot) = v^\star(\cdot)$ exists and is unique for all $t \geq 0$ and for all $x(0) \in D$. Furthermore, if $\mathfrak{d}_1 \leq 0$, then the result holds with $D = \text{int}(S_S)$.*

Proof. The proof is based on [131, Theorem 3.18.1]. Using [131, Theorem 3.15.1] and choosing a Lyapunov candidate $\mathfrak{v} = \frac{1}{2}|y|^2$, it can be shown that $y \equiv 0$ is the unique solution of $\dot{y} = 0$ for $y(0) = 0$. Theorem 4.2 guarantees that the solution of the QP (4.16) is continuous on $\text{int}(S_S)$, which implies continuity of the closed-loop system dynamics (4.1) when $u(x) := v^\star(x)$. Note that $h_G(x) = 0$ for $x \in \partial S_G$ and $h_G(x) > 0$ for $x \notin S_G$, i.e., the function h_G is positive definite with respect to the set S_G. Define $\phi(y) := \mathfrak{d}_1 y - \alpha_1 \,\text{sign}(y)|y|^{\gamma_1} - \alpha_2 \,\text{sign}(y)|y|^{\gamma_2}$. Per Theorem 3.3, it holds that there exists a neighborhood $D_y \subset \mathbb{R}$ of the origin such that for all $y \in D_y$, $\phi(y) \leq 0$. Thus, there exists a function g defined as $g(t, V) = 0$ that satisfies condition (i) of [131, Theorem 3.18.1], the closed-loop dynamics of (4.1) satisfies the condition (ii), and there exists a function V defined as $V(x) = h_G(x)$ that satisfies the condition (iii). Thus, using [131, Theorem 3.18.1], there exists $\tau > 0$ such that the solution of the closed-loop system (4.1) exists and is unique for

all $x(0) \in D = \{x \mid V(x) \in D_y\}$ and all $t \in [0, \tau)$. Since the closed-loop solution $x(t)$ is bounded in the compact set D, the solution is complete (see [135, Ch2., Theorem 1]), and thus, $\tau = \infty$.

Finally, in the case when $\mathfrak{d}_1 \leq 0$, it holds that the $D_y = \mathbb{R}$, and thus, the result holds with $D = \text{int}(S_S)$. □

4.2.4 Safety and fixed-time convergence

Finally, it is shown that under certain conditions, solution of (4.16) solves Problem 4.1.

Theorem 4.4 (Closed-loop properties). *Let Assumptions 4.1-4.4 hold. If the solution of (4.16), given as $z^\star = [v^\star(\cdot)^T \ \delta_1^\star(\cdot) \ \delta_2^\star(\cdot)]^T$, satisfies $\delta_1^\star(x) \leq 0$ for all $x \in \text{int}(S_S)$, then, $u(\cdot) = v^\star(\cdot)$ solves Problem 4.1 for all $x(0) \in \text{int}(S_S)$.*

Proof. First, the convergence of the closed-loop trajectories $x(t)$ to the set S_G within the user-defined time T_{ud} is shown. Since $\delta_1^\star(x) \leq 0$, per Theorem 3.3, it holds that the closed-loop trajectories of (4.1) with $u(x) := v^\star(x)$ reach the set S_G within fixed time $T \leq \frac{\mu\pi}{2(\alpha_1\alpha_2)^{\frac{1}{2}}} = T_{ud}$, i.e., within the user-defined time T_{ud} for all $x(0) \in \text{int}(S_S)$.

Next, it is shown that the closed-loop trajectories of (4.1) satisfy $x(t) \in \text{int}(S_S)$ for all $t \geq 0$ under $u(x) := v^\star(x)$. From Theorem 4.3, it holds that the closed-loop solution of (4.1) exists and is unique under $u = v^\star$ for all $t \geq 0$ and for all $x(0) \in \text{int}(S_S)$. Thus, Nagumo's theorem can be applied to guarantee forward invariance of $\text{int}(S_S)$, i.e., that $x(t) \in \text{int}(S_S)$ for all $t \geq 0$. Therefore, the control input $u(x) := v^\star(x)$ solves Problem 4.1 for all $x(0) \in \text{int}(S_S)$. □

Utilizing the notion of FxT-CLF-S_G, it can be shown that if $h_G(x)$ is a FxT CLF-S_G, then there exists a control input $u \in \mathcal{U}$ such that the closed-loop trajectories of (4.1) reach the set S_G within fixed time T.

Corollary 4.2. *Let Assumptions 4.1-4.4 hold. If h_G is an FxT CLF-S_G for (4.1) with parameters $\alpha_1, \alpha_2, \gamma_1, \gamma_2$ as defined in (4.16), then the QP (4.16) with $\delta_1 = 0$ is feasible for all $x \in \text{int}(S_S) \setminus S_G$, i.e., the solution $(v^\star(x), \delta_2^\star(x))$ of the QP (4.16) after fixing $\delta_1 = 0$ exists for all $x \in \text{int}(S_S) \setminus S_G$. Furthermore, if the solution $(v^\star(x), \delta_2^\star(x))$ is continuous for all $x \in \text{int}(S_S) \setminus S_G$ with $\mathfrak{d}_2 := \sup_{\text{int}(S_S)\setminus S_G} |\delta_2^\star(x)| < \infty$, then the control input $u(x) := v^\star(x)$ solves Problem 4.1 for all $x(0) \in \text{int}(S_S)$.*

Proof. Since h_G is FxT CLF-S_G, there exists $v(x) \in \mathcal{U}$ such that (4.16c) is satisfied with $\delta_1 = 0$. Given that $x \in \text{int}(S_S)$, i.e., $h_S(x) < 0$, one can let $\delta_2(x) := \frac{L_f h_S(x) + L_g h_S(x) v(x)}{-h_S(x)}$ so that (4.16d) is satisfied. Thus, the QP (4.16) is feasible with $\delta_1 = 0$ for all $x \in \text{int}(S_S)$. From Theorem 4.2, it follows that the control input $u = v^\star$ is continuous. Theorem 4.3 can be used to show existence and uniqueness of the solution $x(t)$ of the closed-loop system (4.1) for $t \geq 0$ and for all $x(0) \in \text{int}(S_S)$. Thus, the control input $u(x) := v^\star(x)$ renders the set $\text{int}(S_S)$ forward invariant. Next, it is shown that the closed-loop trajectories remain in the interior of the safe set, i.e., $x(t) \in \text{int}(S_S)$ for all $0 \leq t \leq T_{ud}$. For $\mathfrak{d}_2 < \infty$, and for all $t \leq T_{ud}$, it holds that (4.16d) yields:

$$\dot{h}_S(x(t)) \leq -\mathfrak{d}_2 h_S(x(t)) = \psi(-h_S(x(t))),$$

where $\psi(r) := \mathfrak{d}_2\, r$ is a Lipschitz continuous class-$\mathcal{K}$ function. Thus, using the Comparison Lemma ([122, Lemma 3.4]) and [122, Lemma 4.4], it follows that there exists a class-$\mathcal{KL}$ function κ such that $h_S(x(t)) \leq -\kappa\left(-h_S(x(0)), t\right)$. To see this, consider $\dot{y} = \psi(-y)$ with $y(0) = h_S(x(0))$, and define $z := -y$ to obtain $\dot{z} = -\psi(z)$. Then, using [122, Lemma 4.4], it follows that $z(t) = \kappa(z(0), t)$, or equivalently, $y(t) = -\kappa(-y(0), t)$. Furthermore, using the Comparison Lemma, it follows that $h_S(x(t)) \leq y(t)$, i.e., $h_S(x(t)) \leq -\kappa(-h_S(x(0)), t)$. Since $\kappa\left(-h_S(x(0)), t\right) > 0$ for all $t \leq T_{ud} < \infty$, it follows that $h_S(x(t)) \leq -\kappa\left(-h_S(x(0)), t\right) < 0$ for all $t \leq T_{ud}$, i.e., $x(t) \in \text{int}(S_S)$ for all $t \leq T_{ud}$. Finally, under the assumption that $\delta_1 = 0$, Theorem 4.4 ensures the convergence of the closed-loop trajectories $x(t)$ to the set S_G within a fixed time T_{ud}; therefore, it follows that $u(x) := v^\star(x)$ solves Problem 4.1 for all $x(0) \in \text{int}(S_S)$. □

Remark 4.2. *Corollary 4.2 gives one sufficient condition under which the solution of QP (4.16) solves Problem 4.1. As pointed out in [53], the conflict between safety and the convergence constraint require a non-zero slack term for satisfaction of (4.16c)-(4.16d) together. With this observation and keeping in mind the discussion in Section 3.2.3, one can readily conclude that if the control input constraints set or the user-defined time T_{ud} is sufficiently large, and the goal set is in the interior of safe set, i.e., $S_G \subset \text{int}(S_S)$, then it is possible to satisfy (4.16c) with $\delta_1 \leq 0$. The authors in [58] argue that in the absence of such a conflict, a larger weight w_1 on δ_1 in (4.16) results in solution of the QP with $\delta_1 \approx 0$.*

Next, the cases are discussed when the solution of QP (4.16) might not solve Problem 4.1 with the specified time constraint, and from all initial conditions, but it still renders the closed-loop trajectories safe, and convergent to the set S_G within a fixed time.

Theorem 4.5. *Let Assumptions 4.1-4.4 hold. If the solution of (4.16), given as* $z^\star(x) = [v^\star(x)^T \ \delta_1^\star(x) \ \delta_2^\star(x)]^T$*, satisfies*

$$\mathfrak{d}_1 \coloneqq \sup_{x \in S_S \setminus S_G} \delta_1^*(x) < 2\sqrt{\alpha_1 \alpha_2}, \tag{4.17}$$

then, for all $x(0) \in \text{int}(S_S)$*, the closed-loop trajectories* $x(t)$ *of (4.1) under* $u(x) \coloneqq v^*(x)$ *reach the set* S_G *in a fixed time, while satisfying* $x(t) \in \text{int}(S_S)$ *for all* $t \geq 0$*. If (4.17) does not hold, then for all* $x(0) \in D_S$*, the closed-loop trajectories satisfy* $x(t) \in \text{int}(S_S)$ *for all* $t \geq 0$ *and reach the goal set* S_G *within a fixed time, where* D_S *is the largest sub-level set of the function* h_G *in the set* $D \cap \text{int}(S_S)$*, with* $D = \left\{ x \mid h_G(x) \leq k^\mu \left(\frac{\mathfrak{d}_1 - \sqrt{\mathfrak{d}_1 - 4\alpha_1\alpha_2}}{2\alpha_1} \right)^\mu \right\}$.

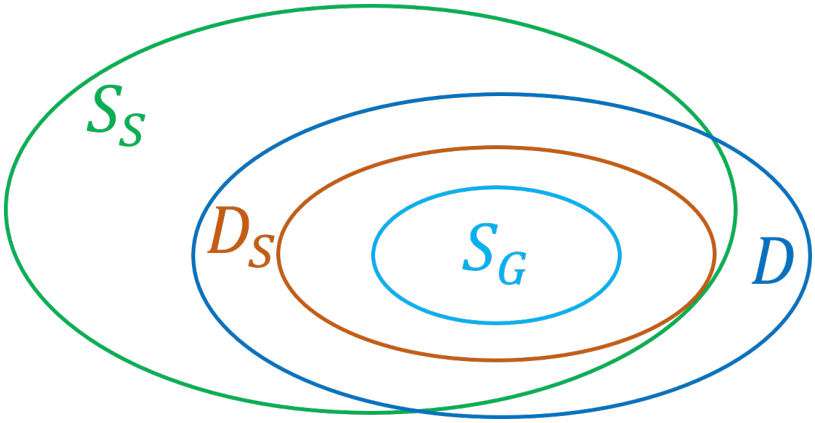

Figure 4.3: Illustration of the safe set S_S (shown in green), the goal set S_G (shown in light blue), FxT DoA D (shown in dark blue) and the domain D_S (shown in brown).

Proof. In both cases, following the proof of Theorem 4.4, it holds that the closed-loop trajectories satisfy $x(t) \in \text{int}(S_S)$ for all $t \geq 0$. When (4.17) holds, using Theorem 3.3, it follows that there exists T_1 satisfying

$$T_1 \leq \frac{\mu}{\alpha_1 \mathrm{k}_1} \left(\frac{\pi}{2} - \tan^{-1} \mathrm{k}_2 \right),$$

where $\mathrm{k}_1 \coloneqq \sqrt{\frac{4\alpha_1\alpha_2 - \mathfrak{d}_1}{4\alpha_1^2}}$ and $\mathrm{k}_2 \coloneqq -\frac{\mathfrak{d}_1}{\sqrt{4\alpha_1\alpha_2 - \mathfrak{d}_1}}$, such that the closed-loop trajectories $x(t)$ reach the set S_G within fixed time T_1. Also, per (4.17), it holds that $\mathrm{k}_1 > 0$ and so, $T_1 < \infty$, i.e., the closed-loop trajectories $x(t)$ of (4.1) under $u(x) \coloneqq v^\star(x)$ reach the set S_G in fixed time T_1.

For the case when (4.17) does not hold, using Theorem 3.3, it holds that there exists

$D \coloneqq \{x \mid h_G(x) \leq k^\mu \left(\frac{\mathfrak{d}_1 - \sqrt{\mathfrak{d}_1 - 4\alpha_1\alpha_2}}{2\alpha_1}\right)^\mu\}$ and a fixed time T_2 such that

$$T_2 \leq \frac{\mu}{\alpha_1(b-a)}\left(\log\left(\frac{b-ka}{a(1-k)}\right) - \log\left(\frac{b}{a}\right)\right),$$

where a, b are defined as in Theorem 3.3 with $\delta_1 = \mathfrak{d}_1$, and $0 < k < 1$, such that for all $x(0) \in D$, the closed-loop trajectories reach the set S_G within time T_2. Since it is also required that $x(0) \in \text{int}(S_S)$, define D_S as the largest sub-level set of the function h_G in the set $D \cap \text{int}(S_S)$, so that D_S is forward invariant (see Figure 4.3). Therefore, for all $x(0) \in D_S$, the closed-loop trajectories of (4.1) reach the set S_G within the fixed time T_2, while maintaining safety at all times. □

In brief, the solution of the QP (4.16) always exists, is a continuous function of x, and renders the interior of the safe set $\text{int}(S_S)$ forward invariant, i.e., guarantees safety. Furthermore, the control input is guaranteed to lead fixed-time convergence of the closed-loop trajectories to the goal set S_G. In the case when $\delta_1 \leq 0$, the convergence is guaranteed for all $x(0) \in \text{int}(S_S)$, and within the user-defined fixed time T_{ud}. If δ_1 satisfies (4.17), then also, fixed-time convergence is guaranteed for all $x(0) \in \text{int}(S_S)$, but the time of convergence T may exceed the time T_{ud}. Finally, if (4.17) does not hold, fixed-time convergence is guaranteed for all $x(0) \in D_S \subset \text{int}(S_S)$, however, the time of convergence T may exceed the time T_{ud}.

4.3 Quadratic program formulation: perturbed case

4.3.1 Problem setup

Building upon the results in 4.2, a robust control design based on QP formulation is presented in this section. Consider a perturbed dynamical system:

$$\dot{x}(t) = f(x(t)) + g(x(t))u + d(t, x), \tag{4.18}$$

where $x \in \mathbb{R}^n, u \in \mathcal{U} \subset \mathbb{R}^m$ are the state and the control input vectors, respectively, with $\mathcal{U}$ the control input constraint set, $f : \mathbb{R}^n \to \mathbb{R}^n$ and $g : \mathbb{R}^n \to \mathbb{R}^{n\times m}$ are continuous functions and $d : \mathbb{R}_+ \times \mathbb{R}^n \to \mathbb{R}^n$ is an unknown additive disturbance. The following assumption is made.

Assumption 4.5 (Disturbance bound). *There exists $\gamma > 0$ such that for all $t \geq 0$ and $x \in \mathcal{D} \subset \mathbb{R}^n$, $\|d(t, x)\| \leq \gamma$, where $\mathcal{D}$ is a compact domain.*

Assumption 4.5 implies that the disturbance d is uniformly bounded in the domain $\mathcal{D}$. This is a standard model to account for modeling uncertainties, environmental noises, and external disturbances (see, e.g. [57]). It is assumed that under the effect of the additive disturbance d, the solutions of system (4.18) are well-defined. Furthermore, it is assumed that the state x is not perfectly known, to account for sensor noises and uncertainties. More specifically, consider that only an estimate of the system state, denoted as $\hat{x}$, is available, that satisfies:

$$\dot{\hat{x}} = f(\hat{x}) + g(\hat{x})u. \tag{4.19}$$

The following assumption is made on the state-estimation error $\|x - \hat{x}\|$.

Assumption 4.6 (Estimation error bound). *There exists an $\epsilon > 0$ such that $\|\hat{x}(t) - x(t)\| \leq \epsilon$, for all $t \geq 0$.*

The notations and functions necessary to state the main problem are defined now. Let $h_S : \mathbb{R}^n \to \mathbb{R}$ be a continuously differentiable function defining the *static* safe set $S_S := \{x \mid h_S(x) \leq 0\}$, as in the nominal case in Section 4.2. To encode safety with respect to a general time-varying safe sets, let $h_T : \mathbb{R}_+ \times \mathbb{R}^n \to \mathbb{R}$ be a continuously differentiable function defining the *time-varying* safe set $S_T(t) = \{x \mid h_T(t, x) \leq 0\}$. Finally, let $h_G : \mathbb{R}^n \to \mathbb{R}$ a continuously differentiable function defining the goal set $S_G = \{x \mid h_G(x) \leq 0\}$.

Remark 4.3. *The set $S_T(t)$ encodes a dynamically-changing safe set arising, for instance, due to the presence of moving obstacles or other agents in a multi-agent scenario. In such a case, a centralized collision avoidance scheme might require each agent i to be in a safe set defined as $\{x_i(t) \mid h(x_i(t), x_j(t)) \leq 0\}$ for all $j \neq i$, where $x_i, x_j \in \mathbb{R}^n$ are the states of the agents i and j. In this case, one can use a smooth approximation for the* max *function, e.g., $h_T := \log(\sum_j e^{h_{ij}})$, so that the resulting function h_T is continuously differentiable (see [64]). The interested reader is also referred to [61] for a discussion on how to compose multiple safety constraints.*

Similar to Problem 4.1, the problem formulation can be stated as follows.

Problem 4.3. *Find a control input $u(t) \in \mathcal{U} = \{v \in \mathbb{R}^m \mid u_{j,min} \leq v \leq u_{j,max}, j = 1, 2, \ldots, m\}$, $t \geq 0$, and a set $D \subset S_S \cap S_T(0)$, such that for all $x(0)$, the closed-loop trajectories of (4.18) satisfy*

(i) $x(T_{ud}) \in S_G$ for a user-defined $T_{ud} > 0$;

(ii) $x(t) \in S_S$ *for all* $t \geq 0$*;*

(iii) $x(t) \in S_T$ *for all* $t \geq 0$*.*

First, conditions for robust CBFs are presented so that the safety requirements (ii) and (iii) in Problem 4.3 can be satisfied in the presence of the disturbance d and state-estimation error ϵ. The following is assumed.

Assumption 4.7 (Lipschitz continuity). *There exist* $l_S, l_G, l_T > 0$ *such that*

$$\left\| \frac{\partial h_S}{\partial x}(x) \right\| \leq l_S, \quad \left\| \frac{\partial h_G}{\partial x}(x) \right\| \leq l_G, \quad \left\| \frac{\partial h_T}{\partial x}(t,x) \right\| \leq l_T,$$

for all $x \in \mathcal{D} \subset \mathbb{R}^n$*, and all* $t \geq 0$*.*

Since the functions h_S, h_T are continuously differentiable, Assumption 4.7 holds on compact domains.

4.3.2 Robust CBF and robust FxT-CLF

Corresponding to the set $S(t) = \{x \mid h(t,x) \leq 0\}$ where $h : \mathbb{R}_+ \times \mathbb{R}^n \to \mathbb{R}$ is continuously differentiable, define $\hat{S}_\epsilon(t) = \{\hat{x} \mid h(t,\hat{x}) \leq -l\epsilon\}$, where $l = \sup \|\frac{\partial h(t,x)}{\partial x}\|$ is the Lipschitz constant of the function h. Inspired from [58], the notion of a robust CBF is defined as follows.

Definition 4.9 (Robust CBF). *A continuously differentiable function* $h : \mathbb{R}_+ \times \mathbb{R}^n \to \mathbb{R}$ *is called a robust CBF for* (4.18) *with respect to a disturbance* d *satisfying Assumption 4.5 if there exists a locally Lipschitz class-*$\mathcal{K}$ *function* α *such that the following condition holds*

$$\inf_{u \in \mathcal{U}} \left\{ L_f h(t,x(t)) + L_g h(t,x(t))u + \frac{\partial h}{\partial t}(t,x(t)) \right\} \leq \alpha(-h(t,x(t))) - l\gamma, \tag{4.20}$$

for all $x(t) \in S(t)$ *and* $t \geq 0$*.*

Note that the worst-case bound $l\gamma$ of the term $\|L_d h(t,x)\|$ is used to define the robust CBF. This condition can be relaxed if more information than just the upper bound of the disturbance is known, or can be adapted online to reduce the conservatism. The following lemma can be stated now that relates the robust CBF condition with the forward invariance of the set $S(t)$ in the presence of disturbance d.

Lemma 4.4 (Robust forward invariance). *Assume that the function $b(t,\hat{x}) \coloneqq h(t,\hat{x}) + l\epsilon$ is a robust CBF for (4.18), i.e., there exists $\alpha \in \mathcal{K}$ and a control input $u \in \mathcal{U}$ such that*

$$L_f b(t,\hat{x}(t)) + L_g b(t,\hat{x}(t))u + \frac{\partial b}{\partial t}(t,\hat{x}(t)) \leq \alpha(-b(t,\hat{x}(t))) - l\gamma, \tag{4.21}$$

holds for all $\hat{x}(t) \in \hat{S}_\epsilon(t)$. If the resulting closed-solution $x(t)$ of (4.18) exists and is unique in forward time, then, the set $S(t)$ forward invariant for all $\hat{x}(0) \in \hat{S}_\epsilon(0)$.

Proof. The time derivative of the function b along the trajectories of (4.18) satisfies

$$\begin{aligned}
\dot{b}(t,\hat{x}) &= L_f b(t,\hat{x}) + L_g b(t,\hat{x})u + L_d b(t,\hat{x}) + \frac{\partial b}{\partial t}(t,\hat{x}) \\
&= L_f h(t,\hat{x}) + L_g h(t,\hat{x})u + L_d h(t,\hat{x}) + \frac{\partial h}{\partial t}(t,\hat{x}) \\
&\leq L_f h(t,\hat{x}) + L_g h(t,\hat{x})u + \left\| \frac{\partial h}{\partial x} d(t,\hat{x}) \right\| + \frac{\partial h}{\partial t}(t,\hat{x}) \\
&\leq L_f h(t,\hat{x}) + L_g h(t,\hat{x})u + \frac{\partial h}{\partial t}(t,\hat{x}) + l\gamma \\
&\overset{(4.20)}{\leq} \alpha(-h(t,\hat{x}) - l\epsilon) = \alpha(-b(t,\hat{x})),
\end{aligned}$$

for all $t \geq 0$. Thus, it follows that $b(t,\hat{x}(t)) \leq 0$ (or, $h(t,\hat{x}(t)) \leq -l\epsilon$) for all $t \geq 0$. Using the mean value theorem, there exists $z \in \mathbb{R}^n$ such that

$$\begin{aligned}
h(t,x) = h(t,\hat{x} + (x-\hat{x})) &= h(t,\hat{x}) + \frac{\partial h}{\partial x}(t,z)(x-\hat{x}) \\
&\leq h(t,\hat{x}) + \left\| \frac{\partial h}{\partial x}(t,z) \right\| \|(x-\hat{x})\| \leq h(t,\hat{x}) + l\epsilon.
\end{aligned}$$

Thus, $h(t,\hat{x}) \leq -l\epsilon$ implies that $h(t,x) \leq 0$, and it follows that $h(t,x) \leq 0$ for all $t \geq 0$, implying forward invariance of set $S(t)$ for all $\hat{x}(0) \in \hat{S}_\epsilon(0)$. □

Thus, the condition (4.20) can be used to satisfy the safety requirements (ii)-(iii) in Problem 4.3. Intuitively, Lemma 4.4 guarantees that if $\hat{x}(t) \in S_\epsilon(t)$, then $x(t) \in S(t)$ for all $t \geq 0$.

Remark 4.4. *Note that for the robust CBF condition, if the set $\hat{S}_\epsilon(0)$ is empty, then there exists no initial condition for which forward invariance of the set S can be guaranteed based on Lemma 4.4. Thus, for forward invariance of S_S and S_T, it is assumed that the sets $\hat{S}_{S,\epsilon}, \hat{S}_{T,\epsilon}(0)$, defined as $S_{S,\epsilon} \coloneqq \{\hat{x} \mid h_S(\hat{x}) \leq -l_S\epsilon\}, S_{T,\epsilon}(0) \coloneqq \{\hat{x} \mid h_S(0,\hat{x}) \leq -l_T\epsilon\}$, are non-empty.*

Next, a robust FxT-CLF condition is presented to guarantee FxTS of the closed-loop trajectories to the goal set. Consider a continuously differentiable function $V : \mathbb{R}^n \to \mathbb{R}$ with Lipschitz constant l_V.

Definition 4.10 (Robust FxT-CLF-S). *A continuously differentiable function $V : \mathbb{R}^n \to \mathbb{R}$ is called a robust FxT-CLF-S for a set S with respect to a disturbance d satisfying Assumption 4.5 if V is positive definite and radially unbounded w.r.t. the set S, $V(x) < 0$ for $x \in \text{int}(S)$, and satisfies*

$$\inf_{u \in \mathcal{U}} \{L_f V(x) + L_g V(x) u\} \leq -\alpha_1 V(x)^{\gamma_1} - \alpha_2 V(x)^{\gamma_2} + \delta_1 V(x) - l_V \gamma, \tag{4.22}$$

with $\alpha_1, \alpha_2 > 0$, $\delta_1 \in \mathbb{R}$, $\gamma_1 = 1 + \frac{1}{\mu}$, $\gamma_2 = 1 - \frac{1}{\mu}$ for $\mu > 1$, along the trajectories of (4.18).

Using the mean value theorem, the following inequality can be obtained:

$$V(x) \leq V(\hat{x}) + l_V \epsilon, \tag{4.23}$$

which implies that if $V(\hat{x}) \leq -l_V \epsilon$, then $V(x) \leq 0$. Based on this, the following result can be stated.

Lemma 4.5 (Robust fixed-time convergence). *Let $\hat{V} : \mathbb{R}^n \to \mathbb{R}$ defined as $\hat{V}(\hat{x}) = V(\hat{x}) + l_V \epsilon$ be a robust FxT-CLF-S_G. Then, there exists $u \in \mathcal{U}$, and a neighborhood D of the set S_G such that for all $\hat{x}(0) \in D$, the closed-loop trajectories of (4.18) reach the goal set S_G within a fixed time $T < \infty$.*

Proof. Note that (4.22) implies that there exists $u \in \mathcal{U}$ such that

$$\begin{aligned}
\dot{\hat{V}}(\hat{x}) &= L_f \hat{V}(\hat{x}) + L_g \hat{V}(\hat{x}) u + L_d \hat{V}(\hat{x}) \\
&= L_f V(\hat{x}) + L_g V(\hat{x}) u + L_d V(\hat{x}) \\
&\leq L_f V(\hat{x}) + L_g V(\hat{x}) u + l_V \gamma \\
&\leq -\alpha_1 \hat{V}(\hat{x})^{\gamma_1} - \alpha_2 \hat{V}(\hat{x})^{\gamma_2} + \delta_1 \hat{V}(\hat{x}).
\end{aligned}$$

Thus, from Theorem 3.3, it follows that there exists a domain D and fixed time $T < \infty$ such that $\hat{V}(\hat{x}(T)) = 0$ for all $\hat{x}(0) \in D$. Thus, it holds that $V(\hat{x}(T)) \leq -l_V \epsilon$, which, in light of (4.23), implies that $V(x(T)) = 0$ for all $\hat{x}(0) \in D$. Since $V(x) \geq \alpha(\|x\|_{S_G})$, $V(x(T)) \leq 0$ implies that $\alpha(\|x(T)\|_{S_G}) \leq 0$, i.e., $x(T) \in S_G$, which completes the proof. □

The robust FxT-CLF condition guarantees that if the state estimate $\hat{x}$ reaches a certain level set in the interior of the set S_G, quantitatively given as $\{x \mid V(\hat{x}) \leq -l_V \epsilon\}$, then the actual state x reaches the zero sub-level set of the function V, and thus, reaches the set S_G.

Remark 4.5. *For Lemma 4.5, it is required that the set* $\{\hat{x} \mid h_G(\hat{x}) \leq -l_G\epsilon\} \neq \emptyset$. *Otherwise, if the minimum value of the function* h_G *exceeds* $-l_G\epsilon$, *i.e.,* $h_{G,min} := \min_{x \in S_G} h_G(x) > -l_G\epsilon$, *so that* $\{\hat{x} \mid h_G(\hat{x}) \leq -l_G\epsilon\} = \emptyset$, *it is not possible for* $\hat{h}_G(\hat{x})$ *to take non-positive values. In such cases, the condition* (4.22) *implies that the closed-loop trajectories only reach the set* $\{x \mid h_G(x) \leq h_{G,min} + l_G\epsilon\}$ *and not the zero sub-level set of the function* h_G. *One such example is the case when the goal set is a singleton, i.e.,* $S_G = \{x \mid \|x - x_G\| \leq 0\} = \{x_G\}$ *where* $x_G \in \mathbb{R}^n$; *in this case* $\text{int}(S_G)$ *is empty and* $\min_{x \in S_G} h_G(x) = 0$, *and thus, condition* (4.22) *only guarantees that the closed-loop trajectories reach the set* $\{x \mid \|x - x_G\| \leq l_G\epsilon\}$.

4.3.3 QP formulation

With robust CBF and robust FxT-CLF conditions at hand, it can be determined whether a given control input can render a safe set forward invariant, and drive the closed-loop trajectories to the desired goal set in the presence of disturbances and state-estimation error. Next, the problem of computing such a control input that satisfies the robust CBF and robust FxT-CLF condition simultaneously, along with the input constraints is addressed. To this end, the QP-based method similar to the ideal case as in Section 4.2 is utilized. The result in Lemma 4.4 is used to formulate robust CBF constraints for the sets S_S and S_T, and that in Lemma 4.5, to formulate the robust FxT-CLF-S_G constraint for the goal set S_G. Define $z = \begin{bmatrix} u^T & \delta_1 & \delta_2 & \delta_3 \end{bmatrix}^T \in \mathbb{R}^{m+3}$, and consider the following optimization problem

$$\min_{z \in \mathbb{R}^{m+3}} \quad \frac{1}{2} z^T H z + F^T z \tag{4.24a}$$

$$\text{s.t.} \quad A_u u \leq b_u, \tag{4.24b}$$

$$L_f \hat{h}_G(\hat{x}) + L_g \hat{h}_G(\hat{x}) u \leq \delta_1 \hat{h}_G(\hat{x}) - \alpha_1 \hat{h}_G(\hat{x})^{\gamma_1} - \alpha_2 \hat{h}_G(\hat{x})^{\gamma_2} - l_G\gamma \tag{4.24c}$$

$$L_f \hat{h}_S(\hat{x}) + L_g \hat{h}_S(\hat{x}) u \leq -\delta_2 \hat{h}_S(\hat{x}) - l_S\gamma, \tag{4.24d}$$

$$L_f \hat{h}_T(t, \hat{x}) + L_g \hat{h}_T(t, \hat{x}) u \leq -\delta_3 \hat{h}_T(t, \hat{x}) - \frac{\partial \hat{h}_T}{\partial t}(t, \hat{x}) - l_T\gamma, \tag{4.24e}$$

where $H = \text{diag}\{\{w_{u_l}\}, w_1, w_2, w_3\}$ is a diagonal matrix consisting of positive weights $w_{u_l}, w_1, w_2, w_3 > 0$ for $l = 1, 2, \ldots, m$, $F = \begin{bmatrix} \mathbf{0}_m^T & q & 0 & 0 \end{bmatrix}^T$ with $q > 0$ and functions

$\hat{h}_G, \hat{h}_S$ (respectively, $\hat{h}_T$) are functions of $\hat{x}$ (respectively, $(t, \hat{x})$) defined as

$$\begin{aligned}\hat{h}_G(\hat{x}) &= h_G(\hat{x}) + l_G\epsilon,\\ \hat{h}_S(\hat{x}) &= h_S(\hat{x}) + l_S\epsilon,\\ \hat{h}_T(t,\hat{x}) &= h_T(t,\hat{x}) + l_T\epsilon.\end{aligned}$$

The parameters $\alpha_1, \alpha_2, \gamma_1, \gamma_2$ are fixed, and are chosen as $\alpha_1 = \alpha_2 = \mu\pi/(2T_{ud})$, $\gamma_1 = 1 + \frac{1}{\mu}$ and $\gamma_2 = 1 - \frac{1}{\mu}$ with $\mu > 1$ and T_{ud} the user-defined time in Problem 4.3. Define $\hat{S}_G = \{\hat{x} \mid h_G(\hat{x}) \leq -l_G\epsilon\}$ so that $\hat{x} \in \hat{S}_G \implies x \in S_G$.
Let the solution of (4.24) be denoted as $z^\star(\cdot) = \begin{bmatrix} v^\star(\cdot)^T & \delta_1^\star(\cdot) & \delta_2^\star(\cdot) & \delta_3^\star(\cdot)\end{bmatrix}^T$. The following result can be stated now.

Theorem 4.6 (Closed-loop properties). *The following holds:*

(i) The QP (4.24) is feasible for all $\hat{x}(t) \in \mathcal{D} \bigcap \left(\text{int}\left(\hat{S}_S\right) \cap \text{int}\left(\hat{S}_T(t)\right)\right) \setminus \hat{S}_G$ for all $t \geq 0$;

(ii) If the solution $z^\star$ is continuous in its arguments and $\max_{0\leq\tau\leq T_{ud}} \delta_1(\hat{x}(\tau)) \leq 0$, then the control input defined as $u = v^\star$ guarantees convergence of the closed-loop trajectories to the goal set S_G within time T_{ud}, i.e., the control input $u = v^\star$ solves Problem 4.3 for all $\hat{x}(0) \in \left(\mathcal{D} \cap \text{int}(\hat{S}_S) \cap \text{int}(\hat{S}_T(0))\right)$.

Proof. Part (i): For $t \geq 0$ such that $\hat{x}(t) \in \mathcal{D} \bigcap (\text{int}(\hat{S}_S \cap \text{int}(\hat{S}_T(t))) \setminus S_G$, it holds that $\hat{h}_S(\hat{x}), \hat{h}_T(t,\hat{x}), \hat{h}_G(\hat{x}) \neq 0$. Choose $v = \bar{v} \in \mathcal{U}$ and define

$$\delta_1 = \frac{L_f\hat{h}_G + L_g\hat{h}_G\bar{v} + \alpha_1\hat{h}_G^{\gamma_1} + \alpha_2\hat{h}_G^{\gamma_2} + l_V\gamma}{\hat{h}_G},$$

which is well-defined for all $\hat{x} \notin \hat{S}_G$, so that (4.24c) is satisfied with equality. Similarly, define $\bar{\delta}_2, \bar{\delta}_3$ so that (4.24d)-(4.24e) are satisfied with equality. Thus, there exists $\bar{z} = \begin{bmatrix}\bar{v}^T & \bar{\delta}_1 & \bar{\delta}_2 & \bar{\delta}_3\end{bmatrix}^T$ such that all the constraints of QP (4.24) are satisfied.

Part (ii): The condition (4.24c) implies that the time derivative of $\hat{h}_G(\hat{x}(t))$ satisfies (3.15) for all $\hat{x}(t) \in \mathcal{D} \cap \text{int}(\hat{S}_S) \cap \text{int}(\hat{S}_T(t))$. Thus, using Lemma 4.5 and Theorem 3.3, it follows that $\hat{h}_G(\hat{x}(t)) \leq 0$ for $t \geq T_{ud}$, which implies that $h_G(\hat{x}(t)) \leq -L_G\epsilon$, which in turn implies $h_G(x(t)) \leq 0$ for $t \geq T_{ud}$ for all $\hat{x}(0) \in \mathcal{D} \cap \text{int}(\hat{S}_S) \cap \text{int}(\hat{S}_T(0))$. Furthermore, conditions (4.24d) and (4.24e) imply that the functions h_S and h_T are robust CBFs for (4.18), and thus, the set $S_S \cap S_T$ is forward invariant. Thus, the control input $u = v^\star$ solves Problem 4.3 for all $\hat{x}(0) \in D = \mathcal{D} \cap \text{int}(\hat{S}_S) \cap \text{int}(\hat{S}_T(0))$. □

It is worth noting that the constraints in the QP (4.24) are a function of the state estimate $\hat{x}$, and not the actual state x, which is unknown. Thus, the resulting control input $u = v^\star(\hat{x})$ is realizable. A couple of remarks on the main result of this section are provided now.

Remark 4.6. *Theorem 4.6 guarantees that starting from the intersection of the interiors of the safe sets, the closed-loop trajectories remain inside the interior of these sets, which, with the help of slack variables in (4.24d)-(4.24e), guarantees recursive feasibility of the QP. The case when the initial conditions lie on the intersection of the boundaries of the safe sets requires strong viability assumptions such as the existence of u such that (4.3) holds for both h_S and h_T for all $x \in \partial S_S \cap \partial S_T$. Under this condition, the result in Theorem 4.6 can be extended to the set $D = \mathcal{D} \cap (\hat{S}_S) \cap (\hat{S}_T(t))$.*

Remark 4.7. *Note that the result in part (iii) of Theorem 4.6 requires $\delta_1 \leq 0$ so that the control input u solves the convergence requirement of Problem 4.3. When this condition does not hold, the closed-loop trajectories, while still satisfying safety requirements, may not converge to the goal set within the required time T_{ud}, or from an arbitrary initial condition $x(0) \notin S_G$.*

4.4 Simulations

Two case studies are presented to illustrate the efficacy of the proposed method. In the numerical case studies, Euler discretization is used to discretize the continuous-time dynamics, and the MATLAB function `quadprog` to solve the QP at each discrete time step.

4.4.1 Nominal case: 2 agents case study

Consider a two-agent motion planning problem under spatiotemporal specifications, where the objectives for the agents are to visit goal regions in a given time sequence while remaining in a safe set at all times, and maintaining a safe distance from each other. For the sake of simplicity, the agent dynamics are modeled via single integrators as:

$$\dot{x}_i = u_i,$$

where $x_i, u_i \in \mathbb{R}^2$ for $i = 1, 2$. The closed-loop trajectories for the respective agents, starting from $x_1(0) \in C_1$ and $x_2(0) \in C_3$, are required to satisfy the following STL specifications

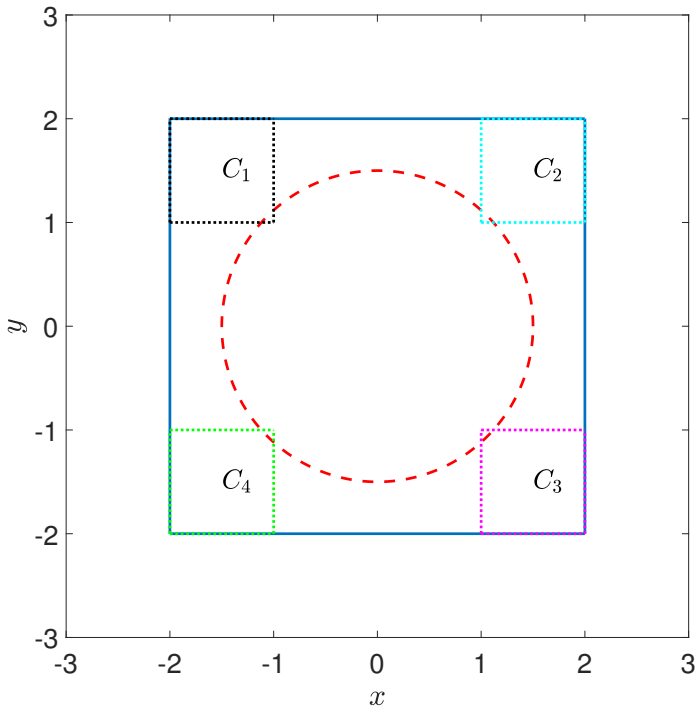

Figure 4.4: Problem setting for the 2 agent scenario.

$$(x_1, t) \models G_{[0,T_4]}\phi_s \wedge F_{[0,T_1]}\phi_2 \wedge F_{[T_1,T_2]}\phi_3 \wedge F_{[T_2,T_3]}\phi_4 \wedge F_{[T_3,T_4]}\phi_1,$$
$$(x_2, t) \models G_{[0,T_4]}\phi_s \wedge F_{[0,T_1]}\phi_2 \wedge F_{[T_1,T_2]}\phi_1 \wedge F_{[T_2,T_3]}\phi_4 \wedge F_{[T_3,T_4]}\phi_3$$

which is explained in details below (see Figure 4.4):

- $x_1(t), x_2(t) \in S_S = \{x \mid \|x\|_1 \leq 2, \|x\|_2 \geq 1.5\}$ for all $t \geq 0$, i.e., the closed-loop trajectories of the two agents should stay inside the solid-blue square and outside the red-dotted circle, and maintain a minimum separation d_m at all times;
- On or before a given T_1 satisfying $0 < T_1 < \infty$, agent 1 and 2 should reach the square C_2;
- On or before a given T_2 satisfying $T_1 < T_2 < \infty$, agent 1 should reach the square C_3 and agent 2 should reach the square C_1;
- On or before a given T_3 satisfying $T_2 < T_3 < \infty$, agent 1 and 2 should reach the square C_4;
- On or before a given T_4 satisfying $T_3 < T_4 < \infty$, agent 1 should reach the square C_1 and agent 2 should reach the square C_3;

This problem is an extended version of the case study considered in [110, 136]. Note that the sets C_i are not overlapping with each other, and the corresponding functions $h_i(x)$ are not continuously differentiable. Now, in order to be able to use QP-based formulation (4.16), Assumption 4.1 needs to hold, i.e., the sets $\bar{S}_i$ should be constructed such that $\bar{S}_i \bigcap \bar{S}_{i+1} \neq \emptyset$. In order to address this problem, construct auxiliary sets $\bar{S}_i$, $i \in \{1, 2, \cdots, 8\}$ as shown in Figure 4.5.

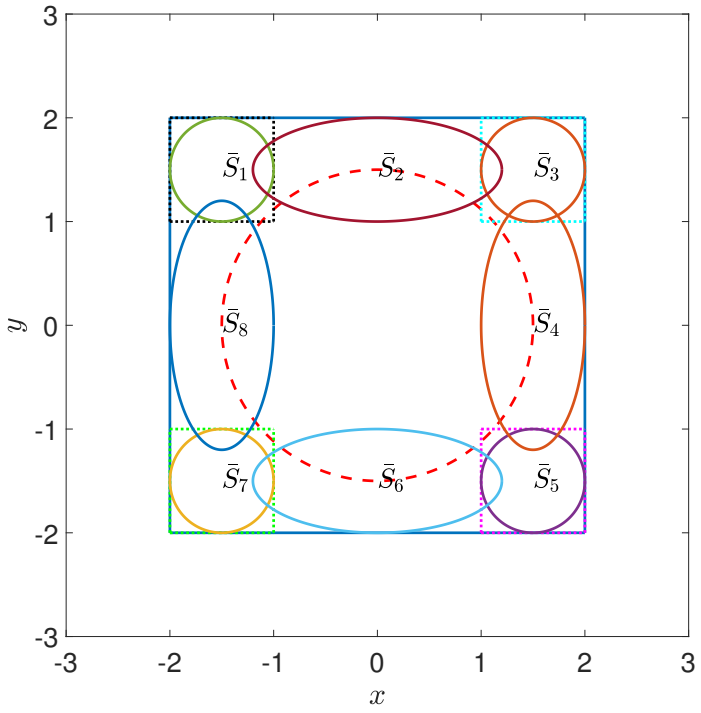

Figure 4.5: Construction of sets $\bar{S}, \bar{S}_1, \cdots, \bar{S}_8$.

The set $\bar{S} = \{x \mid \|x\|_2 \leq 1.5\}$ and sets $\bar{S}_i$ are defined as follows:

$$\bar{S}_1 = \{x \mid \|(x - [-1.5\ 1.5]^T)\| \leq 0.5\}, \qquad \bar{S}_2 = \{x \mid \|(x - [0\ 1.5]^T)\|_{P_1} \leq 1\},$$
$$\bar{S}_3 = \{x \mid \|(x - [1.5\ 1.5]^T)\| \leq 0.5\}, \qquad \bar{S}_4 = \{x \mid \|(x - [1.5\ 0]^T)\|_{P_2} \leq 1\},$$
$$\bar{S}_5 = \{x \mid \|(x - [1.5\ -1.5]^T)\| \leq 0.5\}, \qquad \bar{S}_6 = \{x \mid \|(x - [0\ -1.5]^T)\|_{P_1} \leq 1\},$$
$$\bar{S}_7 = \{x \mid \|(x - [-1.5\ -1.5]^T)\| \leq 0.5\}, \qquad \bar{S}_8 = \{x \mid \|(x - [-1.5\ 0]^T)\|_{P_2} \leq 1\}.$$

where $\|z\|_{P_1} := \sqrt{\frac{z_1^2}{1.2^2} + \frac{z_2^2}{0.5^2}}$ and $\|z\|_{P_2} := \sqrt{\frac{z_1^2}{0.5^2} + \frac{z_2^2}{1.2^2}}$ where $z = [z_1\ z_2]^T \in \mathbb{R}^2$. Now, in order to visit square C_2, agent 1 can go to set $\bar{S}_2 \setminus \bar{S}$ within a time $0 < t_0 < T_1$ and then to $\bar{S}_3$ before $t = T_1$. Hence, for agent 1, for time interval $[0, t_0]$, the safe set is defined by function $h_S = \max\{h_{s1}, h_{s2}, h_{s3}, h_{s4}\}$, where $h_{s1} = \|x\|_1 - 2, h_{s2} = 1.5 - \|x\|, h_{s3} = d_m - \|x - x_2\|$ and $h_{s4} = \|x - [-1.5\ 1.5]^T\| - 0.5$, and the goal set is defined by function

$h_G = \|x - [0\ 1.5]^T\|_{P_1} - 1$. For time interval $[t_0, T_1]$, the functions h_{s4} and h_G change, while other things remain same. With these new sets, the problem can be re-formulated for agent 1 to design a control input $u_1(t)$ such that for $x_1(0) \in \bar{S}_1$,

- For a given t_0 satisfying $0 < t_0 < T_1$, $x_1(t_0) \in \bar{S}_2 \setminus \bar{S}$ and $x_2(t_0) \in \bar{S}_4 \setminus \bar{S}$;
- For a given t_1 satisfying $t_0 < t_1 \leq T_1$, $x_1(t_1) \in \bar{S}_3$ and $x_2(t_1) \in \bar{S}_3$;
- For a given t_2 satisfying $T_1 < t_2 < T_2$, $x_1(t_2) \in \bar{S}_4 \setminus \bar{S}$ and $x_2(t_2) \in \bar{S}_2 \setminus \bar{S}$;
- For a given t_3 satisfying $t_2 < t_3 \leq T_2$, $x_1(t_3) \in \bar{S}_5$ and $x_2(t_3) \in \bar{S}_1$;
- For a given t_4 satisfying $T_2 < t_4 < T_3$, $x_1(t_4) \in \bar{S}_6 \setminus \bar{S}$ and $x_2(t_4) \in \bar{S}_8 \setminus \bar{S}$;
- For a given t_5 satisfying $t_4 < t_5 \leq T_3$, $x_1(t_5) \in \bar{S}_7$ and $x_2(t_5) \in \bar{S}_7$;
- For a given t_6 satisfying $T_3 < t_6 < T_4$, $x_1(t_6) \in \bar{S}_8 \setminus \bar{S}$ and $x_2(t_6) \in \bar{S}_6 \setminus \bar{S}$;
- For a given t_7 satisfying $t_6 < t_7 \leq T_4$, $x_1(t_7) \in \bar{S}_1$ and $x_2(t_7) \in \bar{S}_5$,
- For all $t \geq 0$, $x_1(t), x_2(t) \in S_S$ and $\|x_1(t) - x_2(t)\| \geq d_m$.

One can readily write the requirements for agent 2 in the similar manner. The formulation (4.16) can now be used to compute the control input by solving (4.16) sequentially, i.e., for agent 1, for $t \in [0, t_0)$, $S_G = \bar{S}_2$, then for $t \in [t_0, T_1)$, $S_G = \bar{S}_3$, and so on. The input constraints are chooses as $|u_i| \leq 10$ for $i = 1, 2$. In order to translate the input constraint in the form of (4.16b), define $A_u = \begin{bmatrix} 1 & 0 \\ -1 & 0 \\ 0 & 1 \\ 0 & -1 \end{bmatrix}$ and $b_u = \begin{bmatrix} 7 & 7 & 7 & 7 \end{bmatrix}^T$, so that $u_{1x}, u_{1y}, u_{2x}, u_{2y} \in [-7,\ 7]$. The time constraints are chosen as $T_i = 2$ for $i \in \{1, 2, 3, 4\}$ and $t_j = 1$ for $j \in \{t_0, t_1, \cdots, t_7\}$, and $\mu = 5$, so that $\gamma_1 = 1.2$ and $\gamma_2 = 0.8$. The safety distance is chosen as $d_m = 0.1$.

Figure 4.6 shows the control inputs for the two robots, and their inter-agent distance with time. The control input constraint $\|u_i(t)\| \leq 10$ is satisfied for both $i = 1, 2$ at all times. Red-dotted line shows the minimum required inter-agent distance $d_m = 0.1$ for safety. It is clear that the control input and safety constraints are satisfied at all times.

Figures 4.7 and 4.8 shows the closed-loop trajectories of the two robots. The safe region $S_S \bigcap (\bigcup_{i=1}^{8} \bar{S}_i)$ is highlighted in grey color. Purple and green lines plot the paths taken by agent 1 and 2, respectively. The agents visit all the required sets, while maintaining safe distance from each other when they meet in the sets $\bar{S}_3$ and $\bar{S}_7$. The figure shows snapshots

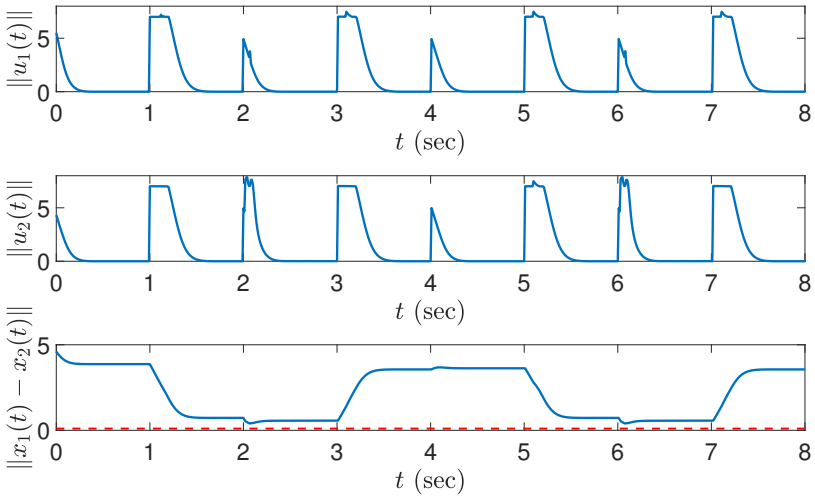

Figure 4.6: Norm of the control inputs $\|u_1(t)\|, \|u_2(t)\|$ and inter-agent distance $\|x_1(t) - x_2(t)\|$ between the agents.

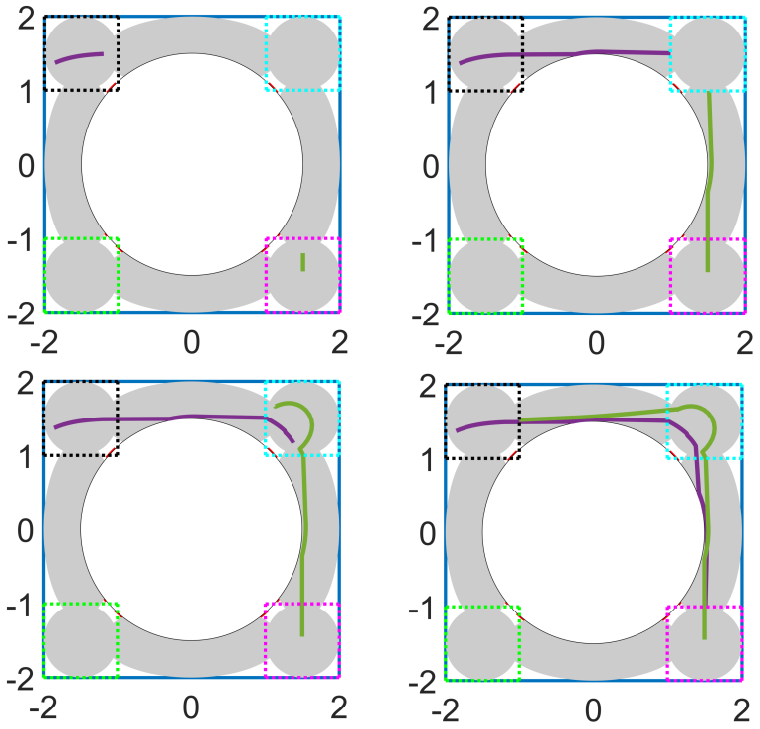

Figure 4.7: Closed-loop trajectories of the two robots: snapshot at $t = 1, 2, 3$ and 4 sec.

at the instants when the agents reach the next goal set in the sequence, i.e., first snapshot at $t = 1$ is taken when agent 1 reaches the set $\bar{S}_2$, i.e., $x_1(t) \in \bar{S}_2$ and agent 2 reaches the set $\bar{S}_4$, i.e., $x_2(t) \in \bar{S}_4$. Snapshots at various time instants illustrate that the closed-loop trajectories satisfy the temporal constraints as well.

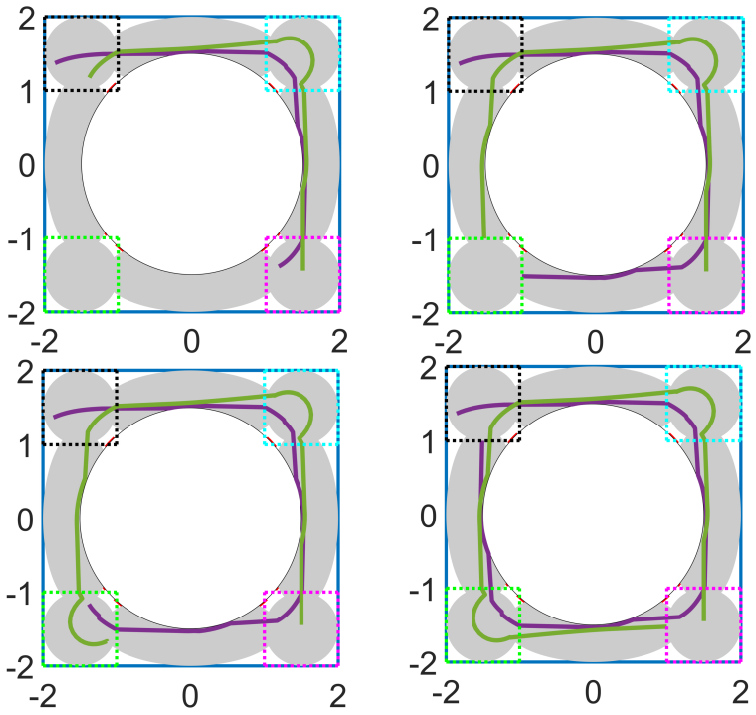

Figure 4.8: Closed-loop trajectories of the two robots: snapshot at $t = 5, 6, 7$ and 8 sec.

4.4.2 Robust control: 4 agents case study

Consider a numerical case-study involving underactuated underwater autonomous vehicles with state $X_i \in \mathbb{R}^6$, modeled as

$$\begin{bmatrix} \dot{x}_i \\ \dot{y}_i \\ \dot{\phi}_i \\ m_{11}\dot{u}_i \\ m_{22}\dot{v}_i \\ m_{33}\dot{r}_i \end{bmatrix} = \begin{bmatrix} u_i \cos\phi_i - v_i \sin\phi_i \\ u_i \sin\phi_i + v_i \cos\phi_i \\ r_i \\ m_{22}v_i r_i + X_u u_i + X_{u|u|}|u_i|u_i \\ -m_{11}u_i r_i + Y_v v_i + Y_{v|v|}|v_i|v_i \\ (m_{11} - m_{22})u_i v_i + N_r r_i + N_{r|r|}|r_i|r_i \end{bmatrix} + \begin{bmatrix} 0 \\ 0 \\ 0 \\ \tau_{u,i} \\ 0 \\ \tau_{r,i} \end{bmatrix} + \begin{bmatrix} V_w \cos(\theta_w) \\ V_w \sin(\theta_w) \\ 0 \\ 0 \\ 0 \\ 0 \end{bmatrix} \tag{4.25}$$

where $z_i = [x_i,\ y_i,\ \phi_i]^T$ is the configuration vector of the i-th agent, $[u_i,\ v_i,\ r_i]^T$ are the velocities (linear and angular) w.r.t the body-fixed frame, $\tau_i = [\tau_{u,i},\ \tau_{r,i}]^T$ is the control input vector where $\tau_{r,i}$ are the control input along the surge (x-axis) and yaw degree of freedom, respectively, X_u, Y_v, N_r are the linear drag terms, and $X_{u|u|}, Y_{v|v|}, N_{r|r|}$ are the non-linear drag terms (see [137] for more details). The parameters used in the case study are given in Table 4.1:

The additive disturbance $d = \begin{bmatrix} V_w(X_i,t)\cos(\theta_w(X_i,t)) \\ V_w(X_i,t)\sin(\theta_w(X_i,t)) \end{bmatrix}$ with $|V_w(X_i,t)| \leq \gamma$ models the effect of an unknown, time-varying water current acting on the system dynamics of

Table 4.1: Dynamic parameters as taken from [137].

m_{11}	5.5404	X_u	-2.3015	$X_{u\|u\|}$	-8.2845
m_{22}	9.6572	Y_v	-8.0149	$Y_{v\|v\|}$	-23.689
m_{22}	1536	N_r	-0.0048	$N_{r\|r\|}$	-0.0089

each agent. Errors in the state estimates are also considered as stated in Assumption 4.6. Note that the system dynamics is under-actuated since there is no control input in the sway degree of freedom (y-axis). The multi-task problem considered for the case study consists of the following objective: find a control input $\tau_i \in \mathcal{U}_i = [-\tau_{u,m}, \tau_{u,m}] \times [-\tau_{r,m}, \tau_{r,m}]$, $\tau_{u,m}, \tau_{r,m} > 0$, such that each agent

(i) Reaches an assigned goal region around a point $g_i \in \mathbb{R}^2$ within a user-defined time T, i.e., $\begin{bmatrix} x_i(t) & y_i(t) \end{bmatrix}^T \to g_i$ as $t \to T$;

(ii) Keeps their respective point-of-interest $p_i \in \mathbb{R}^2$ in their field of view (given as a sector of radius $R > 0$ and angle $\alpha > 0$), i.e., $z_i(t) \in \mathcal{F} = \{z \in \mathbb{R}^3 \mid \| \begin{bmatrix} x_i & y_i \end{bmatrix}^T - p_i \| \leq R, |\angle \left(p_i - \begin{bmatrix} x_i & y_i \end{bmatrix}^T \right) - \phi_i| \leq \alpha\}$ for all $t \geq 0$ (see Figure 4.9);

(iii) Maintains a safe distance d_s with respect to other agents, i.e., $\| \begin{bmatrix} x_i(t) & y_i(t) \end{bmatrix}^T - \begin{bmatrix} x_j(t) & y_j(t) \end{bmatrix}^T \| \geq d_s$ for all $t \geq 0$, $i \neq j$,

where $\angle(\cdot)$ is the angle of the vector $(\cdot)$ with respect to the x-axis of the global frame. Note that (ii) requires safety with respect to a static safe set, while requires (iii) safety with respect to a time-varying safe set.

First, the CLF and CBFs to guarantee convergence to the desired location, and invariance of the required safe sets, respectively are constructed. Consider the function $h_{ij} = d_s^2 - \left\| \begin{bmatrix} x_i(t) & y_i(t) \end{bmatrix}^T - \begin{bmatrix} x_j(t) & y_j(t) \end{bmatrix}^T \right\|^2$, defined for $i \neq j$, so that $h_{ij} \leq 0$ implies that the agents maintain the safe distance d_s. Since the function h_{ij} is relative degree two function with respect to the dynamics (4.25), the second order safety condition discussed in [138] is used. Similarly, for keeping the point-of-interest in the field of view, two separate CBFs are used, defined as $h_\phi = \left| \angle \left(p_i - \begin{bmatrix} x_i & y_i \end{bmatrix}^T \right) - \phi_i \right|^2 - \alpha^2, h_R = \left\| \begin{bmatrix} x_i & y_i \end{bmatrix}^T - p_i \right\|^2 - R^2$, so that $h_\phi(z_i) \leq 0, h_R(z_i) \leq 0$ implies that $z_i \in \mathcal{F}$. For h_ϕ, h_R, a different relative degree 2 condition is used as discussed next. Following the results in [59], it can be shown that satisfaction of

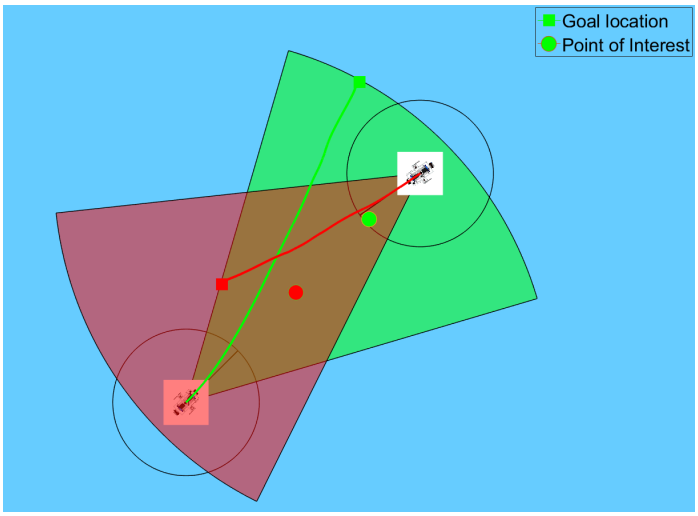

Figure 4.9: Problem setting for the two-agent case.

the inequality

$$L_f^2 h_S(x) + L_g L_f h_S(x) u + 2 L_f h_S(x) + h_S(x) \leq \alpha(-L_f h_S(x) - h_S(x)), \tag{4.26}$$

for all $x \in \bar{S}_S \coloneqq \{x \mid L_f h_S(x) + h_S(x) \leq 0\}$, with $\alpha \in \mathcal{K}$, implies that the set $\bar{S}_S$ is forward-invariant. In this case, one can define $\bar{h}_S = L_f h_S + h_S$ so that (4.26) reads

$$L_f \bar{h}_S(x) + L_g \bar{h}_S(x) u \leq \alpha(-\bar{h}_S(x)), \tag{4.27}$$

which is the same as (4.7), thus guaranteeing forward invariance of the set $\bar{S}_S$. Note that the inequality $L_f h_S(x) + h_S(x) \leq 0$ can also be written as $\dot{h}_S(x) + h_S(x) \leq 0$, satisfaction of which, using Nagumo's theorem, implies forward invariance of the set S_S, and thus, it holds that $\bar{S}_S \subset S_S$.

Finally, the CLF is chosen as $V = \frac{1}{2}(X_i - X_{di})^T (X_i - X_{di})$, where $X_i \in \mathbb{R}^6$ is the state vector of the i-th agent, and $X_{di} \in \mathbb{R}^6$ its desired state, defined as

$$X_{di} = \begin{bmatrix} g_i \\ \theta_g \\ c_1 \left\| g_i - \begin{bmatrix} x_i & y_i \end{bmatrix}^T \right\| \cos(\theta_g - \phi_i) \\ c_1 \left\| g_i - \begin{bmatrix} x_i & y_i \end{bmatrix}^T \right\| \sin(\theta_g - \phi_i) \\ c_2(\theta_g - \phi_i) \end{bmatrix}$$

where $\theta_g = \angle \left(g_i - \begin{bmatrix} x_i & y_i \end{bmatrix}^T \right)$ and $c_1, c_2 > 0$ are constants.

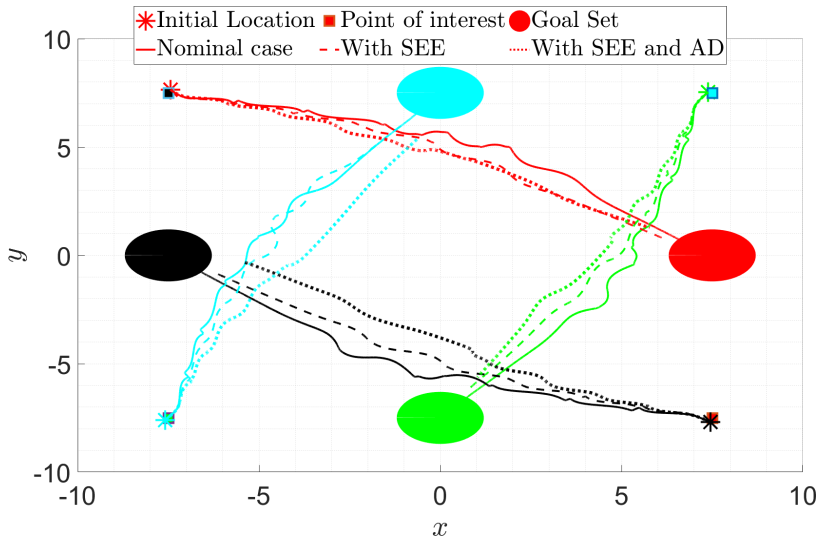

Figure 4.10: Closed-loop paths traced by agents.

Four agents are considered for the numerical experiments, and the bounds on the additive disturbance d and the state-estimation errors are chosen as $\gamma = 0.5$ and $\epsilon = 0.5$, respectively. The simulations are performed for 3 scenarios: the case without disturbances, shown in solid lines, with only state estimation error (SEE), shown in dashed lines, and with both SEE and additive disturbance (AD), shown in dotted lines. Figure 4.10 shows the path traced by 4 agents. The solid circular region represents the goal set defined as $\{X \mid V(X) \leq 0.1\}$, and the square boxes denote the point of interests p_i for each agent i.[1]

Figure 4.11 plots $V_M = \max_i\{V_i\}$ showing the convergence of the agents to their respective goal sets, while satisfying all the safety constraints, as can be seen from Figure 4.12, which plots $h_M = \max\{h_{ij}, h_R, h_\phi\}$ showing that all the CBFs are non-positive at all times for all the three cases.

4.5 Discussion

The QP based formulation for control synthesis proposed in this chapter assumes that the underlying optimization problem is solved for each x which is continuously evolving in time, which requires that the QP is solved instantly for each x. However, as argued in [57], such methods are not directly implementable for mechanical systems, which are typically controlled digitally, in which sensors are used to take measurements, the required input is computed, and the computed control is implemented over a sampling period. The authors in [57] address the issue of sampling effects in the implementation of QP-based controllers.

[1] A video of the simulation is available at https://tinyurl.com/y32oa4p4.

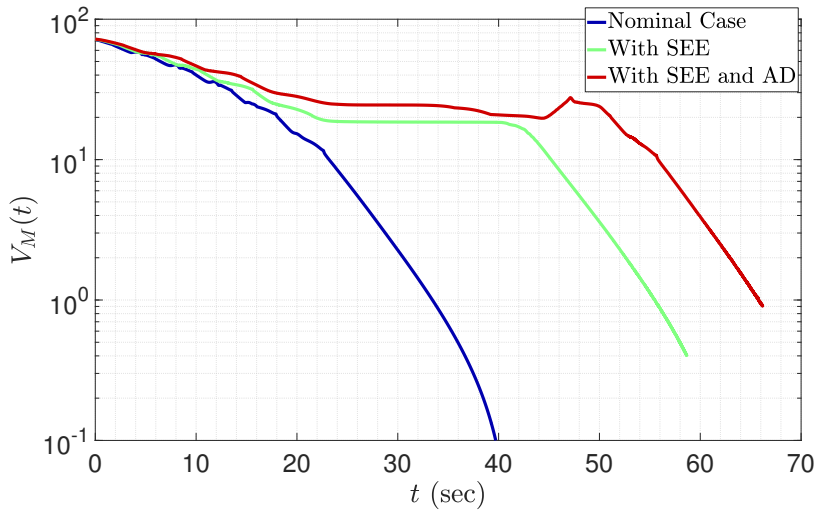

Figure 4.11: Point-wise maximum of Lyapunov functions $V_M(t) = \max_i\{V_i(t)\}$ with time for the three cases.

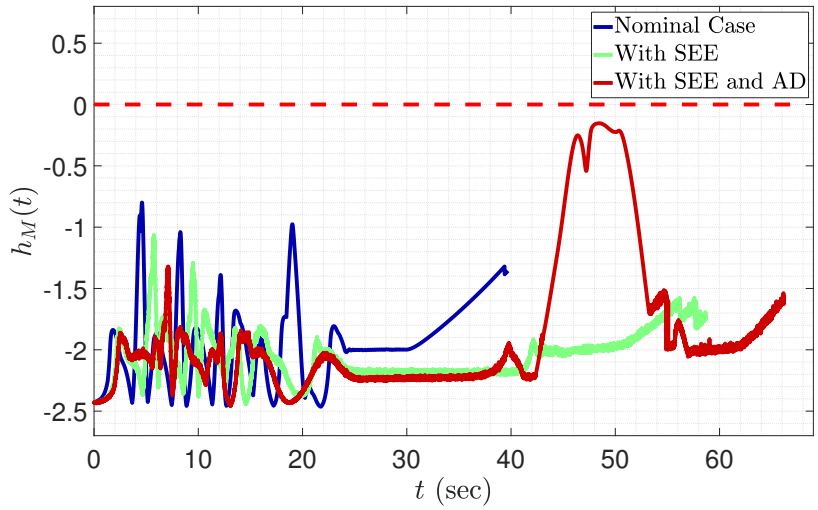

Figure 4.12: Point-wise maximum of CBFs h_{ij}, h_R, h_ϕ, showing satisfaction of all the safety constraints for the three cases.

They consider safety constraints for discretized continuous-time systems in the presence of additive disturbances. More specifically, they discuss how to modify the CBF in the QP to guarantee forward invariance of a set so that satisfaction of the safety constraints at the discrete-time steps via robust CBF results in safety at all times. In the numerical case studies presented at the end of this chapter, Euler discretization is used to implement the proposed method. Although a discrete implementation of the presented method without accounting for discretization errors might lead to a safety violation, one can adopt a robust CLF method as discussed in [57] to guarantee that safety is preserved. Other relevant work

on sampled-data controller design in the context of safety includes [139–143]. A thorough analysis of safety and fixed-time convergence for the discrete-time approximation of QP-based methods is out of the scope of this dissertation, and is left for future work.

4.6 Conclusions

The problem of satisfying spatiotemporal constraints requiring that the closed-loop trajectories of a class of nonlinear, control-affine systems remain in a safe set at all times, and reach a goal set within a fixed time in the presence of control input constraints is considered in this chapter. A novel QP formulation is proposed and it is shown that under the assumption of the existence of a control input that renders the safe set forward invariant, it is feasible and that the solution of the proposed QP is a continuous function of state variable under certain conditions. Various cases under which the solution of the QP solves the considered problem are discussed.

Then, additive disturbances in the system dynamics and bounded error in the available state estimation are considered. The notion of robust CBFs are utilized to guarantee safety, and that of robust FxT-CLF, to guarantee fixed-time reachability to the given goal set. Finally, a QP is formulated, incorporating safety and convergence constraints using slack variables so that its feasibility is guaranteed. It is shown that under certain conditions, the control input defined as the solution of the proposed QP solves the underlying constrained control problem in the presence of the considered disturbances and input constraints.

CHAPTER 5

Finite-time Stability of Switched and Hybrid Systems

Up to now, results were presented for dynamical systems having continuous right-hand side. As discussed in Chapter 1, there are plenty of design and analysis problems that require the study of hybrid dynamical systems. In this chapter, results on finite-time stability of switched and hybrid systems are presented. Inspired by classical stability results for the aforementioned systems using multiple-Lyapunov functions, their extension to finite-time stability is investigated. A new notion of FTS for hybrid systems is introduced so that it does not restrict each mode of the hybrid system to be FTS in itself. Then, sufficient conditions for FTS of the origin of a class of hybrid systems in terms of multiple Lyapunov functions are developed in Section 5.2. The requirements in [77, 82] that the Lyapunov function is non-increasing at the discrete jumps, and strictly decreasing during the continuous flow are relaxed; instead, the Lyapunov functions are allowed to increase both during the continuous flow and at the discrete jumps, as long as these increments are bounded. In this respect, the hybrid system is allowed to have unstable modes while still guaranteeing FTS. The main result is that if the origin is stable under arbitrary switching, and if there exists an FTS mode that is active for a sufficient cumulative time, then the origin of the resulting hybrid system is FTS. The results in this section are based on [113].

Then, FTS of a class of switched systems using multiple Lyapunov functions is studied in Section 5.3. The proposed framework is utilized in designing a switching signal so that the origin of the resulting switched system is FTS. As an application, the problem of stabilizing the origin of a switched linear system using output feedback is studied for the case when only one of the subsystems (or modes) is controllable and observable. The results in this section are based on [114].

The following notation is frequently used in this chapter:

$\mathbb{R}$ Set of real numbers

$\mathbb{R}_+$	Set of non-negative reals
$\mathbb{R}_-$	Set of non-positive reals
$\|\cdot\|$	Euclidean norm of $(\cdot)$
$\|\cdot\|$	Absolute value if $(\cdot)$ is scalar and the length if $(\cdot)$ is a time interval
int(S)	Interior of the set S
t^-	Time just before the time instant t
t^+	Time just after the time instant t
Σ_f	Set of indices of continuous modes
σ_f	Switching signal
t_{i_k}	Time instant when the $i-$th mode becomes active for $k-$th time
t_{i_k+1}	Time instant when the $i-$th mode becomes de-active for $k-$th time
T_{i_k}	Interval $[t_{i_k}, t_{i_k+1})$ in which $i-$th mode is active for the $k-$th time
t_d^m	Time instant when the $m-$th discrete jump takes place
J_i	Set of discrete jumps for the $i-$th mode
$\bar{T}_{i_k}$	Largest connected subset $[\bar{t}_{i_k}, \bar{t}_{i_k+1})$ of T_{i_k} without a discrete jump
$\bar{V}_{F_i}$	Value of V_F at the time instant $\bar{t}_{F_i}$

5.1 Preliminaries

Consider the class of hybrid systems $\mathcal{H} = \{C, \mathcal{F}, D, \mathcal{G}\}$ described as

$$\begin{aligned} \dot{x}(t) &= f_{\sigma_f(t,x)}(x(t)), \qquad && x(t) \in C, \\ x(t^+) &= g(x(t^-)), && x(t^-) \in D, \end{aligned} \tag{5.1}$$

where $x \in \mathbb{R}^n$ is the state vector with $x(t_0) = x_0$, $f_i \in \mathcal{F} \triangleq \{f_k : \mathbb{R}^n \to \mathbb{R}^n\}$ for $k \in \Sigma_f \triangleq \{1, 2, \ldots, N_f\}$ is the continuous flow (called thereafter, continuous-time mode, or simply, mode) allowed on the subset of the state space $C \subset \mathbb{R}^n$, and $\mathcal{G} = \{g\}$ where $g : \mathbb{R}^n \to \mathbb{R}^n$ defines the discrete behavior (called thereafter discrete-jump dynamics), which is allowed on the subset $D \subset \mathbb{R}^n$.

At a jump instant $t \in \mathbb{R}_+$, the state $x(t)$ is characterized by multiple values, namely the value just before the jump at time t, which is denoted as $x(t^-)$, and the value just after the jump at time t, which is denoted as $x(t^+)$ (satisfying $x(t^+) = g(x(t^-))$). The reason for using the t^-, t^+ notation is to highlight the "pre"-jump and the "post"-jump values of the state in the Lyapunov conditions of the main theorems. The switching signal $\sigma_f : \mathbb{R}_+ \times \mathbb{R}^n \to \Sigma_f$ can depend on both t and x, and is assumed to be piecewise continuous (from the right) in time and continuous in x. The arguments (t, x) from σ_f are omitted for the sake

of brevity. Systems of the form (5.1) have been studied in [76], while [77] considers the form (5.1) without the discrete-jump dynamics. Denote by $T_{i_k} = [t_{i_k}, t_{i_k+1}) \subset \mathbb{R}_+$, with $t_{i_k+1} \geq t_{i_k} \geq t_0$, the interval in which the flow f_i is active for the $k-$th time for $i \in \Sigma_f$ and $k \in \mathbb{N}$, and $t = t_m^d$ the time when discrete jump $x(t^+) = g(x(t^-))$ takes place for the $m-$th time, $m \in \mathbb{N}$. Define $J_i = \{t_m^d \mid t_m^d \in T_{i_k}, m \in \mathbb{N}\}$ as the set of all time instances when a discrete jump takes place when the continuous flow f_i is active, and $\mathcal{J} = \bigcup_{i \in \Sigma_f} J_i$ as the set of all times when the state of (5.1) undergoes a discrete jump. Without loss of generality, assume that the switching signal σ_f is minimal, i.e., for all $i \in \Sigma_f$, $t_{i_{k+1}} \neq t_{i_k+1}$ for all $k \in \mathbb{N}$, and that there are no two discrete jumps at the same time instant. The following assumptions is also required.

Assumption 5.1. *The functions f_i are continuous for all $i \in \Sigma_f$ and the origin is the only equilibrium point of* (5.1).

The case when there exists a closed set $\bar{D} \neq \{0\}$ such that $g(x) = 0$ for all $x \in \bar{D} \subset D$ can be treated by studying stability of closed sets; see [82,144]. To study the stability properties of hybrid dynamical systems, a special class of functions is defined below.

Definition 5.1. *A continuous function $\alpha : \mathbb{R}_+ \to \mathbb{R}_+$ is called*

- ***Class-$\mathcal{K}$ function**: if it is increasing, i.e., for all $x > y \geq 0$, $\alpha(x) > \alpha(y)$;*
- ***Class-$\mathcal{K}_\infty$ function**: if it is a class-$\mathcal{K}$ function, and $\lim_{r \to \infty} \alpha(r) = \infty$.*

The solution of the hybrid system (5.1) can be defined as follows: a function $x : \mathbb{R}_+ \to \mathbb{R}^n$ is a solution of (5.1) if

- it is absolutely continuous between two consecutive jump instants and satisfies $\dot{x}(t) = f_k(t, x)$ for almost all $t \in \mathbb{R}_+ \setminus \mathcal{J}$ such that $x(t) \in C$, where $k = \sigma(t, x)$;
- it satisfies $x(t^+) = g(x(t))$, for all $t \in \mathcal{J}$ such that $x(t) \in D$.

The interested reader is referred to [74, Chapter 2] for a detailed presentation on the solution notion of hybrid systems.
Before presenting the main result, the following assumption on the solution of (5.1) is stated.

Assumption 5.2 (Existence of solution). *The solution of* (5.1) *exists for all $t \geq 0$, and is non-Zeno.*

Similar assumptions have been used in literature (e.g., [77, 82, 145]) in order to analyze stability properties of the origin of hybrid systems.

Next, the notion of FTS for hybrid systems is defined. Note that a mode $F \in \Sigma_f$ is called an FTS subsystem or FTS mode if the origin of $\dot{y} = f_F(y)$ is FTS. The standard notion of stability under arbitrary switching, as employed in [75–77, 85, 146], is restrictive in the following sense. The conditions therein require every single mode of the system (5.1) to be LS, AS or FTS for the origin of the system (5.1) to be LS, AS or FTS, respectively. This restriction can be overcome by defining the corresponding notions of stability for hybrid system (inspired in part, from [147, Theorem 1]) as following. Let $\Pi \subset \text{PWC}(\mathbb{R}_+ \times \mathbb{R}^n, \Sigma_f)$ denote the set of all possible switching signals, where PWC is the set of all piecewise constant functions mapping from $\mathbb{R}_+ \times \mathbb{R}^n$ to Σ_f.

Definition 5.2 (FTS of hybrid systems). *The origin of the hybrid system (5.1) is called LS, AS or FTS, if there exists an open neighborhood $X \subset \mathbb{R}^n$ such that for all $y \triangleq x(0) \in X$, there exists a subset of switching signals $\Pi_y \subset \Pi$ such that the origin of the system (5.1) is LS, AS or FTS, respectively, with respect to all $\sigma_f \in \Pi_y$. The origin is called globally AS or FTS if $X = \mathbb{R}^n$.*

The following Lemma is presented before proceeding to the main results.

Lemma 5.1. *Let $a_i \geq b_i \geq 0$ for all $i \in \{1, 2, \ldots, K\}$ where $K \in \mathbb{N}$. Then, for all $0 < r < 1$, we have*

$$\sum_{i=1}^{K} (a_i^r - b_i^r) \leq \sum_{i=1}^{K} (a_i - b_i)^r. \tag{5.2}$$

Proof. Lemma 3.3 [51] establish the following inequality for $z_i \geq 0$ and $0 < r \leq 1$,

$$\left(\sum_{i=1}^{M} z_i \right)^r \leq \sum_{i=1}^{M} z_i^r. \tag{5.3}$$

Hence, it holds that for $a \geq b \geq 0$ and $0 < r \leq 1$, $a^r = (b + (a - b))^r \leq b^r + (a - b)^r$, or equivalently,

$$a^r - b^r \leq (a - b)^r. \tag{5.4}$$

Hence, for all $0 < r \leq 1$, the following holds:

$$\sum_{i=1}^{k}(a_i^r - b_i^r) \leq \sum_{i\in I_1}(a_i^r - b_i^r) \leq \sum_{i\in I_1}(a_i - b_i)^r.$$

□

5.2 Finite-time stability of hybrid systems

Before presenting the main results, the necessary notation is defined. For each interval T_{i_k}, define the largest connected sub-interval $\bar{T}_{i_k} \subset T_{i_k}$, such that there is no discrete jump in $\bar{T}_{i_k}$, i.e., $\text{int}(\bar{T}_{i_k}) \bigcap J_i = \emptyset$. For example, if $T_{i_1} = [0, 1)$ and $J_i = \{0.2, 0.4, 0.75\}$, then $\bar{T}_{i_1} = [0.4, 0.75)$. Let $\bar{T}_{F_k} = [\bar{t}_{F_k}, \bar{t}_{F_k+1})$ with $\bar{t}_{F_k+1} - \bar{t}_{F_k} \geq t_d$ where $t_d > 0$, and $\{\bar{V}_{F_1}, \bar{V}_{F_2}, \ldots, \bar{V}_{F_p}\}$ and $\{\bar{V}_{F_1+1}, \bar{V}_{F_2+1}, \ldots, \bar{V}_{F_p+1}\}$ be the sequence of the values of the Lyapunov function V_F at the beginning and at end of the intervals $\bar{T}_{i_k}$ for $k = \{1, 2, \ldots, p\}$, respectively, i.e., $\bar{V}_{F_k} \triangleq V_F(x(\bar{t}_{F_k}))$ and $\bar{V}_{F_k+1} \triangleq V_F(x(\bar{t}_{F_k+1}))$. Let $\{i^0, i^1, \ldots, i^l, \ldots\} \in \Sigma_f$ be the sequence of modes that are active during the intervals $[t_0, t_1), [t_1, t_2), \ldots$, respectively, where t_k denotes the time instant when the continuous-time dynamics switch from f_{i^k} to $f_{i^{k+1}}$. The main result on FTS of hybrid systems can now be stated.

Theorem 5.1 (Lyapunov conditions for FTS). *If there exist Lyapunov functions V_i for each $i \in \Sigma_f$, and a switching signal $\sigma_f \in \Pi$ such that the following hold:*

(i) There exists $\alpha_1 \in \mathcal{K}$, such that

$$\sum_{k=0}^{p}\Big(V_{i^{k+1}}(x(t_{k+1}^+)) - V_{i^k}(x(t_{k+1}^+))\Big) \leq \alpha_1(\|x_0\|), \quad \forall p \in \mathbb{Z}_+; \tag{5.5}$$

(ii) There exists $\alpha_2 \in \mathcal{K}$ such that

$$\sum_{k=0}^{p}\Big(V_{i^k}(x(t_{k+1}^-)) - V_{i^k}(x(t_k^+))\Big) \leq \alpha_2(\|x_0\|), \quad \forall p \in \mathbb{Z}_+; \tag{5.6}$$

(iii) There exists $\alpha_3 \in \mathcal{K}$ such that

$$\sum_{t_{k+1}\in J_{i^{k+1}}}\Big(V_{i^k}(x(t_{k+1}^+)) - V_{i^k}(x(t_{k+1}^-))\Big) \leq \alpha_3(\|x_0\|), \quad \forall k \in \mathbb{Z}_+, \tag{5.7}$$

(iv) There exist an FTS mode $F \in \Sigma_f$, a positive definite, continuously differentiable Lyapunov function V_F and constants $c > 0$, $0 < \beta < 1$ such that

$$\dot{V}_F(x(t)) \leq -c(V_F(x(t)))^{\beta}, \quad \forall t \in \bigcup_k [t_{F_k}, t_{F_k+1}) \setminus J_F; \tag{5.8}$$

(v) The accumulated duration $|\bar{T}_F| \triangleq \sum_k |\bar{T}_{F_k}|$ corresponding to the period of time during which the mode F is active without discrete jumps, satisfies

$$|\bar{T}_F| = \gamma(\|x_0\|) \triangleq \frac{(\alpha(\|x_0\|))^{1-\beta}}{c(1-\beta)} + \frac{M^{-\beta}(\bar{\alpha}(\|x_0\|))^{1-\beta}}{c(1-\beta)},$$

where $\alpha = \alpha_0 + \alpha_1 + \alpha_2 + N_f\alpha_3$, $\bar{\alpha} = 2M\alpha$ and $\alpha_0 \in \mathcal{K}$, and $M \in \mathbb{Z}_+$ is the number of times the mode F is activated,

then, the origin of (5.1) is FTS with respect to the switching signal σ_f. Moreover, if all the conditions hold globally, the functions V_i are radially unbounded for all $i \in \Sigma_f$, and $\alpha_1, \alpha_2, \alpha_3, \alpha_4 \in \mathcal{K}_\infty$, then the origin of (5.1) is globally FTS.

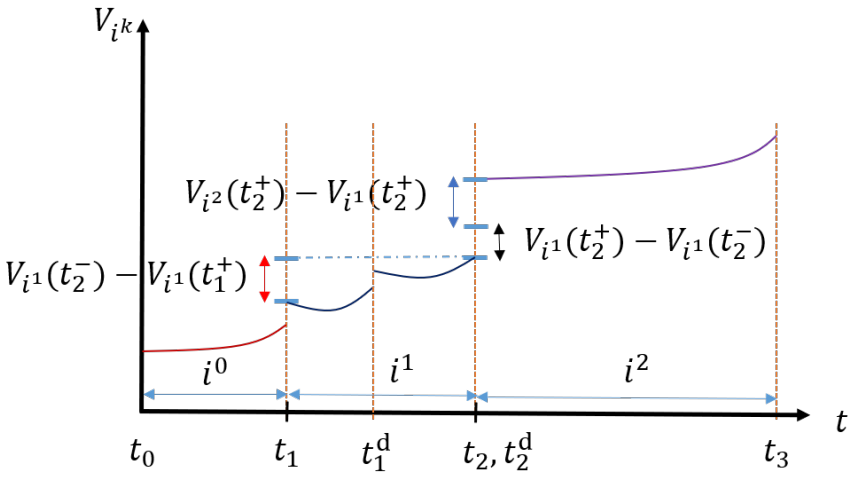

Figure 5.1: Conditions (i), (ii) and (iii) of Theorem 5.1.

Before presenting the proof, an intuitive explanation of the conditions of Theorem 5.1 is provided. Figure C.1 shows the allowable changes in the values of the Lyapunov functions. The increments shown by blue, red and black double-arrows pertain to condition (i), (ii) and (iii), respectively, as explained below:

- Condition (i) means that the cumulative value of the differences between the consecutive Lyapunov functions at the switching instants of the dynamics of continuous

flows (i.e., at switches of the signal σ_f) is bounded by a class-$\mathcal{K}$ function. The functions are evaluated at the post-jump value of the state to include the case when a discrete-jump happens to occur at $t = t_{k+1}$. If there is no discrete-jump at $t = t_{k+1}$, then simply $V_{i^{k+1}}(x(t_{k+1}^+)) - V_{i^k}(x(t_{k+1}^+)) = V_{i^{k+1}}(x(t_{k+1})) - V_{i^k}(x(t_{k+1}))$.

- Condition (ii) means that the cumulative increment in the values of the individual Lyapunov functions when the respective modes are active (evaluated before and after a discrete-jump at t_{k+1} and t_k, respectively) is bounded by a class-$\mathcal{K}$ function. A few authors use the time derivative condition, i.e., $\dot{V}_i \leq \lambda V_i$ with $\lambda > 0$, in place of condition (ii), to allow growth of V_i, hence, requiring the function to be continuously differentiable (see, e.g., [148]). The condition (ii) allows the use of non-differentiable Lyapunov functions. Note that $x(t_{k+1}^-) = x(t_{k+1})$ if $t_{k+1} \notin \bigcup_i J_i$ and $x(t_k^+) = x(t_k)$ if $t_k \notin \bigcup_i J_i$.

- Condition (iii) means that the cumulative increment in the value of the Lyapunov function V_i is bounded by a class-$\mathcal{K}$ function at the discrete jumps occurring at the switching instants, i.e., $t_{k+1} \in J_i$. Condition (5.6) inherently accommodates discrete jumps occurring in the interior of the time interval $[t_k, t_{k+1})$, i.e., in between two switching instants, for all modes $i \neq F$. Thus, only the discrete jumps occurring at the boundaries of these intervals through (5.7) are needed to be accounted for. This condition is going to be useful in proving LS of the origin.

- Condition (iv) means that there exists an FTS mode $F \in \Sigma$ and a Lyapunov function V_F satisfying (2.4) for $\dot{x}(t) = f_F(x(t))$ on $[t_{F_k}, t_{F_k+1}) \setminus J_F$ for all $k \in \mathbb{Z}_+$.

- Condition (v) means that the FTS mode F is active for a sufficiently long cumulative time $\gamma(\|x_0\|)$ without a discrete jump occurring in that cumulative period.

The proof of Theorem 5.1 is provided in Appendix C.1.

Remark 5.1. *Theorem 5.1 essentially says that a set of sufficient conditions for FTS of the origin of (5.1) is that the origin is stable under a given switching signal $\sigma_f \in \Pi$ and the FTS mode F is active for a sufficient amount of cumulative time without a discrete jump. This is formally stated in the following corollary.*

Corollary 5.1. *Suppose that the origin of (5.1) is LS for $\sigma_f \in \Pi$, and that there exists an FTS mode $F \in \Sigma_f$ and a corresponding positive definite function V_F satisfying (5.8). Then, the origin is FTS if $|\bar{T}_F| = \bar{\gamma}(\|x_0\|)$, i.e., the FTS mode F is active for a cumulative time without a discrete jump, where $\bar{\gamma} \in \mathcal{K}$.*

Proof. Since the origin is stable, it follows that there exist $\alpha_4 \in \mathcal{K}$ and a constant $c > 0$ such that

$$\|x(t)\| \leq \alpha_4(\|x_0\|), \tag{5.9}$$

for all $t \geq 0$ and all $\|x_0\| < c$ ([122, Lemma 4.5]). Now, since the function V_F is positive definite, it holds that there exists $\alpha_5 \in \mathcal{K}$ such that ([122, Lemma 4.3])

$$V_F(x(t)) \leq \alpha_5(\|x(t)\|) \overset{(5.9)}{\leq} \alpha_5(\alpha_4(\|x_0\|)) = \alpha(\|x_0\|),$$

where $\alpha = \alpha_5 \circ \alpha_4 \in \mathcal{K}$. Using this, $\bar{T}_F$ can be bounded as follows:

$$\bar{T}_F = \sum_{k=1}^{M} |\bar{T}_{F_k}| \leq \sum_{k=1}^{M} \Big(\frac{\bar{V}_{F_k}^{1-\beta}}{c(1-\beta)} - \frac{\bar{V}_{F_k+1}^{1-\beta}}{c(1-\beta)} \Big) \leq \sum_{k=1}^{M} \frac{\bar{V}_{F_k}^{1-\beta}}{c(1-\beta)} \leq \sum_{k=1}^{M} \frac{(\alpha(\|x_0\|))^{1-\beta}}{c(1-\beta)}.$$

Define $\bar{\gamma} = \sum_{k=1}^{M} \frac{\alpha^{1-\beta}}{c((1-\beta)} \in \mathcal{K}$ to complete the proof. □

In light of this observation, Theorem 5.1 can be further interpreted as follows: If the stability of the origin can be established for all switching signals $\sigma_f \in \Pi$, then the presence of an FTS mode such that the latter is active for a sufficient amount of time $|\bar{T}_F(\|x_0\|)| = \bar{\gamma}(\|x_0\|)$ without a discrete jump guarantees FTS of the origin. Depending upon the application at hand, and available authority on the design of the switching signal, the FTS mode can be made active for the required cumulative duration in one activation period, or multiple activation periods. The motivation of studying FTS using multiple Lyapunov functions comes from applications where the switching law is not under the user's control authority, or where keeping the FTS mode active for a long period leads to undesirable behavior. As an example, consider a spacecraft that tracks the desired trajectory, with the on-board communication and the controller module requiring a certain minimum energy threshold to function. The charge-level of the spacecraft battery can be modeled as a hybrid system, where being in the path of sunlight would be an FTS mode, leading to an increase in the charging level, and tracking the desired trajectory in an unstable mode since it depletes the charge. Now, keeping the FTS mode active for a long duration might lead to the spacecraft losing track of its desired trajectory, and thus, the switching signal between the two modes cannot be designed arbitrarily. At the same time, FTS is desired so that the spacecraft can activate its communication module for crucial communications with the ground station and/or the control module to compute inputs for the next part of the journey. Thus, for the applications where the FTS mode cannot be kept active at all times, or the

switching signal is not under the user's control, it is essential to study FTS under switching laws that allow the FTS mode to become inactive, and unstable modes to become active.

Comparison with earlier results: Compared to [82, 144], the presented results are less conservative in the sense that the Lyapunov functions are allowed to increase during the continuous flows (per (5.6)), as well as at the discrete jumps (per (5.7)). In other words, Theorem 5.1 allows unstable modes to be present in the hybrid system while still guaranteeing FTS of the origin under certain switching signals. Also, during the continuous flows, the Lyapunov functions are allowed to grow when switching from one continuous flow to another (per (5.5)), whereas the aforementioned work imposes that the common Lyapunov function is always non-increasing. In contrast to the previous work e.g., [82, 84, 148, 149], except for V_F we do not require the Lyapunov functions to be differentiable.

5.3 Finite-time stability result for switched systems

In this section, it is illustrated how the case of switched systems, i.e., of systems without discrete jumps in their states, is a special case of the results derived in the previous section. In summary, in the case of a switched system, Theorem 5.1 guarantees FTS of the origin under conditions (i), (ii), (iv) and (v); condition (iii) is obsolete since there are no discrete jumps. As a side note, if in addition to $D = \emptyset$, one has that $N_f = 1$, i.e., if the system (5.1) reduces to a continuous-time dynamical system, Theorem 5.1 reduces to Theorem 2.1. Thus, the seminal result on FTS of continuous-time systems is a special case of Theorem 5.1.

Consider a switched system given as

$$\dot{x}(t) = f_{\sigma(t,x)}(x(t)), \quad x(t_0) = x_0, \tag{5.10}$$

where $x \in \mathbb{R}^n$ is the system state, $\sigma_f : \mathbb{R}_+ \times \mathbb{R}^n \to \Sigma$ is the switching signal that can depend on both t and x, and is assumed to be piecewise continuous (from the right) in time and continuous in x, with $\Sigma \triangleq \{1, 2, \ldots, N\}$ with $N < \infty$, and $f_{\sigma(\cdot,\cdot)} : \mathbb{R}^n \to \mathbb{R}^n$ is the system vector field describing the active subsystem (called thereafter mode) under $\sigma(\cdot, \cdot)$. Note that (5.10) is a special case of (5.1) with $D = \emptyset$. Thus, the solution of (5.10) is defined as follows: an absolutely continuous function $x : \mathbb{R}_+ \to \mathbb{R}^n$ is a solution of (5.10) if it satisfies $\dot{x}(t) = f_k(t, x)$ for almost all $t \in \mathbb{R}_+$ where $k = \sigma(t, x)$. Similarly, FTS of the origin of (5.10) is defined per Definition 5.2 with $\Pi \subset \text{PWC}(\mathbb{R}_+ \times \mathbb{R}^n, \Sigma)$. The following assumption for (5.10) is made.

Assumption 5.3. *The solution of* (5.10) *exists and satisfies Assumption 5.2.*

Based on Theorem 5.1, the following result proposing sufficient conditions for FTS of the origin for (5.10) can be stated.

Corollary 5.2. *If there exist Lyapunov functions V_i for each $i \in \Sigma \in \Pi$, and a switching signal σ such that the following hold:*

(i) There exists $\alpha_1 \in \mathcal{K}$, such that

$$\sum_{k=0}^{p} \Big(V_{i^{k+1}}(x(t_{k+1})) - V_{i^k}(x(t_{k+1})) \Big) \leq \alpha_1(\|x_0\|), \quad \forall p \in \mathbb{Z}_+; \tag{5.11}$$

(ii) There exists $\alpha_2 \in \mathcal{K}$ such that

$$\sum_{k=0}^{p} \Big(V_{i^k}(x(t_{k+1})) - V_{i^k}(x(t_k)) \Big) \leq \alpha_2(\|x_0\|), \quad \forall p \in \mathbb{Z}_+; \tag{5.12}$$

(iii) There exist an FTS mode $F \in \Sigma$, a positive definite, continuously differentiable Lyapunov function V_F and constants $c > 0$, $0 < \beta < 1$ such that

$$\dot{V}_F(x(t)) \leq -c(V_F(x(t)))^{\beta}, \quad \forall t \in \bigcup_k [t_{F_k}, t_{F_k+1}); \tag{5.13}$$

(iv) The accumulated duration $|T_F| \triangleq \sum_k |T_{F_k}|$ corresponding to the period of time during which the mode F is active, satisfies

$$|T_F| = \gamma(\|x_0\|) \triangleq \frac{(\alpha(\|x_0\|))^{1-\beta}}{c(1-\beta)} + \frac{M^{-\beta}(\bar{\alpha}(\|x_0\|))^{1-\beta}}{c(1-\beta)},$$

where $\alpha = \alpha_0 + \alpha_1 + \alpha_2$, $\bar{\alpha} = M(\alpha_1 + \alpha_2)$ and $\alpha_0 \in \mathcal{K}$, where $M \in \mathbb{Z}_+$ is the number of times the mode F is activated,

then, the origin of (5.10) is FTS with respect to the switching signal σ. Moreover, if all the conditions hold globally, the functions V_i are radially unbounded for all $i \in \Sigma$, and $\alpha_1, \alpha_2 \in \mathcal{K}_\infty$, then the origin of (5.10) is globally FTS.

5.3.1 Finite-time stabilizing switching signal

In this section, based on Corollary 5.2, a method of designing a switching signal is presented so that the origin of the switched system is FTS. The approach is inspired from [77]

where a method of designing an asymptotically stabilizing switching signal is presented. Suppose there exist continuous functions $\mu_{ij} : \mathbb{R}^n \to \mathbb{R}$ satisfying:

$$\begin{aligned} \mu_{ij}(0) &= 0, \\ \mu_{ii}(x) &= 0 \quad \forall\, x \in \mathbb{R}^n, \\ \mu_{ij}(x) + \mu_{jk}(x) &\leq \min\{0, \mu_{ik}(x)\},\ \forall x \in \mathbb{R}^n, \end{aligned} \tag{5.14}$$

for all $i, j, k \in \Sigma$. Define the following sets:

$$\begin{aligned} \Omega_i &= \{x \mid V_i(x) - V_j(x) + \mu_{ij}(x) \leq 0, j \in \Sigma\}, \\ \Omega_{ij} &= \{x \mid V_i(x) - V_j(x) + \mu_{ij}(x) = 0, i \neq j\}, \end{aligned} \tag{5.15}$$

where V_i is a Lyapunov function for each $i \in \Sigma$. Let $\sigma(t_0, x(t_0)) = i$ and $i, j \in \Sigma$ be arbitrary modes. For all times $t \geq t_0$, define the finite-time stabilizing switching signal as:

$$\sigma(t, x) = \begin{cases} i, & \sigma(t^-, x(t^-)) = i,\ x(t^-) \in \text{int}(\Omega_i); \\ j, & \sigma(t^-, x(t^-)) = i,\ x(t^-) \in \Omega_{ij}; \end{cases}. \tag{5.16}$$

The following result can be stated now.

Theorem 5.2 (Finite-time stabilizing switching law). *Assume that the solution of* (5.10) *under* σ *in* (5.16) *satisfy Assumption 5.3. Let* V_i *are Lyapunov functions for* $i = 1, 2, \ldots, N$, *and* μ_{ij} *satisfy* (5.14). *Assume that the following hold:*

(I) There exists continuous functions $\beta_{ij} : \mathbb{R}^n \to \mathbb{R}_-$ *for* $i, j \in \Sigma$ *such that*

$$\frac{\partial V_i}{\partial x} f_i(x) + \sum_{j=1}^{N_f} \beta_{ij}(x)(V_i(x) - V_j(x) + \mu_{ij}(x)) \leq 0, \quad \forall i \in \Sigma, \forall x \in \mathbb{R}^n; \tag{5.17}$$

(II) There exists a finite-time stable mode $F \in \Sigma$ *satisfying condition (iii) and (iv) of Corollary 5.2;*

(III) The functions μ_{ij} *are continuously differentiable and satisfy*

$$\frac{\partial \mu_{ij}}{\partial x} f_i \leq 0,\ i, j = 1, 2, \ldots, N. \tag{5.18}$$

(IV) No sliding mode occurs at all switching surface.

Then, the origin of (5.10) *under* σ *in* (5.16) *is FTS.*

Proof. The strategy of the proof is to show that all the conditions of Corollary 5.2 and Assumption 5.3 are satisfied to establish FTS of the origin for (5.10), when the switching signal is defined as per (5.16). As per the analysis in [77, Theorem 3.18], it follows that the conditions (i)-(ii) of Corollary 5.2 are satisfied with

$$\alpha_1(r) = \max_{\|x\| \leq r,\, i,j \in \Sigma_f} |\mu_{ij}(x)|, \tag{5.19}$$

$$\alpha_2(r) = 0, \tag{5.20}$$

for all $r \geq 0$. From (II), we obtain that conditions (iii) and (iv) of Corollary 5.2 hold as well. Thus, all the conditions of the Corollary 5.2 and Assumption 5.3 are satisfied. Hence, it follows that the origin of (5.10) with switching signal defined as per (5.16) is FTS. □

Remark 5.2. *Note that an arbitrary switching signal σ may not satisfy the conditions of Corollary 5.2, particularly condition (v), where the mode F is required to be active for $T_F(x_0)$ time duration. For all initial conditions x_0, the switching signal can be defined as per (5.16) to render the origin of (5.10) FTS. Definition 5.2 allows to choose the switching signal σ as per (5.16) so that the switched system (5.10) satisfies the conditions of Corollary 5.2. Note that there is no difference in the switching signal defined in (5.16) and the one in [77]. This observation re-emphasizes the fact that a system whose origin is uniformly stable can be made FTS by ensuring that the cumulative activation time requirement is satisfied for an FTS mode.*

A note on construction of functions μ_{ij}, V_i: For a class of switched systems consisting of $N-1$ linear modes and one FTS mode F, one can follow a design procedure similar to [77, Remark 3.21] to construct the functions μ_{ij}, as well as the Lyapunov functions V_i, for all $i \neq F$. The design procedure includes choosing quadratic functions $\mu_{ij} = x^T P_{ij} x$ and $V_i = x^T R_i x$ with R_i as positive definite matrices, and using the conditions (5.14) and (5.18) along with the conditions of Corollary 5.2, to formulate a linear matrix inequality (LMI) based optimization problem. For system consisting of polynomial dynamics f_i, one can formulate a sum-of-square (SOS) problem to find polynomial functions V_i, μ_{ij} and β_{ij} by posing (5.14), (5.17) and (5.18) inequalities as SOS constraints (see [150] for an overview of SOS programming and [151] for methods of solving SOS problems). The "min-switching" law as described in [152], can be defined by setting the functions $\mu_{ij} = 0$, which would imply that the Lyapunov functions should be non-increasing at the switching instants. The conditions in Theorem 5.2, on the lines of the generalization of min-switching law as presented in [77], overcome this limitation and allow the Lyapunov functions to increase at the switching instants.

5.3.2 Finite-time stable output-feedback for switched systems

In this section, a switched linear system with N modes is considered such that only one mode is both observable and controllable, and an output-feedback is designed to stabilize the system trajectories at the origin in a finite time. Consider the linear switched system:

$$\begin{aligned} \dot{x} &= A_{\sigma(t,x)}x + B_{\sigma(t,x)}u, \\ y &= C_{\sigma(t,x)}x, \end{aligned} \tag{5.21}$$

where $x \in \mathbb{R}^n, u \in \mathbb{R}, y \in \mathbb{R}$ are the system states, and input and output of the system, respectively, with $A_i \in \mathbb{R}^{n\times n}, B_i \in \mathbb{R}^{n\times 1}$ and $C_i \in \mathbb{R}^{1\times n}$. The switching signal $\sigma : \mathbb{R}_+ \times \mathbb{R}^n \to \Sigma \triangleq \{1, 2, \ldots, N\}$ is a piecewise constant, right-continuous function. The following assumption is made.

Assumption 5.4. *There exists a mode $\sigma_0 \in \Sigma$ such that $(A_{\sigma_0}, B_{\sigma_0})$ is controllable and $(A_{\sigma_0}, C_{\sigma_0})$ is observable.*

Without loss of generality, one can assume that the pair $(A_{\sigma_0}, C_{\sigma_0})$ is in the controllable canonical form and $(A_{\sigma_0}, C_{\sigma_0})$ is in the observable canonical form, i.e., $A_{\sigma_0} = \begin{bmatrix} 0_n & \begin{bmatrix} I_{n-1} \\ 0_{n-1}^T \end{bmatrix} \end{bmatrix}$, $B_{\sigma_0} = \begin{bmatrix} 0 & 0 & 0 & \cdots & 0 & 1 \end{bmatrix}^T$ and $C_{\sigma_0} = \begin{bmatrix} 1 & 0 & 0 & \cdots & 0 & 0 \end{bmatrix}$, where $I_{n-1} \in \mathbb{R}^{n-1\times n-1}$ is an identity matrix and $0_k = \begin{bmatrix} 0 & 0 & \cdots & 0 & 0 \end{bmatrix}^T \in \mathbb{R}^{k\times 1}$. It is also assumed that the switching signal $\sigma(t, x)$ is known at all times even if the state x is not known. The objective is to design an output feedback for (5.21) so that the closed loop trajectories $x(\cdot)$ reach the origin in a finite time. To this end, an FTS observer is designed and the estimated states $\hat{x}$ are used to design the control input u. The form of the observer is:

$$\dot{\hat{x}} = A_\sigma \hat{x} + g_\sigma(C_\sigma x - C_\sigma \hat{x}) + B_\sigma u. \tag{5.22}$$

Following [153, Theorem 10], define the function $g : \mathbb{R} \to \mathbb{R}^n$ as:

$$g(y) = \begin{bmatrix} l_1 \operatorname{sign}(y)|y|^{\alpha_1} \\ \vdots \\ l_n \operatorname{sign}(y)|y|^{\alpha_n} \end{bmatrix} \tag{5.23}$$

where l_i are chosen so that the matrix $\bar{A}$ defined as

$$\bar{A} := \begin{bmatrix} -\bar{l} & \begin{bmatrix} I_{n-1} \\ 0_{n-1} \end{bmatrix} \end{bmatrix},$$

with $\bar{l} = \begin{bmatrix} l_1 & l_2 & \cdots & l_n \end{bmatrix}^T$ is Hurwitz, and the exponents α_i are chosen as $\alpha_i = i\alpha - (i-1)$ for $1 < i \leq n$, where $1 - \frac{n-1}{n} < \alpha < 1$. Define the function g_σ as:

$$g_\sigma(y) = \begin{cases} g(y), & \sigma(t) = \sigma_0; \\ 0, & \sigma(t) \neq \sigma_0; \end{cases} \tag{5.24}$$

Let the observation error be $e = x - \hat{x}$, with $e_i = x_i - \hat{x}_i$ for $i = 1, 2, \ldots, N$. Its time derivative reads:

$$\dot{e} = A_\sigma e - g_\sigma(C_\sigma e). \tag{5.25}$$

Next, a feedback $u = u(\hat{x})$ is designed so that the origin is FTS for the closed-loop trajectories of (5.21). Inspired from control input defined in [117, Proposition 8.1], define the control input as

$$u = \begin{cases} -\sum_{i=1}^{n} k_i \operatorname{sign}(\hat{x}_i)|\hat{x}_i|^{\beta_i}, & \sigma = \sigma_0; \\ 0, & \sigma) \neq \sigma_0; \end{cases}, \tag{5.26}$$

where $\beta_{j-1} = \frac{\beta_j \beta_{j+1}}{2\beta_{j+1} - \beta_j}$ with $\beta_{n+1} = 1$ and $0 < \beta_n = \beta < 1$, and k_i are such that the polynomial $s^n + k_n s^{n-1} + \cdots + k_2 s + k_1$ is Hurwitz. The following result can now be stated.

Theorem 5.3 (Closed-loop properties). *Let the switching signal σ for (5.21) be given by (5.16) with $F = \sigma_0$. Assume that there exist functions μ_{ij} as defined in (5.14), and that the conditions (i)-(iii) of Theorem 5.2 are satisfied. Then, the origin of the closed-loop system (5.21) under the effect of control input (5.26) is an FTS equilibrium.*

Proof. First, it is shown that there exists $T_1 < \infty$ such that for all $t \geq T_1$, $\hat{x}(t) = x(t)$. Note that the origin is the only equilibrium of (5.25). From the analysis in Theorem 5.2, it follows that the conditions (i) and (ii) of Corollary 5.2 are satisfied. The observation-error

dynamics for mode σ_0 reads:

$$\dot{e} = \begin{bmatrix} e_2 - l_1 \text{sign}(e_1)|e_1|^{\alpha_1} \\ e_3 - l_2 \text{sign}(e_1)|e_1|^{\alpha_2} \\ \vdots \\ e_n - l_{n-1} \text{sign}(e_1)|e_1|^{\alpha_{n-1}} \\ -l_n \text{sign}(e_1)|e_1|^{\alpha_n} \end{bmatrix}. \tag{5.27}$$

Now, using [153, Theorem 10], it follows that the origin is an FTS equilibrium for (5.27), i.e., for mode σ_0 of (5.25). From [153, Lemma 8], it follows that (5.27) is homogeneous with degree of homogeneity $d = \alpha - 1 < 0$. Hence, using [117, Theorem 7.2], it holds that there exists a Lyapunov function V_o satisfying $\dot{V}_o \leq -cV_o^\beta$ where $c > 0$ and $0 < \beta < 1$. Hence, condition (iii) of Corollary 5.2 is also satisfied. From the proof of Theorem 5.2, it follows that the condition (iv) of Corollary 5.2 and Assumption 5.3 are also satisfied. Hence, it holds that the origin of (5.25) is an FTS equilibrium. Thus, there exists $T_1 < \infty$ such that for all $t \geq T$, $\hat{x}(t) = x(t)$. So, for $t \geq T_1$, the control input satisfies $u = u(\hat{x}) = u(x)$. Again, it is easy to verify that the origin is the only equilibrium for (5.21) under the effect of control input (5.26). The closed-loop trajectories take the following form for the mode $\sigma = \sigma_0$

$$\dot{x} = \begin{bmatrix} x_2 \\ x_3 \\ \vdots \\ x_{n-1} \\ x_n - \sum_{i=1}^{n} k_i \text{sign}(x_i)|x_i|^{\beta_i} \end{bmatrix}. \tag{5.28}$$

From [117, Proposition 8.1], it follows that the origin of the closed-loop trajectories for mode $\sigma = \sigma_0$ is FTS. Hence, repeating same set of arguments as above, it holds that there exists $T_2 < \infty$ such that the closed-loop trajectories of (5.21) satisfy $x(t) = 0$ for all $t \geq T_1 + T_2$. □

5.4 Simulations

Two numerical examples are presented to demonstrate the efficacy of the proposed methods. The first example considers an instance of the hybrid system (5.1) with five modes, where one mode is FTS, one is AS, and three are unstable. It is demonstrated that if the

conditions of Theorem 5.1 are satisfied, then the trajectories of the considered system reach the origin in finite time even in the presence of unstable modes.

The second example considers a switched linear control system with five modes such that only one mode is both controllable and observable. An FTS output controller is designed for the considered switched system, and it is demonstrated that the closed-loop trajectories reach the origin despite the presence of unobservable modes and the presence of uncontrollable modes that are unstable.

The simulation results have been obtained by discretizing the continuous-time dynamics using Euler discretization. A step size of $dt = 10^{-3}$ is used, and the simulations are run till the norm of the states drops below 10^{-10}. At this point, it is important to emphasize that while the theoretical results hold for the continuous-time dynamics, and not for the implemented discretized dynamics, still the simulations reflect stable behavior that meets the theoretical bounds on the sufficiently long active time of the finite-time stable mode. In other words, the simulations are included for the sake of visualizing the theoretical results despite the discrepancy between continuous and discretized dynamics. The study of discretization methods for finite-time stable systems is left open for future investigation.

5.4.1 Example 1: finite-time stable hybrid system

A numerical example is presented to illustrate the FTS results on a hybrid system given as

$$
\begin{aligned}
&\mathcal{H} = \{C, \mathcal{F}, D, \mathcal{G}\}, \quad \mathcal{F} = \{f_1, f_2, f_3, f_4, f_5\}, \quad \mathcal{G} = \{g_1\}, \\
&f_1 = \begin{bmatrix} 0.01x_1^2 + x_2 \\ -0.01x_1^3 + x_2 \end{bmatrix}, \quad f_2 = \begin{bmatrix} 0.01x_1 - x_2 \\ -x_1^2 + 0.01x_2 \end{bmatrix}, \\
&f_3 = \begin{bmatrix} -x_1 - x_2 \\ x_1 - x_2 \end{bmatrix}, \quad f_4 = \begin{bmatrix} 0.01x_1^2 + 0.01x_1x_2 \\ -0.01x_1^3 + x_2^2 \end{bmatrix}, \\
&f_5 = \begin{bmatrix} x_2 - 20\text{sign}(x_1)|x_1|^{\alpha} \\ -10\text{sign}(x_1)|x_1|^{2-2\alpha} \end{bmatrix}, \\
&g_1 = \begin{bmatrix} -1.1x_1 \\ -1.1x_2 \end{bmatrix}, \quad C = \mathbb{R}^2, \quad D = \mathbb{R}^2,
\end{aligned}
\tag{5.29}
$$

with $\alpha = 0.98$, where the fifth mode is FTS, and thus $F = 5$. Note that the states x_1 and x_2 change sign and increase in magnitude at the discrete jumps. The Lyapunov functions are defined as $V_i(x) = x^T P_i x$, for $i \in \{1, 2, 3, 4\}$, with $P_1 = \begin{bmatrix} 1 & 0 \\ 0 & 1 \end{bmatrix}$, $P_2 = \begin{bmatrix} 5 & 2 \\ 2 & 4 \end{bmatrix}$, $P_3 =$

$\begin{bmatrix} 1 & 0 \\ 0 & 3 \end{bmatrix}$, $P_4 = \begin{bmatrix} 6 & 1 \\ 1 & 3 \end{bmatrix}$, and $V_5(x) = \frac{k_2}{2\alpha}|x_1|^{2\alpha} + \frac{1}{2}|x_2|^2$. Note that this example is more general than the examples considered in [82], as the dynamics is allowed to have unstable modes. In this example, the switches in the continuous flows occur after 0.2 sec, i.e., $|T_{i_k}| = 0.2$ sec, $k \in \mathbb{Z}_+$, and discrete jumps occur after 0.1 sec. for all $i \in \{1, 2, \ldots, 5\}$.

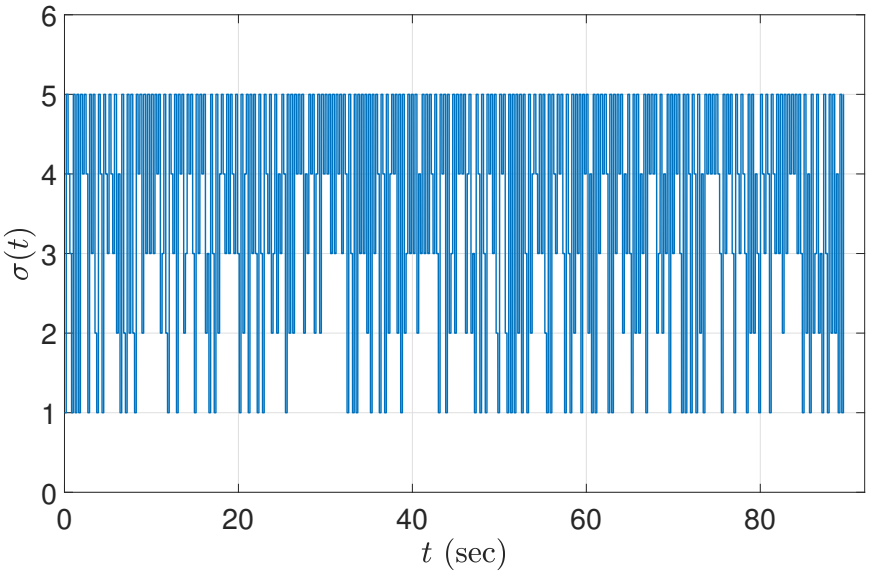

Figure 5.2: Switching signal $\sigma_f(t)$ for the considered hybrid system (5.29).

Figure 5.2 depicts the considered switching signal $\sigma_f(t)$. The switching signal is designed so that the Lyapunov candidates V_i satisfy conditions (i) and (iii) of Theorem 5.1. Mode 3 and 5, being stable, satisfy condition (ii) with $\alpha_2 = 0$, and modes 1, 2 and 4, being active for a finite interval each time, satisfy condition (ii) with $\alpha_2 = k\|x_0\|^2$ where $k > 0$, and so $\alpha_2 = k\|x_0\|^2$ satisfy (ii) for all the modes. It can be verified that f_5 is homogeneous with degree of homogeneity $d = \alpha - 1 < 0$. Thus, using [117, Theorem 7.2], the origin is FTS under the system dynamics f_5, and there exists a V_5 satisfying (5.8); therefore, condition (iv) is satisfied. Finally, the switching signal is designed so that mode 5 is active for a sufficient amount of time that satisfies condition (v).

Figure 5.3 illustrates the state trajectories $x_1(t)$ and $x_2(t)$. The states can be seen as switching signs during discrete jumps. Note that the states change sign at the discrete jumps. Figure 5.4 depicts the norm of the state vector $x(t)$ on a logarithmic scale; note that $\|x(t)\|$ is increasing while operating in unstable modes, and decreasing while operating in stable modes. The norm of the states reach a small neighborhood $\|x\| \leq 10^{-10}$ of the origin within a finite time starting from $\|x(0)\| = 10$ within the first 90 seconds of the simulation. Finally, Figure 5.5 illustrates the evolution of the Lyapunov functions V_i with

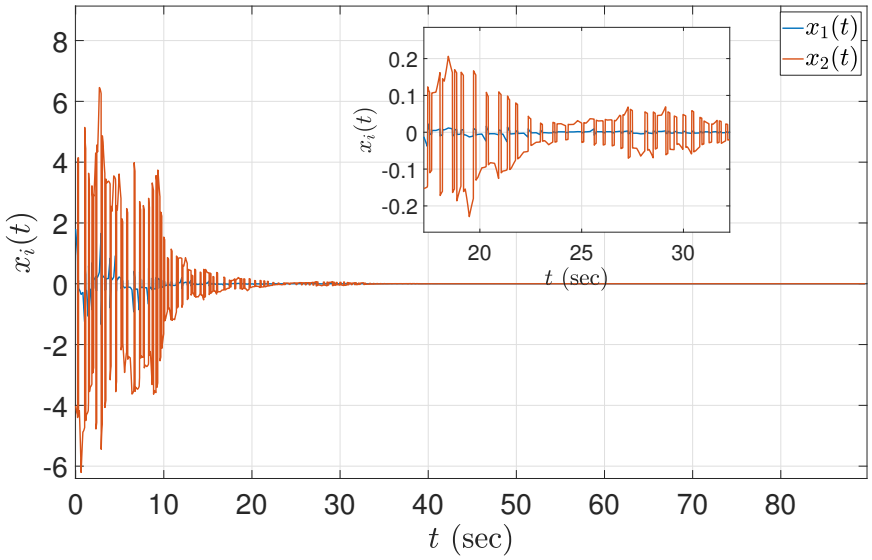

Figure 5.3: The evolution of $x_1(t)$ and $x_2(t)$ for hybrid system (5.29).

respect to time. Note that the Lyapunov functions increase, as expected, at the times of the switches in σ_f, as well as during the continuous flows along the unstable modes 2 and 4. The provided example demonstrates that the origin of the system is FTS even when one or more modes are unstable if the FTS mode is active for a sufficient amount of time.

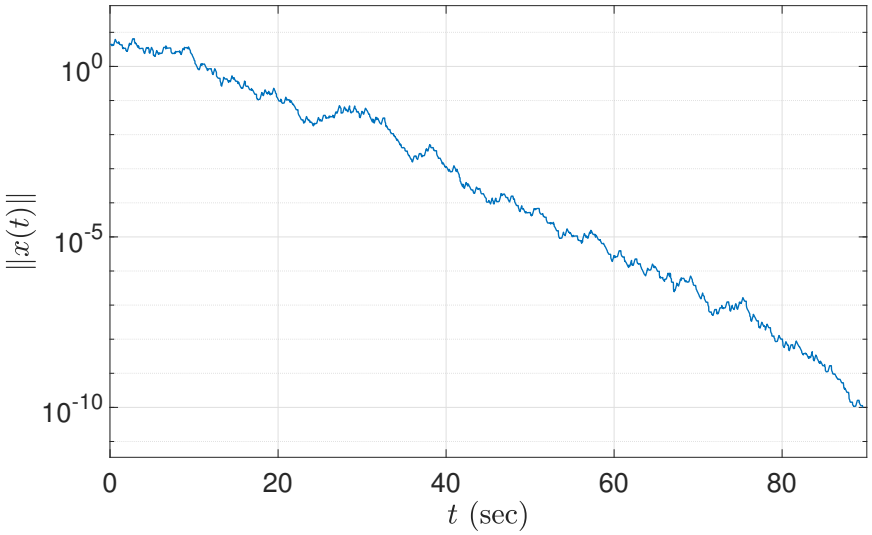

Figure 5.4: The evolution of $\|x(t)\|$ for (5.29).

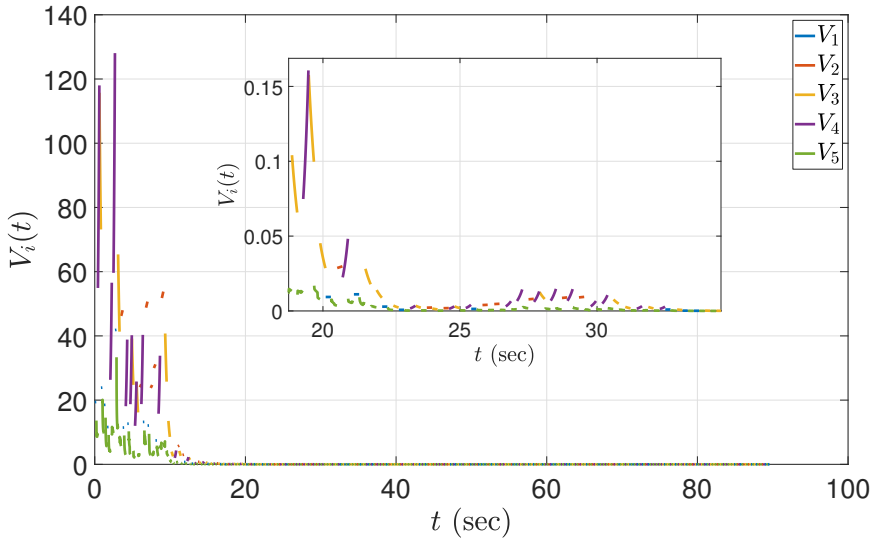

Figure 5.5: The evolution of the Lyapunov functions $V_i(t)$ for $t \in [0, 10]$ sec for (5.29).

5.4.2 Example 2: finite-time stable switched linear control system

In this second example, a linear switched system of the form (5.21) is considered and an output feedback is designed that stabilizes the origin for the closed-loop system in a finite time. For illustration purposes, consider a system of order $n = 2$, $\sigma \in \{1, 2, 3, 4, 5\}$, and assume that mode $\sigma = 5 \triangleq \sigma_0$ is controllable and observable, i.e., that the pair $(A_{\sigma_0}, B_{\sigma_0})$ is controllable and $(A_{\sigma_0}, C_{\sigma_0})$ is observable, while other modes are both uncontrollable and unobservable. The simulation parameters are:

- Number of modes $N = 5$, FTS mode $F = 5$, $|T_{i_k}| = 0.1$, $\alpha = 0.9$, $\beta = .9$ $k_1 = 20$ and $k_2 = 10$;
- The matrices A_i, B_i, C_i are chosen as $A_1 = \begin{bmatrix} 0 & 1 \\ -1 & 0 \end{bmatrix}, A_2 = \begin{bmatrix} 0.1 & 0 \\ 0 & 0.1 \end{bmatrix}, A_3 = \begin{bmatrix} -1 & 0 \\ 0 & -1.2 \end{bmatrix}, A_4 = \begin{bmatrix} 1 & 0.1 \\ 0.1 & 2 \end{bmatrix}, A_5 = \begin{bmatrix} 0 & 1 \\ 0 & 0 \end{bmatrix}, B_1 = B_2 = B_3 = B_4 = \begin{bmatrix} 0 \\ 0 \end{bmatrix}, B_5 = \begin{bmatrix} 0 \\ 1 \end{bmatrix}$ and $C_1 = C_2 = C_3 = C_4 = \begin{bmatrix} 0 & 0 \end{bmatrix}, C_5 = \begin{bmatrix} 1 & 0 \end{bmatrix}$.
- Generalized Lyapunov functions are chosen as $V_i(x) = x^T P_i x$ where matrices P_i are chosen as $P_1 = \begin{bmatrix} 1 & 0 \\ 0 & 1 \end{bmatrix}, P_2 = \begin{bmatrix} 5 & 2 \\ 2 & 4 \end{bmatrix}, P_3 = \begin{bmatrix} 1 & 0 \\ 0 & 3 \end{bmatrix}, P_4 = \begin{bmatrix} 6 & 1 \\ 2 & 3 \end{bmatrix}$, and $V_5(x) = \frac{k_2}{2\alpha}|x_1|^{2\alpha} + \frac{1}{2}|x_2|^2$;

- Functions μ_{ij} as

$$\mu_{ij}(x) = \begin{cases} -\|x\|^2, & i \in \{1,2,4\}; \\ 0, & i \in \{3,5\}; \end{cases}$$

  for all $j \in \sigma$.

Note that modes 1, 2, 3, and 4 are both uncontrollable and unobservable, and the origin of the open-loop is LS for mode 1, AS for mode 3 is asymptotically stable, and unstable for modes 2 and 4. The generalized Lyapunov candidates V_i, being quadratic, satisfy condition (i) of Corollary 5.2. Modes 1, 3 and 5, being stable, satisfy condition (ii) with $\alpha_2 = 0$, and modes 2 and 4, being active only for a finite time, satisfy condition (ii) with $\alpha_2 = k\|x_0\|^2$ where $k > 0$. Conditions (iii) and (iv) are satisfied by carefully designing the switching signal, as discussed in Section 5.3.1.

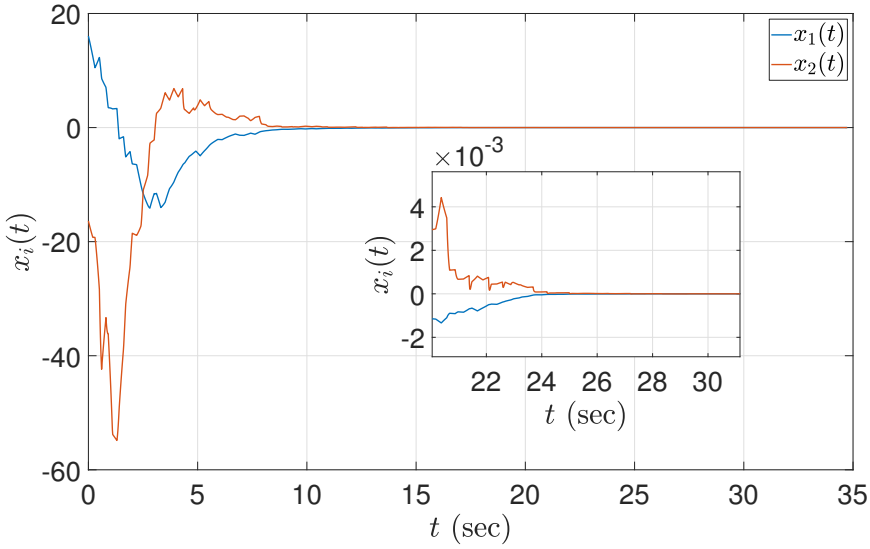

Figure 5.6: Closed-loop system states $x_1(t), x_2(t)$ with time for linear switched system.

Figure 5.6 illustrates the state trajectories $x_1(t), x_2(t)$ of the closed-loop system over time for randomly chosen initial conditions, and Figure 5.7 depicts the norm of the states $\|x(t)\|$. Figure 5.8 plots the norm of the state-estimation error, $\|x - \hat{x}\|$ with time. It can be seen from the these figures that both the norms $\|x\|$ and $\|x - \hat{x}\|$ go to zero in finite time.

Figure 5.9 shows the evolution of Lyapunov functions $V_i(x - \hat{x})$ for the FTS observer of the linear switched system. It can be seen that there are unstable modes in the observer, where the value of the functions increase when the respective modes are active (e.g., mode 2 and 4). Finally, Figure 5.10 plots the switching signal σ with time. The switching signal is designed as per the design procedure listed in Section 5.3.1. It can be seen that all the five

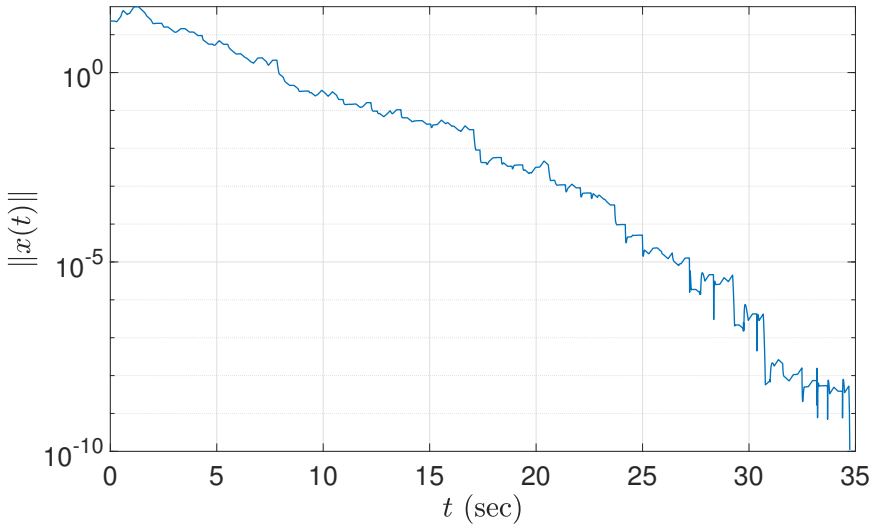

Figure 5.7: The norm of the state vector $x(t)$ for the closed-loop trajectories of linear switched system with time.

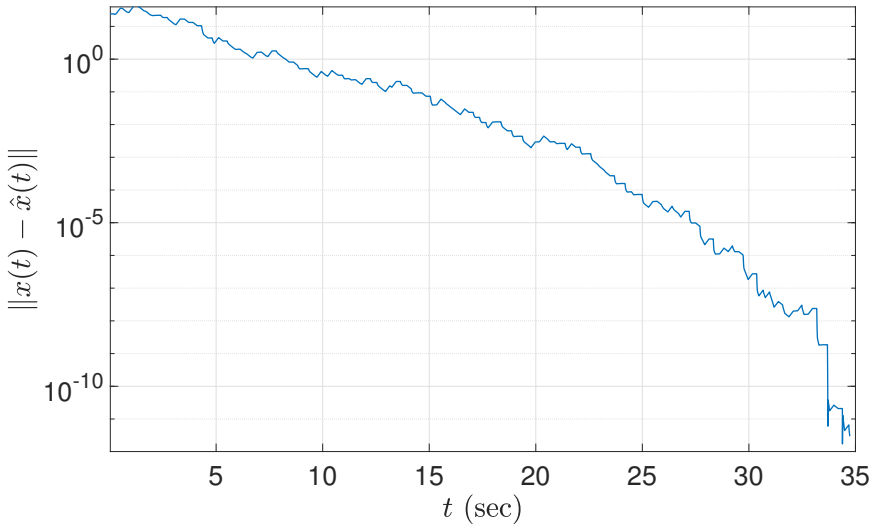

Figure 5.8: The norm of the state-estimation error $x(t) - \hat{x}(t)$ for the linear switched system with time.

modes (including the unstable modes) get activated for the switched linear system, while FTS of the origin is still ensured.

The provided examples validate that the system can achieve FTS even when one or more modes are unstable if the FTS mode is active for long enough.

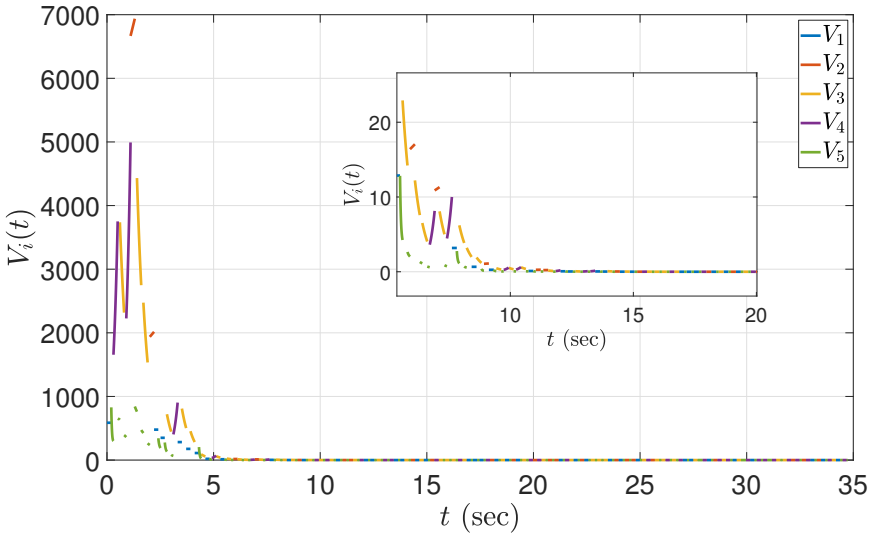

Figure 5.9: The evolution of the Lyapunov functions $V_i(t)$ for the FTS observer of the linear switched system.

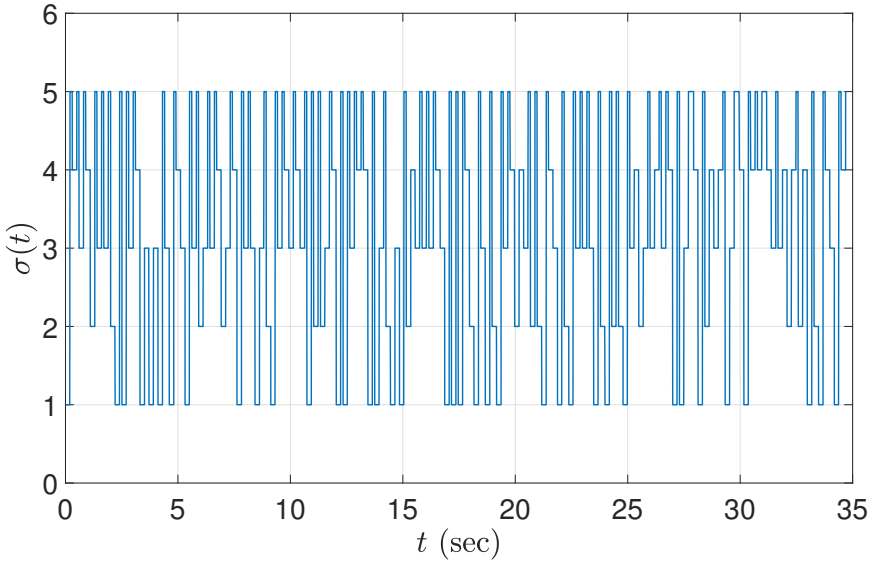

Figure 5.10: Switching signal for the linear switched system.

5.5 Conclusions

In this chapter, FTS of a class of switched and hybrid systems is studied via a multiple Lyapunov function approach. It is showed that under certain mild conditions on the bounds on the difference of the values of Lyapunov functions, if the FTS mode is active for a sufficient cumulative time, then the origin of the hybrid or the switched system is FTS. In other words, the results demonstrate that under mild conditions, the stability of the origin and

sufficient cumulative activation of an FTS mode implies FTS of the origin. The proposed method allows the individual Lyapunov functions to increase both during the continuous flows as well as at the discrete state jumps, i.e., it allows the system to have unstable modes. Using the multiple Lyapunov function conditions, a method of designing a finite-time stabilizing switching signal is proposed. As an application, an FTS output feedback for a class of linear switched systems is designed in the case when only one of the modes is both controllable and observable.

CHAPTER 6

Continuous-time Optimization

This chapter develops novel gradient-flow schemes that yield convergence to the optimal point of a convex optimization problem within a *fixed* time from all initial conditions for unconstrained optimization, constrained optimization, and min-max problems. It is shown that the solution of the modified gradient flow dynamics exists and is unique under certain regularity conditions on the objective function. The application of the modified gradient flow to unconstrained optimization problems is studied under the assumption of gradient dominance, a relaxation of strong convexity. Then, a modified Newton's method is presented that exhibits fixed-time convergence under certain mild conditions on the objective function. Building upon this method, a novel technique for solving convex optimization problems with linear equality constraints that yield convergence to the optimal point in a fixed time is developed. It is also noted that the constrained optimization problem can be reformulated as a min-max problem. Motivated from this, the general min-max problem is considered where an objective function needs to be minimized over one set of variables and maximized over another set of variables, and a modified scheme to obtain the optimal solution of the min-max problem in a fixed time is developed. To the best of the author's knowledge, this is the first work that establishes FxTS of gradient flow-based techniques and demonstrates their application to nonlinear constrained optimization and saddle-point dynamics. The results in this Chapter are based on [115].

The following notation is frequently used in this chapter:

$\mathbb{R}$	The set of real numbers
$\mathbb{R}_+$	The set of non-negative reals
$\|\cdot\|$	Euclidean norm of $(\cdot)$
$\mathcal{C}^k$	$k-$times continuously differentiable functions
$x^\star$	Optimal value of the variable x
f^*	Conjugate of the function f given as $f^*(y) = \sup_{x\in\mathbb{R}^n}(y^T x - f(x))$

∇f	Gradient of a $\mathcal{C}^1$ function f
$\nabla^2 f$	Hessian of a $\mathcal{C}^2$ function f
$\nabla_{x_1} f$	Partial derivative of f with respect to x_1
$A \succ 0$	Positive definite matrix A
$A \succeq 0$	Positive semi-definite matrix A
$A \succ B$	Inequality $A - B \succ 0$
$A \succeq B$	Inequality $A - B \succeq 0$

Note the difference between * for optimality and * for the conjugate.

6.1 Fixed-time stable gradient flows

6.1.1 Mathematical preliminaries

Various notions of convexity, and first and second order conditions for convexity are summarized below (see [128, Chapter 3] for more details).

Definition 6.1. *A $\mathcal{C}^1$ function $f : D \to \mathbb{R}$, where $D \subset \mathbb{R}^n$ is a convex set, is called*

- ***Convex*** *if for all $x, y \in D$ and all $\alpha \in (0,1)$, $f(\alpha x + (1-\alpha)y) \leq \alpha f(x) + (1-\alpha) f(y)$;*
- ***Concave*** *if $(-f)$ is convex;*
- ***Strictly convex*** *if for all $x, y \in D$ and all $\alpha \in (0,1)$, $f(\alpha x + (1-\alpha)y) < \alpha f(x) + (1-\alpha) f(y)$;*
- *m-**Strongly convex** if there exists $m > 0$ such that $f(y) \geq f(x) + \nabla f(x)^T (y-x) + \frac{m}{2}\|x-y\|^2$, for all $x, y \in D$;*
- *β-**Strongly smooth** if for all $x, y \in D$, $f(y) \leq f(x) + \nabla f(x)^T (y-x) + \frac{\beta}{2}\|x-y\|^2$, where $\beta > 0$.*

Lemma 6.1. ***First-order conditions**: A $\mathcal{C}^1$ function $f : D \to \mathbb{R}$, where $D \subset \mathbb{R}^n$ is a convex set, is called*

- ***Convex*** *if and only if for all $x, y \in D$, $f(y) \geq f(x) + \nabla f(x)^T (y-x)$;*
- *m-**Strongly convex** if and only if there exists $m > 0$ such that for all $x, y \in D$, $(\nabla f(x) - \nabla f(y))^T (x-y) \geq m\|x-y\|^2$.*

***Second-order conditions**: A function $f : D \to \mathbb{R}$ such that $f \in \mathcal{C}^2$, where $D \subset \mathbb{R}^n$ is a convex set, is called*

- ***Convex** if and only if for all $x \in D$, $\nabla^2 f(x) \succeq 0$;*
- ***Strictly convex** if for all $x \in D$, $\nabla^2 f(x) \succ 0$;*
- *m-**Strongly convex** if and only if there exists $m > 0$ such that for all $x \in D$, $\nabla^2 f(x) \succeq mI$.*
- *β-**Strongly smooth** if and only if there exists $\beta > 0$ such that for all $x \in D$, $\nabla^2 f(x) \preceq \beta I$.*

It follows that strong convexity implies strict convexity, which implies convexity.

Definition 6.2 (Convexity-concavity). *A function $F : D_1 \times D_2 \to \mathbb{R}$, where $D_1 \subset \mathbb{R}^n, D_2 \subset \mathbb{R}^m$, is called locally convex-concave (respectively, locally strongly or locally strictly convex-concave) if for all $\bar{z} \in U_z \subset D_2$, $F(x, \bar{z})$ is convex (respectively, strongly or strictly convex) for all $x \in U_x \subset D_1$, and for all $\bar{x} \in U_x \subset D_1$, $F(\bar{x}, z)$ is concave (respectively, strongly or strictly concave) for all $z \in U_z \subset D_2$.*

The Lyapunov conditions for FxTS from Chapter 3 are revisited here for the sake of completeness. Consider a dynamical system

$$\dot{x}(t) = \phi(x(t)), \tag{6.1}$$

where $\phi : \mathbb{R}^n \to \mathbb{R}^n$ is continuous, and assume that the origin is the unique equilibrium point of (6.1).

Theorem 6.1 (Lyapunov conditions for FxTS). *Suppose there exists a continuously differentiable, positive definite, radially unbounded function $V : \mathbb{R}^n \to \mathbb{R}$ such that $\dot{V}(x) \leq -\alpha_1 V(x)^{\gamma_1} - \alpha_2 V(x)^{\gamma_2}$ holds along the trajectories of (6.1) for all $x \in \mathbb{R}^n \setminus \{0\}$, with $\alpha_1, \alpha_2 > 0$, $\gamma_1 > 1$ and $0 < \gamma_2 < 1$. Then, the origin of (6.1) is FxTS with continuous settling-time function T that satisfies $T \leq \frac{1}{\alpha_1(\gamma_1 - 1)} + \frac{1}{\alpha_2(1-\gamma_2)}$.*

First, conditions for the existence and uniqueness of the solutions of dynamical systems are reviewed, which would be instrumental in proving the main results in this chapter. The following result from [131] is stated here for the sake of completeness.

Lemma 6.2 ([131, Theorem 3.18.1]). *Assume that*

i) The function $g : \mathbb{R} \to \mathbb{R}$ is continuous and $y(t) = 0$ is the unique solution of the dynamical system $\dot{y}(t) = g(y(t))$;

ii) The function $\phi : \mathbb{R}^n \to \mathbb{R}$ is continuous; and

iii) There exists a positive definite, $\mathcal{C}^1$ function $V : \mathbb{R}^n \to \mathbb{R}_+$ such that $\dot{V}(x) \leq g(V(x))$ for all $x \neq 0$.

Then, the dynamical system $\dot{x}(t) = \phi(x(t))$ has a unique solution for all $t \geq 0$.

Theorem 6.2 (Uniqueness of system trajectory). *Suppose that there exists a positive definite $\mathcal{C}^1$ function $V : \mathbb{R}^n \to \mathbb{R}_+$ such that $\dot{V}(x) \leq -c_1 V(x)^{\alpha_1} - c_2 V(x)^{\alpha_2}$ for all $x \neq 0$, where $c_1, c_2 > 0$, $0 < \alpha_1 < 1$ and $\alpha_2 > 1$. Then the solution $x(t)$ of (6.1) exists and is unique for all $x(0) \in \mathbb{R}^n$ and for all $t \geq 0$.*

Proof. Similar strategy as in the proof of Theorem 4.3 can be used to prove the result. For existence, the result in [135, Ch2., Theorem 1] is used. Since the map ϕ is a single-valued, continuous function, it satisfies all the conditions of [135, Ch2., Theorem 1], and thus, existence of a solution is guaranteed for (6.1) on $[0, \tau)$ where $\tau > 0$. Now, since the solution $x(t)$ remains bounded in the open set $\{x \mid V(x) < V(x(0)) + c\}$ for all $c > 0$, it follows that the solution of (6.1) is complete, i.e., $\tau = \infty$. For uniqueness, the strategy is to verify that all the conditions of Lemma 6.2 are satisfied for (6.1). To this end, consider the dynamical system

$$\dot{y}(t) = g(y) \coloneqq 0, \quad y(0) = 0. \tag{6.2}$$

Note that $g(y)$ is continuous for all $y \in \mathbb{R}$. Choose $\mathfrak{v}(y) = \frac{1}{2}|y|^2$ so that its time derivative along the trajectories of (6.2) satisfies $\dot{\mathfrak{v}}(y) \leq 0$ for all y. Thus, using [131, Theorem 3.15.1], it holds that $y(t) \equiv 0$ is the unique solution of (6.2). Hence, condition (i) of Lemma 6.2 is satisfied. Now, since $\phi \in \mathcal{C}^0$, condition (ii) of Lemma 6.2 is also satisfied. Note that the function V is positive definite, continuously differentiable, and satisfies $\dot{V}(x) \leq -c_1 V(x)^{\alpha_1} - c_2 V(x)^{\alpha_2} \leq 0 = g(V(x))$ for all $x \neq 0$. Thus, condition (iii) of Lemma 6.2 is also satisfied, and therefore, the solution of (6.1) exists and is unique for all $x(0) \in \mathbb{R}^n$ and for all $t \geq 0$, which completes the proof. □

Next, novel gradient flow schemes are proposed for unconstrained and constrained convex optimization problems. First, unconstrained optimization problems are considered.

6.1.2 Unconstrained optimization

Consider the unconstrained minimization problem

$$\min_{x \in \mathbb{R}^n} f(x), \tag{6.3}$$

where $f : \mathbb{R}^n \to \mathbb{R}$. The following assumption is made about the problem (6.3).

Assumption 6.1 (Unique minimizer). *The minimum value of $f(x)$ is attained, i.e., there exists $x^\star \in \mathbb{R}^n$ such that $-\infty < f^\star = f(x^\star)$.*

Remark 6.1. *For (6.3), Assumption 6.1 is a necessary condition for convergence of gradient-based methods to an optimal solution. Coercivity, or equivalently, compactness of the sub-level sets of the convex function f is a sufficient condition to guarantee existence of a minimizer [154, Chapter 2].*

Lemma 6.3 ([128])**.** *If a $\mathcal{C}^1$ function $f : \mathbb{R}^n \to \mathbb{R}$ is convex, then a point $x^\star$ is the global optimal point of the function f if and only if $\nabla f(x^\star) = 0$. Furthermore, if f is strictly convex, then the optimal point $x^\star$ is unique.*

6.1.2.1 Finite-time stable gradient flow

There has been a lot of research on developing discrete-time optimization schemes with convergence rate faster than linear (see [10, 95] and references therein). The continuous variant of such discrete-time schemes are also studied by various authors. Based on the GF defined as

$$\dot{x} = -\nabla f(x), \tag{6.4}$$

the authors in [10] discuss the following scheme

$$\dot{x} = -\frac{\nabla f(x)}{\|\nabla f(x)\|^{\frac{p-2}{p-1}}}, \tag{6.5}$$

where $p > 2$ as a modification of GF. It is shown that the convergence rate for the solutions of (6.5) is given as

$$f(x(t)) - f^\star \leq O\left(\frac{1}{t^{p-1}}\right), \tag{6.6}$$

under the assumption that the level-sets of $f(x)$ are bounded. The flow in (6.5) is referred to as *rescaled* GF in the subsequent text. In this section, it is shown that the optimal

point of (6.3) is actually an FTS equilibrium of (6.5). Then, in the subsequent sections, modifications of (6.5) are presented with fixed-time convergence guarantees.

Theorem 6.3. *If a $\mathcal{C}^2$ function $f : \mathbb{R}^n \to \mathbb{R}$ is k-strongly convex where $k > 0$, then for all $p > 2$, the trajectories of (6.5) converge to the optimal point $x^\star$ in finite time $T = T(x(0))$ satisfying*

$$T(x(0)) \leq \frac{\|\nabla f(x(0))\|^{2(1-\beta_1)}}{k_1 2^{1-\beta_1}(1-\beta_1)}, \tag{6.7}$$

where $k_1 = 2^{\frac{p}{2(p-1)}} k$ and $\beta_1 = \frac{p}{2(p-1)}$.

Proof. First, using Lemma 6.1, one has that strong convexity of f implies that the optimal solution $x^\star$ of (6.3) is unique and satisfies $\nabla f(x^\star) = 0$. Choose $V(x) = \frac{1}{2}\|\nabla f(x)\|^2$ as the candidate Lyapunov function. k-strong convexity of f implies that $\nabla^2 f(x) \succeq kI$ for all $x \in \mathbb{R}^n$. Using this, one obtains that the time derivative of V along (6.5) satisfies

$$\begin{aligned}
\dot{V}(x) &= \nabla f(x)^T \nabla^2 f(x) \dot{x} = -\nabla f(x)^T \nabla^2 f(x) \frac{\nabla f(x)}{\|\nabla f(x)\|^{\frac{p-2}{p-1}}} \\
&\leq -k \nabla f(x)^T \frac{\nabla f(x)}{\|\nabla f(x)\|^{\frac{p-2}{p-1}}} = -k \|\nabla f(x)\|^{2-\frac{p-2}{p-1}} \\
&= -k \|\nabla f(x)\|^{\frac{p}{p-1}} = -k \left(2V(x)\right)^{\frac{p}{2(p-1)}}.
\end{aligned}$$

Define $k_1 = 2^{\frac{p}{2(p-1)}} k$ so that $k_1 > 0$, and $\beta_1 = \frac{p}{2(p-1)}$, so that $0 < \beta_1 < 1$, and one obtains $\dot{V}(x) \leq -k_1 V(x)^{\beta_1}$ for all $x \in \mathbb{R}^n$. Using Theorem 2.1, one obtains that $\|\nabla f(x(t))\| = 0$ for all $t \geq T$ where $T \leq \frac{V(x(0))^{1-\beta_1}}{k_1(1-\beta_1)}$. Since the function is strongly convex, the sublevel sets of the norm of ∇f are bounded. Thus, V is radially unbounded, and hence, the result holds for all $x(0) \in \mathbb{R}^n$. □

Remark 6.2. *For a given $p > 2$, denote the bound on the time of convergence as $\bar{T}_p$. As noted in [10], the limiting case of (6.5) as $p \to \infty$, called normalized GF, is studied in [93], and it is shown that the time of convergence is upper bounded by $\frac{1}{k}\|\nabla f(x(0))\|$ under the assumption of strong convexity. The same bound on the time of convergence is recovered by allowing $p \to \infty$ in the bound of the settling time $\bar{T}_\infty$ in Theorem 6.3.*

It is clear from the expression of the upper-bound on the settling time T in Theorem 6.3 that it grows unbounded as the distance of $x(0)$ increases from the optimal point $x^\star$. Inspired from (6.5) and noting its finite-time convergence guarantees, a modified GF is

designed in this section with fixed-time convergence guarantees, so that the optimal point of (6.3) can be obtained within a fixed time for all $x(0) \in \mathbb{R}^n$.

Consider the flow equation

$$\dot{x} = \begin{cases} -c_1 \dfrac{\nabla f(x)}{\|\nabla f(x)\|^{\frac{p_1-2}{p_1-1}}} - c_2 \dfrac{\nabla f(x)}{\|\nabla f(x)\|^{\frac{p_2-2}{p_2-1}}}; & \nabla f(x) \neq 0, \\ 0; & \nabla f(x) = 0, \end{cases} \tag{6.8}$$

where $c_1, c_2 > 0$, $p_1 > 2$ and $1 < p_2 < 2$. In what follows, (6.8) is referred to as *FxTS-GF*. First, it is shown that the equilibrium points of the right-hand side of (6.8) are critical points[1] of the function f, and that the dynamics in (6.8) is continuous for all $x \in \mathbb{R}^n$.

Lemma 6.4. *A point $\bar{x} \in \mathbb{R}^n$ is an equilibrium point of (6.8) if and only if $\|\nabla f(\bar{x})\| = 0$.*

Proof. One has that $x = \bar{x}$ is an equilibrium of (6.8) if and only if

$$\begin{aligned} \dot{\bar{x}} = 0 &\iff -c_1 \frac{\nabla f(\bar{x})}{\|\nabla f(\bar{x})\|^{\frac{p_1-2}{p_1-1}}} - c_2 \frac{\nabla f(\bar{x})}{\|\nabla f(\bar{x})\|^{\frac{p_2-2}{p_2-1}}} = 0 \\ &\iff c_1 \frac{\|\nabla f(\bar{x})\|}{\|\nabla f(\bar{x})\|^{\frac{p_1-2}{p_1-1}}} + c_2 \frac{\|\nabla f(\bar{x})\|}{\|\nabla f(\bar{x})\|^{\frac{p_2-2}{p_2-1}}} = 0 \\ &\iff c_1 \|\nabla f(\bar{x})\|^{1-\frac{p_1-2}{p_1-1}} + c_2 \|\nabla f(\bar{x})\|^{1-\frac{p_2-2}{p_2-1}} = 0, \\ &\iff \|\nabla f(\bar{x})\| = 0, \end{aligned}$$

since $1 - \frac{p_1-2}{p_1-1}, 1 - \frac{p_2-2}{p_2-1} > 0$ for $p_1 > 2$ and $1 < p_2 < 2$. This completes the proof. □

Lemma 6.5 (Continuity of modified GF). *If $f : \mathbb{R}^n \to \mathbb{R}$ is $\mathcal{C}^1$, then the right-hand side of (6.8) is continuous for all $x \in \mathbb{R}^n$.*

Proof. Let $\mathcal{X} = \{x \mid \nabla f(x) = 0\}$. Since $f \in \mathcal{C}^1$, continuity of right-hand side of (6.8) is immediate on $\mathbb{R}^n \setminus \mathcal{X}$. Let $\bar{x} \in \mathcal{X}$ so that one has

$$\begin{aligned} \left\| \lim_{x \to \bar{x}} c_1 \frac{\nabla f(x)}{\|\nabla f(x)\|^{\frac{p_1-2}{p_1-1}}} \right\| &= \lim_{x \to \bar{x}} c_1 \left\| \frac{\nabla f(x)}{\|\nabla f(x)\|^{\frac{p_1-2}{p_1-1}}} \right\| \\ &= c_1 \lim_{x \to \bar{x}} \|\nabla f(x)\|^{1-\frac{p_1-2}{p_1-1}} \\ &= c_1 \lim_{x \to \bar{x}} \|\nabla f(x)\|^{\delta_1} = 0, \end{aligned}$$

[1] Recall that a point x is called a critical point of a C^1 function f if $\nabla f(x) = 0$.

where the last equality follows from continuity of ∇f since $\delta_1 = 1 - \frac{p_1-2}{p_1-1} > 0$ for $p_1 > 2$. Hence, one has that $\lim_{x\to\bar{x}} c_1 \frac{\nabla f(x)}{\|\nabla f(x)\|^{\frac{p_1-2}{p_1-1}}} = 0$. Similarly, it can be shown that $\lim_{x\to\bar{x}} c_2 \frac{\nabla f}{\|\nabla f\|^{\frac{p_2-2}{p_2-1}}} = 0$, since $\delta_2 = 1 - \frac{p_2-2}{p_2-1} > 0$ for all $1 < p_2 < 2$. Per Lemma 6.4, one has that $\bar{x}$ is an equilibrium of (6.8). This implies that the right-hand side of (6.8) is continuous at $x = \bar{x}$, for all $\bar{x} \in \mathcal{X}$, and hence, is continuous for all $x \in \mathbb{R}^n$. □

Next, it is shown that the solutions of (6.8) exist and are unique in the forward time.

Proposition 6.1. *If a $\mathcal{C}^1$ function $f : \mathbb{R}^n \to \mathbb{R}$ is convex with unique minimizer, then for all $x(0) \in \mathbb{R}^n$, the solution of (6.8) exists and is unique for all $t \geq 0$.*

Proof. Note that right-hand side of the dynamics in (6.8) is continuous for all $x \in \mathbb{R}^n$, and therefore, it satisfies the conditions of Theorem 6.2. Furthermore, the function $V = f(x) - f(x^\star)$ is positive definite (since f is convex and $x^\star$ is assumed to be unique), and is continuously differentiable, satisfying all the requirements as in Theorem 6.2. Thus, the solution of (6.8) exists and is unique for all $x(0) \in \mathbb{R}^n$ and for all $t \geq 0$. □

6.1.2.2 FxTS under gradient dominance

In the section, the notion of PL inequality, or gradient dominance, as defined in [94], is assumed on the objective function f.

Definition 6.3 (PL inequality). *The $\mathcal{C}^1$ function $f : \mathbb{R}^n \to \mathbb{R}$ is said to satisfy the PL inequality, or is gradient dominated, with $\mu_f > 0$, i.e., for all $x \in \mathbb{R}^n$,*

$$\frac{1}{2}\|\nabla f(x)\|^2 \geq \mu_f (f(x) - f^\star). \tag{6.9}$$

Based on this, the following assumption is made on the objective function f.

Assumption 6.2. *The function f is $\mathcal{C}^1$, has a unique minimizer, and satisfies PL inequality with $\mu_f > 0$.*

Remark 6.3. *Strong convexity of the objective function is a standard assumption used in the literature to show exponential convergence for gradient flows. As noted in [94], PL inequality is the weakest condition among other similar conditions popularly used in the literature to show linear convergence in discrete-time (exponential, in continuous-time) gradient-based algorithms. Particularly, a $\mathcal{C}^1$ strongly convex function f satisfies PL inequality. Note that under Assumption 6.2, it is not required that the objective function f is convex.*

It is shown in [94, Theorem 2] that satisfaction of PL inequality implies that the function f has *quadratic growth*, i.e.,

$$f(x) - f^\star \geq \frac{\mu_f}{2}\|x - x^\star\|^2. \tag{6.10}$$

for all x, where μ_f is as defined in (6.9). The following result can now be stated.

Theorem 6.4 (FxTS under PL inequality). *If the objective function f satisfies Assumptions 6.1 and 6.2, then, the trajectories of (6.8) converge to the optimal point $x^\star$ in a fixed time T_1 for all $x(0)$ such that*

$$T_1 \leq \frac{4}{k_1(2-\alpha_1)} + \frac{4}{k_2(\alpha_2 - 2)}, \tag{6.11}$$

where $\alpha_1 = 2 - \frac{p_1-2}{p_1-1}, \alpha_2 = 2 - \frac{p_2-2}{p_2-1}, k_1 = c_1 2^{\frac{2+3\alpha_1}{4}} \mu_f^{\frac{\alpha_1}{2}}$ *and* $k_2 = c_2 2^{\frac{2+3\alpha_2}{4}} \mu_f^{\frac{\alpha_2}{2}}$.

Proof. Proposition 6.1 is invoked for existence and uniqueness of the solutions. Note that the convexity requirement in Proposition 6.1 is required for positive definiteness of the function $V = \frac{1}{2}(f(x) - f(x^\star))^2$. For the case when the optimal point $x^\star$ is unique and f satisfies the PL inequality, the function V is positive definite, and therefore, under Assumption 6.2, the solution of (6.8) exists and is unique for all $x(0) \in \mathbb{R}^n$ and $t \geq 0$.

Now, consider the candidate Lyapunov function $V(x) = \frac{1}{2}(f(x) - f(x^\star))^2$. It follows from (6.10) that V is radially unbounded. The time derivative along the trajectories of (6.8) reads

$$\begin{aligned}
\dot{V}(x) &= (f(x) - f(x^\star))(\nabla f(x))^T \left(-c_1 \frac{\nabla f(x)}{\|\nabla f(x)\|^{\frac{p_1-2}{p_1-1}}} - c_2 \frac{\nabla f(x)}{\|\nabla f(x)\|^{\frac{p_2-2}{p_2-1}}} \right) \\
&= -c_1 (f(x) - f(x^\star))\|\nabla f(x)\|^{2-\frac{p_1-2}{p_1-1}} - c_2 (f(x) - f(x^\star))\|\nabla f(x)\|^{2-\frac{p_2-2}{p_2-1}} \\
&= -c_1 (f(x) - f(x^\star))\|\nabla f(x)\|^{\alpha_1} - c_2 (f(x) - f(x^\star))\|\nabla f(x)\|^{\alpha_2} \\
&\overset{(6.9)}{\leq} -c_1 (2\mu_f)^{\frac{\alpha_1}{2}} (f(x) - f(x^\star))^{1+\frac{\alpha_1}{2}} - c_2 (2\mu_f)^{\frac{\alpha_2}{2}} (f(x) - f(x^\star))^{1+\frac{\alpha_2}{2}} \\
&= -c_1 2^{\frac{2+3\alpha_1}{4}} \mu_f^{\frac{\alpha_1}{2}} V(x)^{\frac{2+\alpha_1}{4}} - c_2 2^{\frac{2+3\alpha_2}{4}} \mu_f^{\frac{\alpha_2}{2}} V(x)^{\frac{2+\alpha_2}{4}} \\
&= -k_1 V(x)^{\frac{2+\alpha_1}{4}} - k_2 V(x)^{\frac{2+\alpha_2}{4}},
\end{aligned}$$

where $\alpha_1 = 2 - \frac{p_1-2}{p_1-1}, \alpha_2 = 2 - \frac{p_2-2}{p_2-1}, k_1 = c_1 2^{\frac{2+3\alpha_1}{4}} \mu_f^{\frac{\alpha_1}{2}}$ and $k_2 = c_2 2^{\frac{2+3\alpha_2}{4}} \mu_f^{\frac{\alpha_2}{2}}$. Since $\alpha_1 < 2$ and $\alpha_2 > 2$, one has $\frac{2+\alpha_1}{4} < 1$ and $\frac{2+\alpha_2}{4} > 1$. Hence, from Theorem 6.1, one obtains that for $t \geq T_1$, $f(x(t)) = f^\star$, which is equivalent to $x(t) = x^\star$ under Assumption

6.2, where $T_1 \leq \frac{4}{k_1(2-\alpha_1)} + \frac{4}{k_2(\alpha_2-2)}$. Hence, the trajectories of (6.8) converge to the optimal point $x^\star$ of (6.3) in a fixed time. □

Remark 6.4. *Note that the difference between the proposed modified gradient flow* (6.8) *and the rescaled gradient flow* (6.5) *is the second term with exponent* $1 < p_2 < 2$*. This term results into the second term* $-V^\beta$ *in* (3.4)*, while the first term, with exponent* $p_1 > 2$*, results into the first term* $-V^\alpha$ *in* (3.4)*. Since* (6.5) *contains only the first term, which dominates when* V *is small, the time of convergence, though finite, grows larger as the initial distance from the equilibrium increases (see also Remark 3.1).*

It is showed that the FxTS-GF in (6.8) can be used to find the optimal solution of (6.3) in fixed time. As mentioned in Remark 6.3, Assumption 6.2 is a relaxation used to show exponential convergence of gradient flow. Hence, all such problems which have been shown to have exponential convergence under strong-convexity can be solved within fixed time using (6.8). It is easy to show that if a function $f : \mathbb{R}^m \to \mathbb{R}$ is strongly convex, then the function $g : \mathbb{R}^n \to \mathbb{R}$, defined as $g(x) = f(Ax)$, $A \in \mathbb{R}^{n\times m}$, is strongly convex if A is full row-rank. If matrix A is not full row-rank, then g may not be strongly convex. On the other hand, as shown in [94, Appendix 2.3], g still satisfies PL inequality for all matrices $A \in \mathbb{R}^{n\times m}$. Below, two important classes of problems are given for which, the objective function satisfies PL inequality (see [94] for more examples on useful functions that satisfy PL inequality).

Example 6.1. ***Least squares****: Consider the optimization problem*

$$\min_{x\in\mathbb{R}^n} f(Ax) = \|Ax - b\|^2, \tag{6.12}$$

where $x \in \mathbb{R}^n, A \in \mathbb{R}^{n\times n}$ *and* $b \in \mathbb{R}^n$*. Here, the function* $f(x) = \|x - b\|^2$ *is strongly-convex, and hence,* $g(x) = \|Ax - b\|^2$ *satisfies PL inequality for all matrices* A*.*
Linear regression: *Consider the optimization problem*

$$\min_{x\in\mathbb{R}^n} f(Ax) = \sum_{i=1}^{m} \log(1 + b_i a_i^T x), \tag{6.13}$$

where $x \in \mathbb{R}^n, a_i \in \mathbb{R}^n$ *and* $b \in \mathbb{R}$ *for* $i = 1, 2, \ldots, m$*. Here, the function* $g(x) = f(Ax)$ *satisfies PL inequality for all matrices* A*. The objective functions in* (6.12) *and* (6.13) *satisfies PL inequality, but need not be strongly convex for all matrices* A*; if additionally, uniqueness of the optimal solutions of* (6.12) *and* (6.13) *is assumed, one can use* (6.8) *to find the optimal solutions for* (6.12) *and* (6.13)*, respectively, in fixed time. These are important classes of functions in machine learning problems.*

6.1.2.3 FxTS under strict convexity

In this section, the modification of the Newton's method based GF is presented to guarantee FxTS for a class of functions that do not satisfy Assumption 6.2. The *nominal* Newton's method is defined as

$$\dot{x} = -\left(\nabla^2 f(x)\right)^{-1} \nabla f(x). \tag{6.14}$$

It is well-known that under certain conditions on the function f, (6.14) can achieve exponential convergence. The following assumption is made about the objective function f.

Assumption 6.3 (Strict convexity). *The function $f : \mathbb{R}^n \to \mathbb{R}$ is C^2 and is strictly convex. Furthermore, the Hessian $\nabla^2 f(x)$ invertible for all $x \in \mathbb{R}^n$, and the norm of the gradient, $\|\nabla f\|$ is radially unbounded.*

Per Assumption 6.3, $\nabla^2 f(x) \succ 0$ for all $x \in \mathbb{R}^n$,[2] and with Assumption 6.1, using Lemma 6.3, one has that the optimal point $x^\star$ is unique. Note that if f satisfies Assumption 6.3, it is not necessary that it satisfies Assumption 6.2. So, for the optimization problem in (6.3), with this class of functions, fixed-time convergence cannot be guaranteed using (6.8). Hence, another modified GF is proposed so that fixed-time convergence for this class of functions can be guaranteed. Consider the flow equation for FxTS Newton's method

$$\dot{x} = \begin{cases} -(\nabla^2 f(x))^{-1} \left(c_1 \frac{\nabla f(x)}{\|\nabla f(x)\|^{\frac{p_1-2}{p_1-1}}} + c_2 \frac{\nabla f(x)}{\|\nabla f(x)\|^{\frac{p_2-2}{p_2-1}}} \right); & \nabla f(x) \neq 0, \\ 0; & \nabla f(x) = 0, \end{cases} \tag{6.15}$$

where $c_1, c_2 > 0$, $p_1 > 2$ and $1 < p_2 < 2$. Under Assumption 6.3, it can be readily shown that the system dynamics in (6.15) is continuous on $\mathbb{R}^n$ and that $x^*\star$ is the unique equilibrium point of (6.15). The following result can now be stated.

Theorem 6.5 (FxTS under strict convexity). *If f satisfies Assumptions 6.1 and 6.3, then the trajectories of (6.15) converge to the optimal point $x^\star$ in fixed time T_{NM} for all initial conditions $x(0) \in \mathbb{R}^n$ such that*

$$T_{NM} \leq \frac{2^{1-\frac{\alpha_1}{2}}}{c_1(2-\alpha_1)} + \frac{2^{1-\frac{\alpha_2}{2}}}{c_2(\alpha_2-2)}, \tag{6.16}$$

where $\alpha_1 = 2 - \frac{p_1-2}{p_1-1}$ and $\alpha_2 = 2 - \frac{p_2-2}{p_2-1}$.

Proof. Note that under Assumption 6.3, per Proposition 6.1, solutions of (6.15) exist and are unique for all $x(0) \in \mathbb{R}^n$. Consider the Lyapunov function $V(x) = \frac{1}{2}\|\nabla f(x)\|^2$.

[2] This is needed so that the right-hand side in the Newton's method is well-defined.

Since the sub-level sets of norm of its gradient ∇f are bounded under Assumption 6.3, the candidate Lyapunov function V is radially unbounded. The time derivative of this function along the trajectories of (6.15) reads

$$\begin{aligned}\dot{V}(x) &= (\nabla f(x))^T(\nabla^2 f(x))\dot{x} \\ &= -(\nabla f(x))^T\left(c_1\frac{\nabla f(x)}{\|\nabla f(x)\|^{\frac{p_1-2}{p_1-1}}} + c_2\frac{\nabla f(x)}{\|\nabla f(x)\|^{\frac{p_2-2}{p_2-1}}}\right) \\ &= -c_1\|\nabla f(x)\|^{2-\frac{p_1-2}{p_1-1}} - c_2\|\nabla f(x)\|^{2-\frac{p_2-2}{p_2-1}} \\ &\leq -c_1 2^{\frac{\alpha_1}{2}} V(x)^{\frac{\alpha_1}{2}} - c_2 2^{\frac{\alpha_2}{2}} V(x)^{\frac{\alpha_2}{2}},\end{aligned}$$

where $\alpha_1 = 2 - \frac{p_1-2}{p_1-1}$ and $\alpha_2 = 2 - \frac{p_2-2}{p_2-1}$. Since $p_1 > 2$ and $1 < p_2 < 2$ one obtains that $1 < \alpha_1 < 2$ and $\alpha_2 > 2$. Hence, using Theorem 6.1, one obtains that the trajectories of (6.15) converge to the optimal point $x^\star$ in the fixed time T_{NM} for all $x(0) \in \mathbb{R}^n$, where $T_{NM} \leq \frac{2^{1-\frac{\alpha_1}{2}}}{c_1(2-\alpha_1)} + \frac{2^{1-\frac{\alpha_2}{2}}}{c_2(\alpha_2-2)}$. □

While strongly-convex functions satisfy PL inequality [94], strictly-convex functions do not satisfy PL inequality in general. Thus, for convex optimization problems with strictly convex objective functions that do not satisfy Assumption 6.2, (6.15) can be used to find the optimal solution of (6.3) within a fixed time. One example is the class of *quartic* functions, which can be used to reformulate a standard QP with sign constraints as an unconstrained optimization problem [155].

Example 6.2. *Consider the optimization problem*

$$\begin{aligned}&\min_x\ x^TQx + c^Tx, \\ &\text{s.t. } x_i \geq 0,\ i = 1, 2, \ldots, n,\end{aligned} \tag{6.17}$$

where $x, c \in \mathbb{R}^n$ and $Q \in \mathbb{R}^{n\times n}$ is a positive definite matrix. Let $z \in \mathbb{R}^n$ be defined as $x_i = z_i^2$ and re-write (6.17) in terms of z

$$\min_z\ z^TZQZz + c^TZz, \tag{6.18}$$

where $Z \in \mathbb{R}^{n\times n}$ is a diagonal matrix consisting of elements z_i, i.e.,

$$Z_{ij} = \begin{cases} z_i, & i = j; \\ 0, & i \neq j, \end{cases}$$

for $i, j = 1, 2, \ldots, n$. The optimal solution $\bar{x}$ of (6.17) is given by $\bar{x}_i = \bar{z}_i^2$, where $\bar{z}$ is the

optimal solution of (6.18).

It is clear that the objective function in (6.18) is a quartic, is not strongly convex, and may not satisfy PL inequality. Nevertheless, it is strictly convex and hence, (6.15) can be used to find the optimal point of (6.18) within a fixed time.

Up to now, unconstrained minimization problems have been considered. Next, constrained minimization problems are studied, and FxTS-GF based methods are proposed with fixed-time convergence guarantees.

6.1.3 Constrained optimization

Consider the optimization problem

$$\begin{aligned} &\min_{x\in\mathbb{R}^n} f(x), \\ &\text{s.t. } Ax = b, \end{aligned} \tag{6.19}$$

where $f : \mathbb{R}^n \to \mathbb{R}$ is convex, $A \in \mathbb{R}^{m\times n}$ and $b \in \mathbb{R}^m$.

Assumption 6.4. *The matrix A is full row-rank and the objective function f is coercive.*

Remark 6.5. *Assumption 6.4 is commonly used in constrained optimization [156]; the matrix A being full row-rank guarantees that the feasible set is non-empty and closed, and thus, coercivity of the convex function f guarantees that the solution of* (6.19) *exists [154, Chapter 2].*

Define $g : \mathbb{R}^m \to \mathbb{R}$ as

$$g(\nu) = \inf_{x\in\mathbb{R}^n} (f(x) + \nu^T(Ax - b)), \tag{6.20}$$

so that the dual problem (see [128, Chapter 5]) for (6.19) is given by

$$\sup_{\nu\in\mathbb{R}^m} g(\nu). \tag{6.21}$$

Using (6.20), rewrite (6.21) as

$$\sup_{\nu\in\mathbb{R}^m} \inf_{x\in\mathbb{R}^n} L(x,\nu) \triangleq f(x) + \nu^T(Ax - b). \tag{6.22}$$

It is clear that (6.22) is a saddle-point problem, where $L(x,\nu)$ needs to be minimized over x and maximized over ν. From (6.20), following the discussion in [128, Section 5.1], one obtains:

$$g(\nu) = -\nu^T b - f^*(-A^T\nu), \tag{6.23}$$

where $f^* : \mathbb{R}^n \to \mathbb{R}$ is the conjugate of f.[3] Note that the function f^* is always convex, whether f is convex or not [128, Chapter 3]. It can be readily seen from (6.23) that g is a concave function (since f^* is convex, $-f^*$ is concave). As shown in [157, Section 3.5], strong convexity of function f and strong smoothness of its conjugate f^* are equivalent. Using this, the following results can be stated.

Lemma 6.6. *If f is a convex, β-strongly smooth function, then the function g defined as per (6.20) is α-strongly concave, where $\alpha > 0$.*

Proof. The convexity and strong-smoothness assumptions on f implies that $f^{**} = f$, i.e., f is the conjugate of its conjugate f^*. Define $\kappa = f^*$ so that one has $\kappa^* = f^{**} = f$. Now, since the function f is the conjugate of κ and is β-strongly smooth, from [157, Section 3.5], one obtains that there exists β^* such that κ is a β^*-strongly convex function. It holds that if A is full row-rank, then β^*-strong-convexity of f^* implies α-strong-convexity of $f^*(-A^T\nu)$, where $\alpha = \lambda\beta^*$ and $\lambda = \lambda_{min}(AA^T)$ is the minimum eigenvalue of AA^T. Since A is full row-rank, it follows that $\lambda > 0$. Finally, using the fact that $f_1 = f^*(-A^T\nu)$ is α-strongly convex and $f_2 = \nu^T b$ is convex, one obtains that $f_1 + f_2 = f^*(-A^T\nu) + \nu^T b = -g(\nu)$ is α-strongly convex, or equivalently, g is α-strongly concave. □

Note that the constrained optimization problem in (6.19) is equivalent to the unconstrained problem in (6.22). Furthermore, under the assumptions of Lemma 6.6 on the function f, the function $-g$ is strongly concave. Thus, if the function f^* is known in closed-form, then (6.8) can be used to find the optimal point of (6.22). Based on this, the following assumption is made on the function f .

Assumption 6.5. *The objective function $f : \mathbb{R}^n \to \mathbb{R}$ is $\mathcal{C}^1$, β_1-strongly convex, β_2-strongly smooth, and its conjugate function $f^* : \mathbb{R}^n \to \mathbb{R}$ is known in closed-form.*

See Remark 6.6 and Corollary 6.2 for the case when f^* is not known in closed-form. For the case when Assumption 6.5 holds, consider the dynamical system

$$\dot{\nu} = \begin{cases} -c_1 \frac{-\nabla g(\nu)}{\|\nabla g(\nu)\|^{\frac{p_1-2}{p_1-1}}} - c_2 \frac{-\nabla g(\nu)}{\|\nabla h(\nu)\|^{\frac{p_2-2}{p_2-1}}}; & \nabla g(\nu) \neq 0, \\ 0; & \nabla g(\nu) = 0, \end{cases} \tag{6.24}$$

where $c_1, c_2 > 0$, $p_1 > 2$ and $1 < p_2 < 2$. Note that the assumptions on functions f, f^*, and matrix A implies $\sup_{\nu} \inf_{x} L(x,\nu) = \inf_{x} \sup_{\nu} L(x,\nu)$ ([128, Section 5.5]). Also, using Proposition 6.1, one has that the solutions of (6.24) exist and are unique for all $\nu(0) \in \mathbb{R}^m$.

[3] Since the considered space is the finite-dimensional vector space $\mathbb{R}^n$ with the Euclidean norm, the dual space is $\mathbb{R}^n$ with the dual norm $\|\cdot\|_* = \|\cdot\|$.

Lemma 6.7 (FxTS of dual variable). *The trajectories of (6.24) reach the optimal point $\nu^\star$ of (6.21) in fixed time T_ν for all initial conditions $\nu(0) \in \mathbb{R}^m$ where*

$$T_\nu \leq \frac{4}{k_3(2-\alpha_1)} + \frac{4}{k_4(\alpha_2-2)}, \tag{6.25}$$

where $\alpha_1 = 2 - \frac{p_1-2}{p_1-1}, \alpha_2 = 2 - \frac{p_2-2}{p_2-1}, k_3 = c_1 2^{\frac{2+3\alpha_1}{4}} \mu_g^{\frac{\alpha_1}{2}}$ *and* $k_4 = c_2 2^{\frac{2+3\alpha_2}{4}} \mu_g^{\frac{\alpha_2}{2}}$.

Proof. Per Lemma 6.6, $-g(\nu)$ is α-strongly convex. Thus, g satisfies PL inequality (6.9) with $\mu_g > 0$. Since g is strongly convex, and the maximizer $\nu^\star$ of g exists, it is also unique. Furthermore, using [157, Theorem 3.5.10], one obtains that $f^* \in \mathcal{C}^1$ if f is strongly convex and so, it holds that $g \in \mathcal{C}^1$. This implies that g satisfies Assumptions 6.1 and 6.2. Hence, using Theorem 6.4, one obtains that the trajectories of (6.24) reach the the maximizer $\nu^\star$ of $g(\nu)$ in a fixed time $T_\nu \leq \frac{4}{k_3(2-\alpha_1)} + \frac{4}{k_4(\alpha_2-2)}$ for all initial conditions $\nu(0)$, where $\alpha_1 = 2 - \frac{p_1-2}{p_1-1}, \alpha_2 = 2 - \frac{p_2-2}{p_2-1}, k_3 = c_1 2^{\frac{2+3\alpha_1}{4}} \mu_g^{\frac{\alpha_1}{2}}$ and $k_4 = c_2 2^{\frac{2+3\alpha_2}{4}} \mu_g^{\frac{\alpha_2}{2}}$. □

Under the assumption of existence (Assumption 6.4) and uniqueness (guaranteed by Assumption 6.5) of the optimal point of (6.19) and using the fact that $-g(\nu)$ is α-strongly convex, one obtains that the minimizer of $L(x, \nu^\star)$ is the optimal solution of (6.19) [128, Section 5.5.5]. Using this, one obtains that

$$x^\star = \arg\min_{x \in \mathbb{R}^n} \; L(x, \nu^\star) \tag{6.26}$$

or, in other words, $x^\star$ satisfies $\nabla_x L(x^\star, \nu^\star) \triangleq \nabla f(x^\star) + \nu^{*T} A = 0$. Hence, the trajectories of the system

$$\dot{x} = \begin{cases} -d_1 \frac{\nabla_x L(x,\nu^\star)}{\|\nabla_x L(x,\nu^\star)\|^{\frac{q_1-2}{q_1-1}}} - d_2 \frac{\nabla_x L(x,\nu^\star)}{\|\nabla_x L(x,\nu^\star)\|^{\frac{q_2-2}{q_2-1}}}; & \nabla_x L(x,\nu^\star) \neq 0, \\ 0; & \nabla_x L(x,\nu^\star) = 0, \end{cases} \tag{6.27}$$

where $d_1, d_2 > 0$, $q_1 > 2$ and $1 < q_2 < 2$, converge to the optimizer of (6.19). The following result can now be stated.

Theorem 6.6 (FxTS of primal variable). *Let Assumptions 6.4 and 6.5 hold. Then, the optimal point $x^\star$ of (6.19) can be found in fixed time T_{eq} by first solving (6.24) for all $\nu(0) \in \mathbb{R}^m$, and then, solving (6.27) for all $x(0) \in \mathbb{R}^n$, with*

$$T_{eq} \leq \frac{4}{k_3(2-\alpha_1)} + \frac{4}{k_4(\alpha_2-2)} + \frac{4}{k_5(2-\alpha_3)} + \frac{4}{k_6(\alpha_4-2)},$$

where $\alpha_1, \alpha_2, k_3, k_4$ *are as defined in Lemma 6.7, and* $\alpha_3 = 2 - \frac{q_1-2}{q_1-1}, \alpha_4 = 2 - \frac{q_2-2}{q_2-1}, k_5 = d_1 2^{\frac{2+3\alpha_3}{4}} \mu_L^{\frac{\alpha_1}{2}}$ *and* $k_6 = d_2 2^{\frac{2+3\alpha_4}{4}} \mu_L^{\frac{\alpha_4}{2}}$

Proof. From Lemma 6.7, one obtains that the trajectories of (6.24) reach the optimizer $\nu^\star$ of (6.21) in fixed time $T_\nu \leq \frac{4}{k_3(2-\alpha_1)} + \frac{4}{k_4(\alpha_2-2)}$. Now, since $f(x)$ is strongly convex, it follows that $L(\cdot, \nu)$ is strongly convex for each $\nu \in \mathbb{R}^m$, and in particular, $L(\cdot, \nu^\star)$ is strongly convex, and hence, also satisfies PL inequality with $\mu_L > 0$. Furthermore, it can be easily shown that $L(\cdot, \nu^\star)$ satisfies Assumptions 6.1 and 6.2. Therefore, from Theorem 6.4, one has that there exists a fixed time T_x such that the trajectories of (6.27) reach the optimal point of (6.26) in $T_x \leq \frac{4}{k_5(2-\alpha_3)} + \frac{4}{k_6(\alpha_4-2)}$ for all initial conditions $x(0)$, where $\alpha_3 = 2 - \frac{q_1-2}{q_1-1}, \alpha_4 = 2 - \frac{q_2-2}{q_2-1}, k_5 = d_1 2^{\frac{2+3\alpha_3}{4}} \mu_L^{\frac{\alpha_1}{2}}$ and $k_6 = d_2 2^{\frac{2+3\alpha_4}{4}} \mu_L^{\frac{\alpha_4}{2}}$. Hence, one has that the optimal point of (6.19) can be obtained in fixed time $T_{eq} \leq T_x + T_\nu$, by first solving (6.24) and then, (6.27). □

A very important class of optimization problems in machine learning and model predictive control (MPC) is the class of QPs. In the following example, it is shown that QPs with equality constraints that satisfy Assumption 6.5 fit into the proposed framework.

Example 6.3. *Consider the following QP with equality constraints*

$$\begin{aligned} &\min_{x \in \mathbb{R}^n} \frac{1}{2} x^T Q x + c^T x, \\ &\text{s.t. } Ax = b, \end{aligned} \tag{6.28}$$

where $Q \in \mathbb{R}^{n \times n}$ *is positive definite and* $A \in \mathbb{R}^{m \times n}$ *has full row-rank. The function* $g(\nu)$ *for (6.28) is given as*

$$\begin{aligned} g(\nu) &= \inf_{x \in \mathbb{R}^n} \left(\frac{1}{2} x^T Q x + c^T x + \nu^T (Ax - b) \right) \\ &= -\nu^T b - \frac{1}{2} (c - A^T \nu)^T Q^{-1} (c - A^T \nu). \end{aligned}$$

Hence, one has that $f^*(-A^T \nu) = -\frac{1}{2}(c - A^T \nu)^T Q^{-1} (c - A^T \nu)$. *It can be readily verified that the functions* f, f^* *satisfy Assumption 6.5.*

6.2 Fixed-time stable saddle-point dynamics

6.2.1 Min-max problem

In this section, min-max problems are considered that can be formulated as saddle-point dynamics, and a modification is studied so that optimal point, which is a saddle-point, can be found within a fixed time. To this end, the general saddle-point problem of minimizing a function $F(x,z)$ over $x \in \mathbb{R}^n$ and maximizing over $z \in \mathbb{R}^m$ is considered, where $F : \mathbb{R}^n \times \mathbb{R}^m \to \mathbb{R}$. Formally, this can be stated as

$$\max_{z\in\mathbb{R}^m} \min_{x\in\mathbb{R}^n} F(x,z). \tag{6.29}$$

A point $(x^\star, z^\star)$ is called as *local saddle-point* of F (as well as local optimal solution of (6.29)), if there exist open neighborhoods $U_x \subset \mathbb{R}^n$ and $U_z \subset \mathbb{R}^m$ of $x^\star$ and $z^\star$, respectively, such that for all $(x,z) \in U_x \times U_z$, one has

$$F(x^\star, z) \leq F(x^\star, z^\star) \leq F(x, z^\star). \tag{6.30}$$

The point $(x^\star, z^\star)$ is *global saddle-point* if $U_x = \mathbb{R}^n$ and $U_z = \mathbb{R}^m$.

6.2.1.1 FxTS under strict convexity-concavity

The results in this section are presented under the following assumption.

Assumption 6.6 (Strict convexity-concavity). *A saddle point $(x^\star, z^\star)$ exists that solves (6.29). Furthermore, the function $F : \mathbb{R}^n \times \mathbb{R}^m \to \mathbb{R}$ is $\mathcal{C}^2$ and locally strictly convex-concave in an open neighborhood $U \subset \mathbb{R}^n \times \mathbb{R}^m$ of the saddle point $(x^\star, z^\star)$. More specifically, $\nabla_{xx} F(x,z) \succ 0$ and $\nabla_{zz} F(x,z) \prec 0$ for all $(x,z) \in U$.*

The local strong or strict convexity-concavity assumption is very commonly used in literature for showing asymptotic convergence of saddle-point dynamics to the optimal solution of (6.29) (see, e.g., [89, 158]). Using this, the following result can be stated.

Lemma 6.8 (Invertiblity of Hessian). *Let Assumption 6.6 hold for an open neighborhood $U \subset \mathbb{R}^n \times \mathbb{R}^m$ of the saddle-point $(x^\star, z^\star)$. Then, the Hessian of F given as*

$$\nabla^2 F(x,z) = \begin{bmatrix} \nabla_{xx} F(x,z) & \nabla_{xz} F(x,z) \\ \nabla_{zx} F(x,z) & \nabla_{zz} F(x,z) \end{bmatrix}, \tag{6.31}$$

is invertible for all $(x,z) \in U$.

Proof. Define $H_{xx} = \nabla_{xx}F$, $H_{xz} = \nabla_{xz}F$ and $H_{zz} = -\nabla_{zz}F$. Since F is twice-continuously differentiable, one has that $\nabla_{zx}F = (\nabla_{xz}F)^T$. Define $H = \nabla^2 F(x,z)$ so that $H = \begin{bmatrix} H_{xx} & H_{xz} \\ H_{xz}^T & -H_{zz} \end{bmatrix}$. Note that H_{xx} and H_{zz} are positive definite for all $(x,z) \in U$ due to Assumption 6.6. The rank of the matrix H satisfies ([159])

$$\operatorname{rank} H = \operatorname{rank} H_{xx} + \operatorname{rank}(-H_{zz} - H_{xz}^T H_{xx}^{-1} H_{xz}).$$

Now, since H_{xx} is invertible for all $(x,z) \in U$, one has that $\operatorname{rank} H_{xx} = n$. Let $H_1 = H_{xx}$ and $H_2 = -H_{zz} - H_{xz}^T H_{xx}^{-1} H_{xz}$. Since H_{xx}, H_{zz} are positive definite matrices, it follows that H_2 is also negative definite. Hence, one obtains that $\operatorname{rank} H_2 = m$. This implies that $\operatorname{rank} H = \operatorname{rank} H_1 + \operatorname{rank} H_2 = n + m$ for all $(x,z) \in U$, i.e., $\nabla^2 F(x,z)$ is full rank and hence, invertible for all $(x,z) \in U$. □

Authors in [89] use the following saddle-point (SP) dynamics

$$\dot{x} = -\nabla F_x(x,z), \quad \dot{z} = \nabla F_z(x,z). \tag{6.32}$$

and show asymptotic convergence to the saddle-point $(x^\star, z^\star)$ under Assumption 6.6. The flow in (6.32) is modified so that fixed-time convergence can be guaranteed. The FxTS Newton's method is used to define the FxTS-SP dynamics as

$$\begin{bmatrix} \dot{x} \\ \dot{z} \end{bmatrix} = \begin{cases} -(\nabla^2 F(x,z))^{-1} \left(c_1 \frac{\nabla F(x,z)}{\|\nabla F(x,z)\|^{\frac{p_1-2}{p_1-1}}} + c_2 \frac{\nabla F(x,z)}{\|\nabla F(x,z)\|^{\frac{p_2-2}{p_2-1}}} \right); & \nabla F(x,z) \neq 0, \\ 0; & \nabla F(x,z) = 0, \end{cases} \tag{6.33}$$

where $c_1, c_2 > 0$, $p_1 > 2, 1 < p_2 < 2$, and $\nabla F(x,z) \triangleq \begin{bmatrix} \nabla_x F(x,z)^T & \nabla_z F(x,z)^T \end{bmatrix}^T$. Note that per Lemma 6.4, the point (x,z) is an equilibrium point of (6.33) if and only if it satisfies $\nabla F(x,z) = 0$. Using strict convexity-concavity of F in U, one obtains that $\nabla F(x,z) = 0$ implies $x = x^\star$ and $z = z^\star$. The first main result of this section is presented below.

Theorem 6.7 (FxTS under strict convexity-concavity). *If F satisfies Assumption 6.6 for $U \subset \mathbb{R}^n \times \mathbb{R}^m$, then the trajectories of (6.33) converge to the saddle point $(x^\star, z^\star)$ in fixed time T_{SP} for all $(x(0), z(0)) \in D \subset U$ where D is the largest compact sub-level set of $V(x,z) = \frac{1}{2}\|\nabla F(x,z)\|^2$ in U and*

$$T_{SP} \leq \frac{2^{1-\frac{\alpha_1}{2}}}{c_1(2-\alpha_1)} + \frac{2^{1-\frac{\alpha_2}{2}}}{c_2(\alpha_2-2)}, \tag{6.34}$$

where $\alpha_1 = 2 - \frac{p_1-2}{p_1-1}$ *and* $\alpha_2 = 2 - \frac{p_2-2}{p_2-1}$. *Furthermore, if* $U = \mathbb{R}^n \times \mathbb{R}^m$, *then the results holds for all* $(x(0), z(0)) \in \mathbb{R}^n \times \mathbb{R}^m$.

Proof. Consider the candidate Lyapunov function $V(x,z) = \frac{1}{2}\|\nabla F(x,z)\|^2$. Define D as the largest compact sub-level set of V. Using analysis similar to the proof of Theorem 6.5, the time derivative of V along the trajectories of (6.33) can be bounded as

$$\dot{V}(x,z) \leq -c_1 2^{\frac{\alpha_1}{2}} V(x,z)^{\frac{\alpha_1}{2}} - c_2 2^{\frac{\alpha_2}{2}} V(x,z)^{\frac{\alpha_2}{2}},$$

where $\alpha_1 = 2 - \frac{p_1-2}{p_1-1}$ and $\alpha_2 = 2 - \frac{p_2-2}{p_2-1}$. It follows that for all $t \geq T_{SP}$, $\nabla F(x(t), z(t)) = 0$, or equivalently, $(x(t), z(t)) = (x^\star, z^\star)$ for all $(x(0), z(0)) \in D$, where $T_{SP} \leq \frac{2^{1-\frac{\alpha_1}{2}}}{c_1(2-\alpha_1)} + \frac{2^{1-\frac{\alpha_2}{2}}}{c_2(\alpha_2-2)}$.

For the case when $U = \mathbb{R}^n \times \mathbb{R}^m$, the sub-level sets of $\|\nabla F\|$ are bounded and therefore, V is radially unbounded. Therefore, the trajectories of (6.33) converge to the saddle-point of (6.29) for all $(x(0), z(0)) \in \mathbb{R}^n \times \mathbb{R}^m$. □

Assumption 6.6 ensures that the Hessian $\nabla^2 F(x,z)$ is invertible for all $(x,z) \in U$ and that the saddle-point of F is the only critical point. Per the analysis in Lemma 6.8, a sufficient condition for the Hessian to be invertible is that $\nabla_{xx} F$ is invertible and $\nabla_{zx} F$ is full row-rank. Based on this observation, the following result can be stated.

Corollary 6.1. *Suppose there exists an open set* $U \subset \mathbb{R}^n \times \mathbb{R}^m$ *such that* $\nabla_{xx} F(x,z)$ *is invertible and* $\nabla_{zx} F(x,z)$ *is full row-rank for all* $(x,z) \in U$. *Then, the trajectories of* (6.33) *converge to the set of the critical points of* F, *defined as* $\Omega_U = \{(x,z) \in U \mid \nabla F(x,z) = 0\}$ *in a fixed time* T_{SP} *for all* $(x(0), z(0)) \in D \subset U$, *where* D *is the largest compact sub-level set of* $V(x,z) = \frac{1}{2}\|\nabla F(x,z)\|^2$ *in* U.

Note that Corollary 6.1 does not require strict convexity-concavity of F. Also, if the set Ω_U contains only the SP, i.e., the only critical point of the function F in Ω_U is the SP, then Corollary 6.1 guarantees local convergence of trajectories of (6.33) to the SP in fixed time.

6.2.1.2 FxTS under strong convexity-concavity

The modified saddle-point dynamics in (6.33) requires the computation of the inverse of the Hessian matrix $\nabla^2 F(x,z)$, which can be computationally expensive for problems with large n, m. In this section, a first-order scheme, i.e., a method only requiring the gradient of the function F, is proposed under a stronger assumption on the function F.

Assumption 6.7 (**Strong convexity-concavity**). *A saddle point $(x^\star, z^\star)$ exists that solves (6.29) and $F : \mathbb{R}^n \times \mathbb{R}^m \to \mathbb{R}$ is $\mathcal{C}^2$ and locally strongly convex-concave on open neighborhood $U \subset \mathbb{R}^n \times \mathbb{R}^m$ of the saddle point $(x^\star, z^\star)$, i.e., there exist $k_x, k_z > 0$ such that $\nabla_{xx} F(x,z) \succeq k_x I$ and $\nabla_{zz} F(x,z) \preceq -k_z I$ for all $(x,z) \in U$.*

Consider the following FxTS-GF based modified SP dynamics

$$\begin{bmatrix} \dot{x} \\ \dot{z} \end{bmatrix} = \begin{cases} -c_1 \frac{\tilde{\nabla} F(x,z)}{\|\nabla F(x,z)\|^{\frac{p_1-2}{p_1-1}}} - c_2 \frac{\tilde{\nabla} F(x,z)}{\|\nabla F(x,z)\|^{\frac{p_2-2}{p_2-1}}}; & \nabla F(x,z) \neq 0, \\ 0; & \nabla F(x,z) = 0, \end{cases} \tag{6.35}$$

where $c_1, c_2 > 0$, $p_1 > 2, 1 < p_2 < 2$, $\tilde{\nabla} F(x,z) \triangleq \begin{bmatrix} \nabla_x F(x,z)^T & -\nabla_z F(x,z)^T \end{bmatrix}^T$. Note that (6.32) is a special case of (6.35) with $c_1 = 1, c_2 = 0$ and $p_1 = 2$. The following result can be readily stated for (6.35).

Theorem 6.8 (**FxTS under strong convexity-concavity**). *Suppose the function F satisfies Assumption 6.7. Then, the trajectories of (6.35) converge to the SP in a fixed time T_{SP2} for all $(x(0), z(0)) \in U$ such that*

$$T_{SP2} \leq \frac{2}{k_7(2-\alpha_7)} + \frac{2}{k_8(\alpha_8 - 2)}, \tag{6.36}$$

where $k_7 = c_1 k\, 2^{\frac{\alpha_7}{2}}, k_8 = c_2 k\, 2^{\frac{\alpha_8}{2}}$, $\alpha_7 = 2 - \frac{p_1-2}{p_1-1}$ and $\alpha_8 = 2 - \frac{p_2-2}{p_2-1}$, with $k = \min\{k_x, k_z\}$. Furthermore, if $U = \mathbb{R}^n \times \mathbb{R}^n$, then the result holds for all $(x(0), z(0)) \in \mathbb{R}^n \times \mathbb{R}^m$.

Proof. Choose the candidate Lyapunov function as $V(x,z) = \frac{1}{2}\|\nabla F(x,z)\|^2$. The time derivative of V along the trajectories of (6.35) reads

$$\begin{aligned} \dot{V} &= \nabla_x F^T \nabla_{xx} F \dot{x} + \nabla_x F^T \nabla_{xz} F \dot{z} + \nabla_z F^T \nabla_{zx} F \dot{x} + \nabla_z F^T \nabla_{zz} F \dot{z} \\ &\overset{(6.35)}{=} \nabla_x F^T \nabla_{xx} F \dot{x} + \nabla_z F^T \nabla_{zz} F \dot{z} \\ &= -\nabla_x F^T \nabla_{xx} F \left(c_1 \frac{\nabla F_x}{\|\nabla F\|^{\frac{p_1-2}{p_1-1}}} + c_2 \frac{\nabla F_x}{\|\nabla F\|^{\frac{p_2-2}{p_2-1}}} \right) \\ &\quad + \nabla_z F^T \nabla_{zz} F \left(c_1 \frac{\nabla F_z}{\|\nabla F\|^{\frac{p_1-2}{p_1-1}}} + c_2 \frac{\nabla F_z}{\|\nabla F\|^{\frac{p_2-2}{p_2-1}}} \right). \end{aligned} \tag{6.37}$$

Now, using the strong convexity-concavity of F, one obtains

$$\begin{aligned}\dot{V} &\leq -c_1 k_x \frac{\|\nabla_x F\|^2}{\|\nabla F\|^{\frac{p_1-2}{p_1-1}}} - c_2 k_x \frac{\|\nabla_x F\|^2}{\|\nabla F\|^{\frac{p_1-2}{p_1-1}}} - c_1 k_z \frac{\|\nabla_z F\|^2}{\|\nabla F\|^{\frac{p_1-2}{p_1-1}}} - c_2 k_z \frac{\|\nabla_z F\|^2}{\|\nabla F\|^{\frac{p_1-2}{p_1-1}}} \\ &\leq -c_1 k \frac{\|\nabla F\|^2}{\|\nabla F\|^{\frac{p_1-2}{p_1-1}}} - c_2 k \frac{\|\nabla F\|^2}{\|\nabla F\|^{\frac{p_1-2}{p_1-1}}} = -k_7 V^{\frac{\alpha_7}{2}} - k_8 V^{\frac{\alpha_8}{2}},\end{aligned}$$

where $k_7 = c_1 k 2^{\frac{\alpha_7}{2}}$, $k_8 = c_2 k 2^{\frac{\alpha_8}{2}}$, $0 < \alpha_7 = 2 - \frac{p_1-2}{p_1-1} < 2$ and $\alpha_8 = 2 - \frac{p_2-2}{p_2-1} > 2$, where $k = \min\{k_x, k_z\}$. Hence, using Theorem 6.1, one obtains that the optimal point of (6.29) can be found in fixed time T_{SP2} satisfying $T_{SP2} \leq \frac{2}{k_7(2-\alpha_7)} + \frac{2}{k_8(\alpha_8-2)}$. Furthermore, the norm of the gradient $\|\nabla F\|$ is radially unbounded on U, and hence, for $U = \mathbb{R}^n \times \mathbb{R}^m$, the result holds globally for all $(x(0), z(0)) \in \mathbb{R}^n \times \mathbb{R}^m$. □

6.2.2 Connections with constrained optimization

The constrained optimization problem in (6.19) can be equivalently posed as a min-max problem via the Lagrangian L given in (6.22). Thus, the modified saddle-point dynamics in (6.33) can be used to solve the constrained optimization of the form (6.19) under certain conditions, as discussed in the remark below.

Remark 6.6. *For problem (6.19) with strictly convex f and full row-rank matrix A, the conditions of Corollary 6.1 are satisfied. Furthermore, it is known that for this problem, the KKT conditions are also sufficient for optimality, i.e., the critical point $(\bar{x}, \bar{z})$ such that $\nabla F(\bar{x}, \bar{z}) \triangleq \begin{bmatrix} \nabla f(\bar{x}) + A^T \bar{z} \\ A\bar{x} - b \end{bmatrix} = 0$ is also the optimal point, i.e., $(x^\star, z^\star) = (\bar{x}, \bar{z})$. Hence, one can use (6.33) with $F(x, z) = L(x, z)$ for the problems of the form (6.19), in the case when the conjugate function f^* is not known in the closed-form.*

This is formally shown in the following result.

Corollary 6.2. *Consider the optimization problem (6.19). Assume that Assumption 6.4 holds and that $f : \mathbb{R}^n \to \mathbb{R}$ is $\mathcal{C}^2$ and strictly convex, and the Hessian $\nabla^2 f$ is invertible. Then, with $F(x, z) = f(x) + z^T(Ax - b)$, the trajectories of (6.33) reach the saddle-point $(x^\star, z^\star)$, where $x^\star$ is the solution of (6.19), in fixed time T_{eq2} for all $(x(0), z(0)) \in D \subset U$, where D is the largest compact sub-level set of $V(x, z) = \frac{1}{2}\|\nabla F(x, z)\|^2$ in U, and*

$$T_{eq2} \leq \frac{2^{1-\frac{\alpha_1}{2}}}{c_1(2-\alpha_1)} + \frac{2^{1-\frac{\alpha_2}{2}}}{c_2(\alpha_2-2)}, \tag{6.38}$$

where where $\alpha_1 = 2 - \frac{p_1-2}{p_1-1}$ and $\alpha_2 = 2 - \frac{p_2-2}{p_2-1}$.

Proof. Define $F(x,z) = f(x) + z^T(Ax-b)$. Note that for strictly convex f, $\nabla_{xx}F = \nabla^2 f(x)$ is invertible. Furthermore, $\nabla_{zx}F = A$ is full row-rank, which implies that the conditions of Corollary 6.1 are satisfied. Hence, the trajectories of (6.33) reach the set of points (x,z) such that $\nabla F(x,z) = 0$. Hence, one obtains that the trajectories of (6.33) for $F(x,z) = f(x) + z^T(Ax-b)$ reach the optimal point of (6.19) in fixed time $T_{eq2} \leq \frac{2^{1-\frac{\alpha_1}{2}}}{c_1(2-\alpha_1)} + \frac{2^{1-\frac{\alpha_2}{2}}}{c_2(\alpha_2-2)}$ where $\alpha_1 = 2 - \frac{p_1-2}{p_1-1}$ and $\alpha_2 = 2 - \frac{p_2-2}{p_2-1}$. □

In summary, (6.33) can be used to solve constrained optimization problems of the form (6.19) as well as min-max problems of the form (6.29), and the optimal solutions can be obtained within a fixed time. Compared to [89, 158], where asymptotic convergence is studied for min-max problems of the form (6.29), and (6.19) posed as saddle-point problem, the proposed method guarantees convergence within a fixed time under relaxed assumptions.

6.3 Simulations

The efficacy of the proposed methods is illustrated via three numerical examples. The computations are done using MATLAB R2018a on a desktop with 32GB DDR3 RAM and an Intel Xeon E3-1245 processor (3.4 GHz). Unless mentioned otherwise, Euler discretization is used for MATLAB implementation with time-step $dt = 10^{-5}$, and with constant step-size, the convergence time T in seconds translates to $T \times 10^5$ iterations. In the first example, an instance of QP with equality constraints is considered as a constrained convex optimization problem (6.19). The FxTS saddle-point dynamics in (6.33) is used to find the optimal point of the problem, and to illustrate that for all initial conditions, the optimal point can be found within a fixed time. Then, an instance of the min-max problem (6.29) is considered, and the FxTS saddle-point dynamics in (6.33) is used to find the saddle-point.

6.3.1 Example 1: quadratic program with equality constraints

Consider (6.28) with $x \in \mathbb{R}^{10}$ and $A \in \mathbb{R}^{5\times 10}$. For simplicity, consider a diagonal matrix Q with positive diagonal elements and a full row-rank matrix A, so that all the conditions of Corollary 6.2 are satisfied. The values of Q, A, b, c are chosen through random matrix generator in MATLAB. The following parameters are used for FxTS-SP dynamics in (6.33): $c_1 = 10,\ c_2 = 10,\ p_1 = 2.2,\ p_2 = 1.8$. With these parameters, the upper bound on the time of convergence in Corollary 6.2 satisfies $T_{eq2} = T_{SP} \leq 1.0025$.

Figure 6.1 compares the performance of the proposed method relative to Newton's method for saddle-point dynamics, i.e., (6.33) with $c_2 = 0$ and $p_2 = 2$. The dotted lines illustrate the evolution of Newton's method, while solid lines illustrate that of FxTS-SP dynamics (6.33).

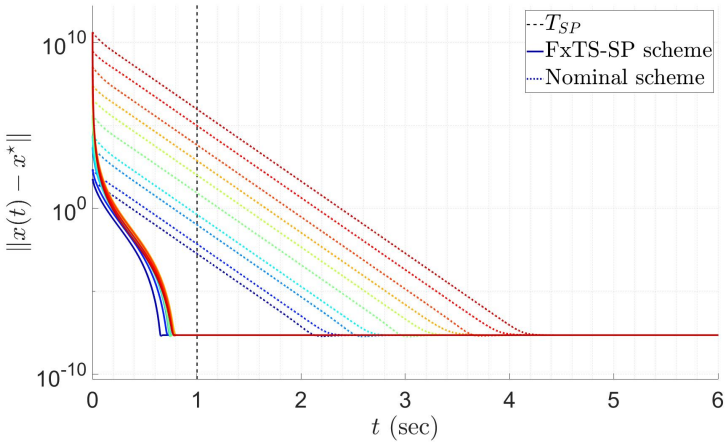

Figure 6.1: The norm $\|x(t) - x^\star\|$ with time for various initial conditions for nominal saddle-point dynamics ($p_1 = 2, c_2 = 0$) and FxTS saddle-point dynamics ($p_1 = 2.2, p_2 = 1.8$).

The vertical black dashed black line corresponds to $T_{SP} = 1.0025$ sec. Figure 6.1 shows the variation of $\|x(t) - x^\star\|$ with time for various initial conditions. The proposed scheme converges to the error of magnitude less than 10^{-8} within T_{SP} sec, while the nominal scheme takes a longer time (and thus, more number of iterations) to achieve the same. It can also be seen that the convergence time is always bounded by T_{SP} for all initial conditions for the proposed method.

6.3.2 Example 2: min-max problem

A numerical example for the min-max problem $\max_z \min_x F(x, z)$ is considered, where the function F is defined as:

$$F(x, z) = (\|x\| - 1)^4 - \|z\|^2\|x\|^2, \tag{6.39}$$

with $x \in \mathbb{R}^n$ and $z \in \mathbb{R}^m$. The dimensions are chosen as $n = 3$ and $m = 1$. The set of optimal points (x, z) satisfy $\|x\| = 1, \|z\| = 0$ [89], i.e., the optimal point is not unique in this case. The parameters c_1, c_2 are chosen as $c_1 = c_2 = 10$.

The first case study considers a varying range of initial conditions $(x(0), z(0))$ and constant values of the parameters p_1, p_2, chosen as $p_1 = 2.2$ and $p_2 = 1.8$. Figure 6.2 shows the convergence time (up to an error of $\|\nabla F(x, z)\| \leq 10^{-15}$) for various initial conditions $x(0), z(0)$. The results illustrate that the time of convergence does not depend upon the initial distance from the saddle point. Also, the actual time of convergence T_c is

lower than the upper bound T_{SP}.

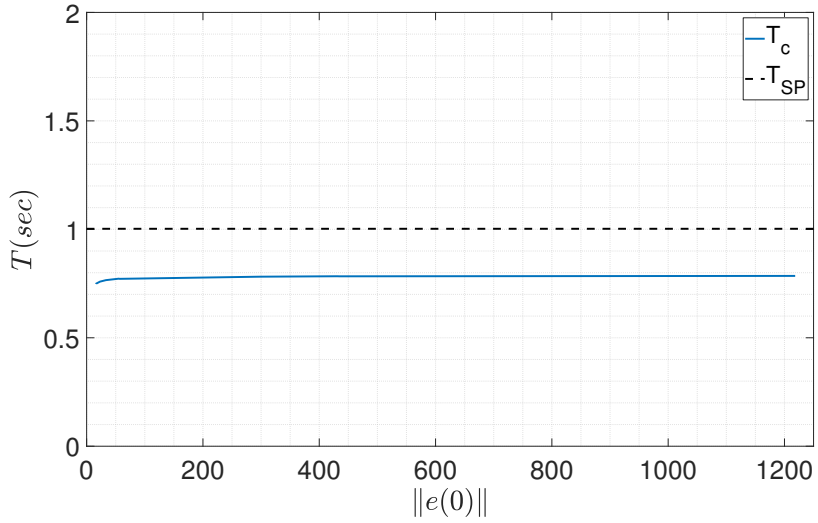

Figure 6.2: Time of convergence T_c with norm of the initial error $\|e(0)\| \triangleq \|[(x(0) - x^\star)^T \ (z(0) - z^\star)^T]^T\|$.

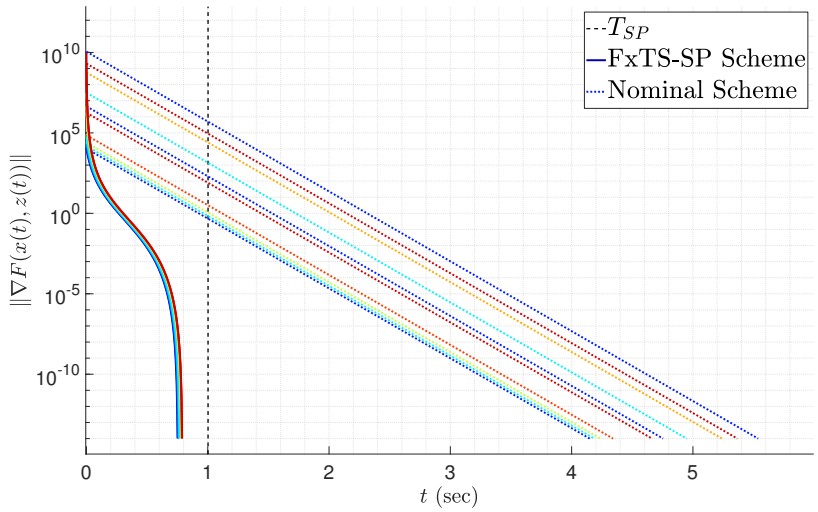

Figure 6.3: The norm of the gradient, $\|\nabla F(x(t), z(t))\|$, with time for various initial conditions for nominal saddle-point dynamics ($p_1 = 2, c_2 = 0$) and FxTS saddle-point dynamics ($p_1 = 2.2, p_2 = 1.8$).

Figure 6.3 illustrates the convergence of norm of the gradient, $\|\nabla F(x, z)\|$, to zero in fixed time for various initial conditions. Figure 6.4 and 6.5 plot the norm of the error $x - x^\star$ and $z - z^\star$, respectively, for various initial conditions. Solid lines show the performance of the proposed method (6.33), and dotted lines show the performance of Newton's method ($c_2 = 0, p_2 = 2$) when solving for saddle-point dynamics.

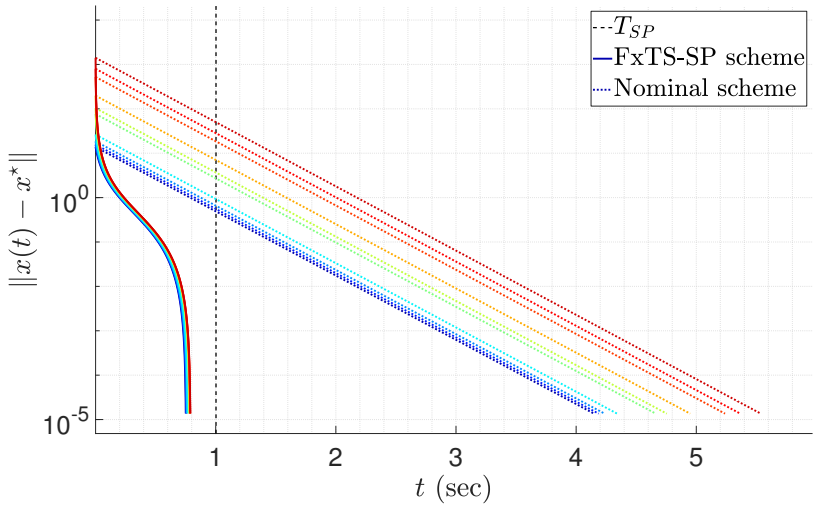

Figure 6.4: The norm $\|x - x^\star\|$ with time for various initial conditions for nominal saddle-point dynamics ($p_1 = 2, c_2 = 0$) and FxTS saddle-point dynamics ($p_1 = 2.2, p_2 = 1.8$).

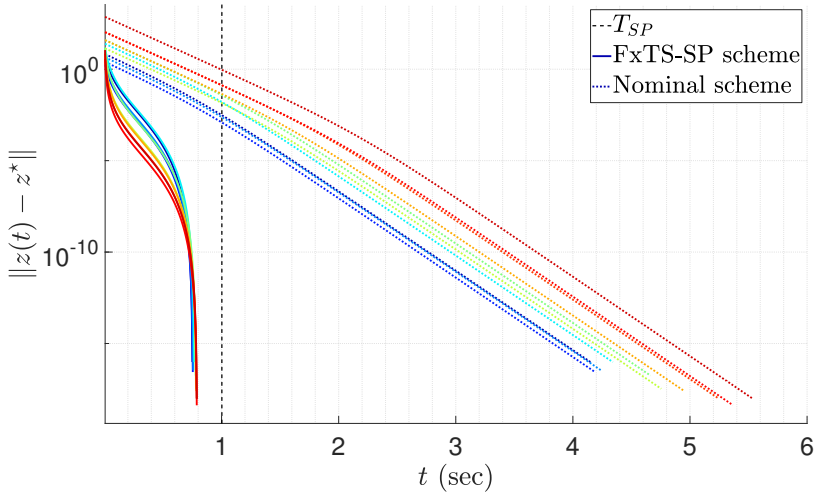

Figure 6.5: The norm $\|z - z^\star\|$ with time for various initial conditions for nominal saddle-point dynamics ($p_1 = 2, c_2 = 0$) and FxTS saddle-point dynamics ($p_1 = 2.2, p_2 = 1.8$).

The second case study considers that the parameters p_1, p_2 are varied in the ranges $[2,\ 2.2]$ and $[1.8,\ 2]$, respectively. Figure 6.6 shows the norm of the gradient, $\|\nabla F(x, z)\|$, with time. As can be seen in the Figure 6.6, the case when $p_1 = p_2 = 2$ has linear convergence (straight line on the $\log$ plot), while for $p_1 > 2$ and $p_2 < 2$, the convergence is super-linear. It can also be observed that as p_1 increases and p_2 decreases, the convergence becomes faster and the time of convergence becomes smaller.

The implementation of the proposed method in numerical studies is done using Euler integration with constant step size. Figure 6.7 shows the performance of the proposed

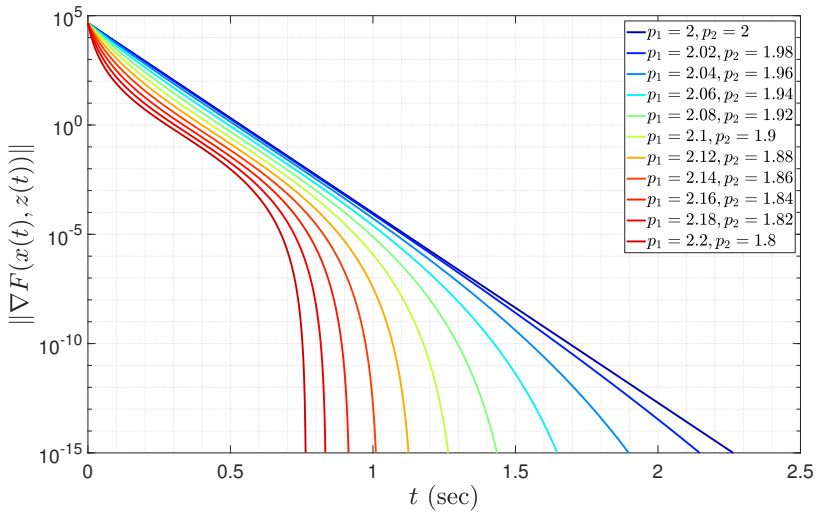

Figure 6.6: The norm of the gradient, $\|\nabla F(x(t), z(t))\|$, with time for various p_1, p_2.

method for various values of discretization steps between 10^{-2} and 10^{-6}. As the figure suggests, the discretization step does not affect the convergence performance of the proposed method.

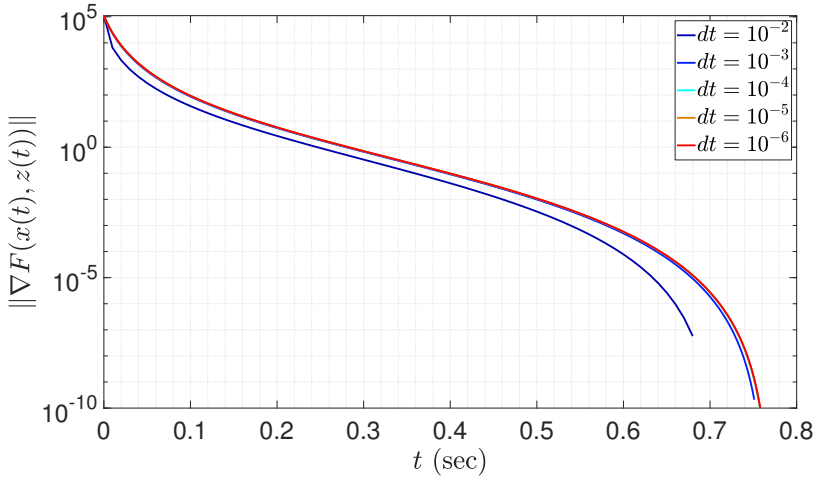

Figure 6.7: The norm of the gradient, $\|\nabla F(x(t), z(t))\|$, with time for various dt.

Finally, the performance of the proposed method is compared with the performance of the rescaled-GF (6.5). More specifically, the considered rescaled-GF scheme is

$$\begin{bmatrix} \dot{x} \\ \dot{z} \end{bmatrix} = \begin{cases} -c_1 \left(\nabla^2 F(x,z)\right)^{-1} \frac{\nabla F(x,z)}{\|\nabla F(x,z)\|^{\frac{p_1-2}{p_1-1}}}; & \nabla F(x,z) \neq 0, \\ 0; & \nabla F(x,z) = 0. \end{cases} . \tag{6.40}$$

where $0 < \theta < 1$. Since the objective function in (6.39) is only strictly convex-concave and

not strongly convex-concave, (6.35) cannot be used, but (6.33) can be used. The dynamical system (6.40) is a Newton's modification of rescaled-GF (6.5) discussed in [10], where Hessian is used so that (6.40) can be used for a strictly convex-concave function.

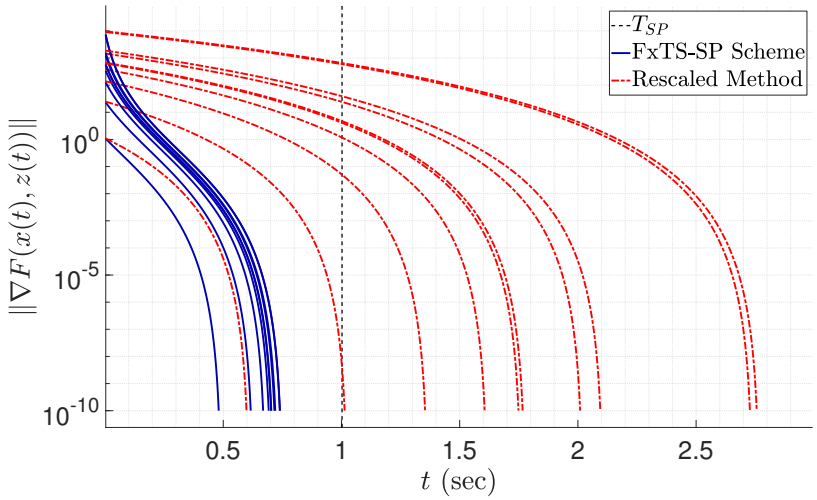

Figure 6.8: The norm of gradient, $\|\nabla F(x(t), z(t))\|$, with time for various initial conditions for the proposed scheme and the rescaled gradient flow scheme.

Figure 6.8 plots the norm of the gradient for various initial conditions, where $p_1 = 2.2, p_2 = 1.8$, $c_1 = c_2 = 10$ for (6.33), $p_1 = 2.2$, $c_1 = 10$ for (6.40). It can be seen that the convergence of the rescaled gradient flow scheme (6.40) is super-linear (finite-time convergence), but slower than the proposed scheme. It is evident from Figure 6.8 that the time of convergence for (6.40) grows as $\|x(0) - x^\star\|$ increases, while that of the proposed scheme (6.33) remains bounded.

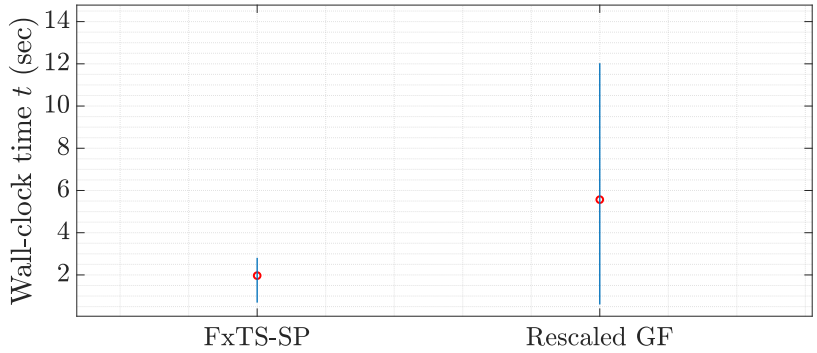

Figure 6.9: The wall-clock time for 1000 trials for the proposed scheme, rescaled gradient flow based scheme.

Figure 6.9 depicts the wall-clock time (i.e., actual run-time) for the two aforementioned schemes. The results are presented for 1000 trials, where the simulations are run until the

norm of the gradient, $\|\nabla F(x(t), z(t))\|$, drops below 10^{-10}. The red dot represents the mean value for the 1000 trials while the vertical lines represent the minimum and maximum values of the respective schemes. It is clear from the figures the proposed scheme takes a smaller computation time than the accelerated scheme while giving a better convergence rate. Note that the wall-clock time, which corresponds to the actual computational time, is different from the convergence time T_{SP}, which, in the discrete setting, corresponds to the number of steps required for the convergence per the relation $N = T_{SP} \times 10^5$. It is evident that the proposed method performs better than the nominal Newton's method, both in terms of the number of iterations required for converging to a small neighborhood of the optimal solution and wall-clock time.

6.4 Discussion

While optimization methods in continuous-time are important and have major theoretical relevance in general, discrete-time algorithms are of more practical use. It is an open question as to how one can discretize the dynamics (6.8) and other schemes presented in this work so that the fixed-time convergence guarantees are provably preserved. While in all the numerical examples the performance of the discretized implementation is at par with the theoretical results, i.e., the convergence is super-linear and the time of convergence is upper bounded by the theoretically established upper bound, the theoretical investigation on how the convergence properties are preserved after discretization is an open problem, and an active field of research (see [12, 13]).

In [12], the authors study a particular class of homogeneous systems and show that there exists a *consistent* discretization scheme that preserves the finite-time convergence. They extend their results to *practically* FxTS systems in [13], where they show that the trajectories of the discretized system reach an arbitrarily small neighborhood of the equilibrium point in a fixed time, independent of the initial condition. Given that the provided numerical examples suggest that the proposed method works efficiently even with constant-step Euler integration, the questions that naturally arise are: (i) how could the theory of consistent discretization be extended to a more general class of FTS and FxTS systems, and (ii) how this theory could be used for the methods developed in this dissertation so that exact convergence of iterative discrete-time optimization schemes for the proposed methods can be guaranteed in a finite or fixed number of steps. These topics are beyond the scope of the current work and are left open for future research.

6.5 Conclusions

This chapter presented modified GF schemes that provide convergence of the solution to the optimal point in a fixed time, under various assumptions such as strict convexity and gradient dominance, which is a relaxation of strong convexity. A modified scheme for the saddle-point dynamics is proposed so that the min-max problem can be solved in a fixed time. Though all the methods are presented for continuous-time optimization, numerical examples illustrate that the proposed schemes have super-linear convergence in the discretized implementation as well, that the time of convergence satisfies the theoretical bound, and that the performance of the proposed method is better than the one of commonly used algorithms, such as Newton's method and the rescaled gradient-based method.

CHAPTER 7

Conclusions and Future Work

7.1 Conclusions

In conclusion, this dissertation advances the theory of finite- and fixed-time stability and explores their applications in the field of robust control design and convex optimization problems.

Chapter 2 studied the problem of distributed control design for agents modeled via double-integrator dynamics moving in an environment consisting of wind disturbances and dynamic obstacles. An FTS controller that uses feedback derived from an FTS observer is designed in a distributed manner with guarantees on provable inter-agent safety, collision avoidance with dynamic obstacles, and finite-time convergence to their respective goal locations. Chapter 3 presented two new results on FxTS by introducing a new term in the Lyapunov conditions and discussed how the newly introduced term explains the relationship between time of convergence, the domain of attraction, and input constraints. The new FxTS results also characterize robustness against a class of disturbances. In particular, it is shown that under the effect of additive, vanishing disturbances, fixed-time convergence is preserved and that under the effect of additive non-vanishing disturbances, there exists a neighborhood of the equilibrium point which is FxTS. Utilizing the new Lyapunov conditions, Chapter 4 introduced the notion of FxT-CLF and presented a combination of FxT-CLF and CBF in a QP formulation with guaranteed feasibility to compute a control input that solves a multi-task problem under input constraints. Continuity of the solution of the proposed QP is discussed so that the resulting closed-loop dynamics are well-defined. A robust control synthesis framework is also presented using the notions of robust FxT-CLFs and robust CBFs in a QP under input constraints.

Chapter 5 studied FTS of a class of hybrid and switched systems via multiple Lyapunov functions. A finite-time stabilizing switching law is designed, and an FTS output-feedback based on an FTS observer is developed for a class of switched linear systems when only one

of the modes is both observable and controllable, demonstrating that the proposed method can incorporate unstable modes. Finally, exploring the applications of FxTS, Chapter 6 proposed FxTS gradient flows to solve convex optimization problems within a fixed time. Numerical case studies show that the proposed methods have super-linear convergence when implemented using a simple Euler discretization scheme.

7.2 Future work

7.2.1 Multi-agent control

An important issue in multi-agent control which is still largely an open problem is deadlock resolution/mitigation. The problem of deadlock occurs in a multi-agent scenario when the relative geometry of the agents and their respective goal locations induce local minima, away from their desired equilibrium points. Thus, a deadlock can be thought of as an *undesirable* equilibrium point. Deadlock mitigation is explored by excluding a set with Lebesgue-measure zero when choosing the initial conditions in [160, 161], and deadlock resolution is addressed by choosing an appropriate direction of motion for each agent in [107]. More recently, the authors in [138] study the problem of deadlock mitigation when the control input is defined as the solution to an optimization problem. They characterize various types of deadlocks depending upon the value of the slack variables in the optimization problem and discuss methods of resolving certain deadlock scenarios. Very recently, the authors in [162] show that a QP formulation consisting of CLF and CBF can induce undesirable equilibrium points, and discuss ways to mitigate such scenarios by reshaping the CLF. The author would like to study similar ideas, and explore other approaches, in a multi-agent setting so that deadlock can be mitigated by appropriately choosing the initial conditions, and for the case when it is not possible to choose the initial conditions arbitrarily, then deadlocks can be resolved effectively.

7.2.2 Forward invariance

One of the biggest assumptions used in the safe control design using CBFs is the knowledge of a *viability* domain, a set that can be made forward invariant (see Assumption 4.2). One way of computing such a viability domain is by computing the backward reachability set of the underlying dynamical system [163]. Various tools have been developed for the computation of the exact reachable sets (see [164, 165]), which tend to be computationally heavy, or an *overapproximation* of the reachability set (see [166–168]), however, they

tend to be very conservative. More recently, learning-based methods have attracted much attention in computing either the CBF (or, equivalently, the safe set) [169, 170] or a safe controller [171]. The author would like to study the utility of the proposed QP framework in the development of online learning tools that can compute the viability domain while maintaining safety.

7.2.3 Discretization of FxTS dynamical systems

One of the future research directions is to investigate discretization schemes for FTS and FxTS systems that can preserve the time of convergence, and translate FTS and FxTS to convergence in a finite and fixed number of steps, respectively. Recent articles [11, 172] show that if FTS dynamical systems are discretized using common discretization schemes such as Euler discretization or Runge-Kutta discretization with a *small enough* discretization step, then the discretized trajectories remain *close enough* to the continuous trajectories, hence, showing convergence to an arbitrarily small neighborhood of the optimal point in a finite number of steps. These works use the ideas from the notion of hybrid systems simulators as defined in [173] to show that the trajectories of the continuous-time gradient flow system and that of the discretized dynamics can be made to remain arbitrarily close and utilize the theory of FTS to show that the trajectories of the discretized dynamics converge to an arbitrarily small neighborhood of the equilibrium point within a finite number of steps. The author would like to explore this idea for FxTS gradient flows in particular, and dynamical systems exhibiting FxTS in general so that similar results showing the convergence of the trajectories of the underlying discretized dynamics to an arbitrarily small neighborhood of the respective equilibrium point within *fixed* number of steps can be obtained.

On similar lines, as discussed in Discussion 4.5, it is important to study practical control design techniques such as zero-order hold control or sampled-data control, using QPs so that they are implementable on real-world systems. This motivates the future work of studying control design for discretized continuous-time dynamical system via a zero-order hold controller so that 1) the safety guarantees in continuous time can be replicated in practice through the zero-order hold controller, and 2) theoretical guarantees of FxT convergence can translate to a fixed number of steps convergence.

7.3 Additional related work

In addition to the main work presented in this dissertation, the author has worked on multi-agent control design for constrained dynamical systems modeled via unicycle dynamics to model the motion of fixed-wing aircraft in [160, 161, 174]. The work in [160] is done in collaboration with Dr. Dongkun Han and presents a robust distributed coordination protocol that achieves the generation of collision-free trajectories for multiple unicycle agents in the presence of stochastic uncertainties. Building upon [160], the work in [161] considers time-varying disturbances and uncertainties to model wind disturbance that can vary both in space and time. In [174], a novel hybrid control protocol for de-conflicting multiple vehicles with constraints on control inputs is proposed. Turning rate and linear speed constraints are considered to represent fixed-wing or car-like vehicles. A set of state-feedback controllers along with a state-dependent switching logic are synthesized in a hybrid system to generate collision-free trajectories that converge to the desired destinations.

Another approach of driving closed-loop trajectories to a goal set within a user-defined time is explored in [175] in collaboration with Dr. Ehsan Arabi, where a time-transformation technique is used for a prescribed-time convergence guarantee, and closed-form controllers are designed using a form that is inspired by Sontag's formula. More recently, relaxing the requirement of continuity of the closed-loop dynamics, the author has done preliminary work in exploring the notion of strong invariance using tools from the nonsmooth analysis in [134] in collaboration with James Usevitch. Sufficient conditions under which the optimization problem is feasible are presented and it is shown that all feasible solutions of the considered optimization problem which is measurable render the multiple safe sets forward invariant.

The author, in collaboration with Dr. Mayank Baranwal, extended the results on FxTS in continuous-time optimization for the problem of distributed optimization in [176], economic dispatch in [177] and sparse recovery (SR) in [178]. The work in [176] presents a novel distributed nonlinear protocol for minimizing the sum of convex objective functions in a fixed time under time-varying communication topology. In a distributed setting, each node in the network has access only to its private objective function, while the exchange of local information, such as state and gradient values, is permitted between the immediate neighbors. The work in [177] proposes a fixed-time convergent, fully distributed economic dispatch algorithm for scheduling optimal power generation among a set of distributed energy resources. The proposed algorithm incorporates both load balance and generation capacity constraints. Finally, [178] develops a novel Continuous-time Accelerated Proximal Point Algorithm (CAPPA) for ℓ_1-minimization problems with provable fixed-time conver-

gence guarantees. CAPPA betters the state-of-the-art methods such as Locally Competitive Algorithm (LCA) and finite-time LCA (recently developed continuous-time dynamical systems for solving SR problems) by exhibiting provable fixed-time convergence to the optimal solution. Consequently, CAPPA is better suited for the fast and efficient handling of SR problems.

Finally, the author would like to mention their most recent work on the topic of QP based control synthesis. One of the drawbacks of using *myopic* QP based approach for control synthesis, as argued in [179], is that they are susceptible to infeasibility, i.e., there is no guarantee that the underlying QP will remain feasible for all future times. To circumvent this issue, combining a high-level planner with a low-level controller has become a popular approach [180]. The author explored such a multi-rate control framework in [181] in collaboration with Ryan K. Cosner, Dr. Ugo Rosoliya, and Dr. Aaron D. Ames, where the notion of periodic safety is studied, requiring the system to evolve in a safe set at all times and visit a subset of this safe set periodically. For high-level planning, a model predictive controller is used to generate a reference trajectory. Then, at a low-level, the notions of the FxT-CLF and CBF are combined to introduce the concept of fixed-time barrier functions, and a QP based controller is proposed to track the reference trajectory.

As mentioned in the previous section, from a practical point of view, it is important to study safety guarantees with zero-order hold controllers. The author explored this direction in [182] in collaboration with Joseph Breeden, where various conditions for guaranteeing forward invariance of safe sets are studied. Two metrics are proposed to compare the conservatism of the proposed set-invariance conditions and it is shown that the proposed results are less conservative as compared to the prior work.

APPENDIX A

Proofs from Chapter 2

A.1 Proof of Lemma 2.1

Proof. It is sufficient to prove that if displaced along γ_i when $\mathbf{F}_i = \mathbf{0}$, the resulting field at the displaced location drives the agent away from the point of deadlock. More specifically, if $\boldsymbol{r}_i$ is the position of the agent i such that $\mathbf{F}_i(\boldsymbol{r}_i) = \mathbf{0}$, then after displacement $\delta\boldsymbol{r}_i$ along the direction γ_i, it is sufficient to show that $\mathbf{F}_i(\boldsymbol{r}_i + \delta\boldsymbol{r}_i) \neq \mathbf{0}$, and that $\angle\mathbf{F}_i(\boldsymbol{r}_i + \delta\boldsymbol{r}_i) = \gamma_i$, which results in agent i moving away from $\boldsymbol{r}_i$ and do not return to the same point.

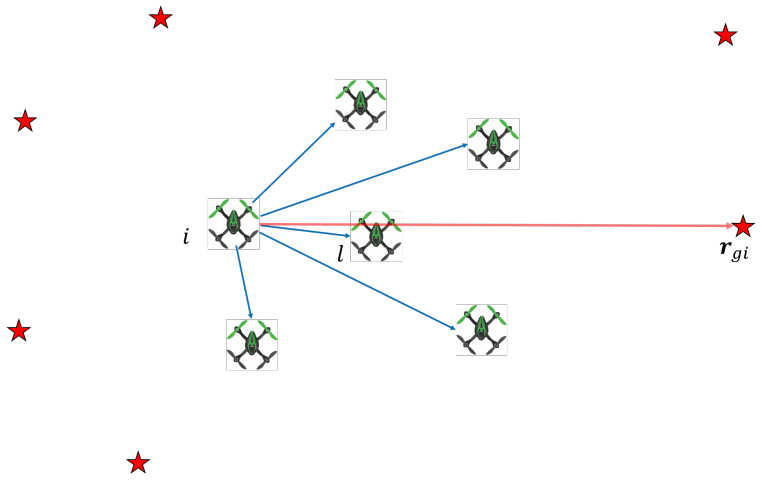

Figure A.1: A scenario with 6 agents located such that their resultant vector fields are $\mathbf{0}$.

Let us consider a scenario with K agents, where $2 \leq K \leq N$, such that for each agent i among these K agents, located at $\boldsymbol{r}_i$, the resulting vector fields $\mathbf{F}_i(\boldsymbol{r}_i) = \mathbf{0}$; an example is shown in Figure A.1 where blue arrows represent the vectors $\boldsymbol{r}_j - \boldsymbol{r}_i$ for each $j \in \mathcal{N}_i$ and red arrow represents the vector $\boldsymbol{r}_{gi} - \boldsymbol{r}_i$. It can be assumed that for all $j \in \mathcal{N}_i$, $\mathbf{F}_j = \mathbf{0}$. If this is not true for some j, then this agent would have a non-zero vector field along which

it moves with a non-zero speed and, hence, it would either go out of the sensing region of the agent i in a finite time, or would reach a location $\boldsymbol{r}_j$ such that $\mathbf{F}_j(\boldsymbol{r}_j) = \mathbf{0}$.

The effect of the rest of the $K-1$ agents on the agent i is denoted by a cumulative repulsive field $\mathbf{F}_{rep}$, so that it holds that:

$$\mathbf{F}_i = \mathbf{F}_{rep} + \prod_j (1-\sigma_{ij})\mathbf{F}_{gi} = \mathbf{0}. \tag{A.1}$$

Let $\bar{\sigma} = \prod_j (1-\sigma_{ij})$. As per the Figure A.1, there is at least one agent i such that $(\boldsymbol{r}_{gi} - \boldsymbol{r}_i)^T(\boldsymbol{r}_j - \boldsymbol{r}_i) \geq 0$ for all $j \in \mathcal{N}_i$ and at least one $l \in \mathcal{N}_i$ such that $(\boldsymbol{r}_{gi} - \boldsymbol{r}_i)^T(\boldsymbol{r}_l - \boldsymbol{r}_i) > 0$. This implies that $\mathbf{F}_{gi}^T\mathbf{F}_{il} < 0$ for at least one $l \in \mathcal{N}_i$ (or, equivalently, $\mathbf{F}_{gi}^T\mathbf{F}_{rep} < 0$), since $\mathbf{F}_{il}$ acts along $-(\boldsymbol{r}_l - \boldsymbol{r}_i)$. Using this, from (A.1), it holds that

$$\mathbf{F}_{gi}^T\mathbf{F}_i = \mathbf{F}_{gi}^T\mathbf{F}_{rep} + \bar{\sigma}\|\mathbf{F}_{gi}\|^2 = 0. \tag{A.2}$$

Since $\mathbf{F}_{gi}^T\mathbf{F}_{rep} < 0$, for (A.2) to hold, it is required that $\bar{\sigma} > 0$. Define an auxiliary agent o located at a location $\boldsymbol{r}_o$ to model the effect of the accumulated repulsive forces on the agent i. Let the repulsive field of agent o on agent i be given by $\mathbf{F}_{io} = \frac{\mathbf{F}_{rep}}{\bar{\sigma}}$ and $\boldsymbol{r}_o$ is such that it satisfies $\frac{\boldsymbol{r}_i - \boldsymbol{r}_o}{\|\boldsymbol{r}_i - \boldsymbol{r}_o\|} = \frac{\mathbf{F}_{rep}}{\bar{\sigma}}$, so that it holds that

$$\mathbf{F}_i(\boldsymbol{r}_i) = \mathbf{F}_{io} + \mathbf{F}_{gi} = \mathbf{0}. \tag{A.3}$$

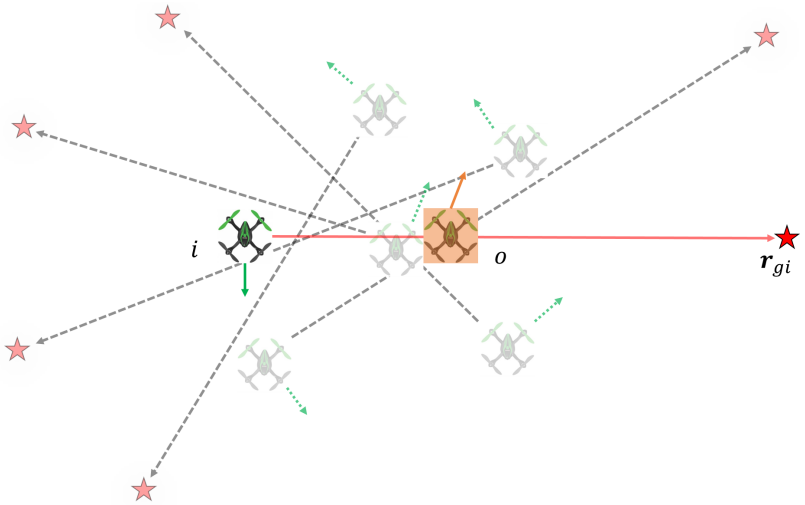

Figure A.2: Motion of the agents along γ_i^0.

The equation (A.3) depicts a two-agent scenario consisting of agents i and o, such that $\mathbf{F}_l(\boldsymbol{r}_l) = \mathbf{0}$ for $l \in \{i, o\}$ as shown in Figure A.2, where gray, dotted arrows show the line

joining an agent and its goal location and green arrows show the instantaneous direction of motion of the agents along their respective directions given by γ_i^0. The agent shown in orange is the *virtual* agent o located at $\boldsymbol{r}_o$, with its resultant direction of motion given by the orange arrow. Since the direction of the motion of the agent i along γ_i^0 is perpendicular to the vector $\boldsymbol{r}_i - \boldsymbol{r}_{gi}$, denote it by the unit vector $(\boldsymbol{r}_i - \boldsymbol{r}_{gi})^\perp$. Hence, the displacement vector for agent i at the location $\boldsymbol{r}_i$ is given by $\delta\boldsymbol{r}_i = \delta_0(\boldsymbol{r}_i - \boldsymbol{r}_{gi})^\perp$, where $\delta_0 > 0$ denotes the infinitesimal length. Note that the resultant motion of the auxiliary agent o may or may not be perpendicular to $\boldsymbol{r}_i - \boldsymbol{r}_{gi}$, since it would depend upon the locations of the rest of the $K-1$ agents. Denote by $\delta\boldsymbol{r}_o$ the displacement of the auxiliary agent o, so that it satisfies:

$$\delta\boldsymbol{r}_o = -\delta_1(\boldsymbol{r}_i - \boldsymbol{r}_{gi})^\perp + \delta_2(\boldsymbol{r}_i - \boldsymbol{r}_{gi})^\parallel, \tag{A.4}$$

with $\delta_1 > 0$ since the motion of the agent o would be in the opposite direction as agent i along the vector $(\boldsymbol{r}_i - \boldsymbol{r}_{gi})^\perp$ and δ_2 can be either positive or negative since its motion can be in the either directions along the vector $(\boldsymbol{r}_i - \boldsymbol{r}_{gi})^\parallel$ where $(\boldsymbol{r}_i - \boldsymbol{r}_{gi})^\parallel$ denotes a unit vector along $(\boldsymbol{r}_i - \boldsymbol{r}_{gi})$,. Using this, the vector field $\mathbf{F}_i$ after this infinitesimal displacement can be expressed as:

$$\begin{aligned}
\mathbf{F}_i(\boldsymbol{r}_i + \delta\boldsymbol{r}_i, \boldsymbol{r}_o + \delta\boldsymbol{r}_o) =& \mathbf{F}_{io}(\boldsymbol{r}_i + \delta\boldsymbol{r}_i, \boldsymbol{r}_o + \delta\boldsymbol{r}_o) + \mathbf{F}_{gi}(\boldsymbol{r}_i + \delta\boldsymbol{r}_i) \\
=& \Big(\mathbf{F}_{io}(\boldsymbol{r}_i, \boldsymbol{r}_o) + \frac{\partial \mathbf{F}_{io}(\boldsymbol{r}_i, \boldsymbol{r}_o)}{\partial \boldsymbol{r}_i}\delta\boldsymbol{r}_i + \frac{\partial \mathbf{F}_{io}(\boldsymbol{r}_i, \boldsymbol{r}_o)}{\partial \boldsymbol{r}_o}\delta\boldsymbol{r}_o\Big) \\
&+ \Big(\mathbf{F}_{gi}(\boldsymbol{r}_i) + \frac{\partial \mathbf{F}_{gi}(\boldsymbol{r}_i)}{\partial \boldsymbol{r}_i}\delta\boldsymbol{r}_i\Big) \\
\overset{(A.3)}{=}& \Big(\frac{\partial \mathbf{F}_{io}(\boldsymbol{r}_i, \boldsymbol{r}_o)}{\partial \boldsymbol{r}_i}\delta\boldsymbol{r}_i + \frac{\partial \mathbf{F}_{io}(\boldsymbol{r}_i, \boldsymbol{r}_o)}{\partial \boldsymbol{r}_o}\delta\boldsymbol{r}_o\Big) + \Big(\frac{\partial \mathbf{F}_{gi}(\boldsymbol{r}_i)}{\partial \boldsymbol{r}_i}\delta\boldsymbol{r}_i\Big) \\
\overset{(A.4)}{=}& \Big(\frac{\partial \mathbf{F}_{io}(\boldsymbol{r}_i, \boldsymbol{r}_o)}{\partial \boldsymbol{r}_i}\delta_0(\boldsymbol{r}_i - \boldsymbol{r}_{gi})^\perp + \Big(\frac{\partial \mathbf{F}_{gi}(\boldsymbol{r}_i)}{\partial \boldsymbol{r}_i}\delta_0(\boldsymbol{r}_i - \boldsymbol{r}_{gi})^\perp\Big) \\
&+ \frac{\partial \mathbf{F}_{io}(\boldsymbol{r}_i, \boldsymbol{r}_o)}{\partial \boldsymbol{r}_o}(-\delta_1(\boldsymbol{r}_i - \boldsymbol{r}_{gi})^\perp + \delta_2(\boldsymbol{r}_i - \boldsymbol{r}_{gi})^\parallel)\Big) \\
\overset{(2.6),(2.7)}{=}& \Big(\frac{\mathbf{I}d_{io}^2 - \boldsymbol{r}_{oi}\boldsymbol{r}_{oi}^T}{d_{io}^3}\delta_0(\boldsymbol{r}_i - \boldsymbol{r}_{gi})^\perp - \Big(\frac{-\mathbf{I}d_{gi}^2 + (\boldsymbol{r}_i - \boldsymbol{r}_{gi})(\boldsymbol{r}_i - \boldsymbol{r}_{gi})^T}{d_{gi}^3} \\
&\delta_0(\boldsymbol{r}_i - \boldsymbol{r}_{gi})^\perp\Big) + \frac{\mathbf{I}d_{io}^2 - \boldsymbol{r}_{oi}\boldsymbol{r}_{oi}^T}{d_{io}^3}(-\delta_1(\boldsymbol{r}_i - \boldsymbol{r}_{gi})^\perp + \delta_2(\boldsymbol{r}_i - \boldsymbol{r}_{gi})^\parallel)\Big),
\end{aligned}$$

where $d_{gi} = \|\boldsymbol{r}_i - \boldsymbol{r}_{gi}\|$, $\boldsymbol{r}_{oi} = \boldsymbol{r}_i - \boldsymbol{r}_o$ and $\mathbf{I} \in \mathbb{R}^{2\times 2}$ is the identity matrix. Note that $\boldsymbol{r}_{oi}$ is

also along $(\boldsymbol{r}_i - \boldsymbol{r}_{gi})^{\parallel}$ and hence, it is perpendicular to $(\boldsymbol{r}_i - \boldsymbol{r}_{gi})^{\perp}$. Using this, it holds that:

$$\begin{aligned}\mathbf{F}_i(\boldsymbol{r}_i + \delta\boldsymbol{r}_i, \boldsymbol{r}_o + \delta\boldsymbol{r}_o) =& \Big(\frac{\delta_0(\boldsymbol{r}_i - \boldsymbol{r}_{gi})^{\perp}}{d_{io}} + \frac{\delta_1(\boldsymbol{r}_i - \boldsymbol{r}_{gi})^{\perp}}{d_{io}} - \frac{\mathbf{I}d_{io}^2 - \boldsymbol{r}_{oi}\boldsymbol{r}_{oi}^T}{d_{io}^3}(\delta_2(\boldsymbol{r}_i - \boldsymbol{r}_{gi})^{\parallel}) \Big) \\ & - \frac{\delta_0(\boldsymbol{r}_i - \boldsymbol{r}_{gi})^{\perp}}{d_{gi}} \\ =& \Big(\frac{\delta_0(\boldsymbol{r}_i - \boldsymbol{r}_{gi})^{\perp}}{d_{io}} + \frac{\delta_1(\boldsymbol{r}_i - \boldsymbol{r}_{gi})^{\perp}}{d_{io}} - \frac{\delta_0(\boldsymbol{r}_i - \boldsymbol{r}_{gi})^{\perp}}{d_{gi}} \\ & - \frac{\mathbf{I}d_{io}^2 - \boldsymbol{r}_{oi}\boldsymbol{r}_{oi}^T}{d_{io}^3}(\delta_2(\boldsymbol{r}_i - \boldsymbol{r}_{gi})^{\parallel}) \Big).\end{aligned}$$

Also note that $(\mathbf{I}d_{io}^2 - \boldsymbol{r}_{oi}\boldsymbol{r}_{oi}^T)\delta_2(\boldsymbol{r}_i - \boldsymbol{r}_{gi})^{\parallel} = \delta_2 d_{io}^2(\boldsymbol{r}_i - \boldsymbol{r}_{gi})^{\parallel} - \delta_2\boldsymbol{r}_{oi}\boldsymbol{r}_{oi}^T(\boldsymbol{r}_i - \boldsymbol{r}_{gi})^{\parallel} = \mathbf{0}$ for all $\boldsymbol{r}_{oi}$. Hence, for $\mathbf{F}_i(\boldsymbol{r}_i + \delta\boldsymbol{r}_i, \boldsymbol{r}_o + \delta\boldsymbol{r}_o) = \mathbf{0}$ to hold, it is required that:

$$\frac{\delta_0 + \delta_1}{d_{io}} = \frac{\delta_0}{d_{gi}}.$$

Equivalently, for $\mathbf{F}_i(\boldsymbol{r}_i + \delta\boldsymbol{r}_i, \boldsymbol{r}_o + \delta\boldsymbol{r}_o) = \mathbf{0}$ to hold, it is required that:

$$d_{gi} = \frac{\delta_0}{\delta_0 + \delta_1} d_{io} < d_{io}. \tag{A.5}$$

Since the agent o is in the sensing radius of the agent i, it follows that $d_{io} \leq R_c$, and using (A.5), it follows that $d_{gi} < d_{io} \leq R_c$. Using the same set of arguments as above for some other agent j from the rest of the $K-1$ agents, one can obtain $d_{gj} < d_{jo'} \leq R_c$, where o' is the auxiliary agent corresponding to agent j. Now, using the above bounds and the fact that $j \in \mathcal{N}_i$, $\|\boldsymbol{r}_{gi} - \boldsymbol{r}_{gj}\|$ can be bounded as

$$\|\boldsymbol{r}_{gi} - \boldsymbol{r}_{gj}\| \leq \|\boldsymbol{r}_{gi} - \boldsymbol{r}_i\| + \|\boldsymbol{r}_{gj} - \boldsymbol{r}_j\| + \|\boldsymbol{r}_i - \boldsymbol{r}_j\| = d_{gi} + d_{gj} + \|\boldsymbol{r} - \boldsymbol{r}_j\| < 3R_c.$$

It follows that $\|\boldsymbol{r}_{gi} - \boldsymbol{r}_{gj}\| < 3R_c$, which violates Assumption 2.3. Hence, if the goal locations are chosen as per Assumption 2.3, the condition $d_{gi} = \frac{\delta_0}{\delta_0+\delta_1} d_{io}$ would never hold, and hence, it holds that $\mathbf{F}_i(\boldsymbol{r}_i+\delta\boldsymbol{r}_i, \boldsymbol{r}_o+\delta\boldsymbol{r}_o) \neq \mathbf{0}$. Furthermore, note that from Assumption 2.3, there is at least one agent i out of the K agents such that $d_{gi} > d_{ij}$, which implies that $\mathbf{F}_i(\boldsymbol{r}_i + \delta\boldsymbol{r}_i, \boldsymbol{r}_o + \delta\boldsymbol{r}_o)$ is along $(\boldsymbol{r}_i - \boldsymbol{r}_{gi})^{\perp}$, making agent i move away from the position $\boldsymbol{r}_i$ for which $\mathbf{F}_i(\boldsymbol{r}_i) = 0$, which completes the proof. □

A.2 Proof of Theorem 2.5

Proof. Before the inter-agent safety is shown, note that the following inequality holds for all $t \geq 0$ and for all $i \neq j$:

$$\hat{d}_{ij} = \|\hat{\boldsymbol{r}}_i - \boldsymbol{r}^i_{js}\| \leq \|\hat{\boldsymbol{r}}_i - \boldsymbol{r}_i\| + \|\boldsymbol{r}^i_{js} - \boldsymbol{r}_j\| + \|\boldsymbol{r}_i - \boldsymbol{r}_j\| \leq \delta_e + \epsilon_s + \|\boldsymbol{r}_i - \boldsymbol{r}_j\|,$$

which means that if $\hat{d}_{ij} = \|\hat{\boldsymbol{r}}_i - \boldsymbol{r}^i_{js}\| \geq d_m + \epsilon_s + \delta_e$, then $d_{ij} = \|\boldsymbol{r}_i - \boldsymbol{r}_j\| \geq d_m$. Hence, it is essential to prove that $\hat{d}_{ij} \geq d_m + \epsilon_s + \delta_e$ holds for all time $t \geq 0$. From Assumption 2.3, it holds that the inter-agent distance $d_{ij}(0) \geq d_m$ which means that all the agents start from a safe distance. Let j be some agent in the sensing region of the agent i at some time instant $t \geq 0$, i.e., $\hat{d}_{ij}(t) \leq R_c$. Denote the steady-state values of the $\hat{\boldsymbol{r}}_i$ and $\hat{\boldsymbol{u}}_i$ as $\hat{\boldsymbol{r}}^{ss}_i$ and $\hat{\boldsymbol{u}}^{ss}_i$, respectively. Note that the steady-state velocity satisfy $\hat{\boldsymbol{u}}^{ss}_i = \boldsymbol{u}_{id}$. Consider the time derivative of the estimated distance, which in the steady state (i.e. when $\hat{\boldsymbol{u}}_i = \hat{\boldsymbol{u}}_{id}$ and $\hat{\boldsymbol{r}}_i = \hat{\boldsymbol{r}}^{ss}_i$) reads:

$$\dot{\hat{d}}_{ij} = \frac{\hat{u}_{id}\,(\hat{\boldsymbol{r}}^{ss}_i - \boldsymbol{r}^i_{js})^T \hat{\boldsymbol{u}}_{idn} - (\hat{\boldsymbol{r}}^{ss}_i - \boldsymbol{r}^i_{js})^T \boldsymbol{u}^i_{js}}{\hat{d}^{ss}_{ij}}. \tag{A.6}$$

The worst-case neighbor is the agent $j \in \{\mathcal{N}_i \mid \hat{J}_i < 0\}$ towards whom the rate of change of the estimated distance $\hat{d}_{ij}$ given by (A.6), due to the motion of agent i, is maximum. More specifically, the term $\hat{J}_i < 0$ describes the set of agents $j \in \mathcal{N}_i$ towards whom agent i is moving in its current direction (see [22] for more details). Consider the worst case, i.e., $\hat{d}^{ss}_{ij} = \|\hat{\boldsymbol{r}}^{ss}_i - \boldsymbol{r}^i_{js}\| = d_s$. The commanded speed $\hat{u}_{id}$ in this case is equal to $\hat{u}_{is|j}$ which is given as per (2.25). Plugging this into (A.6), it follows that:

$$\dot{\hat{d}}_{ij} = \frac{(1-\varepsilon_i)u_e d_s + (\varepsilon_i - 1)(\hat{\boldsymbol{r}}_i - \boldsymbol{r}^i_{js})^T \boldsymbol{u}^i_{js}}{d_s} \tag{A.7}$$

Note that

$$\begin{aligned}(\hat{\boldsymbol{r}}_i - \boldsymbol{r}^i_{js})^T \boldsymbol{u}^i_{js} &= (\hat{\boldsymbol{r}}_i - \hat{\boldsymbol{r}}_j)^T \boldsymbol{u}^i_{js} + (\hat{\boldsymbol{r}}_j - \hat{\boldsymbol{r}}_{js})^T \boldsymbol{u}^i_{js} \\ &= (\hat{\boldsymbol{r}}_i - \hat{\boldsymbol{r}}_j)^T \hat{\boldsymbol{u}}_j + (\hat{\boldsymbol{r}}_i - \hat{\boldsymbol{r}}_j)^T (\boldsymbol{u}^i_{js} - \hat{\boldsymbol{u}}_j) + (\hat{\boldsymbol{r}}_j - \hat{\boldsymbol{r}}_{js})^T \boldsymbol{u}^i_{js}.\end{aligned}$$

Using the fact that either the agent j is moving away from the agent i at the first place or is following the vector field that points away from agent i, it holds that $(\hat{\boldsymbol{r}}_i - \hat{\boldsymbol{r}}_j)^T \hat{\boldsymbol{u}}_j \leq 0$ (where $\hat{\boldsymbol{u}}_j$ is the estimated velocity of agent j, available only to agent j). Furthermore,

using the bounds on the estimation and sensing errors, it follows that

$$(\hat{\boldsymbol{r}}_i - \hat{\boldsymbol{r}}_j)^T \hat{\boldsymbol{u}}_j + (\hat{\boldsymbol{r}}_i - \hat{\boldsymbol{r}}_j)^T (\boldsymbol{u}^i_{js} - \hat{\boldsymbol{u}}_j) + (\hat{\boldsymbol{r}}_j - \hat{\boldsymbol{r}}_{js})^T \boldsymbol{u}^i_{js} \leq (d_s + \epsilon_s)(\delta_e + \epsilon_s) + \epsilon_s \|\boldsymbol{u}^i_{js}\|.$$

Choose u_e as

$$u_e \coloneqq \frac{(d_s + \epsilon_s)(\delta_e + \epsilon_s) + \epsilon_s \|\boldsymbol{u}^i_{js}\|}{d_s} \tag{A.8}$$

Now, from (A.7) and choice of u_e as per (A.8), it holds that

$$\begin{aligned}(1 - \varepsilon_i) u_e d_s + (\varepsilon_i - 1)(\hat{\boldsymbol{r}}_i - \boldsymbol{r}^i_{js})^T \boldsymbol{u}^i_{js} &\geq (1 - \varepsilon_i) u_e d_s - (1 - \varepsilon_i)\big((d_s + \epsilon_s)(\delta_e + \epsilon_s) + \epsilon_s \|\boldsymbol{u}^i_{js}\|\big) \\ &\geq 0,\end{aligned}$$

which implies that the steady-state estimated inter-agent distance $\hat{d}^{ss}_{ij}$ can not become less than d_s. Now, to account for the transient period, consider the time derivative of the velocity error $\hat{\boldsymbol{u}}_{ide}$, which reads

$$\dot{\hat{\boldsymbol{u}}}_{ide} = \dot{\hat{\boldsymbol{u}}}_i - \dot{\hat{\boldsymbol{u}}}_{id} = \boldsymbol{a}_i + k_{i4} \boldsymbol{r}_{ie} \|\boldsymbol{r}_{ie}\|^{\alpha_2 - 1} - \dot{\hat{\boldsymbol{u}}}_{id} \tag{A.9}$$

Substituting (2.27) into (A.9) yields

$$\dot{\hat{\boldsymbol{u}}}_{ide} = -\lambda_i (\hat{\boldsymbol{u}}_i - \hat{\boldsymbol{u}}_{id}) \|\hat{\boldsymbol{u}}_i - \hat{\boldsymbol{u}}_{id}\|^{\beta_2 - 1} = -\lambda_i \boldsymbol{u}_{ide} \|\boldsymbol{u}_{ide}\|^{\beta_2 - 1}, \tag{A.10}$$

where $\lambda_i > 0$. From Theorem 2.3, it follows that the origin is a finite-time stable equilibrium of the system (A.10). Integrating equation (A.10) furthermore yields

$$\boldsymbol{u}_{ide}(t) = \boldsymbol{u}_{ide}(0) \Big(1 - \frac{\lambda_i t (1 - \beta_2)}{\|\boldsymbol{u}_{ide}(0)\|^{1 - \beta_2}}\Big)^{\frac{1}{1 - \beta_2}} = c_1 (1 - c_2 t)^{\xi} \tag{A.11}$$

where, $\boldsymbol{u}_{ide}(0)$ is the initial velocity error, $c_1 = \boldsymbol{u}_{ide}(0)$, $c_2 = \frac{\lambda_i (1 - \beta_2)}{\|\boldsymbol{u}_{ide}(0)\|^{1 - \beta_2}}$, and $\xi = \frac{1}{1 - \beta_2}$. Note that $\boldsymbol{u}_{ide}(t) = 0$ for all $t \geq t^* = \frac{1}{c_2}$. Hence, after this instant, the error in position would not change. By integrating (A.11), the transient position error $\boldsymbol{r}_{ide}(t)$ can be obtained as

$$\boldsymbol{r}_{ide}(t) = \boldsymbol{r}_{ide}(0) + \frac{c_1}{c_2 (1 + \xi)} (1 - (1 - c_2 t)^{1 + \xi}) \tag{A.12}$$

With $\boldsymbol{r}_{ide}(0) = 0$, the maximum position error $\boldsymbol{r}_{ieMax}$, attained at $t^* = \frac{1}{c_2}$, has the form

$$\boldsymbol{r}_{ieMax} = \boldsymbol{r}_{ide}\Big(\frac{1}{c_2}\Big) = \frac{c_1}{c_2(1+\xi)} = \frac{\boldsymbol{u}_{ide}(0)\|\boldsymbol{u}_{ide}(0)\|^{1-\beta_2}}{\lambda_i(2-\beta_2)},$$

where $\boldsymbol{u}_{ide}(0) = \hat{\boldsymbol{u}}_i(0) - u_{id}(0)\boldsymbol{u}_{idn}(0) + \boldsymbol{w}_{av} + k_{i3}\boldsymbol{r}_{ie}(0)\|\boldsymbol{r}_{ie}(0)\|^{\alpha_1-1}$. Define r_e as

$$r_e \coloneqq \max_i \|\boldsymbol{r}_{ieMax}\|. \tag{A.13}$$

Note that from the steady-state analysis, it holds that $\|\hat{\boldsymbol{r}}_i^{ss} - \hat{\boldsymbol{r}}_{js}\| \geq d_s$. Using this, it follows that :

$$\hat{d}_{ij} = \|\hat{\boldsymbol{r}}_i - \hat{\boldsymbol{r}}_{js}\| \geq \|\hat{\boldsymbol{r}}_i^{ss} - \hat{\boldsymbol{r}}_{js}\| - \|\hat{\boldsymbol{r}}_i - \hat{\boldsymbol{r}}_i^{ss}\| \geq d_s - r_e$$

Thus, with $d_s = d_m + \delta_e + \epsilon_s + r_e$, it holds that $\hat{d}_{ij} \geq d_m + \delta_e + \epsilon_s$ and hence, $d_{ij} \geq d_m$, i.e., the resulting agent trajectories are collision free. □

APPENDIX B

Proofs from Chapter 3

B.1 Proof of Lemma 3.1

Proof. It holds that

$$I = \int_{V_0}^{0} \frac{dV}{-\alpha_1 V^{\gamma_1} - \alpha_2 V^{\gamma_2} + \delta_1 V} = \int_{V_0}^{0} \frac{dV}{V(-\alpha_1 V^{\frac{1}{\mu}} - \alpha_2 V^{\frac{-1}{\mu}} + \delta_1)}.$$

Substitute $m = V^{\frac{1}{\mu}}$, so that $dm = \frac{1}{\mu} V^{\frac{1}{\mu}-1} dV$, which implies that $\frac{1}{\mu}\frac{dV}{V} = \frac{dm}{V^{\frac{1}{\mu}}} = \frac{dm}{m}$. Using this, it follows that

$$I = \mu \int_{V_0^{\frac{1}{\mu}}}^{0} \frac{dm}{m(-\alpha_1 m - \alpha_2 \frac{1}{m} + \delta_1)} = \mu \int_{V_0^{\frac{1}{\mu}}}^{0} \frac{dm}{(-\alpha_1 m^2 - \alpha_2 + \delta_1 m)}.$$

Now, consider the three cases, namely, $\delta_1 < 2\sqrt{\alpha_1\alpha_2}$, $\delta_1 = 2\sqrt{\alpha_1\alpha_2}$ and $\delta_1 > 2\sqrt{\alpha_1\alpha_2}$ separately. First, consider the cases when $\delta_1 < 2\sqrt{\alpha_1\alpha_2}$. In the case, can be I re-written as

$$I = \mu \int_{V_0^{\frac{1}{\mu}}}^{0} \frac{dm}{-\alpha_1 \left((m - \frac{\delta_1}{2\alpha_1})^2 + \frac{4\alpha_1\alpha_2 - \delta_1^2}{4\alpha_1^2}\right)}$$

Evaluate the integral to obtain

$$I = \frac{\mu}{-\alpha_1 k_1}(\tan^{-1} k_2 - \tan^{-1} k_3),$$

where $k_1 = \sqrt{\frac{4\alpha_1\alpha_2 - \delta_1^2}{4\alpha_1^2}}$, $k_2 = -\frac{\delta_1}{\sqrt{4\alpha_1\alpha_2 - \delta_1^2}}$ and $k_3 = \frac{2\alpha_1 V_0^{\frac{1}{\mu}} - \delta_1}{\sqrt{4\alpha_1\alpha_2 - \delta_1^2}}$. Hence, it holds that

$$I = \frac{\mu}{\alpha_1 k_1}(\tan^{-1} k_3 - \tan^{-1} k_2) \leq \frac{\mu}{\alpha_1 k_1}(\frac{\pi}{2} - \tan^{-1} k_2),$$

since $\tan^{-1}(\cdot) \leq \frac{\pi}{2}$, which completes the proof of part (i).

Next, the case when $\delta_1 > 2\sqrt{\alpha_1\alpha_2}$ is considered. In this case, the roots of $\gamma(m) = 0$ are real. Let $a \leq b$ be the such that $\alpha_1 m^2 - \delta_1 m + \alpha_2 = \alpha_1(m-a)(m-b)$. This substitution allows to factorize the denominator to evaluate the integral I. The expressions for a, b are given as

$$a = \frac{\delta_1 - \sqrt{\delta_1^2 - 4\alpha_1\alpha_2}}{2\alpha_1}, \quad b = \frac{\delta_1 + \sqrt{\delta_1^2 - 4\alpha_1\alpha_2}}{2\alpha_1}.$$

Note that since $ab = \frac{\alpha_2}{\alpha_1} > 0$ and $a + b = \frac{\delta_1}{\alpha_1}$, it holds that $0 < a \leq b$. Since $V_0^{\frac{1}{\mu}} \leq k\frac{\delta_1 - \sqrt{\delta_1^2 - 4\alpha_1\alpha_2}}{2\alpha_1} = ka$ where $k < 1$, it holds that $\frac{1}{-\alpha_1 V^{\gamma_1} - \alpha_2 V^{\gamma_2} + \delta_1 V} < 0$ for all $V \leq V_0$, i.e., the denominator $\delta_1 V - \alpha_1 V^{\gamma_1} + \alpha_2 V^{\gamma_2}$ does not vanish for $V \in [0, V_0]$. Thus, it holds that

$$\begin{aligned} I &= \mu \int_{V_0^{\frac{1}{\mu}}}^{0} \frac{dm}{(-\alpha_1 m^2 - \alpha_2 + \delta_1 m)} = -\frac{\mu}{\alpha_1} \int_{V_0^{\frac{1}{\mu}}}^{0} \frac{dm}{(m-a)(m-b)} \\ &= -\frac{\mu}{\alpha_1(a-b)} \left(\int_{V_0^{\frac{1}{\mu}}}^{0} \frac{dm}{m-a} - \int_{V_0^{\frac{1}{\mu}}}^{0} \frac{dm}{m-b} \right). \end{aligned}$$

Evaluate the integrals to obtain

$$\begin{aligned} I &= \frac{-\mu}{\alpha_1(a-b)} \left(\log\left(\frac{a}{|V_0^{\frac{1}{\mu}} - a|} \right) - \log\left(\frac{b}{|V_0^{\frac{1}{\mu}} - b|} \right) \right) \\ &= \frac{\mu}{\alpha_1(a-b)} \left(\log\left(\frac{b}{a} \right) + \log\left(\frac{|V_0^{\frac{1}{\mu}} - a|}{|V_0^{\frac{1}{\mu}} - b|} \right) \right) \\ &\leq \frac{\mu}{\alpha_1(b-a)} \left(\log\left(\frac{b - ka}{a(1-k)} \right) - \log\left(\frac{b}{a} \right) \right), \end{aligned}$$

Finally, for the case when $\delta_1 = 2\sqrt{\alpha_1\alpha_2}$, it holds that $a = b = \frac{-\delta_1}{2\alpha_1} = \sqrt{\frac{\alpha_2}{\alpha_1}}$, and thus,

$$I = -\frac{\mu}{\alpha_1} \int_{V_0^{\frac{1}{\mu}}}^{0} \frac{dm}{(m-a)(m-b)} = -\frac{\mu}{\alpha_1} \int_{V_0^{\frac{1}{\mu}}}^{0} \frac{dm}{(m-a)^2}.$$

It is easy to see that for $V_0^{\frac{1}{\mu}} \leq ka < a = \frac{\delta_1}{2\alpha_1} = \sqrt{\frac{\alpha_2}{\alpha_1}}$, the integral I evaluates to a finite

value. Thus, for all $V_0^{\frac{1}{\mu}} \leq k\sqrt{\frac{\alpha_2}{\alpha_1}} < \sqrt{\frac{\alpha_2}{\alpha_1}}$ for $0 < k < 1$, it holds that

$$I = \frac{\mu}{\alpha_1}\Big(-\frac{1}{a} - \frac{1}{-a + V_0^{\frac{1}{\mu}}}\Big) \leq \frac{\mu}{\alpha_1}\Big(-\frac{1}{a} - \frac{1}{-a + k\sqrt{\frac{\alpha_2}{\alpha_1}}}\Big)$$
$$= \frac{\mu}{\alpha_1}\sqrt{\frac{\alpha_1}{\alpha_2}}\Big(-1 - \frac{1}{-1+k}\Big) = \frac{\mu}{\sqrt{\alpha_1\alpha_2}}\Big(\frac{k}{1-k}\Big).$$

This completes the proof of part (ii).

For part (iii), let $\tilde{V} = (\tilde{k}\frac{\delta_1 + \sqrt{\delta_1 - 4\alpha_1\alpha_2}}{2\alpha_1})^{\mu}$ for any $\tilde{k} > 1$. It follows that for all $V_0 \geq V \geq \tilde{V}$ the integrand in (3.10) is negative, and thus, it holds that

$$\int_{V_0}^{\tilde{V}} \frac{dV}{-\alpha_1 V^{\gamma_1} - \alpha_2 V^{\gamma_2} + \delta_1 V} = \frac{\mu}{\alpha_1(b-a)}\left(\log\left(\frac{|\tilde{V}^{\frac{1}{\mu}} - a|}{|V_0^{\frac{1}{\mu}} - a|}\right) - \log\left(\frac{|\tilde{V}^{\frac{1}{\mu}} - b|}{|V_0^{\frac{1}{\mu}} - b|}\right)\right)$$
$$= \frac{\mu}{\alpha_1(b-a)}\left(\log\left(\frac{|\tilde{V}^{\frac{1}{\mu}} - a|}{|\tilde{V}^{\frac{1}{\mu}} - b|}\right) + \log\left(\frac{|V_0^{\frac{1}{\mu}} - b|}{|V_0^{\frac{1}{\mu}} - a|}\right)\right)$$
$$\leq \frac{\mu}{\alpha_1(b-a)}\log\frac{|\tilde{V}^{\frac{1}{\mu}} - a|}{|\tilde{V}^{\frac{1}{\mu}} - b|} = \frac{\mu}{\alpha_1(b-a)}\log\left(\frac{\tilde{k}b - a}{\tilde{k}b - b}\right),$$

since $\tilde{V} = (\tilde{k}b)^{\mu}$ and $\log\left(\frac{|V_0^{\frac{1}{\mu}} - b|}{|V_0^{\frac{1}{\mu}} - a|}\right) \leq 0$ as $a \leq b$. □

B.2 Proof of Lemma 3.3

Proof. For $0 < \bar{\delta}_1 < 2\sqrt{\alpha_1\alpha_2}$, note that $-\alpha_1 V^{\gamma_1} - \alpha_2 V^{\gamma_2} + \bar{\delta}_1 \leq -2\sqrt{\alpha_1\alpha_2}V + \bar{\delta}_1 \leq -2\sqrt{\alpha_1\alpha_2}\bar{V} + \bar{\delta}_1 < 0$ for all $\bar{V} > \frac{\bar{\delta}_1}{2\sqrt{\alpha_1\alpha_2}}$. Since $\frac{\bar{\delta}_1}{2\sqrt{\alpha_1\alpha_2}} < 1$, one can choose $\bar{V} = 1$ so that the integrand in (3.28) is negative for all $V_0 \geq \bar{V} = 1$. Using this, it holds that

$$I = \int_{V_0}^{1} \frac{dV}{-\alpha_1 V^{\gamma_1} - \alpha_2 V^{\gamma_2} + \bar{\delta}_1}.$$

Note that for $V \geq 1$, it holds that $\bar{\delta}_1 \leq \bar{\delta}_1 V$. Using this, it holds that

$$I \leq \int_{V_0}^{1} \frac{dV}{-\alpha_1 V^{\gamma_1} - \alpha_2 V^{\gamma_2} + \bar{\delta}_1 V}.$$

Using Lemma 3.1, it can be shown that the first expression in the above inequality evaluates to

$$\int_{V_0}^{1} \frac{dV}{-\alpha_1 V^{\gamma_1} - \alpha_2 V^{\gamma_2} + \bar{\delta}_1 V} \leq \frac{\mu}{\alpha_1 k_1} \left(\frac{\pi}{2} - \tan^{-1} k_2 \right),$$

where $k_1 = \sqrt{\frac{4\alpha_1\alpha_2 - \bar{\delta}_1^2}{4\alpha_1^2}}$ and $k_2 = \frac{2\alpha_1 - \bar{\delta}_1}{\sqrt{4\alpha_1\alpha_2 - \bar{\delta}_1^2}}$ which completes the proof of (i).

For the case when $\bar{\delta}_1 \geq 2\sqrt{\alpha_1\alpha_2}$, it holds that

$$\bar{V} = (k\frac{\bar{\delta}_1 + \sqrt{\bar{\delta}_1 - 4\alpha_1\alpha_2}}{2\alpha_1})^{\mu} > (\frac{\bar{\delta}_1 + \sqrt{\bar{\delta}_1 - 4\alpha_1\alpha_2}}{2\alpha_1})^{\mu}) > 1,$$

for any $k > 1$. Since $\bar{V} > 1$, it holds that $-\alpha_1 V^{\gamma_1} - \alpha_2 V^{\gamma_2} + \bar{\delta}_1 \leq -\alpha_1 V^{\gamma_1} - \alpha_2 V^{\gamma_2} + \bar{\delta}_1 V$ for all $V \geq \bar{V}$, using which, the following inequality:

$$I \leq \int_{V_0}^{\bar{V}} \frac{dV}{-\alpha_1 V^{\gamma_1} - \alpha_2 V^{\gamma_2} + \bar{\delta}_1 V},$$

can be obtained. Since $\bar{V} = \tilde{V}$ in part (iii) Lemma 3.1, it follows that $I \leq \frac{\mu}{\alpha_1(b-a)} \log\left(\frac{kb-a}{kb-b}\right)$ for any $k > 1$. □

APPENDIX C

Proofs from Chapter 5

C.1 Proof of Theorem 5.1

Proof. First the stability of the origin under conditions (i)-(iii) is shown. Let $x_0 \in D$, where D is some open neighborhood of the origin. For all $p \in \mathbb{Z}_+$, it holds that

$$\begin{aligned} V_{i^p}(x(t_p^+)) &= V_{i^0}(x(t_0)) + \sum_{k=1}^{p} \Big(V_{i^k}(x(t_k^+)) - V_{i^{k-1}}(x(t_k^+)) \Big) \\ &\quad + \sum_{k=0}^{p-1} \Big(V_{i^k}(x(t_{k+1}^-)) - V_{i^k}(x(t_k^+)) \Big) \\ &\quad + \sum_{k=0}^{p-1} \sum_{t_{k+1} \in J_{i^{k+1}}} \Big(V_{i^k}(x(t_{k+1}^+)) - V_{i^k}(x(t_{k+1}^-)) \Big) \\ &\leq \alpha_0(\|x_0\|) + \alpha_1(\|x_0\|) + \alpha_2(\|x_0\|) + N_f \alpha_3(\|x_0\|) \\ &= \alpha(\|x_0\|) \end{aligned}$$

where $\alpha = \alpha_0 + \alpha_1 + \alpha_2 + N_f \alpha_3$ with $\alpha_0(r) = \max_{i \in \Sigma_f,\, \|x\| \leq r} V_i(x)$. Thus, it holds that

$$V_{i^p}(x(t_p^+)) \leq \alpha(\|x_0\|), \tag{C.1}$$

for all $p \in \mathbb{Z}_+$. Let $d_i(c) = \{x \mid V_i(x) \leq c\}$ denote the c sub-level set of the Lyapunov function V_i, $i \in \Sigma_f$, and $B_\rho = \{x \mid \|x\| \leq \rho\}$ denote a ball centered at the origin with radius $\rho \in \mathbb{R}_+$. Define $r(c) = \inf\{\rho \geq 0 \mid d_i(c) \subset B_\rho\}$ as the radius of the smallest ball centered at the origin that encloses the c sub-level sets $d_i(c)$, for all $i \in \Sigma_f$. Figure C.1 shows one such construction where the ball B_ρ with $\rho = \epsilon$, shown in dotted yellow, encloses c sublevel sets of the Lyapunov functions V_i, whose boundaries are shown in solid lines. Since the functions V_i are positive definite, the sub-level sets $d_i(c)$ are bounded for

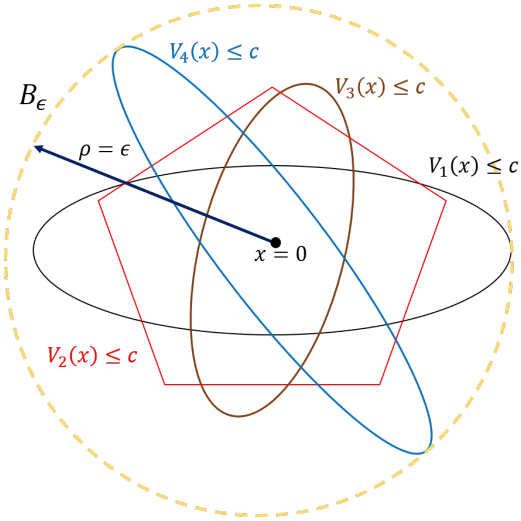

Figure C.1: Construction of the ball B_ρ.

small $c > 0$, and hence, the function r is invertible. The inverse function $c_\epsilon = r^{-1}(\epsilon)$ maps the radius $\epsilon > 0$ to the value c_ϵ such that the sub-level sets $d_i(c_\epsilon)$ are contained in B_ϵ for all $i \in \Sigma_f$. For any given $\epsilon > 0$, choose δ such that $\alpha(\delta) \le (r^{-1}(\epsilon)) > 0$ so that (C.1) implies that for $\|x_0\| \le \delta$, we have $V_{i^p}(x(t_p^+)) \le \alpha(\|x_0\|) \le \alpha(\delta) \le r^{-1}(\epsilon)$, which implies that $\|x(t_p^+)\| \le \epsilon$ for all $p \in \mathbb{Z}_+$, i.e., the origin is LS.

Next, FTS of the origin is shown when conditions (iv)-(v) also hold. From (C.1), it holds that

$$V_F(x(t_{F_i})) \le \alpha(\|x_0\|), \tag{C.2}$$

for all $i \in \mathbb{N}$. By definition, there is no discrete jump during $\bar{T}_{F_k}$, for all $k \in \mathbb{N}$. Let $M \in \mathbb{N}$ denote the total number of times the mode F is activated. From condition (iv), it holds that

$$\dot{V}_F(x(t)) \le -c(V_F(x(t)))^\beta. \tag{C.3}$$

for all $t \in \bigcup \bar{T}_{F_k} \subset (\bigcup [t_{F_k}, t_{F_k+1}) \setminus J_F)$. Using the fact there is no discrete jump in $\bar{T}_{F_k}$, (C.3) can be integrated over the interval $\bar{T}_{F_k}$ to obtain

$$|\bar{T}_{F_k}| \le \frac{\bar{V}_{F_k}^{1-\beta}}{c(1-\beta)} - \frac{\bar{V}_{F_k+1}^{1-\beta}}{c(1-\beta)},$$

where $|\bar{T}_{F_k}| = \bar{t}_{F_k+1} - \bar{t}_{F_k}$. Thus, for any $M \in \mathbb{N}$, it holds that

$$\sum_{k=1}^{M} |\bar{T}_{F_k}| \leq \sum_{k=1}^{M} \left(\frac{\bar{V}_{F_k}^{1-\beta}}{c(1-\beta)} - \frac{\bar{V}_{F_k+1}^{1-\beta}}{c(1-\beta)} \right) = \frac{\bar{V}_{F_1}^{1-\beta}}{c(1-\beta)} + \sum_{i=1}^{M-1} \frac{\bar{V}_{F_{i+1}}^{1-\beta} - \bar{V}_{F_i+1}^{1-\beta}}{c(1-\beta)} - \frac{\bar{V}_{F_M+1}^{1-\beta}}{c(1-\beta)}.$$

Using (C.2), the following inequality can be obtained:

$$\frac{\bar{V}_{F_1}^{1-\beta}}{c(1-\beta)} \leq \frac{(\alpha(\|x_0\|))^{1-\beta}}{c(1-\beta)}. \tag{C.4}$$

Define $\gamma_1(\|x_0\|) \triangleq \frac{(\alpha(\|x_0\|))^{1-\beta}}{c(1-\beta)}$ and note that $\gamma_1 \in \mathcal{K}$. Now, let $F_s = \{q_1, q_2, \ldots, q_k\}, 0 \leq q_l \leq M$, be the set of indices such that $\bar{V}_{F_{i+1}} \geq \bar{V}_{F_i+1}$ for $i \in F_s$. For $a \geq b \geq 0$, it holds that $a^r \geq b^r$ for any $r > 0$. Hence, the following inequality holds:

$$\sum_{i=1}^{M-1} \frac{\bar{V}_{F_{i+1}}^{1-\beta} - \bar{V}_{F_i+1}^{1-\beta}}{c(1-\beta)} \leq \sum_{i \in F_s} \frac{\bar{V}_{F_{i+1}}^{1-\beta} - \bar{V}_{F_i+1}^{1-\beta}}{c(1-\beta)} \tag{C.5}$$

Using Lemma 5.1, the following inequality can be obtained:

$$\sum_{i \in F_s} \frac{\bar{V}_{F_{i+1}}^{1-\beta} - \bar{V}_{F_i+1}^{1-\beta}}{c(1-\beta)} \leq \sum_{i \in F_s} \frac{(\bar{V}_{F_{i+1}} - \bar{V}_{F_i+1})^{1-\beta}}{c(1-\beta)}. \tag{C.6}$$

From the analysis in the first part of the proof, it holds that $V_F(x(t)) \leq \alpha(\|x_0\|)$. Define $\bar{\alpha} = 2M\alpha$ so that the following holds:

$$\sum_{i \in Q} \left(\bar{V}_{F_{i+1}} - \bar{V}_{F_i+1} \right) \leq \bar{\alpha}(\|x_0\|). \tag{C.7}$$

Hence, it holds that

$$\begin{aligned} \sum_{i=1}^{M-1} \frac{\bar{V}_{F_{i+1}}^{1-\beta} - \bar{V}_{F_i+1}^{1-\beta}}{c(1-\beta)} &\overset{\text{(C.6)}}{\leq} \frac{\sum\limits_{i \in F_s} \left(\bar{V}_{F_{i+1}} - \bar{V}_{F_i+1} \right)^{1-\beta}}{c(1-\beta)} \\ &\leq \frac{M^{-\beta} \left(\sum\limits_{i \in F_s} \bar{V}_{F_{i+1}} - \bar{V}_{F_i+1} \right)^{1-\beta}}{c(1-\beta)} \\ &\overset{\text{(C.7)}}{\leq} \frac{M^{-\beta} (\bar{\alpha}(\|x_0\|))^{1-\beta}}{c(1-\beta)}, \end{aligned} \tag{C.8}$$

where the second inequality follows from [51, Lemma 3.4]. Define $\gamma(\|x_0\|) \triangleq \gamma_1(\|x_0\|) +$

$\frac{M^{-\beta}(\bar{\alpha}(\|x_0\|))^{1-\beta}}{c(1-\beta)}$ and $|\bar{T}_F| = \sum_{k=1}^{M} |\bar{T}_{F_k}|$ to obtain:

$$|\bar{T}_F| + \frac{\bar{V}_{F_M+1}^{1-\beta}}{c(1-\beta)} \leq \frac{\bar{V}_{F_1}^{1-\beta}}{c(1-\beta)} + \sum_{i=1}^{M-1} \frac{\bar{V}_{F_{i+1}}^{1-\beta} - \bar{V}_{F_i+1}^{1-\beta}}{c(1-\beta)} \leq \gamma(\|x_0\|).$$

Clearly, $\gamma \in \mathcal{K}$. Now, with $|\bar{T}_F| = \gamma(\|x_0\|)$, the following holds:

$$|\bar{T}_F| + \frac{\bar{V}_{F_M+1}^{1-\beta}}{c(1-\beta)} \leq \gamma(\|x_0\|) = |\bar{T}_F|,$$

which implies that $\frac{\bar{V}_{F_M+1}^{1-\beta}}{c(1-\beta)} \leq 0$. However, $\bar{V}_F \geq 0$ since it is a positive definite function, which further implies that $\bar{V}_{F_M+1} = 0$. Hence, if mode F is active for the accumulated time $|\bar{T}_F| = \gamma(\|x_0\|)$ without any discrete jump in the system state, the value of the function V_F converges to 0 as $t \to \bar{t}_{F_M+1}$, and thus, the origin of (5.1) is FTS.

Finally, if all the conditions (i)-(v) hold globally and the functions V_i are radially unbounded, it holds that α_0 is also radially unbounded and $\alpha_1, \alpha_2, \alpha_3, \alpha_4 \in \mathcal{K}_\infty$. Thus, it follows that $\alpha(\|x_0\|) < \infty$ and $\bar{\alpha}(\|x_0\|) < \infty$ for all $\|x_0\| < \infty$, and hence, $\gamma(\|x_0\|) < \infty$ for all $\|x_0\| < \infty$, which implies global FTS of the origin. □

BIBLIOGRAPHY

[1] E. Ryan, "Finite-time stabilization of uncertain nonlinear planar systems," in *Dynamics and control*. Springer, 1991, vol. 1, pp. 83–94.

[2] S. P. Bhat and D. S. Bernstein, "Finite-time stability of continuous autonomous systems," *SIAM Journal on Control and Optimization*, vol. 38, no. 3, pp. 751–766, 2000.

[3] J. Zhao and M. W. Spong, "Hybrid control for global stabilization of the cart–pendulum system," *Automatica*, vol. 37, no. 12, pp. 1941–1951, 2001.

[4] H. Ishii and B. Francis, "Stabilizing a linear system by switching control with dwell time," *IEEE Transactions on Automatic Control*, vol. 47, no. 12, pp. 1962–1973, 2002.

[5] K. S. Narendra, O. A. Driollet, M. Feiler, and K. George, "Adaptive control using multiple models, switching and tuning," *International Journal of Adaptive Control and Signal Processing*, vol. 17, no. 2, pp. 87–102, 2003.

[6] A. V. Savkin, E. Skafidas, and R. J. Evans, "Robust output feedback stabilizability via controller switching," *Automatica*, vol. 35, no. 1, pp. 69–74, 1999.

[7] A. D. Ames, "Human-inspired control of bipedal walking robots," *IEEE Transactions on Automatic Control*, vol. 59, no. 5, pp. 1115–1130, 2014.

[8] J. W. Grizzle, C. Chevallereau, A. D. Ames, and R. W. Sinnet, "3d bipedal robotic walking: models, feedback control, and open problems," *IFAC Proceedings Volumes*, vol. 43, no. 14, pp. 505–532, 2010.

[9] C. R. He, W. B. Qin, N. Ozay, and G. Orosz, "Optimal gear shift schedule design for automated vehicles: Hybrid system based analytical approach," *IEEE Transactions on Control Systems Technology*, vol. 26, no. 6, pp. 2078–2090, 2017.

[10] A. Wibisono, A. C. Wilson, and M. I. Jordan, "A variational perspective on accelerated methods in optimization," *Proceedings of the National Academy of Sciences*, vol. 113, no. 47, pp. E7351–E7358, 2016.

[11] O. Romero and M. Benosman, "Finite-time convergence in continuous-time optimization," in *International Conference on Machine Learning*. PMLR, 2020, pp. 8200–8209.

[12] A. Polyakov, D. Efimov, and B. Brogliato, "Consistent discretization of finite-time stable homogeneous systems," in *2018-15th International Workshop on Variable Structure Systems*, 2018, pp. 360–365.

[13] ——, "Consistent discretization of finite-time and fixed-time stable systems," *SIAM Journal on Control and Optimization*, vol. 57, no. 1, pp. 78–103, 2019.

[14] K. Klausen, T. I. Fossen, T. A. Johansen, and A. P. Aguiar, "Cooperative path-following for multirotor UAVs with a suspended payload," in *Control Applications, 2015 IEEE Conference on*. IEEE, 2015, pp. 1354–1360.

[15] S. A. Quintero, G. E. Collins, and J. P. Hespanha, "Flocking with fixed-wing UAVs for distributed sensing: A stochastic optimal control approach," in *American Control Conference*, 2013, pp. 2025–2031.

[16] W. Ren and Y. Cao, "Overview of recent research in distributed multi-agent coordination," in *Distributed Coordination of Multi-agent Networks*, ser. Communications and Control Engineering. Springer-Verlag, 2011, ch. 2, pp. 23–41.

[17] S. Knorn, Z. Chen, and R. H. Middleton, "Overview: Collective control of multiagent systems," *IEEE Transactions on Control of Network Systems*, vol. 3, no. 4, pp. 334–347, Dec. 2016.

[18] C. Peterson and D. A. Paley, "Multivehicle coordination in an estimated time-varying flowfield," *Journal of guidance, control, and dynamics*, vol. 34, no. 1, pp. 177–191, 2011.

[19] J.-W. Lee, B. Walker, and K. Cohen, "Path planning of unmanned aerial vehicles in a dynamic environment," in *Infotech@ Aerospace 2011*. AIAA, 2011, p. 1654.

[20] J. Alonso-Mora, T. Naegeli, R. Siegwart, and P. Beardsley, "Collision avoidance for aerial vehicles in multi-agent scenarios," *Autonomous Robots*, vol. 39, no. 1, pp. 101–121, 2015.

[21] Y. Chen, M. Cutler, and J. P. How, "Decoupled multiagent path planning via incremental sequential convex programming," in *2015 IEEE International Conference on Robotics and Automation*. IEEE, 2015, pp. 5954–5961.

[22] D. Panagou, D. M. Stipanović, and P. G. Voulgaris, "Distributed coordination control for multi-robot networks using Lyapunov-like barrier functions," *IEEE Transactions on Automatic Control*, vol. 61, no. 3, pp. 617–632, 2016.

[23] P. Glotfelter, J. Cortés, and M. Egerstedt, "Nonsmooth barrier functions with applications to multi-robot systems," *IEEE Control Systems Letters*, vol. 1, no. 2, pp. 310–315, 2017.

[24] J.-w. Choi, R. Curry, and G. Elkaim, "Real-time obstacle-avoiding path planning for mobile robots," in *AIAA Guidance, Navigation, and Control Conference*, 2010, p. 8411.

[25] J. Wilburm, M. Perhinschi, B. Wilburn, and O. Karas, "Development of a modified voronoi algorithm for uav path planning and obstacle avoidance," in *AIAA Guidance, Navigation, and Control Conference*, 2012, pp. 4904–4915.

[26] T. Chen, G. Zhang, X. Hu, and J. Xiao, "Unmanned aerial vehicle route planning method based on A-star algorithm," in *2018 13th IEEE Conference on Industrial Electronics and Applications*, May 2018, pp. 1510–1514.

[27] G. S. Aoude, B. D. Luders, J. M. Joseph, N. Roy, and J. P. How, "Probabilistically safe motion planning to avoid dynamic obstacles with uncertain motion patterns," *Autonomous Robots*, vol. 35, no. 1, pp. 51–76, 2013.

[28] M. Elbanhawi and M. Simic, "Sampling-based robot motion planning: A review," *IEEE Access*, vol. 2, pp. 56–77, 2014.

[29] E. J. Rodríguez-Seda, C. Tang, M. W. Spong, and D. M. Stipanović, "Trajectory tracking with collision avoidance for nonholonomic vehicles with acceleration constraints and limited sensing," *The International Journal of Robotics Research*, vol. 33, no. 12, pp. 1569–1592, 2014.

[30] T.-H. Cheng, Z. Kan, J. A. Rosenfeld, and W. E. Dixon, "Decentralized formation control with connectivity maintenance and collision avoidance under limited and intermittent sensing," in *American Control Conference*, 2014, pp. 3201–3206.

[31] H. Ahn, A. Colombo, and D. Del Vecchio, "Supervisory control for intersection collision avoidance in the presence of uncontrolled vehicles," in *American Control Conference*, 2014, pp. 867–873.

[32] H. Ahn, A. Rizzi, and A. Colombo, "Robust supervisors for intersection collision avoidance in the presence of legacy vehicles," *International Journal of Control, Automation and Systems*, vol. 18, no. 2, pp. 384–393, 2020.

[33] H. L. Trentelman, K. Takaba, and N. Monshizadeh, "Robust synchronization of uncertain linear multi-agent systems," *IEEE Transactions on Automatic Control*, vol. 58, no. 6, pp. 1511–1523, Jan. 2013.

[34] X. Liu, D. W. Ho, J. Cao, and W. Xu, "Discontinuous observers design for finite-time consensus of multiagent systems with external disturbances," *IEEE Transactions on Neural Networks and Learning Systems*, vol. 28, no. 11, pp. 2826–2830, 2017.

[35] J. Fu and J. Wang, "Fixed-time coordinated tracking for second-order multi-agent systems with bounded input uncertainties," *Systems & Control Letters*, vol. 93, pp. 1–12, 2016.

[36] H. Hong, W. Yu, G. Wen, and X. Yu, "Distributed robust fixed-time consensus for nonlinear and disturbed multiagent systems," *IEEE Transactions on Systems, Man, and Cybernetics: Systems*, vol. 47, no. 7, pp. 1464–1473, 2017.

[37] X. Wang and S. Li, "Distributed finite-time consensus algorithms for leader-follower second-order multi-agent systems with mismatched disturbances," in *American Control Conference*, 2016, pp. 2814–2819.

[38] P. Li, K. Qin, and M. Shi, "Distributed robust H infinity rotating consensus control for directed networks of second-order agents with mixed uncertainties and time-delay," *Neurocomputing*, vol. 148, pp. 332–339, Jan. 2015.

[39] V. Rezaei and M. Stefanovic, "Distributed leaderless and leader-follower consensus of linear multiagent systems under persistent disturbances," in *2016 24th Mediterranean Conference on Control and Automation*. IEEE, 2016, pp. 587–592.

[40] X. Wang, A. Saberi, A. A. Stoorvogel, and H. F. Grip, "Control of a chain of integrators subject to actuator saturation and disturbances," *International journal of robust and nonlinear control*, vol. 22, no. 14, pp. 1562–1570, 2012.

[41] X. Wang, S. Li, X. Yu, and J. Yang, "Distributed active anti-disturbance consensus for leader-follower higher-order multi-agent systems with mismatched disturbances," *IEEE Transactions on Automatic Control*, vol. 62, no. 11, pp. 5795–5801, 2017.

[42] B. Tian, H. Lu, Z. Zuo, and Q. Zong, "Multivariable uniform finite-time output feedback reentry attitude control for RLV with mismatched disturbance," *Journal of the Franklin Institute*, vol. 355, no. 8, pp. 3470–3487, 2018.

[43] X. Wang and Y. Hong, "Finite-time consensus for multi-agent networks with second-order agent dynamics," *IFAC Proceedings Volumes*, vol. 41, no. 2, pp. 15 185–15 190, 2008.

[44] F. Xiao, L. Wang, J. Chen, and Y. Gao, "Finite-time formation control for multi-agent systems," *Automatica*, vol. 45, no. 11, pp. 2605–2611, 2009.

[45] Y. Liu and Z. Geng, "Finite-time formation control for linear multi-agent systems: A motion planning approach," *Systems & Control Letters*, vol. 85, pp. 54–60, 2015.

[46] S. Li and X. Wang, "Finite-time consensus and collision avoidance control algorithms for multiple AUVs," *Automatica*, vol. 49, no. 11, pp. 3359–3367, 2013.

[47] S. Li, H. Du, and X. Lin, "Finite-time consensus algorithm for multi-agent systems with double-integrator dynamics," *Automatica*, vol. 47, no. 8, pp. 1706–1712, 2011.

[48] J. Hu, S. Li, C. Zhao, Q. Pan, B. Fan, Z. Zhang, and H. Li, "Finite-time consensus for multi UAV system with collision avoidance," in *IEEE International Conference on Unmanned Systems*. IEEE, 2017, pp. 517–522.

[49] J. Ma and E. M. Lai, "Finite-time flocking control of a swarm of Cucker-Smale agents with collision avoidance," in *IEEE 24th International Conference on Mechatronics and Machine Vision in Practice*, 2017, pp. 1–6.

[50] L. Wang, S. Sun, and C. Xia, "Finite-time stability of multi-agent system in disturbed environment," *Nonlinear Dynamics*, vol. 67, no. 3, pp. 2009–2016, 2012.

[51] Z. Zuo and L. Tie, "Distributed robust finite-time nonlinear consensus protocols for multi-agent systems," *International Journal of Systems Science*, vol. 47, no. 6, pp. 1366–1375, 2016.

[52] M. Defoort, A. Polyakov, G. Demesure, M. Djemai, and K. Veluvolu, "Leader-follower fixed-time consensus for multi-agent systems with unknown non-linear inherent dynamics," *IET Control Theory & Applications*, vol. 9, no. 14, pp. 2165–2170, 2015.

[53] A. D. Ames, X. Xu, J. W. Grizzle, and P. Tabuada, "Control barrier function based quadratic programs for safety critical systems," *IEEE Transactions on Automatic Control*, vol. 62, no. 8, pp. 3861–3876, 2017.

[54] A. D. Ames, J. W. Grizzle, and P. Tabuada, "Control barrier function based quadratic programs with application to adaptive cruise control," in *53rd Conference on Decision and Control*. IEEE, 2014, pp. 6271–6278.

[55] M. Z. Romdlony and B. Jayawardhana, "Stabilization with guaranteed safety using control Lyapunov-barrier function," *Automatica*, vol. 66, pp. 39–47, 2016.

[56] M. Rauscher, M. Kimmel, and S. Hirche, "Constrained robot control using control barrier functions," in *IEEE/RSJ International Conference on Intelligent Robots and Systems*. IEEE, 2016, pp. 279–285.

[57] W. S. Cortez, D. Oetomo, C. Manzie, and P. Choong, "Control barrier functions for mechanical systems: Theory and application to robotic grasping," *IEEE Transactions on Control Systems Technology*, 2019.

[58] X. Xu, P. Tabuada, J. W. Grizzle, and A. D. Ames, "Robustness of control barrier functions for safety critical control," *IFAC-PapersOnLine*, vol. 48, no. 27, pp. 54–61, 2015.

[59] Q. Nguyen and K. Sreenath, "Exponential control barrier functions for enforcing high relative-degree safety-critical constraints," in *American Control Conference*, 2016, pp. 322–328.

[60] A. D. Ames, K. Galloway, K. Sreenath, and J. W. Grizzle, "Rapidly exponentially stabilizing control Lyapunov functions and hybrid zero dynamics," *IEEE Transactions on Automatic Control*, vol. 59, no. 4, pp. 876–891, 2014.

[61] P. Glotfelter, J. Cortés, and M. Egerstedt, "Boolean composability of constraints and control synthesis for multi-robot systems via nonsmooth control barrier functions," in *2018 IEEE Conference on Control Technology and Applications*. IEEE, 2018, pp. 897–902.

[62] M. Srinivasan, S. Coogan, and M. Egerstedt, "Control of multi-agent systems with finite time control barrier certificates and temporal logic," in *57th Conference on Decision and Control*. IEEE, 2018, pp. 1991–1996.

[63] A. Li, L. Wang, P. Pierpaoli, and M. Egerstedt, "Formally correct composition of coordinated behaviors using control barrier certificates," in *IEEE/RSJ International Conference on Intelligent Robots and Systems*. IEEE, 2018, pp. 3723–3729.

[64] L. Lindemann and D. V. Dimarogonas, "Control barrier functions for signal temporal logic tasks," *IEEE Control Systems Letters*, vol. 3, no. 1, pp. 96–101, 2019.

[65] A. Polyakov, "Nonlinear feedback design for fixed-time stabilization of linear control systems," *IEEE Transactions on Automatic Control*, vol. 57, no. 8, pp. 2106–2110, 2012.

[66] F. Lopez-Ramirez, D. Efimov, A. Polyakov, and W. Perruquetti, "Conditions for fixed-time stability and stabilization of continuous autonomous systems," *Systems & Control Letters*, vol. 129, pp. 26–35, 2019.

[67] ——, "On necessary and sufficient conditions for fixed-time stability of continuous autonomous systems," in *2018 European Control Conference*, 2018, pp. 197–200.

[68] C. Li, X. Yu, X. Zhou, and W. Ren, "A fixed time distributed optimization: A sliding mode perspective," in *43rd Annual Conference of the Industrial Electronics Society*. IEEE, 2017, pp. 8201–8207.

[69] M. L. Corradini and A. Cristofaro, "Nonsingular terminal sliding-mode control of nonlinear planar systems with global fixed-time stability guarantees," *Automatica*, vol. 95, pp. 561–565, 2018.

[70] F. Lopez-Ramirez, D. Efimov, A. Polyakov, and W. Perruquetti, "Fixed-time output stabilization and fixed-time estimation of a chain of integrators," *International Journal of Robust and Nonlinear Control*, vol. 28, no. 16, pp. 4647–4665, 2018.

[71] J. Liu, Y. Yu, J. Sun, and C. Sun, "Distributed event-triggered fixed-time consensus for leader-follower multiagent systems with nonlinear dynamics and uncertain disturbances," *International Journal of Robust and Nonlinear Control*, vol. 28, no. 11, pp. 3543–3559, 2018.

[72] X. Wei, W. Yu, H. Wang, Y. Yao, and F. Mei, "An observer-based fixed-time consensus control for second-order multi-agent systems with disturbances," *IEEE Transactions on Circuits and Systems II: Express Briefs*, vol. 66, no. 2, pp. 247–251, 2018.

[73] M. Jankovic, "Robust control barrier functions for constrained stabilization of nonlinear systems," *Automatica*, vol. 96, pp. 359–367, 2018.

[74] R. Goebel, R. G. Sanfelice, and A. R. Teel, *Hybrid Dynamical Systems: Modeling, Stability, and Robustness*. Princeton University Press, 2012.

[75] D. Liberzon, *Switching in Systems and Control*. Springer Science & Business Media, 2003.

[76] M. S. Branicky, "Multiple Lyapunov functions and other analysis tools for switched and hybrid systems," *IEEE Transactions on Automatic Control*, vol. 43, no. 4, pp. 475–482, 1998.

[77] J. Zhao and D. J. Hill, "On stability, l_2-gain and H_∞ control for switched systems," *Automatica*, vol. 44, no. 5, pp. 1220–1232, 2008.

[78] X. Zhao, L. Zhang, P. Shi, and M. Liu, "Stability of switched positive linear systems with average dwell time switching," *Automatica*, vol. 48, no. 6, pp. 1132–1137, 2012.

[79] X. Liu, D. W. Ho, Q. Song, and J. Cao, "Finite-/fixed-time robust stabilization of switched discontinuous systems with disturbances," *Nonlinear Dynamics*, vol. 90, no. 3, pp. 2057–2068, 2017.

[80] Y. Li and R. G. Sanfelice, "A robust finite-time convergent hybrid observer for linear systems," in *52nd IEEE Conference on Decision and Control*, Dec 2013, pp. 3349–3354.

[81] S. G. Nersesov and W. M. Haddad, "Finite-time stabilization of nonlinear impulsive dynamical systems," in *European Control Conference*. IEEE, 2007, pp. 91–98.

[82] Y. Li and R. G. Sanfelice, "Finite time stability of sets for hybrid dynamical systems," *Automatica*, vol. 100, pp. 200–211, 2019.

[83] H. Ríos, J. Davila, and L. Fridman, "State estimation on switching systems via high-order sliding modes," in *Hybrid Dynamical Systems*. Springer, 2015, pp. 151–178.

[84] B. Zhang, "On finite-time stability of switched systems with hybrid homogeneous degrees," *Mathematical Problems in Engineering*, 2018, Article ID 3096986.

[85] J. Fu, R. Ma, and T. Chai, "Global finite-time stabilization of a class of switched nonlinear systems with the powers of positive odd rational numbers," *Automatica*, vol. 54, pp. 360–373, 2015.

[86] F. Bejarano, A. Pisano, and E. Usai, "Finite-time converging jump observer for switched linear systems with unknown inputs," *Nonlinear Analysis: Hybrid Systems*, vol. 5, no. 2, pp. 174–188, 2011.

[87] A. Brown and M. C. Bartholomew-Biggs, "Some effective methods for unconstrained optimization based on the solution of systems of ordinary differential equations," *Journal of Optimization Theory and Applications*, vol. 62, no. 2, pp. 211–224, 1989.

[88] W. Su, S. Boyd, and E. Candes, "A differential equation for modeling Nesterov's accelerated gradient method: Theory and insights," in *Advances in Neural Information Processing Systems*, 2014, pp. 2510–2518.

[89] A. Cherukuri, B. Gharesifard, and J. Cortes, "Saddle-point dynamics: Conditions for asymptotic stability of saddle points," *SIAM Journal on Control and Optimization*, vol. 55, no. 1, pp. 486–511, 2017.

[90] N. K. Dhingra, S. Z. Khong, and M. R. Jovanović, "The proximal augmented Lagrangian method for nonsmooth composite optimization," *IEEE Transactions on Automatic Control*, vol. 64, no. 7, pp. 2861–2868, 2018.

[91] W. Krichene, A. Bayen, and P. L. Bartlett, "Accelerated mirror descent in continuous and discrete time," in *Advances in Neural Information Processing Systems*, 2015, pp. 2845–2853.

[92] U. Clarenz, S. Henn, M. Rumpf, and K. Witsch, "Relations between optimization and gradient flow methods with applications to image registration," in *Proceedings of the 18th GAMM-Seminar Leipzig on Multigrid and Related Methods for Optimization Problems*, 2002, pp. 11–30.

[93] J. Cortés, "Finite-time convergent gradient flows with applications to network consensus," *Automatica*, vol. 42, no. 11, pp. 1993–2000, 2006.

[94] H. Karimi, J. Nutini, and M. Schmidt, "Linear convergence of gradient and proximal-gradient methods under the Polyak- łojasiewicz condition," in *Joint European Conference on Machine Learning and Knowledge Discovery in Databases*. Springer, 2016, pp. 795–811.

[95] Y. Nesterov, "Accelerating the cubic regularization of Newton's method on convex problems," *Mathematical Programming*, vol. 112, no. 1, pp. 159–181, 2008.

[96] J. Wang and N. Elia, "A control perspective for centralized and distributed convex optimization," in *IEEE Conference on Decision and Control and European Control Conference*. IEEE, 2011, pp. 3800–3805.

[97] X. Ma and N. Elia, "A distributed continuous-time gradient dynamics approach for the active power loss minimizations," in *2013 51st Annual Allerton Conference on Communication, Control, and Computing*. IEEE, 2013, pp. 100–106.

[98] D. Feijer and F. Paganini, "Stability of primal-dual gradient dynamics and applications to network optimization," *Automatica*, vol. 46, no. 12, pp. 1974–1981, 2010.

[99] B. Gharesifard and J. Cortés, "Distributed convergence to Nash equilibria in two-network zero-sum games," *Automatica*, vol. 49, no. 6, pp. 1683–1692, 2013.

[100] M. Benzi, G. H. Golub, and J. Liesen, "Numerical solution of saddle point problems," *Acta numerica*, vol. 14, pp. 1–137, 2005.

[101] F. Chen and W. Ren, "Convex optimization via finite-time projected gradient flows," in *IEEE Conference on Decision and Control*. IEEE, 2018, pp. 4072–4077.

[102] Y. Song and W. Chen, "Finite-time convergent distributed consensus optimisation over networks," *IET Control Theory & Applications*, vol. 10, no. 11, pp. 1314–1318, 2016.

[103] X. Pan, Z. Liu, and Z. Chen, "Distributed optimization with finite-time convergence via discontinuous dynamics," in *2018 37th Chinese Control Conference*. IEEE, 2018, pp. 6665–6669.

[104] J. D. Sánchez-Torres, M. J. Loza-Lopez, R. Ruiz-Cruz, E. N. Sanchez, and A. G. Loukianov, "A fixed time convergent dynamical system to solve linear programming," in *IEEE 53rd Annual Conference on Decision and Control*. IEEE, 2014, pp. 5837–5842.

[105] Z. Feng and G. Hu, "Finite-time distributed optimization with quadratic objective functions under uncertain information," in *2017 IEEE 56th Conference on Decision and Control*. IEEE, 2017, pp. 208–213.

[106] M. Santilli, A. Marino, and A. Gasparri, "A finite-time protocol for distributed continuous-time optimization of sum of locally coupled strictly convex functions," in *IEEE 57th Conference on Decision and Control*. IEEE, 2018, pp. 993–998.

[107] K. Garg and D. Panagou, "Finite-time estimation and control for multi-aircraft systems under wind and dynamic obstacles," *Journal of Guidance, Control, and Dynamics*, vol. 42, no. 7, pp. 1489–1505, 2019.

[108] ——, "Characterization of domain of fixed-time stability under control input constraints," in *American Control Conference*, 2021.

[109] M. Black, K. Garg, and D. Panagou, "A quadratic program based control synthesis under spatiotemporal constraints and non-vanishing disturbances," in *59th Conference on Decision and Control*. IEEE, Dec 2020, pp. 2726–2731.

[110] K. Garg and D. Panagou, "Control-Lyapunov and control-barrier functions based quadratic program for spatio-temporal specifications," in *58th Conference on Decision and Control*. IEEE, Dec 2019, pp. 1422–1429.

[111] K. Garg, E. Arabi, and D. Panagou, "Fixed-time control under spatiotemporal and input constraints: A quadratic program based approach," *IEEE Transactions on Automatic Control*, 2020, submitted, under review.

[112] K. Garg and D. Panagou, "Robust control barrier and control Lyapunov functions with fixed-time convergence guarantees," in *American Control Conference*, 2021.

[113] ——, "Finite-time stability of hybrid systems with unstable modes," *IEEE Control Systems Letters*, 2021, submitted, under review.

[114] ——, "Finite-time stabilization of switched systems with unstable modes," in *Conference on Analysis and Design of Hybrid Systems*. IFAC, 2021, submitted, under review.

[115] ——, "Fixed-time stable gradient flows: Applications to continuous-time optimization," *IEEE Transactions on Automatic Control*, vol. 66, no. 5, 2021.

[116] D. Panagou, "A distributed feedback motion planning protocol for multiple unicycle agents of different classes," *IEEE Transactions on Automatic Control*, vol. 62, no. 3, pp. 1178–1193, Mar. 2017.

[117] S. P. Bhat and D. S. Bernstein, "Geometric homogeneity with applications to finite-time stability," *Mathematics of Control, Signals and Systems*, vol. 17, no. 2, pp. 101–127, 2005.

[118] K. Garg and D. Panagou, "New results on finite-time stability: Geometric conditions and finite-time controllers," in *2018 Annual American Control Conference*, June 2018, pp. 442–447.

[119] X. Ma, Z. Jiao, Z. Wang, and D. Panagou, "3-d decentralized prioritized motion planning and coordination for high-density operations of micro aerial vehicles," *IEEE Transactions on Control Systems Technology*, vol. 26, no. 3, pp. 939–953, May 2017.

[120] Y. Shen and X. Xia, "Semi-global finite-time observers for nonlinear systems," *Automatica*, vol. 44, no. 12, pp. 3152–3156, 2008.

[121] A. G. Kartsatos, *Advanced Ordinary Differential Equations*. Mariner, 1980.

[122] H. K. Khalil, *Nonlinear Systems*. Prentice hall Upper Saddle River, NJ, 2002, vol. 3.

[123] Q. Hui, W. M. Haddad, and S. P. Bhat, "Semistability, finite-time stability, differential inclusions, and discontinuous dynamical systems having a continuum of equilibria," *IEEE Transactions on Automatic Control*, vol. 54, no. 10, pp. 2465–2470, 2009.

[124] E. Moulay and W. Perruquetti, "Finite time stability of differential inclusions," *IMA Journal of Mathematical Control and Information*, vol. 22, no. 4, pp. 465–475, 2005.

[125] A. Polyakov, D. Efimov, and W. Perruquetti, "Finite-time and fixed-time stabilization: Implicit Lyapunov function approach," *Automatica*, vol. 51, pp. 332–340, 2015.

[126] A. Polyakov, "Characterization of finite/fixed-time stability of evolution inclusions," in *2019 IEEE 58th Conference on Decision and Control*, 2019, pp. 4990–4995.

[127] S. Parsegov, A. Polyakov, and P. Shcherbakov, "Nonlinear fixed-time control protocol for uniform allocation of agents on a segment," in *51st Conference on Decision and Control*. IEEE, 2012, pp. 7732–7737.

[128] S. Boyd and L. Vandenberghe, *Convex Optimization*. Cambridge University Press, 2004.

[129] F. Blanchini, "Set invariance in control," *Automatica*, vol. 35, no. 11, pp. 1747–1767, 1999.

[130] E. D. Sontag, "A universal construction of Artstein's theorem on nonlinear stabilization." *Systems & Control Letters*, vol. 13, no. 2, pp. 117–123, 1989.

[131] R. P. Agarwal and V. Lakshmikantham, *Uniqueness and Nonuniqueness Criteria for Ordinary Differential Equations*. World Scientific Publishing Company, 1993, vol. 6.

[132] S. M. Robinson, "Perturbed Kuhn-Tucker points and rates of convergence for a class of nonlinear-programming algorithms," *Mathematical Programming*, vol. 7, no. 1, pp. 1–16, 1974.

[133] A. V. Fiacco, "Sensitivity analysis for nonlinear programming using penalty methods," *Mathematical Programming*, vol. 10, no. 1, pp. 287–311, 1976.

[134] J. Usevitch, K. Garg, and D. Panagou, "Strong invariance using control barrier functions: A Clarke tangent cone approach," in *59th Conference on Decision and Control*. IEEE, Dec 2020, pp. 2044–2049.

[135] J. P. Aubin and A. Cellina, *Differential Inclusions: Set-valued Maps and Viability Theory*. Springer Science & Business Media, 2012, vol. 264.

[136] L. Lindemann and D. V. Dimarogonas, "Robust motion planning employing signal temporal logic," in *American Control Conference*, 2017, pp. 2950–2955.

[137] D. Panagou and K. J. Kyriakopoulos, "Dynamic positioning for an underactuated marine vehicle using hybrid control," *International Journal of Control*, vol. 87, no. 2, pp. 264–280, 2014.

[138] L. Wang, A. D. Ames, and M. Egerstedt, "Safety barrier certificates for collisions-free multirobot systems," *IEEE Transactions on Robotics*, vol. 33, no. 3, pp. 661–674, 2017.

[139] I. M. Mitchell, S. Kaynama, M. Chen, and M. Oishi, "Safety preserving control synthesis for sampled data systems," *Nonlinear Analysis: Hybrid Systems*, vol. 10, pp. 63–82, 2013.

[140] A. Ghaffari, I. Abel, D. Ricketts, S. Lerner, and M. Krstić, "Safety verification using barrier certificates with application to double integrator with input saturation and zero-order hold," in *2018 Annual American Control Conference*, 2018, pp. 4664–4669.

[141] T. Gurriet, P. Nilsson, A. Singletary, and A. D. Ames, "Realizable set invariance conditions for cyber-physical systems," in *2019 Annual American Control Conference*, 2019, pp. 3642–3649.

[142] J. Usevitch and D. Panagou, "Adversarially resilient control barrier functions in sampled-data systems," in *2021 American Control Conference*, May 2021.

[143] A. Singletary, Y. Chen, and A. D. Ames, "Control barrier functions for sampled-data systems with input delays," in *2020 59th IEEE Conference on Decision and Control*, 2020, pp. 804–809.

[144] Y. Li and R. G. Sanfelice, "Results on finite time stability for a class of hybrid systems," in *2016 American Control Conference*, July 2016, pp. 4263–4268.

[145] R. G. Sanfelice, R. Goebel, and A. R. Teel, "Invariance principles for hybrid systems with connections to detectability and asymptotic stability," *IEEE Transactions on Automatic Control*, vol. 52, no. 12, pp. 2282–2297, 2007.

[146] H. Lin and P. J. Antsaklis, "Stability and stabilizability of switched linear systems: a survey of recent results," *IEEE Transactions on Automatic control*, vol. 54, no. 2, pp. 308–322, 2009.

[147] P. Peleties and R. DeCarlo, "Asymptotic stability of m-switched systems using Lyapunov-like functions," in *American Control Conference*, 1991, pp. 1679–1684.

[148] Y.-E. Wang, H. R. Karimi, and D. Wu, "Conditions for the stability of switched systems containing unstable subsystems," *IEEE Transactions on Circuits and Systems II: Express Briefs*, vol. 66, no. 4, pp. 617–621, 2018.

[149] C. Cai, A. R. Teel, and R. Goebel, "Smooth Lyapunov functions for hybrid systems part ii:(pre) asymptotically stable compact sets," *IEEE Transactions on Automatic Control*, vol. 53, no. 3, pp. 734–748, 2008.

[150] P. A. Parrilo, "Structured semidefinite programs and semialgebraic geometry methods in robustness and optimization," Ph.D. dissertation, California Institute of Technology, 2000, PhD Thesis.

[151] S. Prajna, A. Papachristodoulou, and P. A. Parrilo, "Introducing SOSTOOLS: a general purpose sum of squares programming solver," in *41st IEEE Conference on Decision and Control*, Dec 2002, pp. 741–746.

[152] D. Liberzon and A. S. Morse, "Basic problems in stability and design of switched systems," *IEEE Control Systems Magazine*, vol. 19, no. 5, pp. 59–70, 1999.

[153] W. Perruquetti, T. Floquet, and E. Moulay, "Finite-time observers: application to secure communication," *IEEE Transactions on Automatic Control*, vol. 53, no. 1, pp. 356–360, 2008.

[154] A. Beck, *Introduction to Nonlinear Optimization: Theory, Algorithms, and Applications with MATLAB*. SIAM, 2014, vol. 19.

[155] I. M. Bomze and L. Palagi, "Quartic formulation of standard quadratic optimization problems," *Journal of Global Optimization*, vol. 32, no. 2, pp. 181–205, 2005.

[156] G. Qu and N. Li, "On the exponential stability of primal-dual gradient dynamics," *IEEE Control Systems Letters*, vol. 3, no. 1, pp. 43–48, 2019.

[157] C. Zalinescu, *Convex Analysis in General Vector Spaces*. World Scientific, 2002.

[158] A. Cherukuri, E. Mallada, S. Low, and J. Cortés, "The role of convexity on saddle-point dynamics: Lyapunov function and robustness," *IEEE Transactions on Automatic Control*, vol. 63, no. 8, pp. 2449–2464, 2017.

[159] C. Paige, G. P. Styan, B.-Y. Wang, and F. Zhang, "Hua's matrix equality and Schur complements," *International Journal of Information & Systems Sciences*, vol. 4, no. 1, p. 124, 2008.

[160] K. Garg, D. Han, and D. Panagou, "Robust semi-cooperative multi-agent coordination in the presence of stochastic disturbances," in *2017 IEEE 56th Annual Conference on Decision and Control*, Dec 2017, pp. 3443–3448.

[161] K. Garg and D. Panagou, "A robust coordination protocol for safe multi-agent motion planning," in *AIAA Guidance, Navigation, and Control Conference*, Jan 2018, p. 0605.

[162] M. F. Reis, A. P. Aguiar, and P. Tabuada, "Control barrier function-based quadratic programs introduce undesirable asymptotically stable equilibria," *IEEE Control Systems Letters*, vol. 5, no. 2, pp. 731–736, 2021.

[163] J. N. Maidens, S. Kaynama, I. M. Mitchell, M. M. Oishi, and G. A. Dumont, "Lagrangian methods for approximating the viability kernel in high-dimensional systems," *Automatica*, vol. 49, no. 7, pp. 2017–2029, 2013.

[164] I. M. Mitchell, A. M. Bayen, and C. J. Tomlin, "A time-dependent hamilton-jacobi formulation of reachable sets for continuous dynamic games," *IEEE Transactions on automatic control*, vol. 50, no. 7, pp. 947–957, 2005.

[165] M. Chen and C. J. Tomlin, "Hamilton–jacobi reachability: Some recent theoretical advances and applications in unmanned airspace management," *Annual Review of Control, Robotics, and Autonomous Systems*, vol. 1, pp. 333–358, 2018.

[166] N. Kochdumper and M. Althoff, "Sparse polynomial zonotopes: A novel set representation for reachability analysis," *IEEE Transactions on Automatic Control*, 2020.

[167] P.-J. Meyer, A. Devonport, and M. Arcak, "TIRA: Toolbox for interval reachability analysis," in *Proceedings of the 22nd ACM International Conference on Hybrid Systems: Computation and Control*, ser. HSCC '19. New York, NY, USA: Association for Computing Machinery, 2019, p. 224–229.

[168] A. Girard and C. Le Guernic, "Zonotope/hyperplane intersection for hybrid systems reachability analysis," in *International Workshop on Hybrid Systems: Computation and Control*. Springer, 2008, pp. 215–228.

[169] A. Robey, H. Hu, L. Lindemann, H. Zhang, D. V. Dimarogonas, S. Tu, and N. Matni, "Learning control barrier functions from expert demonstrations," in *59th IEEE Conference on Decision and Control*, 2020, pp. 3717–3724.

[170] L. Lindemann, H. Hu, A. Robey, H. Zhang, D. V. Dimarogonas, S. Tu, and N. Matni, "Learning hybrid control barrier functions from data," in *Conference on Robot Learning*. PMLR, 2020.

[171] A. Taylor, A. Singletary, Y. Yue, and A. Ames, "Learning for safety-critical control with control barrier functions," in *Learning for Dynamics and Control*. PMLR, 2020, pp. 708–717.

[172] M. Benosman, O. Romero, and A. Cherian, "Optimizing deep neural networks via discretization of finite-time convergent flows," 2020, arXiv:2010.02990.

[173] R. G. Sanfelice and A. R. Teel, "Dynamical properties of hybrid systems simulators," *Automatica*, vol. 46, no. 2, pp. 239–248, 2010.

[174] K. Garg and D. Panagou, "Hybrid planning and control for multiple fixed-wing aircraft under input constraints," in *AIAA Scitech 2019 Forum*, 2019, p. 0655.

[175] K. Garg, E. Arabi, and D. Panagou, "Prescribed-time convergence with input constraints: A control Lyapunov function based approach," in *2020 Annual American Control Conference*, 2020, pp. 962–967.

[176] K. Garg, M. Baranwal, and D. Panagou, "A fixed-time convergent distributed algorithm for strongly convex functions in a time-varying network," in *59th Conference on Decision and Control*. IEEE, Dec 2020, pp. 4405–4410.

[177] M. Baranwal, K. Garg, D. Panagou, and A. O. Hero, "Robust distributed fixed-time economic dispatch under time-varying topology," *IEEE Control Systems Letters*, vol. 5, no. 4, pp. 1183–1188, 2021.

[178] K. Garg and M. Baranwal, "CAPPA: Continuous-time accelerated proximal point algorithm for sparse recovery," *IEEE Signal Processing Letters*, vol. 27, pp. 1760–1764, 2020.

[179] M. H. Cohen and C. Belta, "Approximate optimal control for safety-critical systems with control barrier functions," in *2020 59th IEEE Conference on Decision and Control*. IEEE, 2020, pp. 2062–2067.

[180] U. Rosolia and A. D. Ames, "Multi-rate control design leveraging control barrier functions and model predictive control policies," *IEEE Control Systems Letters*, vol. 5, no. 3, pp. 1007–1012, 2021.

[181] K. Garg, R. K. Cosner, U. Rosoliya, A. D. Ames, and D. Panagou, "Multi-rate control design under input constraints via fixed-time barrier functions," *IEEE Control Systems Letters, under review*, 2021, arXiv:2103.03695.

[182] J. Breeden, K. Garg, and D. Panagou, "Control barrier functions in sampled-data systems," *IEEE Control Systems Letters, under review*, 2021, arXiv:2103.03677.